EXTRACELLULAR VESICLES IN SYNOVIAL FLUID

Dynamics during joint inflammation and articular development and promise for joint regeneration and restoration of joint homeostasis

MEMBRAANBLAASJES IN GEWRICHTSVLOEISTOF
Dynamiek tijdens artritis en gewrichtsontwikkeling en de mogelijke rol
bij regeneratie van gewrichten en herstel van gewrichtshomeostase

(met een samenvatting in het Nederlands)

Proefschrift

ter verkrijging van de graad van doctor aan de Universiteit Utrecht
op gezag van de rector magnificus, prof.dr. G.J. van der Zwaan,
ingevolge het besluit van het college voor promoties in het openbaar te verdedigen
op donderdag 7 september 2017 des middags te 12.45 uur

door

Janneke Boere
geboren op 16 juli 1985 te Maastricht

Zo, laat ons dan proberen om de berg op te klimmen,
niet door te trappen op wat onder ons ligt,
maar door ons op te trekken aan wat zich boven ons bevindt,
voor mijn part aan de sterren...

(M.C. Escher)

Voor mama en papa

CONTENTS

1

General Introduction

It is only fifty years ago that vesicle-like structures were for the first time described in cartilage as "roundish bodies" that form nucleation centers in which calcification is initiated for the formation of bone [1,2]. Later, these shedding vesicles became known as matrix vesicles. In 1983, new research from two independent groups showed that also an endocytic form of vesicle formation and excretion existed [3,4]. These important discoveries were the basis for future research on extracellular vesicles (EVs). Since then, various EV types have been discovered and have gained increasing recognition for regulating complex pathways in many biological systems. Not surprisingly, EVs are candidates for regulating local joint homeostasis as well.

In this general introduction the current positioning of EV research in the field of joint biology and joint disease is outlined. The original discovery of matrix vesicles and their role in physiological joint development is explained in more detail. The knowledge on EVs in inflammatory joint disease and the opportunities for EVs in articular tissue repair are reviewed briefly and will be dealt with in more detail in later chapters in this thesis.

SIGNIFICANCE OF JOINT DISORDERS IN HUMANS AND HORSES

Global burden of joint disease
Musculoskeletal diseases in humans, with osteoarthritis (OA), rheumatoid arthritis (RA), gout, low back pain and neck pain as major disorders, are estimated to cause a staggering 21.3% of the total years lived with disability (YLDs) globally, which comes second only to mental and behavioral problems (23.2%) [5]. With increasing life expectancy, decreasing mortality in low-income and middle-income countries, the increase in obesity and the adoption of a lifestyle that promotes musculoskeletal problems (sedentary lifestyle in the Western world; harsh working conditions in low-income and middle-income countries), these numbers can only be expected to increase in the coming decades.
Osteoarthritis and RA have a high prevalence specifically in the Western world [6,7]. They are an enormous burden to healthcare systems and cost governments billions each year. Most importantly, they dramatically impact on the quality of life, which justifies the substantial amount of scientific research focusing on OA and RA.

Osteoarthritis is more common in middle-aged and elderly people and typically presents with chronic pain due to structural damage of the articular cartilage and subchondral bone, including osteophyte formation, and concomitant deterioration of tendons and ligaments. More recently, it has been acknowledged that OA is also characterised by chronic synovial inflammation and inflammation of the cartilage, which is instrumental for progression of the disease [8,9]. Although in OA inflammation

may be low-grade and is not always reflected by elevated leukocyte counts in the synovial fluid (SF) and swelling of the synovial membrane (as is the case in RA [10]), it has been proposed that local inflammation could be the trigger for primary cartilage injury. Upon release of catabolic factors, the surrounding tissue (and the synovial membrane) become stressed, starting a vicious cycle of progressive tissue breakdown and further inflammation; in other words, disturbance of local homeostasis [11].

In contrast to OA, RA is a systemic auto-immune disorder characterised by flares and remissions of severe synovitis in multiple joints, resulting in joint swelling, tissue damage, joint instability and ultimately severe cartilage and bone erosion [10]. In RA, inflammatory responses of the tissue are obvious and disease progression is therefore easier to monitor, but the auto-immune and systemic character makes it into a difficult disease to target therapeutically.

For both OA and RA, and also for most other joint diseases, the exact etiology and pathogenesis is still not fully known and only slowly we begin to understand what the molecular mechanisms are that cause initial tissue injury and inflammation in the different types of arthritis. At the moment, treatment options only achieve symptom relief and prevention (or delay) of severe complications, but complete remission is hardly, if ever, accomplished. The study of these processes in more detail will provide clues for more adequate and effective therapeutic targeting and disease prevention. In this same line, early detection of joint disease by biomarker analysis is an important motive for pursuing in-depth analysis and molecular profiling of SF and synovial tissues during health and disease.

Animal models for joint disease

To study joint diseases, various animal models, most of them for OA, have been developed, which all have their practical considerations and drawbacks regarding translation to the human situation [12]. Overall, the horse is seen as one of the best large animal models for musculoskeletal disease and specifically suitable to study OA [13,14]. Not only do horses, as a species, suffer from spontaneous OA, and is OA a highly significant problem in this species, they also have the best equivalent of the human musculoskeletal system with comparable biochemical and biomechanical properties, cartilage structure and cartilage thickness [14-16]. In both humans and horses, two routes for the initiation of OA can be distinguished: 1) the combination of healthy cartilage with abnormal stresses on the joint (due to *e.g.* bone or ligament damage, developmental defects, or sports injuries), or 2) normal stresses on a joint with abnormal cartilage (for instance due to trauma, synovitis, ageing, or osteochondrosis) [13]. Because of these similarities and the clinical need in the species, the horse serves as an experimental animal and at the same time as a therapeutic target animal

1

for OA and cartilage repair studies [14]. The species is also an excellent study model for (inducible) synovitis [17-20].

Detection of joint disease and monitoring its progression can be performed in blood, articular tissue biopsies and in SF [8]. Synovial fluid in particular has been shown to be an excellent representation of molecular joint homeostasis in horses, especially for inflammatory joint disease [11,17].

In view of the impact that joint diseases have on both humans and horses, and the advantages of using equine specimens as translational study material, for this thesis equine SF was chosen for detection of EVs to investigate potential EV engagement in normal and imbalanced joint homeostasis.

THE JOINT AS AN ORGAN

Synovial joints are complex structures in the musculoskeletal system. They are the physiologic connectors of long bones and enable motion and flexibility by permitting the gliding of the thin layers of hyaline cartilage covering the epiphyseal bone surfaces, over each other [21]. The synovial cavity, which is the connecting compartment, is filled with SF, serving both as a lubricant and as nutritional fluid for the cartilage. Nutrition through diffusion is necessary, since cartilage is aneural, avascular and alymphatic. Enclosing the joint space is the synovial membrane, or synovium, a specialised cell layer of fibroblast-like and macrophage-like synoviocytes (intima), lined by connective and adipose tissue (subintima). Synovial fibroblasts take care of production of SF components (mainly hyaluronic acid, lubricin and glycoproteins) and provide nutrients for the cartilage, whereas the macrophages are responsible for phagocytosis of local debris [22]. As outer layer, the joint is surrounded by a fibrous capsule, protecting the delicate intra-articular structures [21].

With respect to joint homeostasis, synovial joints can be envisioned as complex organs in which the articular tissues act as an entity and synovial membrane and cartilage stay in close contact via the SF, maintaining a healthy steady state [22]. As a consequence, imbalance in one of the tissues, due to trauma, infection or inflammation, will ultimately have impact on the entire joint [11,23]. Communication between tissues is of great importance to adequately stabilise these impaired conditions. Although responses to undesirable situations most often comprise production of catabolic cytokines, enzymes and inflammatory mediators [24], parallel intercellular communication via EVs is highly likely in order to regulate immunologic processes to maintain joint homeostasis.

EXTRACELLULAR VESICLES (EVs)

Biogenesis and characteristics of EVs

Extracellular vesicles are small, lipid-bilayer enclosed, cell-derived particles, specialised to facilitate cell-cell communication [25,26]. Their membrane contains proteins and lipids that make adherence to target cells possible, upon which active interaction takes place by several routes (Figure 1): a) fusion with the plasma membrane for releasing their cargo into the cytosol, b) ligand-receptor binding at the plasma membrane for direct intracellular pathway activation, or c) complete endocytosis for downstream fusion with intracellular compartments. In addition, soluble factors in the microenvironment of EVs can bind to their membrane and use EVs as shuttle vehicles for directed transport towards target cells [27,28].

The biogenesis of EVs follows generally one of two pathways (Figure 1): intraluminal vesicles (ILVs) can be produced within endosomes of the donor cells, resulting in multivesicular bodies (MVB). After subsequent fusion of MVBs with the plasma membrane, ILVs are released in the environment and are called "exosomes". Alternatively, EVs originate directly from budding from the cell membrane, referred to as "microvesicles" [25,29]. Often, the terms exosomes and microvesicles are used as equivalent for small and larger vesicles, but this classification is incorrect. Indeed, exosomes are generally smaller (as there is a limiting size for endosomal formation) and microvesicles are often detected as larger particles. However, both exosomes ($\sim$ 30-200 nm) and microvesicles ($\sim$ 50 nm – 1 µm) can either be very small or relatively large [26]. Vesicles shedding from apoptotic cells, including apoptotic bodies, are even more heterogeneous with diameters up to 5 µm. Alternative names used for EVs (*e.g.* matrix vesicles [30], prostasomes [31], oncosomes [32] etc.) usually refer to the research field or cell type studied. In order to halt and further avoid confusion and misinterpretation of nomenclature, the International Society for Extracellular Vesicles (ISEV) has advised in 2011 that, unless investigations can show the pathway of origin of EVs, or if there are clear indications that EVs are derived from specific cell types, the use of the generic term "extracellular vesicles" (EVs) is preferred [33].

Extracellular vesicles are very efficient in bringing complex signals across, since they are unique combinations of biologically active signaling molecules packaged into one small vesicle [34,35]. Their lipid bilayer protects proteins and nucleic acids from the degradative extravesicular environment (the extracellular space), making stable transfer of proteins, rRNA, tRNA, miRNA, lncRNA and (mitochondrial) DNA possible, over short and longer distances [36,37]. Also, specialised enzymes can be carried by EVs, which hence provide a tool to biologically activate precursor molecules in the EV or in the recipient cell [35].
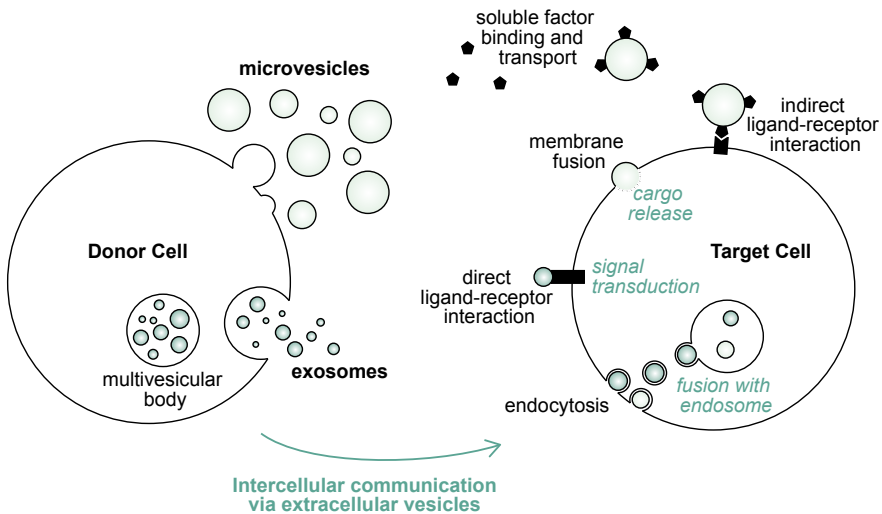
Figure 1 EV biogenesis and routes of communication with the target cell.

Extracellular vesicles typically have specific protein and lipid signatures of the cells of origin [38]. In general, the EV membrane is composed of a bilayer of phospholipids, interspersed with glyco(sphingo)lipids, cholesterol, sphingomyelin, prostaglandins, integrins, tetraspanins, cell adhesion molecules and growth factor receptors [28,37,39]. These molecules facilitate adhesion and/or fusion with recipient cells and may serve in ligand-receptor signaling. The EV membrane can also contain membrane transport proteins (*e.g.* sodium-dependent inorganic phosphate transporters) [30] and ion channels (*e.g.* annexins function as Ca^{2+} channels in matrix vesicles) [40]. These characteristics enable EVs to act as sites of active processing of (signaling) molecules, in addition to being shuttling vehicles for passive transport of biologically active factors.

Extracellular vesicles are produced by all cell types and EV production and release are tightly regulated processes which may vary between normal physiological and pathophysiological processes [28,41]. In addition, the stimulation of cells by external stimuli can drastically change the EV-production rate and EV content or composition [42,43]. The pool of EVs found in biological fluids represents vesicles from the various cell types which are in direct contact with the fluid, or from infiltrating pathogens (since these produce EVs as well) [44,45]. In some cases, EVs can even cross epithelial and endothelial barriers, which has been shown for the blood brain barrier [46]. Thus, the EV pool in body fluids reflects the systemic activity of the body as a whole

(for example when measured in blood) or of specific organs (for example when measured in urine) and can be a monitoring tool ("liquid biopsy") for active disease processes [47-49].

EVs in synovial fluid

Synovial fluid can be seen as the extension of the cartilage and synovium extracellular matrix (ECM) [22]. It is a clear, viscous fluid, containing paracrine and autocrine molecules produced by synovial cells, or infiltrating immune cells during inflammation. The interstitial spaces in the synovial membrane (average width = 2 μm) enable small molecule diffusion [50], making SF a blood plasma dialysate. The permeability of the synovial membrane could also facilitate cross-barrier diffusion of EVs between blood plasma and SF, but up to now there is no evidence for this to happen.

So far only a limited number of studies have been performed on EV analysis in SF, with almost all using human SF obtained from patients with joint disease [51-68]. Considering a role for EVs in normal homeostasis as well, EVs can be expected to be also present in SF from healthy individuals. However, no data are available to confirm this conjecture. Also, all current studies are cross-sectional in nature and there is no information on the dynamics of the EV concentration, EV populations or EV characteristics between healthy and diseased joints.

Besides this gap in general knowledge about normal function of EVs in the joint, technical aspects complicate the interpretation of data from the few studies performed so far. What makes EV isolation from SF very challenging is the very specific composition of the fluid. Especially the high concentration of hyaluronic acid in SF [22], causing its typical high viscosity, makes sedimentation of EVs by differential ultracentrifugation difficult. Furthermore, the highly variable SF composition and viscosity, which is associated with different joint diseases [22,69], hinder consistent EV isolation. The lack of consensus on how to consistently isolate EVs from SF and the incompatibility of analysis techniques urge the need for a more standardised protocol.

Cartilage matrix vesicles: the ancestors of EV research

The discovery of matrix vesicles is historically important for the general recognition of cell-derived vesicles being functional instead of being cell debris. Matrix vesicles, for the first time described in independent parallel research by Bonucci and Anderson in 1967 [1,2,70] are a specialised type of EVs, known for their function in endochondral ossification, the process during which embryonic cartilage is converted into bone. This process takes place in the hypertrophic zone of the epiphyseal growth plates. Here, matrix vesicles are formed by budding from the plasma membrane of maturing chondrocytes and osteoblasts. These vesicles subsequently collect calcium and phosphorus in their lumina and increase the concentration of phosphate through the

1

action of alkaline phosphatase, hereby facilitating mineralisation of the tissue [71,72] (Figure 2). Very uniquely, this process takes place in a polarised fashion: vesicles pinch off from the lateral side of growth plate chondrocytes and from the osteoid-facing surface of osteoblasts, in the longitudinal direction of the bone [70,73].

Matrix vesicles are 30-500 nm in diameter and typically carry inorganic phosphate (P_i) and mitochondrial derived calcium (Ca^{2+}) ions derived from their parental cells. Further influx of extracellular P_i and Ca^{2+} results in intraluminal hydroxyapatite formation, which later is deposited as hydroxyapatite crystals in the ECM [72,74]. Unlike lysosomes, matrix vesicles lack acid phosphatases [74] and carry several annexin proteins in their membrane (mediating Ca^{2+} influx and promoting interaction of the vesicle with collagen type 2 and type 10 in the ECM) [40,72,75]. In order to degrade the surrounding ECM to generate better accessibility of the ion channels in the vesicle membrane, luminal matrix metalloproteinases MMP-2, MMP-3, MMP-9 and MMP-13 are secreted, suggestively under the influence of vitamin-D metabolites and phospholipase-A2 (PLA_2) [76-78].

The cues for the very precisely timed matrix vesicle biogenesis during endochondral ossification have not yet been completely elucidated, but an increase in intracellular Ca^{2+} concentration has been shown to induce matrix vesicle production in growth plate-derived chondrocytes *in vitro* [79]. Furthermore, matrix vesicle production has been suggested to be the result of a specific form of programmed cell death by which hypertrophic chondrocytes are cleared from the growth plate and replaced by osteoblasts, leading to events of vesiculation [80].

Perhaps unsurprisingly, dysregulation of matrix vesicle induced calcification of tissue is a feature of several joint-related diseases [81]. In OA for example, it has been suggested that prematurely differentiated chondrocytes release increased amounts of alkaline phosphatase and BMP-loaded matrix vesicles into the ECM, thereby possibly stimulating osteosclerosis of subchondral bone and osteophyte formation [72].

The potential role of EVs in embryonic joint biology

In addition to bone matrix vesicles, it is highly likely that other EV types play a role in the embryonic stages of skeletal and joint development, although direct evidence is lacking thus far. Skeletogenesis and synovial joint formation are highly orchestrated processes regulated by at least two important signaling pathways, Wnt and Hedgehog [88]. These pathways steer chondrogenesis, osteoblast development and angiogenesis in concert with other regulatory factors that are expressed in the developing cartilage and perichondrium, such as BMPs, fibroblast growth factors (FGFs), TGFβ and VEGF [89-91]. These factors also have a role in homeostasis of the mature joint and all of them have been related to EVs, or found to be involved in (the regulation of) EV production

CARTILAGE

CARTILAGE CALCIFICATION IN THE CARTILAGE-BONE INTERFACE

CALCIFIED BONE

Recruitment and accumulation of Ca^{2+}
and phosphate from the extracellular space

Intraluminal hydroxyapatite (HA)
crystal formation

PPi → **2Pi + Ca^{2+}** → HA crystals

ATP → phosphocholine
phosphoethanolamine

ATP
NTP

Pi
transporter

HA crystal deposition
in the ECM

Anx

neovascularization

ECM degradation to increase
vesicle ion channel accessibility

stimulate cell differentiation

hypertrophic chondrocyte

chondrocyte
matrix vesicle

osteoblast
matrix
vesicle

osteoblast

Ca^{2+}
Pi
PPi
BMPs
VEGF
MMPs

Membrane components
caveolin-1
cholesterol
sphingomyelin
phosphatidylserine
annexins (Anx)

Luminal proteins promoting calcification
bone sialoprotein (BSP)
osteopontin (OPN)
osteocalcin (OCN)
osteonectin (ON)

Membrane associated enzymes
alkaline phosphatase (TNAP)
ATPases
pyrophosphatase
ATP-pyrophosphohydrolase
glycoprotein-1 (PC-1/NPP-1)

Other luminal proteins, growth factors and enzymes
bone morphogenetic proteins (BMPs) 1-7
vascular endothelial growth factor (VEGF)
matrix metalloproteinases (MMPs) 2, 3, 9, 13
PHOSPHO1

Ca^{2+} (mitochondrial derived) calcium

Pi inorganic phosphate

PPi inorganic pyrophosphate

extracellular matrix (ECM):
proteoglycans and
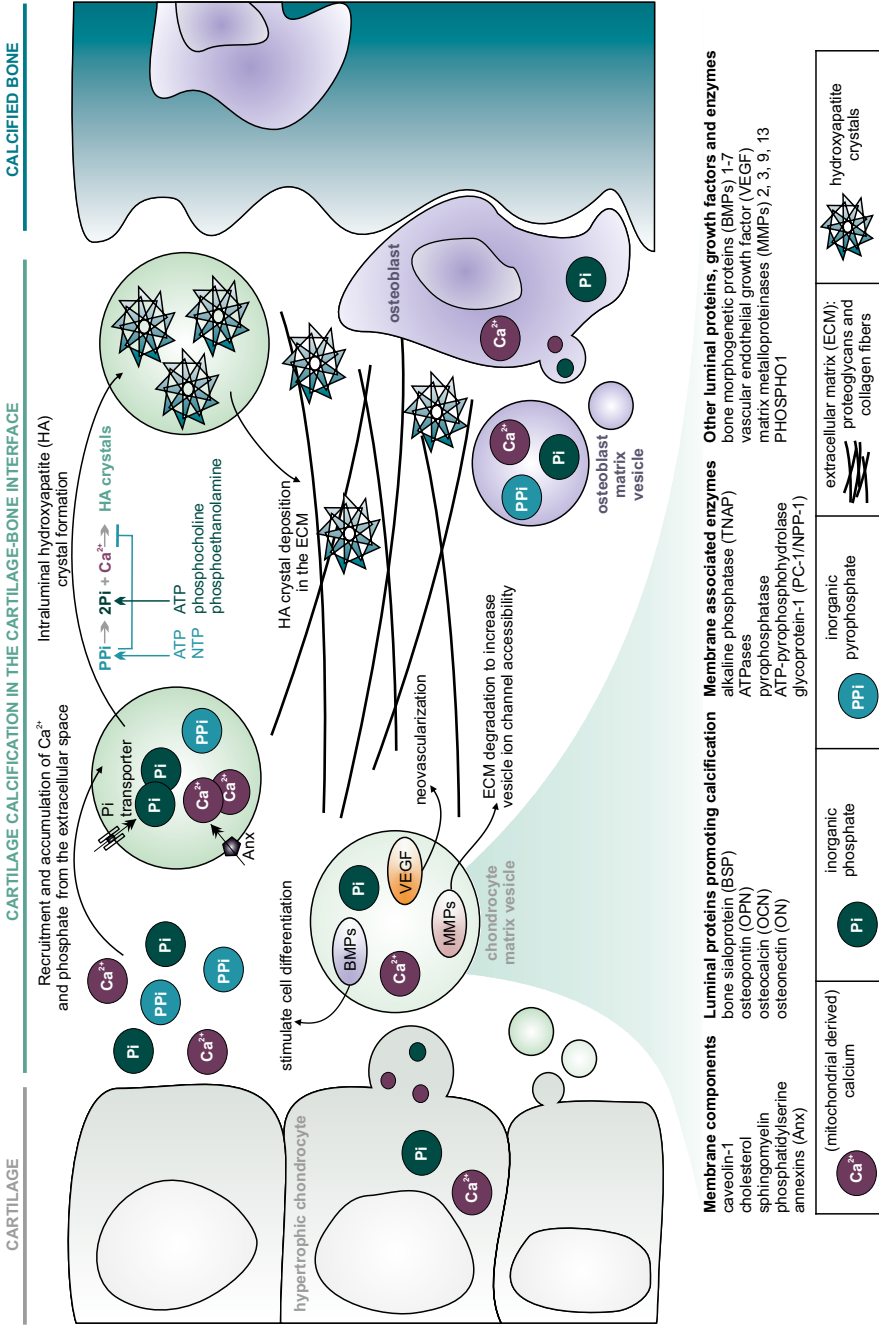collagen fibers

hydroxyapatite
crystals

1

Figure 2 Matrix vesicles start cartilage calcification during endochondral ossification. Vesicles originating from maturing (hypertrophic) chondrocytes and osteoblasts accumulate calcium and phosphate ions in their lumen for the formation of hydroxyapatite (HA) crystals. Deposition of HA crystals in the extracellular matrix (ECM), together with calcification promoting proteins, leads to complete transformation of cartilage into bone. It is hypothesised that other factors found in matrix vesicles, such as BMPs, VEGF, and MMPs, could be involved in chondrocyte and osteoblast differentiation, neovascularisation and ECM degradation, respectively [82,83].

The electrophoretic profile of matrix vesicles is characterised by mineralisation promoting enzymes (TNAP, ATPases, etc.) that hydrolyze adenosine triphosphate (ATP) and nucleoside triphosphate (NTP) into inorganic pyrophosphate (PP_i) and PP_i into inorganic phosphate (P_i), thereby increasing concentrations of P_i and decreasing concentrations of PP_i in the vesicle lumen and its surrounding matrix [73,84]. Keeping PP_i concentrations low at sites of active mineralisation is critical, since PP_i is the most important physiologic suppressor of hydroxyapatite crystal deposition [85]. To further increase the pool of P_i in the vesicle lumen, the enzyme PHOSPHO1 is suggested to hydrolyse luminal phosphoethanolamine and phosphocholine (derived from membrane phospholipids) in order to produce P_i [84,86,87]. Active phosphate transporters in the vesicle membrane facilitate further influx of P_i from the ECM [30].

and function [92,93]. It is, for example, known for Wnt signaling molecules that these are expressed on EVs derived from both Drosophila and human cells [94], indicating an evolutionary conserved process. The same holds true for Notch signaling. Notch modulates endochondral ossification [95], is required for articular cartilage and joint maintenance [96], and has been reported in multiple studies to be regulated in an EV-dependent manner [97,98]. The investigation of the role of these EVs during joint development is a new interesting avenue for joint biology research with potential benefits for regenerative medicine of the joint.

EVs IN JOINT DISEASES AND THERAPY

EVs in inflammatory joint diseases
Extracellular vesicles have first been isolated from SF two decades ago [57]. Much later, their increased concentration in SF from RA and OA patients [51] suggested a role in pathophysiological processes. Since then, EV-mediated communication in the joint has become a new field of interest, especially in relation to inflammatory joint disease [99-102].

In inflammatory SF, EVs have been detected that originated from synovial fibroblasts [103], platelets [56], erythrocytes [51], neutrophils [60], monocytes and T-cells [59,104,105]. Indeed, EVs can, as a result of inflammation, be produced by activated synoviocytes or by

infiltrating immune cells, which are a hallmark of joint inflammation. Alternatively, they can be derived from blood plasma of which SF is an ultra-filtrate. Finally, chondrocytes could also be a possible EV source, but chondrocyte-derived EVs have so far not been detected in SF.

Joint diseases are in most cases associated with (chronic) inflammation [9]. In addition to the high concentrations of cytokines, chemokines, catabolic enzymes and inflammatory mediators that can be measured in the SF [8], also EVs are present in substantial amounts in SF of patients with RA and OA [51,52,59]. Although the exact mode of action of EVs in inflammatory joint diseases has still to be elucidated, several general mechanisms that are related to inflammation have been suggested, such as the recognition of pathogen-derived EVs by immune cells, EV-mediated shuttling of inflammatory cytokines and lipid mediators, and the ability of EVs to carry proteolytic enzymes that cause tissue destruction and further propagation of inflammation [26,99]. Also, a role is claimed for EVs in autoimmune diseases such as RA [106]. Interestingly, whilst most studies so far have suggested a pro-inflammatory function for SF-derived EVs during joint disease, a recent study has suggested that neutrophil-derived EVs from RA SF have a protective phenotype [60]. Probably the most interesting and urgent question at this moment is which role EVs take in different types of joint inflammation and at different timings during the disease process.

Finally, the application of well-defined native EV subsets and the engineering of EVs and EV-inspired drug delivery systems is an emerging research field [101,102]. Within this light, EVs have, in addition to being therapeutic targets in some diseases, great potential to be used as therapeutic applications in others. Furthermore, the cargo-protective properties and regulated release of EVs during (patho)physiologic processes hold promise for a role as SF biomarkers [47].

Articular tissue regeneration: a role for EVs?

Cartilage and bone destruction in joint disorders is essentially irreversible and usually worsens progressively during the course of the disease. The lack of repair capacity of articular cartilage is notorious and has been signalled as early as the mid-1700s by William Hunter in his famous publication on cartilage structure and cartilage diseases [107]. This problem has not yet been solved and the quest for innovative strategies for cartilage repair is more intense than ever, driven by the societal and demographic developments alluded to earlier. An important development in this quest is the introduction of scaffolds constructed from biomaterials that serve as artificial matrix for the repair of (osteo)chondral defects [108]. Such scaffolds can be generated using 3-dimensional (3D)-bioprinting technology [109,110] and they can be seeded with a combination of cells and growth factors of interest [111]. Another development is the

1

use of fibrin matrixes containing chondrons and mesenchymal stem cells (MSCs), which currently shows promising results in a clinical trial of patients with cartilage defects [112,113].

The most difficult challenge is to regain normal joint homeostasis in order to facilitate proper healing of the tissue. To achieve this, the joint environment should be targeted as well, and here it is where EV-mediated therapies might be very effective. The high potential of exploiting EVs for articular tissue regeneration has already stimulated several groups to develop biodegradable EV-like microparticles (usually referred to as microspheres) for controlled delivery in the joint. For example, transforming growth factor beta-1 (TGFβ-1), bone morphogenetic protein 2 (BMP-2) and insulin-like growth factor 1 (IGF-1) have been incorporated successfully into microspheres [114].

Bioactive molecules, such as BMPs and several growth factors, have also been found as cargo transported in EVs [83,115]. For this reason, the use of nanovesicle-mediated delivery is expected to be more efficient than using the soluble form of the proteins, which are usually prone to fast degradation after injection. In addition, since several miRNAs can support chondrogenesis and decrease inflammation, and EVs may serve as protective vehicles against RNA degradation, incorporation of miRNAs into artificial vesicles is an interesting option to assist in regenerative strategies.

MSC-derived EVs

MSCs are seen as a promising cellular source in cartilage tissue engineering [116]. The supposed mechanism through paracrine signaling is supported by several studies showing that conditioned medium from MSCs alone [117,118], or even only the culture medium EV-fraction [119], is sufficient to induce beneficial effects to harmed tissue or to prevent tissue damage. This indicates that soluble biomolecules and possibly EVs are the main effectors in the MSC-driven regeneration cascade and not the capacity of these cells to differentiate into several lineages, as was thought for long.

Indeed, in other research fields it has been postulated that, in case of tissue injury, mRNA and miRNA laden EVs from local MSCs are able to induce dedifferentiation of the damaged tissue cells in order to re-enter the cell cycle and start the regeneration process, suggesting that EVs can genetically reprogram damaged cells by horizontal transfer of RNA [25,120]. The hypothesis that EVs could drive resting cells into re-entry of the cell cycle is of particular interest for chondrocytes as these cells are known to have a naturally low metabolism. Reprogramming inert chondrocytes at a site of cartilage injury, resulting in proliferation of cells and stimulation of matrix production, would be the ultimate goal of cartilage tissue regeneration for which EVs may hence

be suitable tools [121]. In 2016, the first studies on this topic have been performed and showed that MSC-derived EVs indeed were able to promote osteochondral regeneration *in vivo* [122] and cartilage regeneration *in vitro* [123].

In addition to MSCs, synovial membrane-derived cells with the pluripotent characteristics of MSCs can sometimes be detected in SF and their use for treatment of cartilage defects has already shown promising results [124-126]. Also, specific chondrogenic progenitor cells have been found in articular cartilage and are seen as a potentially good cell source for cartilage repair [127,128]. These cells are therefore interesting EV donors for treatment of cartilage damage. Although their natural low abundance in the joint may be not sufficient for endogenous repair of cartilage defects, *in vitro* expansion of these cells and collection of the EVs they produce would allow for intra-articular administration of high concentrations of biologically active EVs.

AIM AND OUTLINE OF THIS THESIS

Notwithstanding the descriptive investigations performed so far that have revealed the presence of EVs in SF, and a small number of elegant studies pointing out specific characteristics of EVs in human joint disease [51-68], the general knowledge on EVs in joint biology is still very limited. In this thesis, we aim at deepening our knowledge on EVs in healthy and diseased joints. This included improvement of isolation protocols that can be used as a standard, in order to perform reproducible in-depth studies of EVs in normal and pathologically altered joints (Figure 3). The horse was chosen as translational animal model, since this animal is both a clinical patient in its own right and a model for human joint disease [14]. With this approach, conclusions from this thesis can be applied in equine veterinary medicine and are highly likely to be relevant to human joint biology as well.

We started with developing and optimizing the urgently needed protocols for EV isolation from SF based on a literature overview of techniques used so far for this purpose (**Chapter 2**). This was done in samples from healthy adult horses, in order to achieve baseline measurements for EVs in normal joint homeostasis. **Chapter 3** investigates SF-derived EVs in a lipopolysaccharide (LPS)-induced model for transient synovitis. This well-described model [20] mimics acute arthritis and enabled us to adequately monitor EVs during a controlled process of inflammation. More detailed investigation of the lipid composition of SF EVs from this LPS-induced synovitis revealed the presence of so far unknown phosphatidylserine species. These new lipids are described in **Chapter 4**. Next, in the quest for identifying possible functions of EVs in the joint, SF derived EVs were investigated for their involvement in

early joint development (**Chapter 5**). This was based on the unique capacity of juvenile joints to orchestrate growth and to repair injuries effectively, such as for instance happens in osteochondrosis. These are all potentially EV-driven mechanisms. Finally, in **Chapter 6**, perspectives are sketched for the possible future use of specialised (biological or artificial) EVs to control joint inflammation and to repair injured articular tissues.
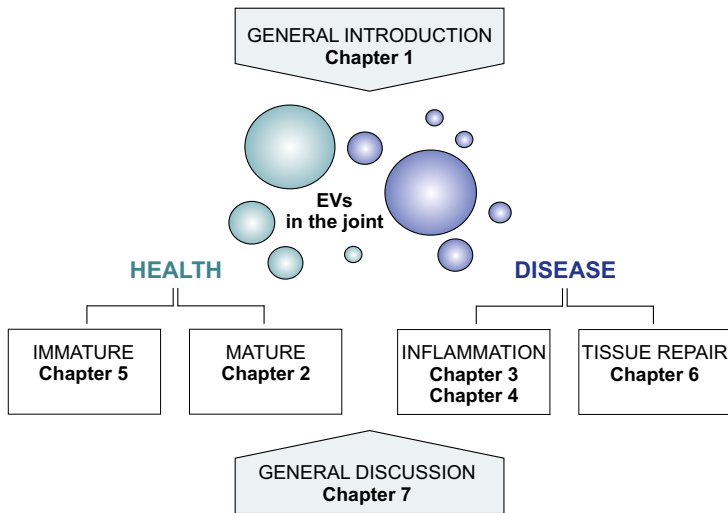

Figure 3 Thesis outline.

REFERENCES

1. Anderson, H. C. Electron microscopic studies of induced cartilage development and calcification. *J. Cell Biol.* **1967***, 35*, 81-101.

2. Bonucci, E. Fine structure of early cartilage calcification. *J. Ultrastruct. Res.* **1967***, 20*, 33-50.

3. Harding, C.; Heuser, J.; Stahl, P. Receptor-mediated endocytosis of transferrin and recycling of the transferrin receptor in rat reticulocytes. *J. Cell Biol.* **1983***, 97*, 329-339.

4. Pan, B. T.; Johnstone, R. M. Fate of the transferrin receptor during maturation of sheep reticulocytes in vitro: selective externalization of the receptor. *Cell* **1983***, 33*, 967-978.

5. Hoy, D. G.; Smith, E.; Cross, M.; Sanchez-Riera, L.; Blyth, F. M.; Buchbinder, R.; Woolf, A. D.; Driscoll, T.; Brooks, P.; March, L. M. Reflecting on the global burden of musculoskeletal conditions: lessons learnt from the global burden of disease 2010 study and the next steps forward. *Ann. Rheum. Dis.* **2015***, 74*, 4-7.

6. Cross, M.; Smith, E.; Hoy, D.; Nolte, S.; Ackerman, I.; Fransen, M.; Bridgett, L.; Williams, S.; Guillemin, F.; Hill, C. L.; Laslett, L. L.; Jones, G.; Cicuttini, F.; Osborne, R.; Vos, T.; Buchbinder, R.; Woolf, A.; March, L. The global burden of hip and knee osteoarthritis: estimates from the global burden of disease 2010 study. *Ann. Rheum. Dis.* **2014***, 73*, 1323-1330.

7. Cross, M.; Smith, E.; Hoy, D.; Carmona, L.; Wolfe, F.; Vos, T.; Williams, B.; Gabriel, S.; Lassere, M.; Johns, N.; Buchbinder, R.; Woolf, A.; March, L. The global burden of rheumatoid arthritis: estimates from the global burden of disease 2010 study. *Ann. Rheum. Dis.* **2014***, 73*, 1316-1322.

8. Rahmati, M.; Mobasheri, A.; Mozafari, M. Inflammatory mediators in osteoarthritis: A critical review of the state-of-the-art, current prospects, and future challenges. *Bone* **2016***, 85*, 81-90.

9. Attur, M. G.; Dave, M.; Akamatsu, M.; Katoh, M.; Amin, A. R. Osteoarthritis or osteoarthrosis: the definition of inflammation becomes a semantic issue in the genomic era of molecular medicine. *Osteoarthritis Cartilage* **2002***, 10*, 1-4.

10. McInnes, I. B.; Schett, G. The pathogenesis of rheumatoid arthritis. *N. Engl. J. Med.* **2011***, 365*, 2205-2219.

11. de Grauw, J. C. Molecular monitoring of equine joint homeostasis. *Vet. Q.* **2011***, 31*, 77-86.

12. Teeple, E.; Jay, G. D.; Elsaid, K. A.; Fleming, B. C. Animal models of osteoarthritis: challenges of model selection and analysis. *AAPS J.* **2013***, 15*, 438-446.

13. McIlwraith, C. W.; Frisbie, D. D.; Kawcak, C. E. The horse as a model of naturally occurring osteoarthritis. *Bone Joint Res.* **2012***, 1*, 297-309.

14. McIlwraith, C. W.; Fortier, L. A.; Frisbie, D. D.; Nixon, A. J. Equine Models of Articular Cartilage Repair. *Cartilage* **2011***, 2*, 317-326.

15. Malda, J.; Benders, K. E.; Klein, T. J.; de Grauw, J. C.; Kik, M. J.; Hutmacher, D. W.; Saris, D. B.; van Weeren, P. R.; Dhert, W. J. Comparative study of depth-dependent characteristics of equine and human osteochondral tissue from the medial and lateral femoral condyles. *Osteoarthritis Cartilage* **2012***, 20*, 1147-1151.

16. McCoy, A. M. Animal Models of Osteoarthritis: Comparisons and Key Considerations. *Vet. Pathol.* **2015***, 52*, 803-818.

17. de Grauw, J. C.; van de Lest, C. H.; Brama, P. A.; Rambags, B. P.; van Weeren, P. R. In vivo effects of meloxicam on inflammatory mediators, MMP activity and cartilage biomarkers in equine joints with acute synovitis. *Equine Vet. J.* **2009***, 41*, 693-699.

18. Ross, T. N.; Kisiday, J. D.; Hess, T.; McIlwraith, C. W. Evaluation of the inflammatory response in experimentally induced synovitis in the horse: a comparison of recombinant equine interleukin 1 beta and lipopolysaccharide. *Osteoarthritis Cartilage* **2012***, 20*, 1583-1590.

19. Palmer, J. L.; Bertone, A. L. Experimentally-induced synovitis as a model for acute synovitis in the horse. *Equine Vet. J.* **1994***, 26*, 492-495.

20. de Grauw, J. C.; van de Lest, C. H.; van Weeren, P. R. Inflammatory mediators and cartilage biomarkers in synovial fluid after a single inflammatory insult: a longitudinal experimental study. *Arthritis Res. Ther.* **2009***, 11*, R35.

21. Ateshian, G. A.; Mow, V. C. Friction, lubrication, and wear of articular cartilage and diarthrodial joints. In *Basic Orthopaedic Biomechanics and Mechano-Biology*; Mow, V. C., Huiskes, R., Eds.; Lippincott Williams & Wilkins: Philadelphia, 2005; pp 447-494.

22. Hui, A. Y.; McCarty, W. J.; Masuda, K.; Firestein, G. S.; Sah, R. L. A systems biology approach to synovial joint lubrication in health, injury, and disease. *Wiley Interdiscip. Rev. Syst. Biol. Med.* **2012***, 4*, 15-37.

23. Goldring, M. B.; Marcu, K. B. Cartilage homeostasis in health and rheumatic diseases. *Arthritis Res. Ther.* **2009***, 11*, 224.

24. Wojdasiewicz, P.; Poniatowski, L. A.; Szukiewicz, D. The role of inflammatory and anti-inflammatory cytokines in the pathogenesis of osteoarthritis. *Mediators Inflamm.* **2014***, 2014*, 561459.

25. Camussi, G.; Deregibus, M. C.; Bruno, S.;

1

Cantaluppi, V.; Biancone, L. Exosomes/microvesicles as a mechanism of cell-to-cell communication. *Kidney Int.* **2010***, 78*, 838-848.

26. Thery, C.; Ostrowski, M.; Segura, E. Membrane vesicles as conveyors of immune responses. *Nat. Rev. Immunol.* **2009***, 9*, 581-593.

27. Mulcahy, L. A.; Pink, R. C.; Carter, D. R. Routes and mechanisms of extracellular vesicle uptake. *J. Extracell Vesicles* **2014***, 3*, 10.3402/jev.v3.24641. eCollection 2014.

28. Yanez-Mo, M.; Siljander, P. R.; Andreu, Z.; Zavec, A. B.; Borras, F. E.; Buzas, E. I.; Buzas, K.; Casal, E.; Cappello, F.; Carvalho, J.; Colas, E.; Cordeiro-da Silva, A.; Fais, S.; Falcon-Perez, J. M.; Ghobrial, I. M.; Giebel, B.; Gimona, M.; Graner, M.; Gursel, I.; Gursel, M.; Heegaard, N. H.; Hendrix, A.; Kierulf, P.; Kokubun, K.; Kosanovic, M.; Kralj-Iglic, V.; Kramer-Albers, E. M.; Laitinen, S.; Lasser, C.; Lener, T.; Ligeti, E.; Line, A.; Lipps, G.; Llorente, A.; Lotvall, J.; Mancek-Keber, M.; Marcilla, A.; Mittelbrunn, M.; Nazarenko, I.; Nolte-'t Hoen, E. N.; Nyman, T. A.; O'Driscoll, L.; Olivan, M.; Oliveira, C.; Pallinger, E.; Del Portillo, H. A.; Reventos, J.; Rigau, M.; Rohde, E.; Sammar, M.; Sanchez-Madrid, F.; Santarem, N.; Schallmoser, K.; Ostenfeld, M. S.; Stoorvogel, W.; Stukelj, R.; Van der Grein, S. G.; Vasconcelos, M. H.; Wauben, M. H.; De Wever, O. Biological properties of extracellular vesicles and their physiological functions. *J. Extracell Vesicles* **2015***, 4*, 27066.

29. Thery, C.; Zitvogel, L.; Amigorena, S. Exosomes: composition, biogenesis and function. *Nat. Rev. Immunol.* **2002***, 2*, 569-579.

30. Solomon, D. H.; Browning, J. A.; Wilkins, R. J. Inorganic phosphate transport in matrix vesicles from bovine articular cartilage. *Acta Physiol. (Oxf)* **2007***, 190*, 119-125.

31. Brouwers, J. F.; Aalberts, M.; Jansen, J. W.; van Niel, G.; Wauben, M. H.; Stout, T. A.; Helms, J. B.; Stoorvogel, W. Distinct lipid compositions of two types of human prostasomes. *Proteomics* **2013***, 13*, 1660-1666.

32. Di Vizio, D.; Kim, J.; Hager, M. H.; Morello, M.; Yang, W.; Lafargue, C. J.; True, L. D.; Rubin, M. A.; Adam, R. M.; Beroukhim, R.; Demichelis, F.; Freeman, M. R. Oncosome formation in prostate cancer: association with a region of frequent chromosomal deletion in metastatic disease. *Cancer Res.* **2009***, 69*, 5601-5609.

33. Lotvall, J.; Hill, A. F.; Hochberg, F.; Buzas, E. I.; Di Vizio, D.; Gardiner, C.; Gho, Y. S.; Kurochkin, I. V.; Mathivanan, S.; Quesenberry, P.; Sahoo, S.; Tahara, H.; Wauben, M. H.; Witwer, K. W.; Thery, C. Minimal experimental requirements for definition of extracellular vesicles and their functions: a position statement from the International Society for Extracellular Vesicles. *J. Extracell Vesicles* **2014***, 3*, 26913.

34. Subra, C.; Grand, D.; Laulagnier, K.; Stella, A.; Lambeau, G.; Paillasse, M.; De Medina, P.; Monsarrat, B.; Perret, B.; Silvente-Poirot, S.; Poirot, M.; Record, M. Exosomes account for vesicle-mediated transcellular transport of activatable phospholipases and prostaglandins. *J. Lipid Res.* **2010***, 51*, 2105-2120.

35. Record, M.; Carayon, K.; Poirot, M.; Silven-te-Poirot, S. Exosomes as new vesicular lipid transporters involved in cell-cell communication and various pathophysiologies. *Biochim. Biophys. Acta* **2014***, 1841*, 108-120.

36. Valadi, H.; Ekstrom, K.; Bossios, A.; Sjostrand, M.; Lee, J. J.; Lotvall, J. O. Exosome-mediated transfer of mRNAs and microRNAs is a novel mechanism of genetic exchange between cells. *Nat. Cell Biol.* **2007***, 9*, 654-659.

37. Yoon, Y. J.; Kim, O. Y.; Gho, Y. S. Extracellular vesicles as emerging intercellular communicasomes. *BMB Rep.* **2014***, 47*, 531-539.

38. Subra, C.; Laulagnier, K.; Perret, B.; Record, M. Exosome lipidomics unravels lipid sorting at the level of multivesicular bodies. *Biochimie* **2007***, 89*, 205-212.

39. Llorente, A.; Skotland, T.; Sylvanne, T.; Kauhanen, D.; Rog, T.; Orlowski, A.; Vattulainen, I.; Ekroos, K.; Sandvig, K. Molecular lipidomics of exosomes released by PC-3 prostate cancer cells. *Biochim. Biophys. Acta* **2013***, 1831*, 1302-1309.

40. Kirsch, T.; Harrison, G.; Golub, E. E.; Nah, H. D. The roles of annexins and types II and X collagen in matrix vesicle-mediated mineralization of growth plate cartilage. *J. Biol. Chem.* **2000***, 275*, 35577-35583.

41. De Toro, J.; Herschlik, L.; Waldner, C.; Mongini, C. Emerging roles of exosomes in normal and pathological conditions: new insights for diagnosis and therapeutic applications. *Front. Immunol.* **2015***, 6*, 203.

42. Nolte-'t Hoen, E. N.; Wauben, M. H. Immune cell-derived vesicles: modulators and mediators of inflammation. *Curr. Pharm. Des.* **2012***, 18*, 2357-2368.

43. van der Vlist, E. J.; Arkesteijn, G. J.; van de Lest, C. H.; Stoorvogel, W.; Nolte-'t Hoen, E. N.; Wauben, M. H. CD4(+) T cell activation promotes the differential release of distinct populations of nanosized vesicles. *J. Extracell Vesicles* **2012***, 1*, 10.3402/jev.v1i0.18364. eCollection 2012.

44. Kim, J. H.; Lee, J.; Park, J.; Gho, Y. S. Gram-negative and Gram-positive bacterial extracellular vesicles. *Semin. Cell Dev. Biol.* **2015***, 40*, 97-104.

45. Szempruch, A. J.; Dennison, L.; Kieft, R.; Harrington, J. M.; Hajduk, S. L. Sending a message: extracellular vesicles of pathogenic protozoan parasites. *Nat. Rev. Microbiol.* **2016***, 14*, 669-675.

46. Alvarez-Erviti, L.; Seow, Y.; Yin, H.; Betts, C.; Lakhal, S.; Wood, M. J. Delivery of siRNA to the mouse brain by systemic injection of targeted exosomes. *Nat. Biotechnol.* **2011***, 29*, 341-345.

47. Boukouris, S.; Mathivanan, S. Exosomes in bodily fluids are a highly stable resource of disease biomarkers. *Proteomics Clin. Appl.* **2015***, 9*, 358-367.

48. Verma, M.; Lam, T. K.; Hebert, E.; Divi, R. L. Extracellular vesicles: potential applications in cancer diagnosis, prognosis, and epidemiology. *BMC Clin. Pathol.* **2015***, 15*, 6-015-0005-5. eCollection 2015.

49. Gamez-Valero, A.; Lozano-Ramos, S. I.; Bancu, I.; Lauzurica-Valdemoros, R.; Borras, F. E. Urinary extracellular vesicles as source of biomarkers in kidney diseases. *Front. Immunol.* **2015***, 6*, 6.

50. Levick, J. R.; McDonald, J. N. Ultrastructure of transport pathways in stressed synovium of the knee in anaesthetized rabbits. *J. Physiol.* **1989***, 419*, 493-508.

51. Berckmans, R. J.; Nieuwland, R.; Tak, P. P.; Boing, A. N.; Romijn, F. P.; Kraan, M. C.; Breedveld, F. C.; Hack, C. E.; Sturk, A. Cell-derived microparticles in synovial fluid from inflamed arthritic joints support coagulation exclusively via a factor VII-dependent mechanism. *Arthritis Rheum.* **2002***, 46*, 2857-2866.

52. Berckmans, R. J.; Nieuwland, R.; Kraan, M. C.; Schaap, M. C.; Pots, D.; Smeets, T. J.; Sturk, A.; Tak, P. P. Synovial microparticles from arthritic patients modulate chemokine and cytokine release by synoviocytes. *Arthritis Res. Ther.* **2005***, 7*, R536-44.

53. Biro, E.; Nieuwland, R.; Tak, P. P.; Pronk, L. M.; Schaap, M. C.; Sturk, A.; Hack, C. E. Activated complement components and complement activator molecules on the surface of cell-derived microparticles in patients with rheumatoid arthritis and healthy individuals. *Ann. Rheum. Dis.* **2007***, 66*, 1085-1092.

54. Boilard, E.; Nigrovic, P. A.; Larabee, K.; Watts, G. F.; Coblyn, J. S.; Weinblatt, M. E.; Massarotti, E. M.; Remold-O'Donnell, E.; Farndale, R. W.; Ware, J.; Lee, D. M. Platelets amplify inflammation in arthritis via collagen-dependent microparticle production. *Science* **2010***, 327*, 580-583.

55. Cloutier, N.; Tan, S.; Boudreau, L. H.; Cramb, C.; Subbaiah, R.; Lahey, L.; Albert, A.; Shnayder, R.; Gobezie, R.; Nigrovic, P. A.; Farndale, R. W.; Robinson, W. H.; Brisson, A.; Lee, D. M.; Boilard, E. The exposure of autoantigens by microparticles underlies the formation of potent inflammatory components: the microparticle-associated immune complexes. *EMBO Mol. Med.* **2013***, 5*, 235-249.

56. Duchez, A. C.; Boudreau, L. H.; Naika, G. S.; Bollinger, J.; Belleannee, C.; Cloutier, N.; Laffont, B.; Mendoza-Villarroel, R. E.; Levesque, T.; Rollet-Labelle, E.; Rousseau, M.; Allaeys, I.; Tremblay, J. J.; Poubelle, P. E.; Lambeau, G.; Pouliot, M.; Provost, P.; Soulet, D.; Gelb, M. H.; Boilard, E. Platelet microparticles are internalized in neutrophils via the concerted activity of 12-lipoxygenase and secreted phospholipase A2-IIA. *Proc. Natl. Acad. Sci. U. S. A.* **2015***, 112*, E3564-73.

57. Fourcade, O.; Simon, M. F.; Viode, C.; Rugani, N.; Leballe, F.; Ragab, A.; Fournie, B.; Sarda, L.; Chap, H. Secretory phospholipase A2 generates the novel lipid mediator lysophosphatidic acid in membrane microvesicles shed from activated cells. *Cell* **1995***, 80*, 919-927.

58. Gyorgy, B.; Modos, K.; Pallinger, E.; Paloczi, K.; Pasztoi, M.; Misjak, P.; Deli, M. A.; Sipos, A.; Szalai, A.; Voszka, I.; Polgar, A.; Toth, K.; Csete, M.; Nagy, G.; Gay, S.; Falus, A.; Kittel, A.; Buzas, E. I. Detection and isolation of cell-derived microparticles are compromised by protein complexes resulting from shared biophysical parameters. *Blood* **2011***, 117*, e39-48.

59. Gyorgy, B.; Szabo, T. G.; Turiak, L.; Wright, M.; Herczeg, P.; Ledeczi, Z.; Kittel, A.; Polgar, A.; Toth, K.; Derfalvi, B.; Zelenak, G.; Borocz, I.; Carr, B.; Nagy, G.; Vekey, K.; Gay, S.; Falus, A.; Buzas, E. I. Improved flow cytometric assessment reveals distinct microvesicle (cell-derived microparticle) signatures in joint diseases. *PLoS One* **2012***, 7*, e49726.

60. Headland, S. E.; Jones, H. R.; Norling, L. V.; Kim, A.; Souza, P. R.; Corsiero, E.; Gil, C. D.; Nerviani, A.; Dell'Accio, F.; Pitzalis, C.; Oliani, S. M.; Jan, L. Y.; Perretti, M. Neutrophil-derived microvesicles enter cartilage and protect the joint in inflammatory arthritis. *Sci. Transl. Med.* **2015***, 7*, 315ra190.

61. Junkar, I.; Sustar, V.; Frank, M.; Jansa, V.; Zavec, A.; Rozman, B.; Mozetic, M.; Hagerstrand, H.; Kralj-Iglic, V. Blood and synovial microparticles as revealed by atomic force and scanning electron microscope. *The Open Autoimmunity Journal* **2009***, 1*, 50-58.

62. Martinez-Lorenzo, M. J.; Anel, A.; Saez-Gutierrez, B.; Royo-Canas, M.; Bosque, A.; Alava, M. A.; Pineiro, A.; Lasierra, P.; Asin-Ungria, J.; Larrad, L. Rheumatoid synovial fluid T cells are sensitive to APO2L/TRAIL. *Clin. Immunol.* **2007***, 122*, 28-40.

63. Matei, C. I.; Boulocher, C.; Boule, C.; Schramme, M.; Viguier, E.; Roger, T.; Berthier, Y.; Trunfio-Sfarghiu, A. M.; Blanchin, M. G. Ultrastructural analysis of healthy synovial fluids in three mammalian species. *Microsc. Microanal.* **2014**, *20*, 903-911.

64. Messer, L.; Alsaleh, G.; Freyssinet, J.; Zobairi, F.; Leray, I.; Gottenberg, J.; Sibilia, J.; Toti-Orfanoudakis, F.; Wachsmann, D. Microparticle-induced release of B-lymphocyte regulators by rheumatoid synoviocytes. *Arthritis Research & Therapy* **2009**, *11*, R40.

65. Pasztoi, M.; Sodar, B.; Misjak, P.; Paloczi, K.; Kittel, A.; Toth, K.; Wellinger, K.; Geher, P.; Nagy, G.; Lakatos, T.; Falus, A.; Buzas, E. I. The recently identified hexosaminidase D enzyme substantially contributes to the elevated hexosaminidase activity in rheumatoid arthritis. *Immunol. Lett.* **2013**, *149*, 71-76.

66. Skriner, K.; Adolph, K.; Jungblut, P. R.; Burmester, G. R. Association of citrullinated proteins with synovial exosomes. *Arthritis Rheum.* **2006**, *54*, 3809-3814.

67. Mustonen, A. M.; Nieminen, P.; Joukainen, A.; Jaroma, A.; Kaariainen, T.; Kroger, H.; Lazaro-Ibanez, E.; Siljander, P. R.; Karja, V.; Harkonen, K.; Koistinen, A.; Rilla, K. First in vivo detection and characterization of hyaluronan-coated extracellular vesicles in human synovial fluid. *J. Orthop. Res.* **2016**, *34*, 1960-1968.

68. Reich, N.; Beyer, C.; Gelse, K.; Akhmetshina, A.; Dees, C.; Zwerina, J.; Schett, G.; Distler, O.; Distler, J. H. Microparticles stimulate angiogenesis by inducing ELR(+) CXC-chemokines in synovial fibroblasts. *J. Cell. Mol. Med.* **2011**, *15*, 756-762.

69. Dahl, L. B.; Dahl, I. M.; Engstrom-Laurent, A.; Granath, K. Concentration and molecular weight of sodium hyaluronate in synovial fluid from patients with rheumatoid arthritis and other arthropathies. *Ann. Rheum. Dis.* **1985**, *44*, 817-822.

70. Anderson, H. C. Vesicles associated with calcification in the matrix of epiphyseal cartilage. *J. Cell Biol.* **1969**, *41*, 59-72.

71. Hessle, L.; Johnson, K. A.; Anderson, H. C.; Narisawa, S.; Sali, A.; Goding, J. W.; Terkeltaub, R.; Millan, J. L. Tissue-nonspecific alkaline phosphatase and plasma cell membrane glycoprotein-1 are central antagonistic regulators of bone mineralization. *Proc. Natl. Acad. Sci. U. S. A.* **2002**, *99*, 9445-9449.

72. Anderson, H. C. Matrix vesicles and calcification. *Curr. Rheumatol. Rep.* **2003**, *5*, 222-226.

73. Anderson, H. C. Molecular biology of matrix vesicles. *Clin. Orthop. Relat. Res.* **1995**, *(314)*, 266-280.

74. Ali, S. Y.; Sajdera, S. W.; Anderson, H. C. Isolation and characterization of calcifying matrix vesicles from epiphyseal cartilage. *Proc. Natl. Acad. Sci. U. S. A.* **1970**, *67*, 1513-1520.

75. Thouverey, C.; Strzelecka-Kiliszek, A.; Balcerzak, M.; Buchet, R.; Pikula, S. Matrix vesicles originate from apical membrane microvilli of mineralizing osteoblast-like Saos-2 cells. *J. Cell. Biochem.* **2009**, *106*, 127-138.

76. Boyan, B. D.; Wong, K. L.; Fang, M.; Schwartz, Z. 1alpha,25(OH)2D3 is an autocrine regulator of extracellular matrix turnover and growth factor release via ERp60 activated matrix vesicle metalloproteinases. *J. Steroid Biochem. Mol. Biol.* **2007**, *103*, 467-472.

77. D'Angelo, M.; Billings, P. C.; Pacifici, M.; Leboy, P. S.; Kirsch, T. Authentic matrix vesicles contain active metalloproteases (MMP). a role for matrix vesicle-associated MMP-13 in activation of transforming growth factor-beta. *J. Biol. Chem.* **2001**, *276*, 11347-11353.

78. Dean, D. D.; Schwartz, Z.; Muniz, O. E.; Gomez, R.; Swain, L. D.; Howell, D. S.; Boyan, B. D. Matrix vesicles are enriched in metalloproteinases that degrade proteoglycans. *Calcif. Tissue Int.* **1992**, *50*, 342-349.

79. Iannotti, J. P.; Naidu, S.; Noguchi, Y.; Hunt, R. M.; Brighton, C. T. Growth plate matrix vesicle biogenesis. The role of intracellular calcium. *Clin. Orthop. Relat. Res.* **1994**, *(306)*, 222-229.

80. Roach, H. I.; Clarke, N. M. Physiological cell death of chondrocytes in vivo is not confined to apoptosis. New observations on the mammalian growth plate. *J. Bone Joint Surg. Br.* **2000**, *82*, 601-613.

81. Morhayim, J.; Baroncelli, M.; van Leeuwen, J. P. Extracellular vesicles: Specialized bone messengers. *Arch. Biochem. Biophys.* **2014**.

82. Cui, L.; Houston, D. A.; Farquharson, C.; MacRae, V. E. Characterisation of matrix vesicles in skeletal and soft tissue mineralisation. *Bone* **2016**, *87*, 147-158.

83. Nahar, N. N.; Missana, L. R.; Garimella, R.; Tague, S. E.; Anderson, H. C. Matrix vesicles are carriers of bone morphogenetic proteins (BMPs), vascular endothelial growth factor (VEGF), and noncollagenous matrix proteins. *J. Bone Miner. Metab.* **2008**, *26*, 514-519.

84. Stewart, A. J.; Roberts, S. J.; Seawright, E.; Davey, M. G.; Fleming, R. H.; Farquharson, C. The presence of PHOSPHO1 in matrix vesicles and its developmental expression prior to skeletal mineralization. *Bone* **2006**, *39*, 1000-1007.

85. Johnson, K. A.; Hessle, L.; Vaingankar, S.; Wennberg, C.; Mauro, S.; Narisawa, S.; Goding, J.

W.; Sano, K.; Millan, J. L.; Terkeltaub, R. Osteoblast tissue-nonspecific alkaline phosphatase antagonizes and regulates PC-1. *Am. J. Physiol. Regul. Integr. Comp. Physiol.* **2000***, 279*, R1365-77.

86. Roberts, S.; Narisawa, S.; Harmey, D.; Millan, J. L.; Farquharson, C. Functional involvement of PHOSPHO1 in matrix vesicle-mediated skeletal mineralization. *J. Bone Miner. Res.* **2007***, 22*, 617-627.

87. Roberts, S. J.; Stewart, A. J.; Sadler, P. J.; Farquharson, C. Human PHOSPHO1 exhibits high specific phosphoethanolamine and phosphocholine phosphatase activities. *Biochem. J.* **2004***, 382*, 59-65.

88. Lefebvre, V.; Bhattaram, P. Vertebrate skeleto-genesis. *Curr. Top. Dev. Biol.* **2010***, 90*, 291-317.

89. Colnot, C. Cellular and molecular interactions regulating skeletogenesis. *J. Cell. Biochem.* **2005***, 95*, 688-697.

90. Kobayashi, T.; Lyons, K. M.; McMahon, A. P.; Kronenberg, H. M. BMP signaling stimulates cellular differentiation at multiple steps during cartilage development. *Proc. Natl. Acad. Sci. U. S. A.* **2005***, 102*, 18023-18027.

91. Mackie, E. J.; Ahmed, Y. A.; Tatarczuch, L.; Chen, K. -.; Mirams, M. Endochondral ossification: How cartilage is converted into bone in the developing skeleton. *Int. J. Biochem. Cell Biol.* **2008***, 40*, 46-62.

92. Corrigan, L.; Redhai, S.; Leiblich, A.; Fan, S. J.; Perera, S. M.; Patel, R.; Gandy, C.; Wainwright, S. M.; Morris, J. F.; Hamdy, F.; Goberdhan, D. C.; Wilson, C. BMP-regulated exosomes from Drosophila male reproductive glands reprogram female behavior. *J. Cell Biol.* **2014***, 206*, 671-688.

93. Wendler, F.; Bota-Rabassedas, N.; Franch-Marro, X. Cancer becomes wasteful: emerging roles of exo-somes(dagger) in cell-fate determination. *J. Extracell Vesicles* **2013***, 2*, 10.3402/jev.v2i0.22390.

94. Gross, J. C.; Chaudhary, V.; Bartscherer, K.; Boutros, M. Active Wnt proteins are secreted on exosomes. *Nat. Cell Biol.* **2012***, 14*, 1036-1045.

95. Hosaka, Y.; Saito, T.; Sugita, S.; Hikata, T.; Kobayashi, H.; Fukai, A.; Taniguchi, Y.; Hirata, M.; Akiyama, H.; Chung, U. I.; Kawaguchi, H. Notch signaling in chondrocytes modulates endochondral ossification and osteoarthritis development. *Proc. Natl. Acad. Sci. U. S. A.* **2013***, 110*, 1875-1880.

96. Mirando, A. J.; Liu, Z.; Moore, T.; Lang, A.; Kohn, A.; Osinski, A. M.; O'Keefe, R. J.; Mooney, R. A.; Zuscik, M. J.; Hilton, M. J. RBP-Jkappa-dependent Notch signaling is required for murine articular cartilage and joint maintenance. *Arthritis Rheum.* **2013***, 65*, 2623-2633.

97. Ristorcelli, E.; Beraud, E.; Mathieu, S.; Lombardo, D.; Verine, A. Essential role of Notch signaling in apoptosis of human pancreatic tumoral cells mediated by exosomal nanoparticles. *Int. J. Cancer* **2009***, 125*, 1016-1026.

98. Sheldon, H.; Heikamp, E.; Turley, H.; Dragovic, R.; Thomas, P.; Oon, C. E.; Leek, R.; Edelmann, M.; Kessler, B.; Sainson, R. C.; Sargent, I.; Li, J. L.; Harris, A. L. New mechanism for Notch signaling to endothelium at a distance by Delta-like 4 incorporation into exosomes. *Blood* **2010***, 116*, 2385-2394.

99. Buzas, E. I.; Gyorgy, B.; Nagy, G.; Falus, A.; Gay, S. Emerging role of extracellular vesicles in inflammatory diseases. *Nat. Rev. Rheumatol.* **2014***, 10*, 356-364.

100. Distler, J. H.; Pisetsky, D. S.; Huber, L. C.; Kalden, J. R.; Gay, S.; Distler, O. Microparticles as regulators of inflammation: novel players of cellular crosstalk in the rheumatic diseases. *Arthritis Rheum.* **2005***, 52*, 3337-3348.

101. Cosenza, S.; Ruiz, M.; Maumus, M.; Jorgensen, C.; Noel, D. Pathogenic or Therapeutic Extracellular Vesicles in Rheumatic Diseases: Role of Mesenchymal Stem Cell-Derived Vesicles. *Int. J. Mol. Sci.* **2017***, 18*, 10.3390/ijms18040889.

102. Kim, I. K.; Kim, S. H.; Choi, S. M.; Youn, B. S.; Kim, H. S. Extracellular Vesicles as Drug Delivery Vehicles for Rheumatoid Arthritis. *Curr. Stem Cell. Res. Ther.* **2016***, 11*, 329-342.

103. Kato, T.; Miyaki, S.; Ishitobi, H.; Nakamura, Y.; Nakasa, T.; Lotz, M. K.; Ochi, M. Exosomes from IL-1beta stimulated synovial fibroblasts induce osteoarthritic changes in articular chondrocytes. *Arthritis Res. Ther.* **2014***, 16*, R163.

104. Jungel, A.; Distler, O.; Schulze-Horsel, U.; Huber, L. C.; Ha, H. R.; Simmen, B.; Kalden, J. R.; Pisetsky, D. S.; Gay, S.; Distler, J. H. Microparticles stimulate the synthesis of prostaglandin E(2) via induction of cyclooxygenase 2 and microsomal prostaglandin E synthase 1. *Arthritis Rheum.* **2007***, 56*, 3564-3574.

105. Distler, J. H.; Jungel, A.; Huber, L. C.; Seemayer, C. A.; Reich, C. F.,3rd; Gay, R. E.; Michel, B. A.; Fontana, A.; Gay, S.; Pisetsky, D. S.; Distler, O. The induction of matrix metalloproteinase and cytokine expression in synovial fibroblasts stimulated with immune cell microparticles. *Proc. Natl. Acad. Sci. U. S. A.* **2005***, 102*, 2892-2897.

106. Turpin, D.; Truchetet, M. E.; Faustin, B.; Augusto, J. F.; Contin-Bordes, C.; Brisson, A.; Blanco, P.; Duffau, P. Role of extracellular vesicles in autoimmune diseases. *Autoimmun. Rev.* **2016***, 15*, 174-183.

107. Hunter, W. Of the structure and disease of articular cartilages. *Phil. Trans.* **1742**, 514-521.

108. Smith, B. D.; Grande, D. A. The current state of scaffolds for musculoskeletal regenerative applications. *Nat. Rev. Rheumatol.* **2015**, *11*, 213-222.

109. Malda, J.; Visser, J.; Melchels, F. P.; Jungst, T.; Hennink, W. E.; Dhert, W. J.; Groll, J.; Hutmacher, D. W. 25th anniversary article: Engineering hydrogels for biofabrication. *Adv Mater* **2013**, *25*, 5011-5028.

110. Visser, J.; Peters, B.; Burger, T. J.; Boomstra, J.; Dhert, W. J.; Melchels, F. P.; Malda, J. Biofabrication of multi-material anatomically shaped tissue constructs. *Biofabrication* **2013**, *5*, 035007-5082/5/3/035007. Epub 2013 Jul 2.

111. Makris, E. A.; Gomoll, A. H.; Malizos, K. N.; Hu, J. C.; Athanasiou, K. A. Repair and tissue engineering techniques for articular cartilage. *Nat. Rev. Rheumatol.* **2014**.

112. US National Library of Medicine. IMPACT: Safety and feasibility of a single-stage procedure for focal cartilage lesions of the knee. https://clinicaltrials.gov/ct2/show/NCT02037204. **2014**.

113. de Windt, T. S.; Vonk, L. A.; Slaper-Cortenbach, I. C.; van den Broek, M. P.; Nizak, R.; van Rijen, M. H.; de Weger, R. A.; Dhert, W. J.; Saris, D. B. Allogeneic Mesenchymal Stem Cells Stimulate Cartilage Regeneration and Are Safe for Single-Stage Cartilage Repair in Humans upon Mixture with Recycled Autologous Chondrons. *Stem Cells* **2016**.

114. Lam, J.; Lu, S.; Kasper, F. K.; Mikos, A. G. Strategies for controlled delivery of biologics for cartilage repair. *Adv. Drug Deliv. Rev.* **2015**, *84*, 123-134.

115. Proia, P.; Schiera, G.; Mineo, M.; Ingrassia, A. M.; Santoro, G.; Savettieri, G.; Di Liegro, I. Astrocytes shed extracellular vesicles that contain fibroblast growth factor-2 and vascular endothelial growth factor. *Int. J. Mol. Med.* **2008**, *21*, 63-67.

116. Savkovic, V.; Li, H.; Seon, J. K.; Hacker, M.; Franz, S.; Simon, J. C. Mesenchymal stem cells in cartilage regeneration. *Curr. Stem Cell. Res. Ther.* **2014**, *9*, 469-488.

117. Gnecchi, M.; He, H.; Liang, O. D.; Melo, L. G.; Morello, F.; Mu, H.; Noiseux, N.; Zhang, L.; Pratt, R. E.; Ingwall, J. S.; Dzau, V. J. Paracrine action accounts for marked protection of ischemic heart by Akt-modified mesenchymal stem cells. *Nat. Med.* **2005**, *11*, 367-368.

118. van Buul, G. M.; Villafuertes, E.; Bos, P. K.; Waarsing, J. H.; Kops, N.; Narcisi, R.; Weinans, H.; Verhaar, J. A.; Bernsen, M. R.; van Osch, G. J. Mesenchymal stem cells secrete factors that inhibit inflammatory processes in short-term osteoarthritic synovium and cartilage explant culture. *Osteoarthritis Cartilage* **2012**, *20*, 1186-1196.

119. Lai, R. C.; Arslan, F.; Lee, M. M.; Sze, N. S.; Choo, A.; Chen, T. S.; Salto-Tellez, M.; Timmers, L.; Lee, C. N.; El Oakley, R. M.; Pasterkamp, G.; de Kleijn, D. P.; Lim, S. K. Exosome secreted by MSC reduces myocardial ischemia/reperfusion injury. *Stem Cell. Res.* **2010**, *4*, 214-222.

120. Bruno, S.; Grange, C.; Deregibus, M. C.; Calogero, R. A.; Saviozzi, S.; Collino, F.; Morando, L.; Busca, A.; Falda, M.; Bussolati, B.; Tetta, C.; Camussi, G. Mesenchymal stem cell-derived microvesicles protect against acute tubular injury. *J. Am. Soc. Nephrol.* **2009**, *20*, 1053-1067.

121. Toh, W. S.; Lai, R. C.; Hui, J. H.; Lim, S. K. MSC exosome as a cell-free MSC therapy for cartilage regeneration: Implications for osteoarthritis treatment. *Semin. Cell Dev. Biol.* **2016**.

122. Zhang, S.; Chu, W. C.; Lai, R. C.; Lim, S. K.; Hui, J. H.; Toh, W. S. Exosomes derived from human embryonic mesenchymal stem cells promote osteochondral regeneration. *Osteoarthritis Cartilage* **2016**, *24*, 2135-2140.

123. Vonk, L. A.; van Dooremalen, S.; Coffer, P. J.; Saris, D. B.; Lorenowicz, M. J. MSC-derived extracellular vesicles stimulate cartilage regeneration and modulate inflammatory responses. Paper presented at the 13th world congress of the International Cartilage Repair Society, Sept 26, 2016, Sorrento, Italy. **2016**.

124. Gullo, F.; De Bari, C. Prospective purification of a subpopulation of human synovial mesenchymal stem cells with enhanced chondro-osteogenic potency. *Rheumatology (Oxford)* **2013**, *52*, 1758-1768.

125. Lee, J. C.; Min, H. J.; Park, H. J.; Lee, S.; Seong, S. C.; Lee, M. C. Synovial membrane-derived mesenchymal stem cells supported by platelet-rich plasma can repair osteochondral defects in a rabbit model. *Arthroscopy* **2013**, *29*, 1034-1046.

126. Murata, D.; Miyakoshi, D.; Hatazoe, T.; Miura, N.; Tokunaga, S.; Fujiki, M.; Nakayama, K.; Misumi, K. Multipotency of equine mesenchymal stem cells derived from synovial fluid. *Vet. J.* **2014**, *202*, 53-61.

127. Jiang, Y.; Tuan, R. S. Origin and function of cartilage stem/progenitor cells in osteoarthritis. *Nat. Rev. Rheumatol.* **2015**, *11*, 206-212.

128. McCarthy, H. E.; Bara, J. J.; Brakspear, K.; Singhrao, S. K.; Archer, C. W. The comparison of equine articular cartilage progenitor cells and bone marrow-derived stromal cells as potential cell sources for cartilage repair in the horse. *Vet. J.* **2012**, *192*, 345-351.

2

Synovial fluid pre-treatment with hyaluronidase facilitates isolation of CD44+ extracellular vesicles

Janneke Boere [a]
Chris H. A. van de Lest [a,b]
Sten F. W. M. Libregts [b]
Ger J. A. Arkesteijn [b,c]
Willie J. C. Geerts [d]
Esther N. M. Nolte-'t Hoen [b]
Jos Malda [a,e]
P. René van Weeren [a]
Marca H. M. Wauben [b]

Departments of Equine Sciences[a], Biochemistry & Cell Biology[b], and Infectious Diseases and Immunology[c] of Faculty of Veterinary Medicine, Utrecht University, Utrecht, the Netherlands; Department of Cryo-Electron Microscopy[d], Bijvoet Center for Biomolecular Research, Utrecht, the Netherlands; Department of Orthopaedics[e], University Medical Center Utrecht, Utrecht, the Netherlands

ABSTRACT

Extracellular vesicles (EVs) in synovial fluid (SF) are gaining increased recognition as important factors in joint homeostasis, joint regeneration, and as biomarkers of joint disease. A limited number of studies have investigated EVs in SF samples of patients with joint disease, but knowledge on the role of EVs in healthy joints is lacking. In addition, no standardised protocol is available for isolation of EVs from SF. Based on the high viscosity of SF caused by high concentrations of hyaluronic acid (HA) – a prominent extracellular matrix component – it was hypothesised that EV recovery could be optimised by pre-treatment with hyaluronidase (HYase). Therefore, the efficiency of EV isolation from healthy equine SF samples was tested by performing sequential ultracentrifugation steps (10,000g, 100,000g and 200,000g) in the presence or absence of HYase. Quantitative EV analysis using high-resolution flow cytometry showed an efficient recovery of EVs after 100,000g ultracentrifugation, with an increased yield of CD44+ EVs when SF samples were pre-treated with HYase. Morphological analysis of SF-derived EVs with cryo-transmission-electron microscopy did not indicate damage by high-speed ultracentrifugation and revealed that most EVs are spherical with a diameter of 20-200 nm. Further protein characterisation by Western blotting revealed that healthy SF-derived EVs contain CD9, Annexin-1, and CD90/Thy1.1. Taken together, these data suggest that EV isolation protocols for body fluids that contain relatively high amounts of HA, such as SF, could benefit from treatment of the fluid with HYase prior to ultracentrifugation. This method facilitates recovery and detection of CD44+ EVs within the HA-rich extracellular matrix. Furthermore, based on the findings presented here, it is recommended to sediment SF-derived EVs with at least 100,000g for optimal EV recovery.

INTRODUCTION

Lately there has been an increased recognition of the role of extracellular vesicles (EVs) in joint regeneration and joint disease, and suggestions have been made for EV-based clinical applications [1]. In this context, EVs derived from synovial fluid (SF) are currently being investigated to unravel their role in these processes and their biomarker potential for joint disease. Several studies have examined EVs isolated from SF [2-19]. In most of these studies EVs have only been isolated from human SF obtained from inflamed joints. The fact that studies did not include samples from healthy controls is mainly because of ethical constraints concerning joint puncture in healthy subjects and the resulting low availability of healthy samples from the clinic. However, in order to fully understand the role of EV-driven (patho)physiological processes in joints, knowledge about EVs in healthy joints is of utmost importance. Animal studies can ultimately give answers, but small animal models (rodents) do not provide sufficient volumes of SF for EV isolation, nor are their joints representative for the human situation in a biomechanical sense. The horse, on the contrary, is a well-suited species for obtaining large volumes of healthy SF. Furthermore, equine and human joints show great similarities [20] and the horse is an acknowledged animal model for human joint disease [21,22].

Since all body fluids have their own characteristic composition, EV isolation protocols need to be tailored for each specific fluid [23-25]. Synovial fluid, especially if derived from healthy joints, is very viscous due to high concentrations of high-molecular-weight hyaluronic acid (HA), also known as *hyaluronan* [26,27]. Although some previous studies included hyaluronidase (HYase) treatment of SF prior to EV isolation [10,11], the effect of HYase treatment on EV recovery has not been investigated in detail. In fact, an optimised protocol for EV recovery from SF is lacking and documented protocols for EV isolation and analysis differ widely and are often incomplete.

In the current study, the recovery of EV subsets from healthy equine joint-derived SF was analysed using different centrifugation protocols in the absence or presence of HYase. Quantitative and qualitative analysis of EV subsets was performed using single-EV-based high-resolution flow cytometric (FCM) analysis [28,29], cryo-transmission-electron microscopy (cryo-TEM) [30], and Western blotting. Based on the results, suggestions are made for an optimised protocol for EV isolation from SF.

2

MATERIALS AND METHODS

Experimental study design, ultracentrifugation steps, and density gradient composition. The complete work flow for this study and the specific EV isolation protocol are depicted in Figure 1. The protocol was based on earlier protocols used for EV isolation from SF as summarised in Table 1 [2-19], but was more comprehensive than most of these, as it was made to meet the recently defined minimal requirements for functional EV studies [31]. The technical specifications of ultracentrifugation steps (centrifugation speeds, rotor types, etc.) and density gradient floatation are indicated in the individual sections. For all ultracentrifugation steps, rotors with swing-out buckets were used. The compositions of the OptiPrep and sucrose density gradients are presented in Supplementary Figure 1.

Reagents and antibodies. HYase type II from sheep testes, PKH67 green fluorescent dye with diluent-C (MIDI-67-1KT kit), and OptiPrep™ density gradient medium (iodixanol 60% w/v) were purchased from Sigma-Aldrich (St. Louis, MO, USA). Phosphate buffered saline (PBS) was purchased from Gibco (Thermo Scientific, Waltham, MA, USA). Protifar protein powder was purchased from Nutricia (Zoetermeer, the Netherlands). Sucrose was purchased from J.T. Baker (Avantor Performance Materials, Center Valley, PA, USA). The following primary antibodies were used for Western blotting and/or high-resolution FCM: anti-CD9 (clone HI9, Biolegend, San Diego, CA, USA), anti-CD44 (clone IM7, PE-conj., eBioscience, San Diego, CA, USA), isotype control for anti-CD44 (rat IgG2bκ, PE-conj., eBioscience), anti-Annexin-1 (clone 29/Annexin-1, BD Transduction Labs, San Jose, CA, USA), and anti-CD90/Thy1.1 (clone MRC-OX-7, PE-conj., Abcam, Cambridge, UK). Secondary antibody for Western blotting was HRP-conjugated goat-anti-mouse IgG (Nordic Immunology Laboratories, Susteren, the Netherlands).

EV depletion of reagents containing BSA and FBS. EV-depleted PBS/0.1% BSA, used for suspension of EV pellets, was prepared by making a stock solution of 5% (w/v) BSA (GE Healthcare, Amersham, UK) in PBS, which was cleared of EVs by ultracentrifugation at 100,000g for 16 h at 4°C (Optima™ L-90K or Optima™ XPN-80 centrifuge; SW28 rotor; 28,000 rpm; relative centrifugation force (RCF) average 103,745g; RCF max 141,371g; κ-factor 245.5; Beckman-Coulter, Fullerton, CA, USA), filtered through a 0.22-µm filter, stored in aliquots at −20°C, and diluted 50× in PBS prior to use.
EV-depleted RPMI/10% FBS, used to stop the PKH67 staining process, was prepared by making a stock solution of 30% (v/v) FBS (PAA Laboratories, GE Healthcare) in roswell park memorial institute medium (RPMI) (Gibco, Thermo Scientific), which was cleared of EVs by ultracentrifugation at 100,000g for 16 h at 4°C (as described above),

filtered through a 0.22-µm filter, stored in aliquots at −20°C, and diluted 3× in RPMI prior to use.

This protocol for EV depletion of reagents is a standard procedure in our lab [29] and results in very few remaining EVs if the following precautions are taken: a) start with dilutions of BSA (max 5%) and FBS (max 30%) in the buffer/medium of choice; b) use a swing-out rotor; c) use a centrifugation time of at least 16 h; d) leave at least 5 ml of supernatant above the EV pellet.

2

Collection of equine SF. Synovial fluid samples were collected post-mortem with owner consent from adult warmblood horses that were euthanised for reasons other than joint disease at the Utrecht University Equine Hospital. Healthy SF (5–10 ml) without blood contamination was collected by arthrocentesis from the carpal joints within 2 h after euthanasia and cleared from cells by centrifugation at 2,700g (4,000 rpm) 30 min at room temperature (RT) in a Hettich Universal 32 centrifuge (Hettich, Tuttlingen, Germany) with rotor 1619. Cell-free samples were aliquoted and stored at −80°C.

EV isolation and labelling for high-resolution FCM and Western blotting (CD9 and CD44). The stored, healthy, cell-free SF of 2 donors (adult horses; 4 ml/donor) was thawed and for each donor divided into 2 aliquots of 2 ml. Aliquots were incubated either with 40 µl PBS or with 40 µl HYase solution (1,500 U/ml in H$_2$O) for 15 min in a water bath at 37°C while vortexing every 5 min. Protein aggregates were removed by centrifugation at 1,000g for 10 min at RT in an Eppendorf centrifuge (Hettich Mikro 200R with rotor 2424A). The supernatants were transferred into SW60 tubes (Beckman-Coulter) and gently mixed with 2 ml PBS. EVs were pelleted with 3 sequential ultracentrifugation steps of 10,000g (35 min, 9,900 rpm; RCF average 10,066g; RCF max 13,205g; κ-factor 1667.7), 100,000g (65 min, 31,300 rpm; RCF average 100,618g; RCF max 132,000g; κ-factor 166.8), and 200,000g (65 min, 44,000 rpm; RCF average 198,835g; RCF max 260,849g; κ-factor 84.4) using an SW60-Ti rotor in a Beckman-Coulter Optima™ L-90K or Optima™ XPN-80 ultracentrifuge at 4°C. EV pellets were suspended in a mixture of 20 µl EV-depleted PBS/0.1% BSA and 30 µl diluent-C. To each sample 4 µl anti-CD44-PE antibody (0.2 mg/ml) or 4 µl anti-IgG2bκ-PE isotype control antibody (0.2 mg/ml) was added and incubated for 1 h at RT on a shaker. Prior to use the anti-CD44-PE and the IgG2bκ-PE stock solutions were centrifuged in order to pellet aggregates (21,000g, 20 min, 4°C; Hettich Mikro 200R with rotor 2424A). After CD44-PE or isotype labelling 50 µl diluent-C was added (to create a total volume of 100 µl) and this was mixed with PKH67 staining mix (1.5 µl PKH67 in 100 µl diluent-C). After 3 min incubation at RT, 50 µl of EV-depleted RPMI/10% FBS was added to stop the staining process. Labelled EVs (250 µl) were then mixed with 1.5 ml pure OptiPrep (iodixanol 60% w/v) and used for density gradient floatation. A dye background control sample (20 µl EV-depleted PBS/0.1%

BSA+30 µl diluent-C, without EVs) was taken along during the entire procedure of PKH67 labelling, anti-CD44 labelling, and OptiPrep gradient floatation. High-resolution FCM of this control sample did not show significant background in gradient fractions of interest (data not shown).

EV isolation and labelling for cryo-TEM and Western blotting (Annexin-1 and CD90/Thy1.1). The stored, healthy, cell-free SF of 2 donors (adult horses; 6 ml/donor) was thawed, pooled, and divided into 6 aliquots of 2 ml. Each aliquot was incubated with HYase and cleared from protein aggregates as described above. Supernatants were pooled, transferred into MLS50 tubes (Beckman-Coulter) (3 ml per tube) and gently mixed with 2 ml PBS. EVs were pelleted with 2 sequential ultracentrifugation steps of 10,000g (35 min, 10,000 rpm; RCF average 8,025g; RCF max 10,730g; -factor 1,777) and 200,000g (120 min, 50,000 rpm; RCF average 200,620g; RCF max 268,240g; -factor 71.7) using an MLS50 rotor in a Beckman-Coulter Optima™ MAX-E ultracentrifuge at 4°C. Note that by omitting the 100,000g centrifugation step, all EVs that would have been recovered in a separate 100,000g step are now recovered in the 200,000g step (in this paper these vesicles will be referred to as "100/200,000g EVs"). The EV pellets of each of 4 corresponding tubes were resuspended in PBS, pooled (final volume 250 µl EVs), and mixed with 1.25 ml 2 M sucrose solution (in PBS) and used for sucrose density gradient floatation.

Density gradient floatation of EVs

OptiPrep™ density gradient floatation. Pelleted 10,000g, 100,000g, or 200,000g EVs, labelled with anti-CD44-PE (or isotype control) and PKH67, mixed with pure OptiPrep (iodixanol 60% w/v) (total volume=1.75 ml) in SW40 tubes (Beckman-Coulter) were carefully overlaid with 15 volumes of 700-µl OptiPrep solutions with decreasing density (pure OptiPrep diluted in PBS) to create continuous gradients of ± 51–0% iodixanol (Supplementary Figure 1). Gradients were centrifuged at 200,000g for 16 h at 15°C (Beckman-Coulter Optima™ L-90K or Optima™ XPN-80 centrifuge; SW40-Ti rotor; 39,000 rpm; RCF average 192,072g; RCF max 270,519g; κ-factor 144.5). After centrifugation 12 fractions of 1 ml were carefully collected from top (fraction 1) to bottom (fraction 12) by using a P1000 pipette and OptiPrep densities were calculated by refractometry [32].

Sucrose density gradient floatation. Pelleted 10,000g or 100/200,000g EVs, mixed with 2 M sucrose solution (total volume=1.5 ml) in MLS50 tubes (Beckman-Coulter) were carefully overlaid with sucrose solutions of 1.4, 0.4, and 0 M (sucrose in PBS) to create 2 discontinuous sucrose gradients (Supplementary Figure 1). Gradients were centrifuged at 200,000g for 16 h at 4°C (Beckman-Coulter Optima™ MAX-E centrifuge; MLS50 rotor; 50,000 rpm; RCF average 200,620g; RCF max 268,240g; κ-factor 71.1).

After centrifugation 5 fractions of 1 ml were collected from bottom (fraction 5) to top (fraction 1) by using a peristaltic pump connected to a capillary tube reaching to the bottom of the centrifuge tube. Fraction densities were calculated by refractometry.

Single-EV-based high-resolution FCM. OptiPrep gradient fractions 1–9 (containing 10,000g, 100,000g, or 200,000g EVs from SF treated with or without HYase) were diluted 1:20 in PBS and single-EV-based high-resolution FCM was performed using an optimised jet-in-air-based BD Influx™ flow cytometer (Becton Dickinson, San Jose, CA, USA), as previously described in detail [28,29,33]. Briefly, detection of EVs by this system is based on threshold triggering by the fluorescence emitted after excitation of fluorescently labelled particles passing the first laser (FL1 signal). The threshold for triggering on FL1 was adjusted to allow an event rate of ≤10 events/s when clean PBS was analysed. The threshold level was kept identical for all measurements in this study. Forward scatter (FSC) of EVs was measured through an adapted small particle detector with a collection angle of 15–25° (reduced wide-angle FSC), by using a high numerical aperture and long working distance lens and by installing a 5-mm obscuration bar in front of the FSC collection lens. These settings allow the best distinction of FSC and FL1 fluorescence for fluorescent 100 nm and 200 nm yellow-green (505/515) carboxylated polystyrene beads (FluoSpheres, Life Technologies, Thermo Scientific, Waltham, MA, USA) with which the flow cytometer was calibrated. For experiments a 140-µm nozzle was used. The sheath fluid pressure was kept between 4.98 and 5.02 psi and was monitored by an external pressure meter. The sample pressure was set to 4.29 psi. Data were acquired using BD FACS™ Sortware v1.0.1.654 (BD Biosciences, San Jose, CA, USA) and analysed with FlowJo v10.07 software (FlowJo, Ashland, OR, USA).

For time-based quantification of EVs per gradient fraction, the amount of PKH67 events (FL1 signal) per 30 s was measured and the percentage of CD44-PE positive events (FL3 signal) was assessed relative to the isotype control condition. Total EV concentrations per ml of SF were calculated based on the event rate measurement per 30 s and a volume measurement of 14.5 µl per 30 s. Volume measurement was performed by a 30–60 min measurement of an H_2O sample and calculating the weight difference of the tube over time.

Western blotting. For OptiPrep gradients, 375 µl of fractions 2–7 were pooled (*i.e.* fractions 2+3, 4+5, and 6+7) since these fractions contained the highest concentration of EVs according to high-resolution FCM. Pooled fractions (750 µl each) were diluted in SW28 tubes (Beckman-Coulter) by adding 37 ml PBS. EVs were pelleted at 100,000g for 60 min at 4°C (Beckman-Coulter Optima™ L-90K or Optima™ XPN-80 centrifuge; SW28 rotor; 28,000 rpm; RCF average 103,745g; RCF max 141,371g; κ-factor 245.5).

For sucrose gradients, fractions 2, 3, and 4 were pooled and 1 ml of pooled sample mixed with 11 ml PBS was centrifuged in SW40 tubes (Beckman-Coulter) to pellet EVs by using the identical protocol as for pelleting EVs for cryo-TEM.

Finally, EV pellets were suspended in 70 µl non-reducing SDS-PAGE sample buffer [50 mM TRIS (pH 6.8), 2% SDS, 10% glycerol, 0.02% bromophenol blue], heated at 100°C, run on 4–20% Criterion TGX gels (Bio-Rad, Hercules, CA, USA), and transferred onto 0.2 µm polyvinylidene difluoride (PVDF) membranes. After blocking (1 h, 5% Protifar in PBS 0.1% Tween-20) proteins were labelled with primary antibodies against CD9 (dilution 1:1,000), CD44 (dilution 1:400), Annexin-1 (dilution 1:400), and CD90/Thy1.1 (dilution 1:400) and a HRP-labelled secondary antibody (dilution 1:5,000) was used for detection by chemiluminescence (SuperSignal West Pico Chemiluminescent Substrate, Thermo Scientific). Chemiluminescence was visualised using a ChemiDoc™ MP Imaging System (Bio-Rad, Hercules, CA, USA) and analysed with Bio-Rad Image Lab V5.1 software (Bio-Rad).

Cryo-TEM. For cryo-TEM, sucrose gradient fractions 2, 3, and 4 (containing 10,000g or 100/200,000g EV) were pooled per gradient and diluted by adding 9 ml PBS to SW40 tubes (Beckman-Coulter). EVs were pelleted at 200,000g for 60 min at 4°C (Beckman-Coulter Optima™ L-90K or Optima™ XPN-80 centrifuge; SW40-Ti rotor; 39,000 rpm; RCF average 192,072g; RCF max 270,519g; -factor 144.5). EV pellets were carefully suspended in 20 µl PBS and stored on ice for 1–2 h until vitrification using a Vitrobot™ Mark IV system (FEI, Eindhoven, Netherlands). Three microlitres of EV sample was directly placed onto a glow-discharged 2/2 copper grid (Quantifoil, Jena, Germany). Excess sample was removed with 595 filter paper (Schleicher & Schuell, Whatman Plc., Kent, UK) in the Vitrobot chamber for 1 s at 100% relative humidity, with subsequent plunging into liquid ethane (3.5 purity). Residual ethane was removed with filter paper and grids were stored in cryo-boxes under liquid N_2 for later imaging. For cryo-TEM, grids were transferred to a Gatan 626 cryo-holder (Gatan Inc., Pleasanton, CA, USA), which was inserted into a Tecnai™ 20 transmission electron microscopy (FEI) with LaB_6 filament operated at 200 kV. Images were acquired with a 4,000×4,000 Eagle charge coupled device (CCD) camera (FEI) at a 19,000× magnification, 5–10 µm under focus.

For morphology of EVs, individual EVs were categorised as "single EVs" (1 EV with a single membrane), "multi-membrane EVs" (2 EVs merged together, or 1 EV with double membrane), "collections of EVs" (more than 2 EVs merged into 1 entity), or "other small particles" (very small vesicle-like particles without clear membrane). Single EVs were further subcategorised into "spherical EVs" (diameter ratio ≥0.7) or "tubular EVs" (diameter ratio <0.7). Multi-membrane EVs and collections of EVs were counted as 1 entity. For size distribution of spherical EVs, the smallest and largest diameter of each individual EV was measured with the "measure tool" in ImageJ
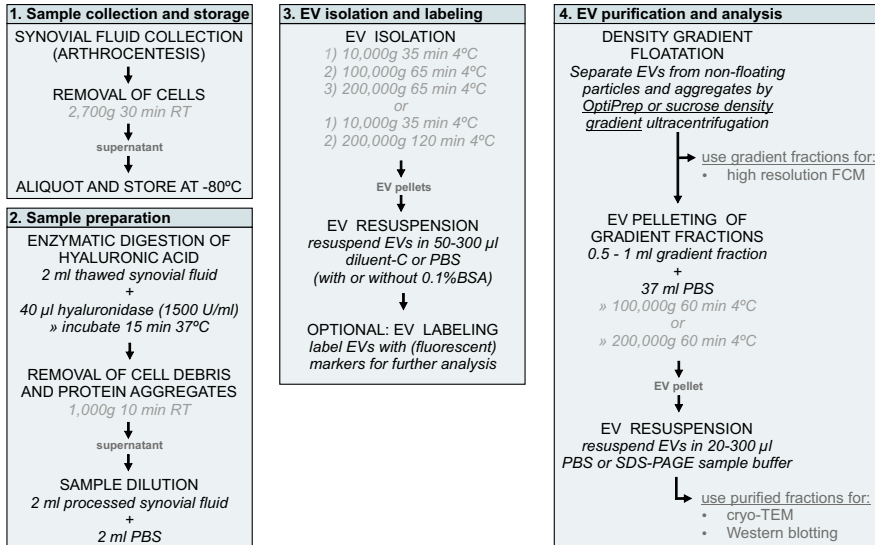
Figure 1 Work flow for isolation of extracellular vesicles from synovial fluid including enzymatic digestion of hyaluronic acid.

(1.48v) and the "diameter ratio" (smallest diameter/largest diameter) was determined. The average diameter for each EV [(smallest+largest diameter)/2] was used for the size distribution graphs.

Statistical analysis. All data in bar graphs are plotted as means of individual measurements of 2 donors. Error bars in all graphs represent the range, indicating the highest and lowest observed values (n=2). Statistical analysis for Figures 6 and 7 was performed on data from 2 donors by using the total EV counts or the relative amount of CD44+ EVs present in the 9 fractions of each gradient as data points. Log-transformation was carried out on total EV counts to gain normal distribution among the 9 fractions. Overall significant differences in all gradient fractions between +HYase and −HYase were calculated in SPSS 22.0 software (IBM, Chicago, USA), using a linear mixed model, with "donor" as a subject and "gradient fraction" (=F1 to F9), "centrifugation step" (=10,000*g* or 100,000*g* or 200,000*g*), and "HYase treatment" (= +HYase or −HYase) as (repeated) fixed factors. Differences with p-values <0.05 were considered significant based on 95% confidence intervals.

Table 1 EV isolation and characterisation methods for SF-derived EVs published between 1995 and 2016.

| Publication | Synovial fluid preparation and storage | | | HA digestion and sample dilution | |
	Anti-coagulant	Removal of cells/ cell debris	Storage	HA digestion	Sample dilution
Fourçade *et al.* 1995 [8]	EDTA	1,500*g* 30 min	not specified	-	-
Berckmans *et al.* 2002 [2]	sodium citrate	1,550*g* 20 min 20°C	fresh samples used	-	0.8x by anti-coagulant
Berckmans *et al.* 2005 [3]	sodium citrate	1,550*g* 20 min 20°C	snap-frozen; -80°C	-	0.8x by anti-coagulant
Skriner *et al.* 2006 [18]	-	300*g* 5 min 4°C, 1,200*g* 5 min 4°C	not specified	-	5x in PBS
Martínez-Lorenzo *et al.* 2007 [13]	-	800*g* 10 min	not specified	-	-
Biró *et al.* 2007 [4]	sodium citrate	1,550*g* 20 min RT	snap-frozen; -80°C	-	diluted by anti-coagulant
Messer *et al.* 2009 [15]	sodium citrate	1,500*g* 15 min RT, 13,000*g* 2 min RT	-80°C	-	diluted by anti-coagulant
Junkar *et al.* 2009 [12]	sodium citrate	1,550*g* 20 min 20°C	not specified	-	0.8x by anti-coagulant
Boillard *et al.* 2010 [5]	-	2 x 600*g* 30 min	not specified	-	-
Reich *et al.* 2011 [17]	-	Not specified	not specified	-	-
György *et al.* 2011 [10]	-	250*g* 10 min, 650*g* 20 min	-20°C	HYase	-
György *et al.* 2012 [9]	-	650*g* 20 min	-20°C	-	-
Cloutier *et al.* 2013 [6]	-	1,900*g* 30 min 4°C	-80°C	-	only for cryo-EM: 10x in HEPES buffer

	EV isolation and purification			EV characterisation	
Start volume	Ultrafiltration and ultracentrifugation	Density gradient	Size distribution	Particle analysis
not specified	2 x 200,000*g* 30 min	-	-	thin-layer chromatography
250 µl	2 x 17,570*g* 15 min 20℃	-	-	FCM
250 µl, 1 or 3ml	for volume 250 µl: 2 x 17,570*g* 30 min 20℃; for volumes 1 or 3 ml: 2 x 17,570*g* 60 min 20℃	-	-	FCM
not specified	10,000*g* 30 min 4℃; 110,000*g* 60 min 4℃	yes	30-200 nm	EM
1 ml	10,000*g* 20 min; 100,000g 6 hours	-	-	-
250 µl	2 x 18,890*g* 60 min 4℃	-	-	-
not specified	2 x 17,000*g* 30 min 4℃	-	-	-
250 µl	for AFM: no ultracentrifugation; for SEM: 2 x 17,570*g* 30 min 20℃; 20,000*g* 60 min 20℃	-	50-250 nm	AFM, SEM
not specified	-	-	-	FCM
not specified	not specified	-	-	-
not specified	3,000*g* 10 min; filtration (800nm filter); 20,500*g* 60 min RT	-	80-400 nm	AFM, immune-TEM, dynamic light scattering, FCM
not specified	for FCM: no ultracentrifugation; for EM, NTA and MS: filtration (800nm filter); 3 x 20,500*g* 60 min	-	80-400 nm	EM, NTA, FCM, MS
not specified	-	-	100-300 nm	cryo-TEM, FC, high-sensitivity FCM

2

Table 1 Continued.

| Publication | Synovial fluid preparation and storage | | | HA digestion and sample dilution | |
	Anti-coagulant	Removal of cells/ cell debris	Storage	HA digestion	Sample dilution
Pásztói *et al.* 2013 [16]	-	3,000*g* 10 min	-20°C	-	-
Matei *et al.* 2014 [14]	-	-	not specified	-	diluted only for rat samples
Duchez *et al.* 2015 [7]	-	-	not specified	-	-
Headland *et al*. 2015 [11]	-	3,000*g* 25 min 4°C	fresh samples	HYase	diluted 1:1 in PBS
Mustonen *et al.*2016 [19]	-	-	-80°C	-	diluted 1:1 in PBS

Abbreviations: AFM, atomic force microscopy; EM, electron microscopy; EV, extracellular vesicle; FCM, flow cytometry; HA, hyaluronic acid; HYase, hyaluronidase; LCM, laser scanning confocal microscopy; MS, mass spectrometry; NTA, nanoparticle tracking analysis; RT, room temperature; SEM, scanning electron microcopy; TEM, transmission electron microcopy; WetSTEM, wet scanning TEM (environmental SEM).

RESULTS

Quantification of EVs from SF with or without HYase treatment and detection of EV markers

To characterise and quantify EVs from healthy SF and to investigate the effect of HYase treatment, EVs from equine SF were isolated based on differential centrifugation followed by density gradient floatation. Equine SF was harvested from healthy joints of 2 donors and the samples were processed as summarised in Figure 1 and Supplementary Figure 1. Previously we analysed whether dilution of fresh SF (1:2 in EV-depleted PBS/0.1% BSA) prior to storage at −80°C would benefit EV isolation and analysis. Since pre-dilution of SF resulted in inconsistent data and loss of EVs (data not shown), in the current protocol, fresh samples were not diluted prior to HYase treatment. After HYase treatment, a 1:1 dilution of the sample was performed.

PKH67-labelled EVs in OptiPrep gradient fractions were measured as single-vesicle events by high-resolution FCM (Figure 2). EVs were detected throughout fractions F2–F7 with densities between 1.02 and 1.16 g/ml. Highest concentration of EVs were found in gradient fractions F3–F5 (density 1.05–1.10 g/ml). The majority of all EVs

	EV isolation and purification			EV characterisation	
Start volume	Ultrafiltration and ultracentrifugation	Density gradient	Size distribution	Particle analysis
1 ml	2 x 20,500g 60 min RT	-	-	-
not specified	-	-	60-500 nm	cryo-TEM, SEM, WetSTEM, LCM
not specified	-	-	-	FCM
not specified	10,000g 10 min RT (EVs stained in supernatant)	-	-	FCM
1 ml	1,000g 10 min; 1,200g 20 min; 110,000g 90 min	-	50-400 nm	NTA, LCM, TEM

2

were recovered in the 100,000g centrifugation step, regardless of HYase treatment (Figure 2A). Total EV recovery (sum of 10,000g EVs + 100,000g EVs + 200,000g EVs in gradient fractions F2–F7) was not significantly affected by pre-treatment with HYase. By using the event rate and the sample volume measurement during high-resolution FCM analysis, the biological concentrations of EVs in healthy equine SF (calculated from the HYase-treated samples after OptiPrep density gradient) could be estimated at 7×10^8 EVs/ml.

Hyaluronidase treatment, however, substantially increased the number of EVs pelleting at 10,000g, whereas in the non-treated samples a higher number of EV tended to pellet at 200,000g (Figure 2A). In addition, differences in light scattering properties of EVs were observed between the HYase-treated and non-treated samples (most clear in arbitrary regions II and III in the 10,000g and 100,000g centrifugation steps and in regions III and IV in the 200,000g centrifugation step). Because light scattering of EVs is dependent on a range of factors, such as size, cargo, and membrane composition, these findings could be indicative for recovery of different EV subsets in HYase-treated and non-treated samples after similar centrifugation conditions (Figure 2B).
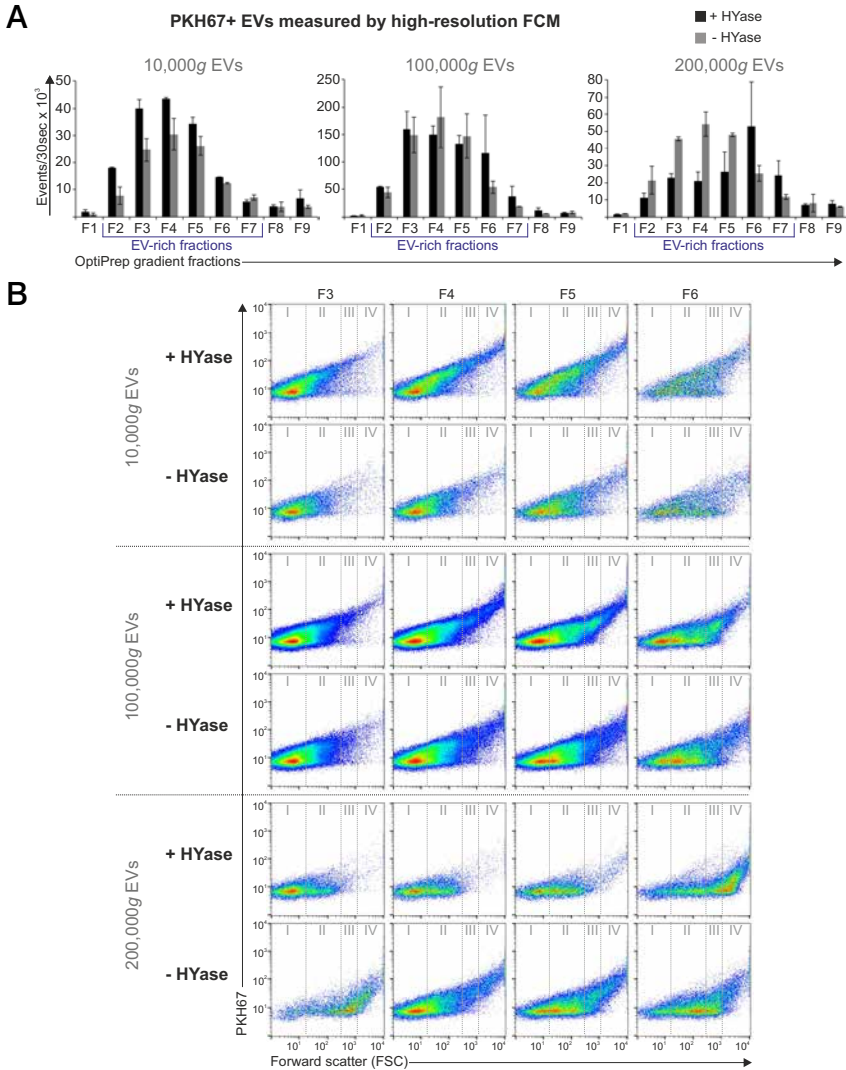
Figure 2 High-resolution FCM of EVs derived from SF; detection of PKH67+ EVs. EVs were isolated from HYase-treated or non-treated healthy SF, labelled with PKH67, floated in OptiPrep gradients, and analysed using high-resolution FCM in gradient fractions F1 (low density) to F9 (high density). **A)** Quantification of PKH67+ events (single EVs) for the subsequent 10,000*g*, 100,000*g*, and 200,000*g* ultracentrifugation steps. Bars represent mean (n=2); error bars represent minimum and maximum observed values. **B)** Representative scatter plots corresponding to Figure 2A for gradient fractions F3–F6. In this figure, the arbitrary regions I–IV were set to indicate observed differences in the light-scattering properties of EVs in each fraction, indicative for the recovery of different EV populations.

The quantitative results obtained with single-EV-based high-resolution FCM (Figure 2A) corroborate with the CD9 Western blot results of EVs in pools of the same gradient fractions (Figure 3; Supplementary Figure 2A). Similar to the recovery of PKH67-labelled EVs, HYase treatment resulted in a more efficient recovery of CD9+ EVs after 10,000*g* pelleting, whereas the additional 200,000*g* step improved the recovery of CD9+ EVs from the non-treated samples. When total CD9 signal (sum) of all gradient fractions was compared, HYase treatment resulted in approximately 10% more CD9+ EVs.

In addition to CD9, selected as general EV marker [31], Annexin-1 and CD90/Thy1.1 were analysed on SF-derived EVs because of their relevance in the joint. Annexin-1 was previously found on neutrophil-derived EVs during inflammatory arthritis [11], and CD90/Thy1.1 is a cell surface marker of fibroblasts in the synovial lining [34]. The latter was verified on primary equine fibroblast-like synoviocytes (Supplementary Figure 3). Indeed, both Annexin-1 and CD90/Thy1.1 could be detected on 10,000*g* and 100/200,000*g* EVs from healthy SF (Supplementary Figure 2B).
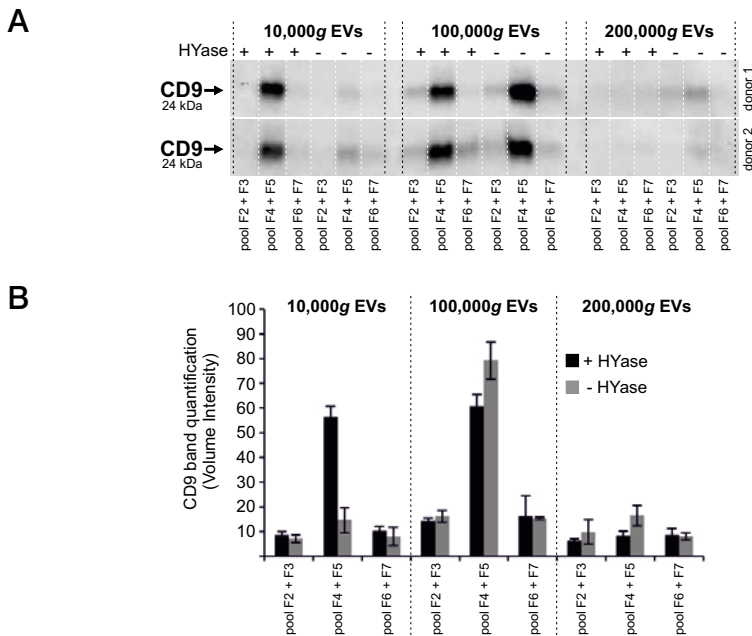
2

Figure 3 Detection of CD9 (tetraspanin; EV marker) on EVs from healthy SF by Western blotting. EVs were isolated from HYase-treated or non-treated healthy SF and floated in OptiPrep gradients. **A)** CD9 detection on EVs in pools of OptiPrep fractions F2–F7 (F2=low density; F7=high density). **B)** Quantification of CD9+ bands from Figure 3A. Bars represent mean (n=2); error bars represent minimum and maximum observed values.

Cryo-TEM of EVs from healthy SF

Cryo-TEM investigation was performed in order to confirm intact EVs in our preparations and to determine size and shape of 10,000g versus 100/200,000g EVs from healthy SF (Figure 4). A typical distribution on the grids showed single intact vesicles (Figure 4A). In both the 10,000g and the 100/200,000g samples, only occasional clusters of EVs were seen (Figure 4B). Further, both the 10,000g and the 100/200,000g ultracentrifugation resulted in a large diversity of EV shapes and sizes, for which the spherical shape was most abundant, comprising about 65% of all EVs (Figure 4C). Of note, about 3–8% of analysed particles were defined as "other small particles" (<20 nm and lacking a clear vesicle membrane) (Figure 4F). When evaluating the size distribution of spherical EVs (Figure 4D), 92–98% of all EVs had diameters between 20 and 200 nm in both centrifugation conditions. The highest frequencies of EVs <100 nm, however, were found in the 100/200,000g centrifugation step (69% vs. 57% in the 10,000g step). The average diameter was 109 nm for 10,000g EVs (n=88) and 90 nm for 100/200,000g EVs (n=105). Occasionally EVs were found with high electron-dense granules in their lumen (not quantified) (Figure 4E).

Quantification of CD44+ EVs from healthy SF and the impact of HYase treatment

Next, the impact of HYase treatment on the identification of specific EV subsets from SF was studied by exploring the detection of CD44+ EVs. CD44 is expressed by various cell types [35], including primary fibroblast-like synoviocytes in the synovial membrane (Supplementary Figure 3). In healthy joints these fibroblasts are the candidate cell type for the production and release of EVs into the SF. Furthermore, CD44 is the HA receptor and – if present on EVs in SF – could be involved in binding to full-length HA in the extracellular matrix. Therefore, degradation of the extracellular matrix by HYase might be beneficial for the recovery of CD44+ EVs. Indeed, CD44 was detected by Western blotting on 10,000g and 100,000g EVs from the HYase-treated samples, whereas for the non-treated samples CD44+ EVs were only present in the 100,000g samples (Supplementary Figure 2C). Since Western blotting does not allow single EV analysis, individual CD44+ EVs were quantified by single-EV-based high-resolution FCM (Figures 5 and 6). CD44+ EVs were detected in all centrifugation steps, with an increased yield for the HYase-treated samples when centrifuged at 10,000g ($p<0.05$) and 100,000g ($p<0.01$) (Figures 5 and 6B). To get more insight into the distribution of the CD44+ EVs throughout the density gradients, the CD44+ population of EVs was compared to the total population of EVs (PKH67+) (Figure 6). Remarkably, the distribution of CD44+ EVs in the density gradient fractions did not fully correlate with the distribution of the total EV population; CD44+ EVs tend to float at a higher density than the bulk of EVs in the gradient (Figure 6).
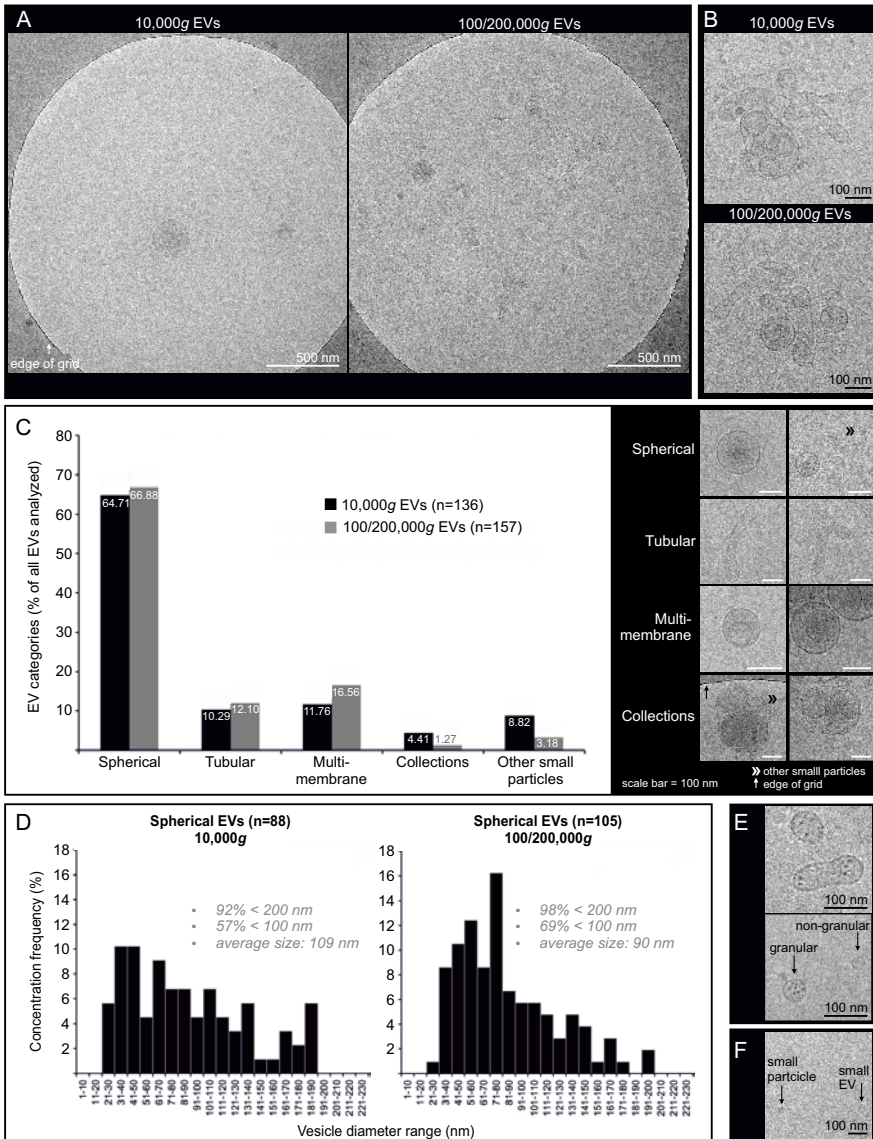
Figure 4 Cryo-transmission-electron microscopy (cryo-TEM) analysis of EVs isolated from HYase-treated healthy SF. EVs were pelleted using centrifugation steps of 10,000g (=10,000g EVs), immediately followed by 200,000g, omitting the 100,000g step (=100/200,000g EVs, representing a pool of all EVs that are pelleted if using subsequent 100,000g and 200,000g centrifugation steps). Isolated EVs were floated in sucrose gradients followed by cryo-TEM analysis. **A)** Representative images of EV distribution in the grid holes as they are most often observed.

Figure 4 (*Continued*)

B) Clusters of EVs occasionally observed for both centrifugation steps. **C)** Quantification of typical EV morphologies found in healthy SF. Note that sometimes vesicle-like structures without clear membrane were also found, here referred to as "other small particles" (see also 4F). **D)** Size distribution for 10,000*g* and 100/200,000g spherical EVs. **E)** For both centrifugation conditions occasionally "granular" EVs were observed containing electron-dense granules. **F)** Comparison of small EVs (with clear membrane; typically 20–40 nm) with "other small particles" (lacking a clear membrane; typically <20 nm) generally found in all images.

In general, centrifugation at 100,000*g* contributes mostly to the recovery of CD44+ EVs. Finally, the cumulative counts of CD44+ EVs in all centrifugation steps (sum of event rates for 10,000*g* EVs+100,000*g* EVs+200,000*g* EVs present in gradient fractions F2–F7) clearly demonstrates a significantly less efficient recovery of these EVs in the 10,000*g* and 100,000*g* centrifugation steps (p<0.01) in the absence of HYase treatment (Figure 7).

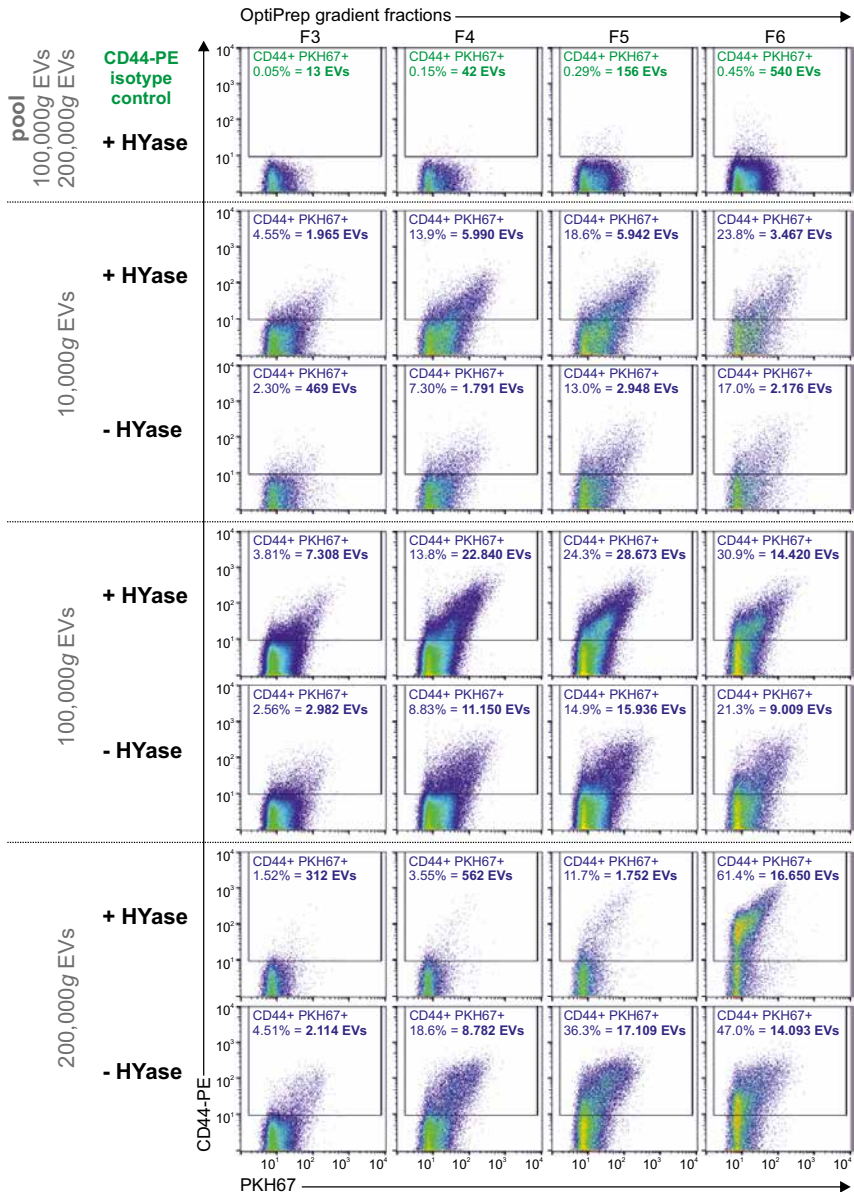**CD44+/PKH67+ EVs measured by high-resolution FCM**

2

Figure 5 High-resolution FCM of SF-derived EVs; detection of CD44+/PKH67+ EVs. EVs were isolated from HYase-treated or non-treated healthy SF, labelled with PKH67 and anti-CD44 antibody (PE-conj.) floated in OptiPrep gradients and analysed using high-resolution FCM.

Figure 5 (*Continued*)

Scatter plots for the subsequent 10,000*g*, 100,000*g*, and 200,000*g* ultracentrifugation steps are shown for gradient fractions F3–F6 corresponding to Figure 2B. Percentages of CD44+ events and absolute CD44+ numbers measured per 30 s were determined using a square gate based on the isotype control (pool of 100,000*g* and 200,000*g* EVS, labelled with PKH67 and CD44-PE isotype antibody).
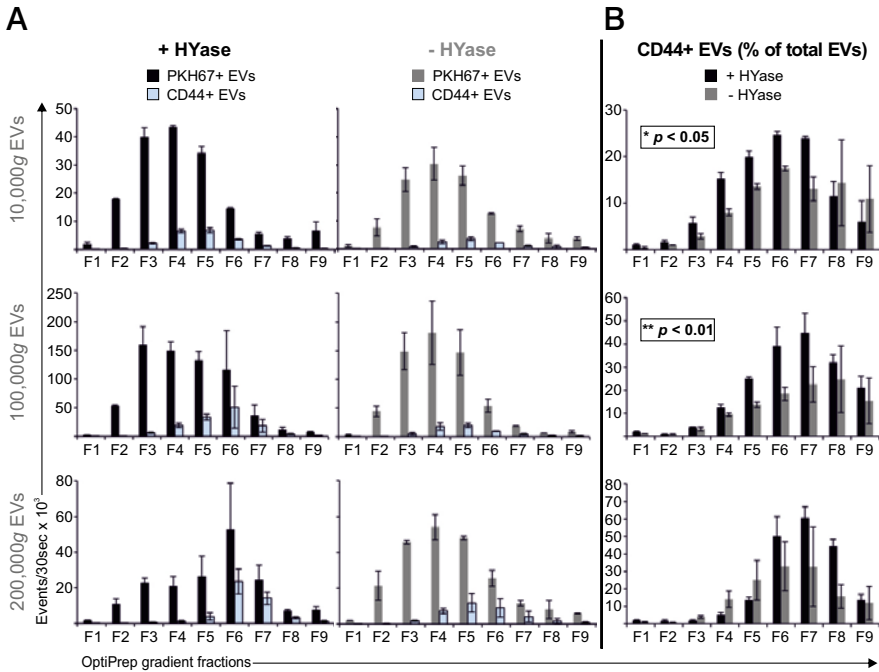

Figure 6 A) Comparison of PKH67+ EVs (black/grey bars) (data from Figure 2) and CD44+/ PKH67+ EVs (blue bars) (data from Figure 5) measured by high-resolution FCM for the conditions +HYase and −HYase. **B)** Ratio of CD44+ EVs relative to total EVs. The p-values indicate significantly higher total yield in the HYase-treated samples in the 10,000*g* and 100,000*g* centrifugation steps (paired analysis). Bars represent mean (n=2); error bars represent minimum and maximum observed values.
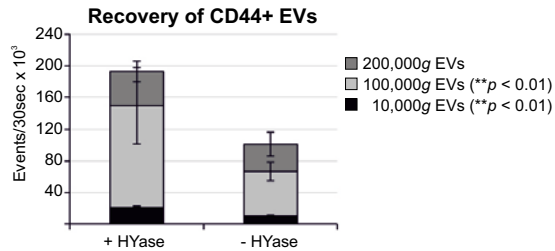
Figure 7 Cumulative yield of CD44+ EVs in all ultracentrifugation steps (sum of event rates for 10,000*g* EVs + 100,000*g* EVs + 200,000*g* EVs present in gradient fractions F2–F7) in HYase-treated and non-treated samples. Bars represent mean (n=2); error bars represent minimum and maximum observed values. The p-values indicate significant higher recovery of CD44+ EVs in HYase-treated samples in the 10,000*g* and 100,000*g* centrifugation step.

DISCUSSION

For developing a tailor-made protocol for EV isolation from SF, previously published reports were first evaluated to determine which protocols to date have been used for EV isolation from SF and to survey which important technical steps should be considered for a standardised protocol. Of 18 articles published between 1995 and 2016 reporting EV isolation from SF (Table 1) [2-19], 17 involved samples from human patients with joint disease. Only one study investigated healthy SF (of rat, canine, and equine origin) [14]. In 6 publications, samples were pre-treated with anticoagulant and in 2 publications enzyme treatment with HYase prior to ultracentrifugation was reported. In most cases, EVs were pelleted with maximally 20,500*g*. In only 4 publications were EVs pelleted at ≥100,000*g*. Strikingly, there was only a single publication in which EVs were purified by floating in density gradients. In all other studies, fresh SF or the total ultracentrifugation pellets – both cleared from large particles, but contaminated with other non-vesicular macromolecular structures in addition to EVs – were used for analysis of SF-derived EVs.

Our protocol considered the earlier published work, but was more comprehensive and included density gradient floatation, as it was designed to meet the recently published minimal requirements for functional EV studies [31]. Importantly, apart from the 10,000*g* and 100,000*g* pelleting steps, which are centrifugation forces most often used in the field to isolate EVs from body fluids, an additional 200,000*g* pelleting step was included to isolate EVs from SF, as this is a very viscous body fluid. Because the

SF samples for this study were taken from healthy joints without blood contamination, anticoagulant treatment was not included. In contrast, HYase treatment appeared to be an important step in our protocol, due to the high concentration of high-molecular-weight HA in SF [26,27]. Hyaluronic acid is a non-sulphated glycosaminoglycan and the most prominent component of the extracellular matrix of SF [27]. Because CD44 is an HA receptor and present on synovial fibroblasts, considered to be important EV producers in SF, we evaluated the recovery of CD44+ EVs in the absence or presence of HYase treatment.

We here showed that enzymatic digestion of the large HA chains with HYase is beneficial for the isolation of CD44 (HA receptor) positive EVs from SF. Only after HYase treatment could the CD44+ EVs be efficiently isolated, mainly after 100,000g ultracentrifugation. Although the recovery of total EVs (PKH67+) was not significantly affected when omitting HYase treatment, significantly less CD44+ EVs were recovered. Very recently the presence of HA-coated EVs was detected in SF [19]. One possible explanation for the lower detection of CD44+ EVs in the absence of HYase treatment in our study could be masking of antibody detection due to HA binding. However, because the epitope of the anti-CD44 antibody (IM7 clone) used for CD44+ EV detection is located outside the HA binding domain of CD44 [36], antibody shielding or steric hindrance of antibody binding is less likely the cause of lack of detection. We therefore conclude that the lower yield of CD44+ EVs from non-HYase-treated samples is most likely due to the formation of complexes of these EVs with the large chains of non-degraded HA in SF and that HYase degrades HA and liberates EVs that are bound via CD44, resulting in increased EV yields. Nevertheless, if steric hindrance of antibody binding by HA did take place on EVs, it could also hamper other antibody-based detection assays, making HYase treatment indispensable.

Based on our data, we propose HYase incubation of SF preceding EV isolation for efficient recovery of CD44+ EVs. However, it should be noted that possible effects of HYase treatment should be evaluated on further downstream processing and analysis steps, for example, (micro)RNA analysis. For protein and lipid analysis, problems due to HYase are not expected, since general biomarker analysis of fresh SF is routinely preceded by HYase treatment.

The fact that most EVs were intact and no debris of damaged EVs was observed by cryo-TEM indicates that these EVs can withstand the high centrifugation forces used in our protocol (>100,000g). Nevertheless, the possibility of (functional) loss due to centrifugation and floatation procedures cannot be ruled out, which is important for future research aiming at functional testing of these EVs. Cryo-TEM analysis of EVs from healthy SF, isolated with 10,000g or 100/200,000g, followed by a sucrose

density gradient, revealed a heterogeneous pool of particles with shapes comparable to findings in other body fluids [24,30,37,38]. For SF, differential centrifugation steps did not separate EVs based on morphology, nor on size, although size distribution of spherical EVs did show a tendency for EVs >100 nm to be recovered at 10,000g (compared to 100/200,000g). The finding that 92–98% of EVs in our study had diameters between 20 and 200 nm is considerably different from the larger particles (up to 400 nm) detected in SF from patients with inflammatory joint disease [6,9,10,19]. These differences could be caused by differences in the methodology used to isolate EVs, for example, centrifugation protocols and density gradients. Alternatively, it might indicate that during disease different EV populations are present in the joint.

Recent data indicate that particular EV types (*e.g.* platelet-derived EVs present in blood plasma) have the tendency to aggregate due to ultracentrifugation, which can lead to false interpretation of particle size and marker analysis [39,40]. However, we have shown here that for SF-derived EVs from healthy joints, clusters of EVs were rarely observed by cryo-TEM analysis, indicating that even 200,000g pelleting did not induce major aggregation artefacts. In addition to very small EVs (20–40 nm), other small particles (typically ≤20 nm) were observed. These structures differed from EVs by not having a clear membrane and usually having a darker and more homogenous core compared to the slightly larger EVs. Possibly, these very small particles could be lipoproteins, resembling cryo-EM preparations of very low density lipoprotein (VLDL) particles from blood [38,41], or ice-crystal artefacts, as has been observed in ejaculates [37].

Extracellular vesicles isolated from healthy equine SF were positive for CD9, Annexin-1, CD90/Thy1.1, and CD44. Whereas CD9 is a common marker for EVs, Annexin-1 has so far – in relation to the joint – been known only as a pro-resolving anti-inflammatory marker on EVs in the inflammatory joints of patients with joint disease [11]. The current data show that Annexin-1 is also present on EVs in healthy SF, although at relatively low abundance. These Annexin-1+ EVs may be derived from the few circulating immune cells present in healthy SF. For the bulk of SF-derived EVs, however, a synoviocytic origin is more likely, because markers found on these EVs, for example, CD90/Thy1.1 and CD44, are also highly expressed on primary fibroblast-like synoviocytes.

The interaction between HA and CD44+ EVs in SF might be of functional interest during joint disease. Because the concentration and chain length of HA is dependent on the disease state of the joint [27], the interaction (or the lack thereof) between CD44+ EVs and HA in the extracellular matrix might be altered when joint homeostasis is disturbed. This could have its functional effect by changing the freedom of movement of CD44+ EVs in the joint space and thus changing the efficiency of

2

interaction with target cells in the synovial membrane or the cartilage. CD44+ EVs could also, by binding free HA chains, serve as transport vehicles for HA between cells and might facilitate its efficient delivery to target cells. *In vitro* studies have shown that when HA is delivered to CD44-expressing cells, the HA–CD44 interaction on these cells results in an anabolic (and anti-inflammatory) cascade by inhibiting TNF-α- or IL-1β-induced matrix metalloproteinase (MMP) production and aggrecanase expression in chondrocytes and synovial cells, explaining the mechanism of action during HA therapy in arthritis [42]. Furthermore, triggering of fibroblast-like synoviocytes with HA evokes the production of more HA, dependent on the type of HA used [26,43]. Finally, cell types with active HA synthesis (for the joint these are fibroblast-like synoviocytes and chondrocytes) contain an "HA coat" on protrusions of their plasma membrane [44]. CD44+ EVs could use these high-affinity HA-coated areas to anchor to cells for further EV uptake or interaction.

While the importance of CD44-dependent EV interaction with HA has already been established in HA-related pathologies, such as cancer progression [45], clarifying the role of EV-associated CD44 in healthy and diseased joints needs to be further substantiated since CD44 is not only a HA receptor, but also an important signalling molecule in various cell types [35]. With respect to the CD44–HA interaction on EVs, it is important to note that only specific forms of HA actively bind to CD44 [27]. The exact interaction and timing of this event during joint homeostasis, or the disturbance thereof, should be further investigated. Insight into this interaction could also be of importance for potential clinical applications, such as the incorporation of CD44+ EVs or liposomes (loaded with pharmaceuticals) into HA-rich scaffolds for local controlled release of treatment during joint regeneration [1].

Ultimately, the CD44+ EV population in SF is likely an important functional EV subset, which might have distinct functions in healthy and diseased joints. Although infiltration of interstitial fluids into the SF during inflammation results in lower viscosity of the fluid, the HYase step needs to be taken into consideration for inflammatory SF as well, because increased production of low-molecular-weight HA during inflammation might provoke even more trapping of CD44+ EVs into the extracellular matrix [27]. In addition, for other HA-containing body fluids, such as pleural fluid, peritoneal fluid, and blood [46,47], sedimentation of EVs could be hampered by omitting the HYase step in the EV isolation protocol. This is an important consideration, since systemic accumulation of HA is often a poor prognostic factor in diseases like rheumatoid arthritis [48], osteoarthritis [49], liver disease [50], and many epithelial cancers [51]. Hence to unveil the role of EVs in (patho)physiologic processes and to search for disease-specific EV-based biomarkers, the addition of HYase during EV isolation from body fluids might be indispensable to avoid the loss of a potentially important CD44+ EV subset.

CONCLUSION

To the best of our knowledge, this is the first detailed investigation in which EVs were isolated and analysed from healthy SF samples. In contrast to reports that claim that high-speed centrifugation of body fluids leads to formation of EV aggregates, EV isolation from SF can be performed with high-speed centrifugation up to 200,000g without substantial aggregate formation or damage to EVs. The majority of EVs from SF can be recovered at 100,000g. However, in the absence of HYase treatment a substantial amount of EVs is only recovered after 200,000g, while the CD44+ EV subset is isolated inefficiently. The beneficial effect of HYase treatment on CD44+ EV recovery from SF stresses the importance of tailor-made protocols for EV isolation from different body fluids. For the case of SF, in most EV isolation protocols up to now, neither HYase treatment nor a 200,000g centrifugation step was applied and often only centrifugation forces of maximally 20,500g were used. Based on our findings, this implies that in these studies EVs are possibly recovered suboptimally and specific subsets, such as the CD44+ EVs, might therefore remain unnoticed. The design of a golden standard protocol for isolation of EVs from SF, however, remains difficult due to differences in SF composition between healthy and diseased joints, within different joint diseases, at different disease stages, and possibly between species. Taking into account that not only EV characteristics, but also the matrix composition wherein these EVs are present, determine the g-forces and time necessary for sedimentation, HYase treatment is an attractive option to at least eliminate HA-dependent matrix variations between SF samples and efficiently recover the biologically relevant CD44+ EVs.

2

ACKNOWLEDGEMENTS

REFERENCES

1. Malda, J.; Boere, J.; van de Lest, C. H.; van Weeren, P.; Wauben, M. H. Extracellular vesicles - new tool for joint repair and regeneration. *Nat. Rev. Rheumatol.* **2016***, 12*, 243-249.

2. Berckmans, R. J.; Nieuwland, R.; Tak, P. P.; Boing, A. N.; Romijn, F. P.; Kraan, M. C.; Breedveld, F. C.; Hack, C. E.; Sturk, A. Cell-derived microparticles in synovial fluid from inflamed arthritic joints support coagulation exclusively via a factor VII-dependent mechanism. *Arthritis Rheum.* **2002***, 46*, 2857-2866.

3. Berckmans, R. J.; Nieuwland, R.; Kraan, M. C.; Schaap, M. C.; Pots, D.; Smeets, T. J.; Sturk, A.; Tak, P. P. Synovial microparticles from arthritic patients modulate chemokine and cytokine release by synoviocytes. *Arthritis Res. Ther.* **2005***, 7*, R536-44.

4. Biro, E.; Nieuwland, R.; Tak, P. P.; Pronk, L. M.; Schaap, M. C.; Sturk, A.; Hack, C. E. Activated complement components and complement activator molecules on the surface of cell-derived microparticles in patients with rheumatoid arthritis and healthy individuals. *Ann. Rheum. Dis.* **2007***, 66*, 1085-1092.

5. Boilard, E.; Nigrovic, P. A.; Larabee, K.; Watts, G. F.; Coblyn, J. S.; Weinblatt, M. E.; Massarotti, E. M.; Remold-O'Donnell, E.; Farndale, R. W.; Ware, J.; Lee, D. M. Platelets amplify inflammation in arthritis via collagen-dependent microparticle production. *Science* **2010***, 327*, 580-583.

6. Cloutier, N.; Tan, S.; Boudreau, L. H.; Cramb, C.; Subbaiah, R.; Lahey, L.; Albert, A.; Shnayder, R.; Gobezie, R.; Nigrovic, P. A.; Farndale, R. W.; Robinson, W. H.; Brisson, A.; Lee, D. M.; Boilard, E. The exposure of autoantigens by microparticles underlies the formation of potent inflammatory components: the microparticle-associated immune complexes. *EMBO Mol. Med.* **2013***, 5*, 235-249.

7. Duchez, A. C.; Boudreau, L. H.; Bollinger, J.; Belleannee, C.; Cloutier, N.; Laffont, B.; Mendoza-Villarroel, R. E.; Levesque, T.; Rollet-Labelle, E.; Rousseau, M.; Allaeys, I.; Tremblay, J. J.; Poubelle, P. E.; Lambeau, G.; Pouliot, M.; Provost, P.; Soulet, D.; Gelb, M. H.; Boilard, E. Platelet microparticles are internalized in neutrophils via the concerted activity of 12-lipoxygenase and secreted phospholipase A2-IIA. *Proc. Natl. Acad. Sci. U. S. A.* **2015***, 112*, E3564-73.

8. Fourcade, O.; Simon, M. F.; Viode, C.; Rugani, N.; Leballe, F.; Ragab, A.; Fournie, B.; Sarda, L.; Chap, H. Secretory phospholipase A2 generates the novel lipid mediator lysophosphatidic acid in membrane microvesicles shed from activated cells. *Cell* **1995***, 80*, 919-927.

9. Gyorgy, B.; Szabo, T.,G.; Turiak, L.; Wright, M.; Herczeg, P.; Ledeczi, Z.; Kittel, A.; Polgar, A.; Toth, K.; Derfalvi, B.; Zelenak, G.; Borocz, I.; Carr, B.; Nagy, G.; Vekey, K.; Gay, S.; Falus, A.; Buzas, E.,I. Improved flow cytometric assessment reveals distinct microvesicle (cell-derived microparticle) signatures in joint diseases. *PloS one* **2012***, 7*, e49726.

10. Gyorgy, B.; Modos, K.; Pallinger, E.; Paloczi, K.; Pasztoi, M.; Misjak, P.; Deli, M. A.; Sipos, A.; Szalai, A.; Voszka, I.; Polgar, A.; Toth, K.; Csete, M.; Nagy, G.; Gay, S.; Falus, A.; Kittel, A.; Buzas, E. I. Detection and isolation of cell-derived microparticles are compromised by protein complexes resulting from shared biophysical parameters. *Blood* **2011***, 117*, e39-48.

11. Headland, S. E.; Jones, H. R.; Norling, L. V.; Kim, A.; Souza, P. R.; Corsiero, E.; Gil, C. D.; Nerviani, A.; Dell'Accio, F.; Pitzalis, C.; Oliani, S. M.; Jan, L. Y.; Perretti, M. Neutrophil-derived microvesicles enter cartilage and protect the joint in inflammatory arthritis. *Sci. Transl. Med.* **2015***, 7*, 315ra190.

12. Junkar, I.; Sustar, V.; Frank, M.; Jansa, V.; Zavec, A.; Rozman, B.; Mozetic, M.; Hagerstrand, H.; Kralj-Iglic, V. Blood and synovial microparticles as revealed by atomic force and scanning electron microscope. *The Open Autoimmunity Journal* **2009***, 1*, 50-58.

13. Martinez-Lorenzo, M. J.; Anel, A.; Saez-Gutierrez, B.; Royo-Canas, M.; Bosque, A.; Alava, M. A.; Pineiro, A.; Lasierra, P.; Asin-Ungria, J.; Larrad, L. Rheumatoid synovial fluid T cells are sensitive to APO2L/TRAIL. *Clin. Immunol.* **2007***, 122*, 28-40.

14. Matei, C. I.; Boulocher, C.; Boule, C.; Schramme, M.; Viguier, E.; Roger, T.; Berthier, Y.; Trunfio-Sfarghiu, A. M.; Blanchin, M. G. Ultrastructural analysis of healthy synovial fluids in three mammalian species. *Microsc. Microanal.* **2014***, 20*, 903-911.

15. Messer, L.; Alsaleh, G.; Freyssinet, J.; Zobairi, F.; Leray, I.; Gottenberg, J.; Sibilia, J.; Toti-Orfanoudakis, F.; Wachsmann, D. Microparticle-induced release of B-lymphocyte regulators by rheumatoid synoviocytes. *Arthritis Research & Therapy* **2009***, 11*, R40.

16. Pasztoi, M.; Sodar, B.; Misjak, P.; Paloczi, K.; Kittel, A.; Toth, K.; Wellinger, K.; Geher, P.; Nagy, G.; Lakatos, T.; Falus, A.; Buzas, E. I. The recently identified hexosaminidase D enzyme substantially contributes to the elevated hexosaminidase activity

2

in rheumatoid arthritis. *Immunol. Lett.* **2013***, 149*, 71-76.

17. Reich, N.; Beyer, C.; Gelse, K.; Akhmetshina, A.; Dees, C.; Zwerina, J.; Schett, G.; Distler, O.; Distler, J. H. Microparticles stimulate angiogenesis by inducing ELR(+) CXC-chemokines in synovial fibroblasts. *J. Cell. Mol. Med.* **2011***, 15*, 756-762.

18. Skriner, K.; Adolph, K.; Jungblut, P. R.; Burmester, G. R. Association of citrullinated proteins with synovial exosomes. *Arthritis Rheum.* **2006***, 54*, 3809-3814.

19. Mustonen, A. M.; Nieminen, P.; Joukainen, A.; Jaroma, A.; Kaariainen, T.; Kroger, H.; Lazaro-Ibanez, E.; Siljander, P. R.; Karja, V.; Harkonen, K.; Koistinen, A.; Rilla, K. First in vivo detection and characterization of hyaluronan-coated extracellular vesicles in human synovial fluid. *J. Orthop. Res.* **2016***, 34*, 1960-1968.

20. Malda, J.; Benders, K. E.; Klein, T. J.; de Grauw, J. C.; Kik, M. J.; Hutmacher, D. W.; Saris, D. B.; van Weeren, P. R.; Dhert, W. J. Comparative study of depth-dependent characteristics of equine and human osteochondral tissue from the medial and lateral femoral condyles. *Osteoarthritis Cartilage* **2012***, 20*, 1147-1151.

21. Hurtig, M. B.; Buschmann, M. D.; Fortier, L. A.; Hoemann, C. D.; Hunziker, E. B.; Jurvelin, J. S.; Mainil-Varlet, P.; McIlwraith, C. W.; Sah, R. L.; Whiteside, R. A. Preclinical Studies for Cartilage Repair: Recommendations from the International Cartilage Repair Society. *Cartilage* **2011***, 2*, 137-152.

22. McIlwraith, C. W.; Frisbie, D. D.; Kawcak, C. E. The horse as a model of naturally occurring osteoarthritis. *Bone Joint Res.* **2012***, 1*, 297-309.

23. Witwer, K. W.; Buzas, E. I.; Bemis, L. T.; Bora, A.; Lasser, C.; Lotvall, J.; Nolte-'t Hoen, E. N.; Piper, M. G.; Sivaraman, S.; Skog, J.; Thery, C.; Wauben, M. H.; Hochberg, F. Standardization of sample collection, isolation and analysis methods in extracellular vesicle research. *J. Extracell Vesicles* **2013***, 2*, 10.3402/jev.v2i0.20360. eCollection 2013.

24. Zonneveld, M. I.; Brisson, A. R.; van Herwijnen, M. J.; Tan, S.; van de Lest, C. H.; Redegeld, F. A.; Garssen, J.; Wauben, M. H.; Nolte-'t Hoen, E. N. Recovery of extracellular vesicles from human breast milk is influenced by sample collection and vesicle isolation procedures. *J. Extracell Vesicles* **2014***, 3*, 10.3402/jev.v3.24215. eCollection 2014.

25. Lacroix, R.; Judicone, C.; Mooberry, M.; Boucekine, M.; Key, N. S.; Dignat-George, F.; The ISTH SSC Workshop Standardization of pre-analytical variables in plasma microparticle determination: results of the International Society on Thrombosis and Haemostasis SSC Collaborative workshop. *J. Thromb. Haemost.* **2013**.

26. Dahl, L. B.; Dahl, I. M.; Engstrom-Laurent, A.; Granath, K. Concentration and molecular weight of sodium hyaluronate in synovial fluid from patients with rheumatoid arthritis and other arthropathies. *Ann. Rheum. Dis.* **1985***, 44*, 817-822.

27. Murai, T. Lipid Raft-Mediated Regulation of Hyaluronan-CD44 Interactions in Inflammation and Cancer. *Front. Immunol.* **2015***, 6*, 420.

28. Nolte-'t Hoen, E. N.; van der Vlist, E. J.; Aalberts, M.; Mertens, H. C.; Bosch, B. J.; Bartelink, W.; Mastrobattista, E.; van Gaal, E. V.; Stoorvogel, W.; Arkesteijn, G. J.; Wauben, M. H. Quantitative and qualitative flow cytometric analysis of nanosized cell-derived membrane vesicles. *Nanomedicine* **2012***, 8*, 712-720.

29. van der Vlist, E. J.; Nolte-'t Hoen, E. N.; Stoorvogel, W.; Arkesteijn, G. J.; Wauben, M. H. Fluorescent labeling of nano-sized vesicles released by cells and subsequent quantitative and qualitative analysis by high-resolution flow cytometry. *Nat. Protoc.* **2012***, 7*, 1311-1326.

30. Arraud, N.; Linares, R.; Tan, S.; Gounou, C.; Pasquet, J. M.; Mornet, S.; Brisson, A. R. Extracellular vesicles from blood plasma: determination of their morphology, size, phenotype and concentration. *J. Thromb. Haemost.* **2014***, 12*, 614-627.

31. Lotvall, J.; Hill, A. F.; Hochberg, F.; Buzas, E. I.; Di Vizio, D.; Gardiner, C.; Gho, Y. S.; Kurochkin, I. V.; Mathivanan, S.; Quesenberry, P.; Sahoo, S.; Tahara, H.; Wauben, M. H.; Witwer, K. W.; Thery, C. Minimal experimental requirements for definition of extracellular vesicles and their functions: a position statement from the International Society for Extracellular Vesicles. *J. Extracell Vesicles* **2014***, 3*, 26913.

32. Graham, J. M. OptiPrep density gradient solutions for nonmammalian organelles. *ScientificWorldJournal* **2002***, 2*, 1444-1448.

33. Groot Kormelink, T.; Arkesteijn, G. J.; Nauwelaers, F. A.; van den Engh, G.; Nolte-'t Hoen, E. N.; Wauben, M. H. Prerequisites for the analysis and sorting of extracellular vesicle subpopulations by high-resolution flow cytometry. *Cytometry A.* **2016***, 89*, 135-147.

34. Bartok, B.; Firestein, G. S. Fibroblast-like synoviocytes: key effector cells in rheumatoid arthritis. *Immunol. Rev.* **2010***, 233*, 233-255.

35. Ponta, H.; Sherman, L.; Herrlich, P. A. CD44:

from adhesion molecules to signalling regulators. *Nat. Rev. Mol. Cell Biol.* **2003***, 4*, 33-45.

36. Mikecz, K.; Dennis, K.; Shi, M.; Kim, J. H. Modulation of hyaluronan receptor (CD44) function in vivo in a murine model of rheumatoid arthritis. *Arthritis Rheum.* **1999***, 42*, 659-668.

37. Hoog, J. L.; Lotvall, J. Diversity of extracellular vesicles in human ejaculates revealed by cryo-electron microscopy. *J. Extracell Vesicles* **2015***, 4*, 28680.

38. Yuana, Y.; Koning, R. I.; Kuil, M. E.; Rensen, P. C.; Koster, A. J.; Bertina, R. M.; Osanto, S. Cryo-electron microscopy of extracellular vesicles in fresh plasma. *J. Extracell Vesicles* **2013***, 2*, 10.3402/jev.v2i0.21494. eCollection 2013 Dec 31.

39. Linares, R.; Tan, S.; Gounou, C.; Arraud, N.; Brisson, A. R. High-speed centrifugation induces aggregation of extracellular vesicles. *J. Extracell Vesicles* **2015***, 4*, 29509.

40. Yuana, Y.; Boing, A. N.; Grootemaat, A. E.; van der Pol, E.; Hau, C. M.; Cizmar, P.; Buhr, E.; Sturk, A.; Nieuwland, R. Handling and storage of human body fluids for analysis of extracellular vesicles. *J. Extracell Vesicles* **2015***, 4*, 29260.

41. van Antwerpen, R.; La Belle, M.; Navratilova, E.; Krauss, R. M. Structural heterogeneity of apoB-containing serum lipoproteins visualized using cryo-electron microscopy. *J. Lipid Res.* **1999***, 40*, 1827-1836.

42. Masuko, K.; Murata, M.; Yudoh, K.; Kato, T.; Nakamura, H. Anti-inflammatory effects of hyaluronan in arthritis therapy: Not just for viscosity. *Int. J. Gen. Med.* **2009***, 2*, 77-81.

43. Smith, M. M.; Ghosh, P. The synthesis of hyaluronic acid by human synovial fibroblasts is influenced by the nature of the hyaluronate in the extracellular environment. *Rheumatol. Int.* **1987***, 7*, 113-122.

44. Rilla, K.; Tiihonen, R.; Kultti, A.; Tammi, M.; Tammi, R. Pericellular hyaluronan coat visualized in live cells with a fluorescent probe is scaffolded by plasma membrane protrusions. *J. Histochem. Cytochem.* **2008***, 56*, 901-910.

45. Mu, W.; Rana, S.; Zoller, M. Host matrix modulation by tumor exosomes promotes motility and invasiveness. *Neoplasia* **2013***, 15*, 875-887.

46. Choi, D. S.; Park, J. O.; Jang, S. C.; Yoon, Y. J.; Jung, J. W.; Choi, D. Y.; Kim, J. W.; Kang, J. S.; Park, J.; Hwang, D.; Lee, K. H.; Park, S. H.; Kim, Y. K.; Desiderio, D. M.; Kim, K. P.; Gho, Y. S. Proteomic analysis of microvesicles derived from human colorectal cancer ascites. *Proteomics* **2011***, 11*, 2745-2751.

47. Park, J. O.; Choi, D. Y.; Choi, D. S.; Kim, H. J.; Kang, J. W.; Jung, J. H.; Lee, J. H.; Kim, J.; Freeman, M. R.; Lee, K. Y.; Gho, Y. S.; Kim, K. P. Identification and characterization of proteins isolated from microvesicles derived from human lung cancer pleural effusions. *Proteomics* **2013***, 13*, 2125-2134.

48. Majeed, M.; McQueen, F.; Yeoman, S.; McLean, L. Relationship between serum hyaluronic acid level and disease activity in early rheumatoid arthritis. *Ann. Rheum. Dis.* **2004***, 63*, 1166-1168.

49. Turan, Y.; Bal, S.; Gurgan, A.; Topac, H.; Koseoglu, M. Serum hyaluronan levels in patients with knee osteoarthritis. *Clin. Rheumatol.* **2007***, 26*, 1293-1298.

50. Wyatt, H. A.; Dhawan, A.; Cheeseman, P.; Mieli-Vergani, G.; Price, J. F. Serum hyaluronic acid concentrations are increased in cystic fibrosis patients with liver disease. *Arch. Dis. Child.* **2002***, 86*, 190-193.

51. Peng, C.; Wallwiener, M.; Rudolph, A.; Cuk, K.; Eilber, U.; Celik, M.; Modugno, C.; Trumpp, A.; Heil, J.; Marme, F.; Madhavan, D.; Nees, J.; Riethdorf, S.; Schott, S.; Sohn, C.; Pantel, K.; Schneeweiss, A.; Chang-Claude, J.; Yang, R.; Burwinkel, B. Plasma hyaluronic acid level as a prognostic and monitoring marker of metastatic breast cancer. *Int. J. Cancer* **2016***, 138*, 2499-2509.

2

SUPPLEMENTARY INFORMATION CHAPTER 2
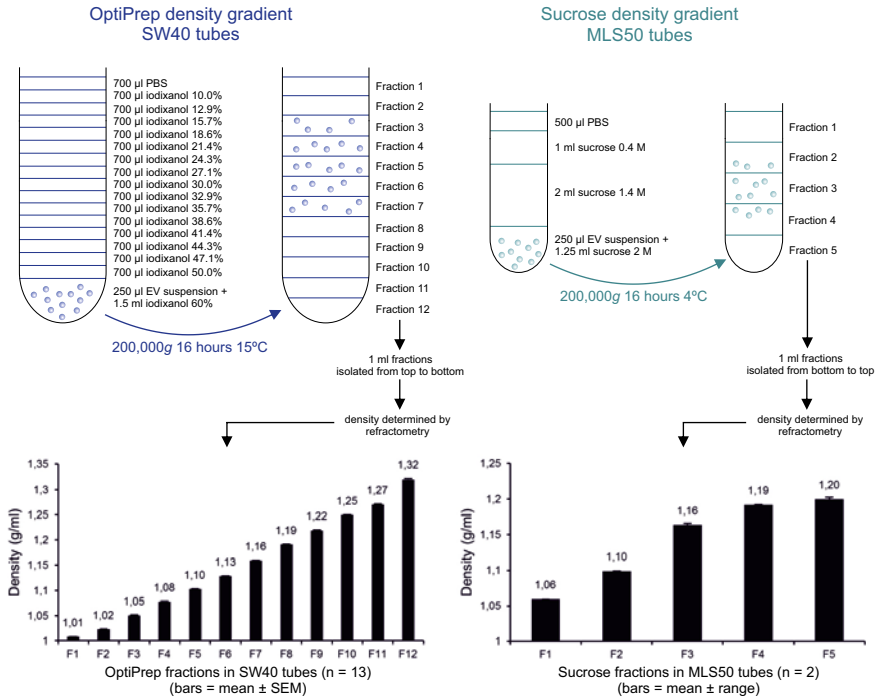
Supplementary Figure 1 Composition of OptiPrep (iodixanol) and sucrose density gradients in, respectively, SW40 tubes (12.95 ml) and MLS50 tubes (5 ml). In OptiPrep, SF-derived EVs float at densities 1.02-1.16 g/ml with highest concentrations at 1.05-1.10 g/ml. In sucrose, similar EVs float at densities 1.10-1.19 g/ml, with highest concentration around 1.16 g/ml. Different floating densities for EVs in iodixanol vs. sucrose gradients can be the result of gradient design, but can also be introduced by density calculation for the two solutions. For sucrose solutions standard refractive indices were used. For iodixanol, density was calculated using the following formula: 3,4394(refractive index)-3,5870 [32].

2
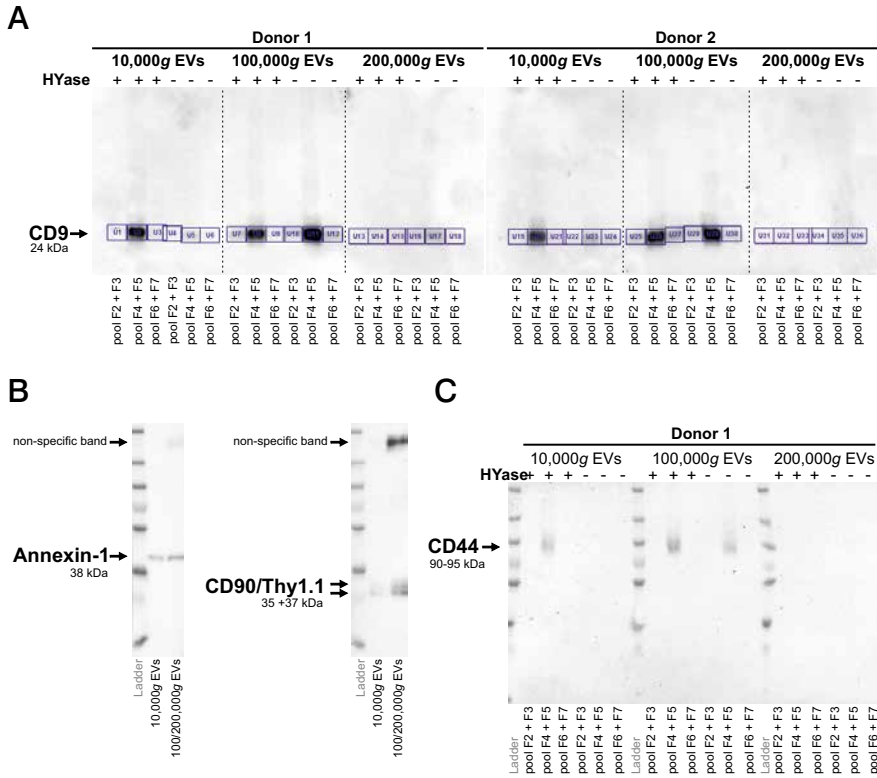
Supplementary Figure 2 Western blotting of SF-derived EV proteins. **A)** Raw data corresponding to Figure 3 including boxes set for band quantification. Detection of CD9 (tetraspanin; EV marker) on EVs from healthy SF. **B)** Detection of Annexin-1 (phospholipid binding protein; EV marker; anti-inflammatory maker) and CD90/Thy1.1 (fibroblast marker) on EVs from healthy SF. For this particular analysis EVs were isolated from HYase-treated healthy SF by using centrifugation steps of 10,000g (= 10,000g EVs), immediately followed by 200,000g omitting the 100,000g step (= 100/200,000g EVs, representing a pool of all EVs that are pelleted if using subsequent 100,000g and 200,000g centrifugation steps). Isolated EVs were floated in sucrose gradients followed by western blotting. **C)** Detection of CD44 (HA receptor; fibroblast-like synovioctye marker) on EVs of healthy SF by western blotting. EVs were isolated from HYase-treated or non-treated healthy SF and floated in OptiPrep gradients. Pools of OptiPrep fractions F2-F7 were analyzed using western blotting (F2 = low density; F7 = high density).
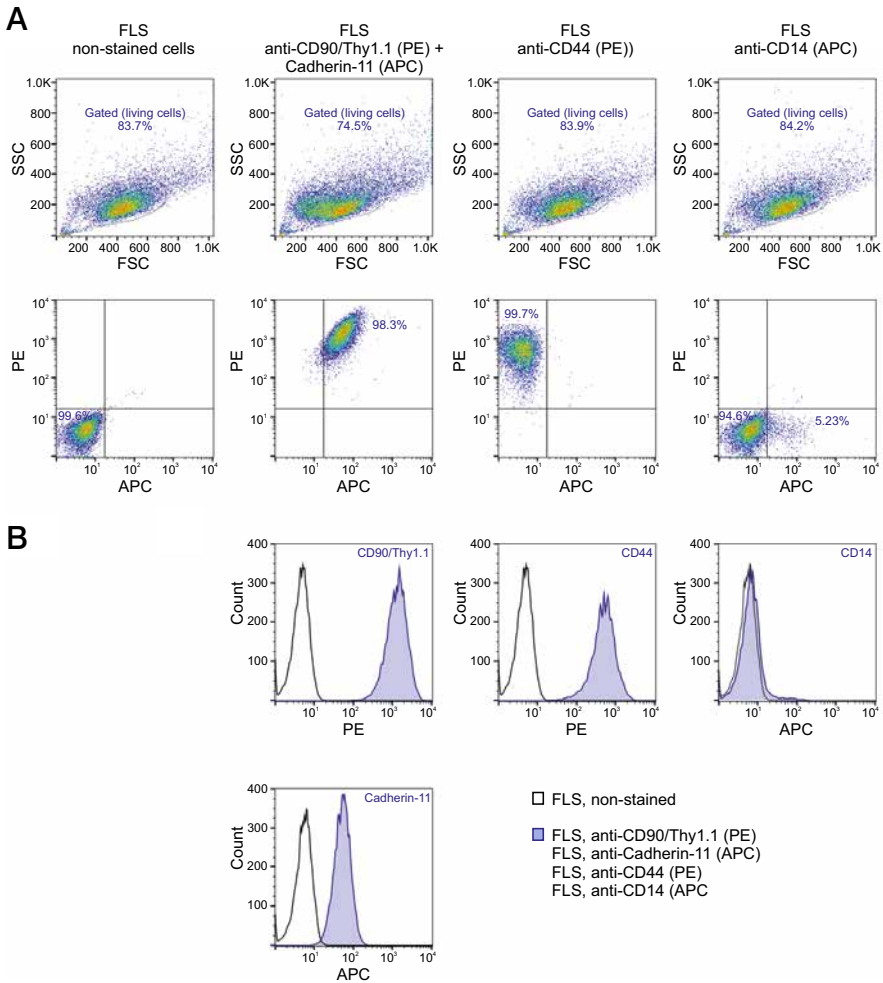
Supplementary Figure 3 Flow cytometry analysis of primary equine fibroblast-like synoviocytes (FLS) stained for CD90/Thy1.1 and Cadherin-11 (both fibroblast markers), for CD44 (HA-receptor) or for CD14 (macrophage marker). **A)** Scatter plots for forward scatter (FSC) x side scatter (SSC) and PE- or APC-signal show that >98% of cells are positive for CD90/Thy1.1 (PE conj.), Cadherin-11 (APC conj.) and CD44 (PE conj.). Only 5% of cells are positive for CD14 (APC-conj.), indicating that the contribution of macrophages in this experiment is negligible. **B)** Overlay histograms of non-stained cells versus cells stained against CD90/Thy1.1, Cadherin-11, CD44 or CD14. A complete population shift of stained cells can be seen for CD90/Thy1.1, Cadherin-11 and CD44. The population shift is absent for CD14 staining. Together, these data verify the fibroblast origin of the cells in this experiment.

Supplementary Figure 2 (*Continued*)

Materials and methods: Synovial membrane was harvested with owner consent from the femoropatellar joints of adult Warmblood horses euthanised at the Utrecht University Equine Hospital (Fac. Veterinary Medicine, Utrecht University, Utrecht, the Netherlands).All horses were euthanised for reasons other than joint disease. Synovial membrane tissue was digested with Type 1 clostridial collagenase (Worthington, Lakewood, NJ, USA) (210 U/ml in RPMI medium) for 3 hours at 37°C. Cells were pelleted and washed during several centrifugation steps and finally filtered through a 70 μm cell strainer, pelleted and suspended in DMEM/F12 culture medium. FLS were cultured for 3-4 days and stored in liquid nitrogen (passage 1). For flow cytometry experiments, stored cells were cultured until passage 3. For single or double antibody staining, $5x10^5$ cells were incubated with 50 μl staining solution containing the following volumes of antibodies: 7 μl anti-CD90/Thy1.1 (clone MRC-OX-7, PE conj., Abcam, Cambridge, UK) and 7 μl anti-cadherin-11 (clone 667039, APC conj., R&D Systems, Minneapolis, MN, USA) or 0.25 μl anti-CD44 (clone IM7, PE-conj., eBioscience, San Diego, CA, USA) or 3.5 μl anti-CD14 (clone 61D3, APC conj., eBioscience, San Diego, CA, USA). Fluorescent PE- or APC-signal was measured on a FACS Calibur flow cytometer (Becton Dickinson) and data were analyzed with FlowJo v10.07 software.

2

3

Dynamics and possible functional role of synovial fluid extracellular vesicles in LPS-induced acute synovitis

Janneke Boere [a]
Chris H. A. van de Lest [a,b]
Sten F. W. M. Libregts [b]
Ger J. A. Arkesteijn [b,c]
Willie J. C. Geerts [d]
Janny C. de Grauw [a]
Stefan M. Cokelaere [a]
Saskia G.M. Plomp [a]
Jos Malda [a,e]
Marca H.M. Wauben [b]
P. René van Weeren [a]

Departments of Equine Sciences[a], Biochemistry & Cell Biology[b], and Infectious Diseases and Immunology[c] of Faculty of Veterinary Medicine, Utrecht University, Utrecht, the Netherlands; Department of Cryo-Electron Microscopy[d], Bijvoet Center for Biomolecular Research, Utrecht, the Netherlands; Department of Orthopaedics[e], University Medical Center Utrecht, Utrecht, the Netherlands

ABSTRACT

Objective. To investigate dynamics and functionality of extracellular vesicles (EVs) in inflammatory joint disease, using a controlled acute synovitis model in horses.

Methods. Extracellular vesicles were isolated from synovial fluid (SF) from equine joints that had been challenged by single intra-articular injections of lipopolysaccharide (LPS), using differential ultracentrifugation and density gradient floatation. With single EV-based high-resolution flow cytometry, quantitative and qualitative EV analysis was performed at 8 hours (LPS-8h), 24 hours (LPS-24h) and 168 hours (LPS-168h) post LPS-injection. Morphology and protein content of EVs were investigated using cryo-transmission-electron microscopy and Western blotting. Ultimately, possible functional effects of these EVs were analysed by in vitro incubation of 3D chondrocyte cultures with EV-enriched ultracentrifugation-pellets (EVp).

Results. Extracellular vesicle concentration in SF peaked at LPS-8h and gradually decreased to baseline at LPS-168h. Remarkably, the percentage of CD44+ EVs was strongly increased at LPS-24h, which was indicative for either specific influx or retention of this EV subset. EVs during inflammation were morphologically similar to EVs in healthy SF and contained, besides CD44 and CD9, Annexin-A1 and MHC-II. Incubation of chondrocytes with EVp from LPS-8h and LPS-24h resulted in upregulation of matrix metalloproteinase (MMP) activity, followed by changes in gene expression that suggest an inflammation-attenuating effect, which was most prominent at LPS-24h for most factors measured.

Conclusion. This study shows the dynamics of total EVs and the CD44+ EV subset in SF during acute joint inflammation and suggests a possible role of EVs in resolving inflammatory effects.

INTRODUCTION

There is general agreement that inflammation is a hallmark of virtually all joint disorders [1], but the intensity may vary according to the specific disease, *e.g.* rheumatoid arthritis (RA) and osteoarthritis (OA), and the stage of the disorder. It has been known for long that joint inflammation is characterised by often substantial increases in the production of chemokines, cytokines and catabolic enzymes [2]. More recently, it has become clear that also extracellular vesicles (EVs) are present in substantial amounts in the synovial fluid (SF) of patients with RA and OA [3-6]. Extracellular vesicles are cell-derived submicron lipid bilayer enclosed particles that facilitate cell-cell communication [7,8]. Since they have been found to be efficient transporters of signalling molecules, such as proteins, lipids and nucleic acids [8,9], the interest in EVs and their potential role in pathological processes has increased considerably in recent years, including in articular pathology [6,10]. The exact role of EVs in the control of joint homeostasis, however, is not fully understood yet. In addition to the catabolic function reported for EVs during joint inflammation [3,11-13], recent insights indicate that subpopulations of EVs might also be involved in protection of articular cartilage [14]. Extracellular vesicles in synovial fluid (SF) have so far been suggested to originate from synovial fibroblasts [15,16], platelets [17], erythrocytes [3], neutrophils [14], monocytes and T-cells [12,13]. They therefore make up a complex and heterogeneous population of which detailed information about characteristics is scant thus far. We recently described the presence of a CD44 positive (CD44+) EV subset in SF of healthy equine joints [15]. CD44 is a transmembrane glycoprotein that is abundantly expressed by synovial fibroblasts and neutrophils [15,18] and serves as the receptor for hyaluronic acid (HA; hyaluronan) [19]. Since HA–CD44 crosslinking has been associated with neutrophil recruitment and activation at sites of chronic inflammation [20], this subset is of particular interest in studying EV dynamics in arthritis.

Based on the close similarities with human joints, especially in a biomechanical sense, large animal models are preferred for the study of molecular mechanisms underlying joint pathology [21]. Experimentally induced synovitis in horses is a well-studied model that resembles septic arthritis in humans [22,23]. Previously, we have investigated inflammatory mediators in a lipopolysaccharide (LPS)-induced synovitis model in horses [24], demonstrating a rapid, local release of pro-inflammatory peptide and lipid mediators and an increase of matrix metalloproteinase (MMP) activity in the SF. In addition, a major influx of leukocytes, predominantly neutrophils, was found. Given the substantial number of EVs in SF of human patients with inflammatory joint diseases, we here analyzed well-preserved SF samples from equine LPS-induced synovitis studies and performed quantitative and qualitative

analyses of EVs, including the CD44+ subset, during the course of acute inflammation. Further, EV-containing ultracentrifugation-pellets (EVp) were tested for functional effects on three-dimensional (3D) healthy chondrocyte cultures *in vitro* to investigate whether EVs in the SF of joints with acute synovitis may have a primarily pro- or anti-inflammatory action.

MATERIALS AND METHODS

An extended description of the methodologies used in this manuscript can be found as supplementary information. Extracellular vesicle isolation and analysis protocols were based on previously published work [15].

Ethical considerations. All *in vivo* experiments were approved by the Utrecht University Animal Ethics Committee (DEC), the Animal Welfare Body (IvD), and the Central Authority for Scientific Procedures on Animals (CCD) under license number 10800, according to the Dutch Experiments on Animals Act and conform the European Directive 2010/63/EU.

Experimental LPS-induced acute synovitis and collection of SF. All *in vivo* experiments were performed with skeletally mature horses with no known history of orthopaedic disorders. Synovial fluid samples originated from 3 different studies (see supplementary information) in which animals received a single-dose intra-articular injection of LPS from *E. Coli* O55:B5 (Sigma Aldrich, St. Louis, MO, USA). Synovial fluid was collected by sterile arthrocentesis prior to LPS-injection (LPS-0h, baseline) and at 8 (LPS-8h), 24 (LPS-24h) or 168 hours (LPS-168h) post LPS-injection. Synovial fluid was cleared from cells by centrifugation at 2,700g, (30 min, RT), aliquoted and stored at -80°C. Fresh aliquots of SF collected at LPS-0h and LPS-8h were used for total nucleated cell count (using an automated particle counter), total protein measurement (by refractometry) and cytology (by smear assessment).

EV isolation from SF. Cell-free SF (starting volumes 0.6-2 ml) was thawed, incubated with hyaluronidase solution (HYase Type II from sheep testes, Sigma-Aldrich, St. Louis, MO, USA) (1500 U/ml in H_2O; 20 μl per ml SF) for 15 min at 37°C, and centrifuged at 1000g (10 min, RT) to remove aggregates. Samples were topped up with PBS and subsequently ultracentrifuged at 10,000g (35 min, 4°C) and 200,000g (120 min, 4°C) resulting in 10K and 200K EV-pellets (EVp).

Single-EV-based high-resolution flow cytometry (FCM). Single-EV-based high-resolution FCM was performed using an optimised jet-in-air-based BD Influx™

flow cytometer (BD Biosciences Europe, Erembodegem, Belgium), as described previously [25,26]. See supplementary information for details. Labelling of EVs with PKH67 and anti-CD44 antibody was performed as described previously [15] with minor modifications, followed by density gradient floatation in sucrose to separate labelled EVs from unbound dye and antibodies. Twelve fractions of 1 ml were collected from top (F1, lowest density) to bottom (F12, highest density). Densities were determined by refractometry. Sucrose fractions were diluted 1:10 in PBS for EVs from healthy SF or diluted 1:66 for EVs from synovitis SF to avoid mass coincidence, so called swarm detection [27].

Cryo-TEM. 10K and 200K EVp were subjected to density gradient floatation in small sucrose block gradients. Five fractions of 1 ml were collected from bottom (F5) to top (F1). Densities were determined by refractometry. Gradient fractions F2, F3, and F4 of each gradient were pooled and diluted (1:10) with PBS. EVs were again pelleted by ultracentrifugation at 200,000g (60 min, 4°C), after which pellets were processed for vitrification and cryo-transmission-electron microscopy (cryo-TEM), as previously described [15]. Morphological analysis of EVs was performed identical to previously described [15].

Western blotting. The same sucrose fractions that were analysed by high-resolution FCM were used for protein identification by Western blotting. Gradient fractions of 375 µl were pooled in pairs (*i.e.* fractions F2+F3 [low density], F4+F5 [medium density], F6+F7 [high density]), diluted in PBS and EVs were pelleted by ultra-centrifugation at 200,000g (90 min, 4°C). Pellets were resuspended in 65 µl non-reducing SDS-PAGE sample buffer and processed for Western Blotting using antibodies against CD9, CD44, major histocompatibility complex II (MHC-II) and Annexin-A1 (AnxA1).

3D primary chondrocyte culture with SF-derived EVp. Because sucrose used for density gradient purification of EVs can induce cell stress in culture, chondrocytes were stimulated with freshly prepared EV pellets ("EVp"); these were pools of the 10K and 200K differential ultracentrifugation pellets enriched for EVs.
Chondrocytes were isolated from fresh full thickness cartilage that was harvested post-mortem, with owner consent, from the distal articular surfaces of the metacarpal bones of two adult Warmblood horses. Frozen chondrocytes (passage 0) were thawed and expanded in monolayer for 7 days, separately for each donor. Confluent cells were seeded (passage 1) in 96-well plates. To form 3D cell cultures, plates were centrifuged at $\sim$ 40g (5 min, RT). 3D cultures were expanded for 48 hours, then transferred to 12-well plates (TC-coated, Greiner Bio-One, Kremsmünster, Austria) and incubated for 24 hours with 100 µl EVp (pooled 10K EVp + 200K EVp isolated

3

from 0.5 ml SF) or 100 µl fresh medium ("no EVp"). Chondrocyte 3D cultures of donor 1 and donor 2 received identical EVp (EVp set 1). In addition, two LPS control conditions were taken along: 1) LPS only (10 ng/ml, 1 µg/ml or 10 µg/ml), and 2) EVp from healthy SF (LPS-0h) spiked with 0.005 ng/ml or 0.05 ng/ml LPS prior to ultra-centrifugation. For details and medium conditions, see supplementary information. Culture medium was collected and stored in aliquots at −80°C for further analysis. Cells were processed for RNA isolation and subsequent qPCR analysis. The experiment was repeated for chondrocyte donor 1 with EVp set 2. See Supplementary Table 1 for conditions and EVp sets used.

Gene expression analysis (qPCR). RNA was isolated from stimulated chondrocytes by use of the RNeasy Mini Isolation Kit (Qiagen, Hilden, Germany), followed by cDNA synthesis with the I-script CDNA synthesis kit (Bio-Rad, Hercules, CA, USA). qPCR was performed and gene expression was normalised according to three reference genes. Primer sets (Eurogentec, Maastricht, The Netherlands) for the equine genes of interest were designed with PerlPrimer v.1.1.14., based on known sequences from public databases (www.ensembl.org/index.html and www.ncbi.nlm.nih.gov) and verified using BLAST (http://blast.ncbi.nlm.nih.gov/). For primer sequences, amplicon size and annealing temperatures see Supplementary Table 2.

MMP assay. A fluorimetric assay to determine overall matrix MMP activity based on cleavage of the fluorogenic peptide substrate FS-6 was used as described previously [24,28] with minor modifications.

CCL2 enzyme-linked immunosorbent assay (ELISA). A sandwich ELISA was designed using rabbit anti-equine C-C motif chemokine 2 (CCL2) (King Fisher, Saint Paul, MN, USA) as capture antibody and biotinylated rabbit anti-equine CCL2 (King Fisher, Saint Paul, MN, USA) as detection antibody. Recombinant CCL2 (King Fisher, Saint Paul, MN, USA) was used to prepare the standard curve (0-2.5 ng/ml).

Prostaglandin measurement. After addition of 100 µl internal standard (25,24-dimethyl-PGF2a, 40 pg/µl) to 200 µl sample (culture medium) and acidifying the solution with 200 µl 0.2 M NH4COOH pH 3.3, eicosanoids were extracted by mixing each sample with 800 µl ethyl acetate 0.002% butylated hydroxytoluene. After thorough mixing and centrifugation at 15,000g for 5 minutes the lower water phase was frozen for 30 min at −80°C and the upper organic (liquid) phase collected. This extraction was repeated with another 800 µl ethyl acetate 0.002% butylated hydroxytoluene. After evaporation of the pooled ethyl acetate extracts (SpeedVac, Savant, Thermo Scientific, Waltham, MA, USA) the dried samples were dissolved in 60 µl 30% methanol and analysed by liquid chromatography-mass spectrometry (LC/

MS), as described earlier [29] using a 4000 QTRAP system (Applied Biosystems, Nieuwerkerk aan den IJssel, The Netherlands). A standard curve of a mixture of prostaglandins (6.25-200 pg/µl) was taken along.

Statistical analysis. Significant gene expression differences relative to "No EVp" or to "EVp LPS-0h" were calculated, after ^{2}log transformation of the relative difference, in SPSS 22.0 software (IBM, Chicago, USA), using a linear mixed model with "EVp donor" as subject (repeated measures) and "chondrocyte donor" as random factor. Since the expected value under the H_0-hypothesis is "0" (*i.e.* ^{2}log(1)), the intercept was omitted in the model. For post-hoc analysis (LPS-8h and LPS-24h vs. LPS-0h), a Šidák-multiple comparison correction was used. Differences with p-values < 0.05 were considered significant.

3

RESULTS

The clear inflammatory effect as described in the original *in vivo* study (study 1 [24]) was confirmed in *in vivo* studies 2 (Cokelaere S.M. *et al.*, manuscript in preparation; data not shown) and 3. In study 3, we found increased numbers of total nucleated cells at LPS-8h (LPS-0h: 0.33x10^9 cells/l; LPS-8h: 22.84x10^9 cells/l) and increased total protein levels (LPS-0h: 1.0 g/dl; LPS-8h: 2.2 g/dl). Subsequent cytological smear assessment indicated that the majority of nucleated cells were white blood cells of which $> 90\%$ were neutrophils. These data confirm that acute joint inflammation was induced at LPS-8h in all animals analysed for the current investigation.

Morphological aspects of EVs in SF from LPS-challenged joints

At LPS-8h, EVs were isolated (n=1 horse) and analysed by cryo-TEM. A total of 197 10K and 485 200K vesicular structures with heterogeneous shapes and sizes were visualised (Figure 1A, 1B). Comparison with data from healthy joints [15] suggested no major differences in the proportion of spherical EVs (82% of 10K EVs and 53% of 200K EVs at LPS-8h were spherical, against 65% and 67% in the healthy sample, respectively), while a substantial difference was observed in the number of "other small particles" (25% compared to 3% in the healthy sample). Size-wise, relatively many very small EVs (20-100 nm) were detected in both the 10K and 200K centrifugation steps, and therefore average vesicle diameters for 10K and 200K spherical EVs in the synovitis sample were slightly smaller than in healthy SF (Figure 1C).
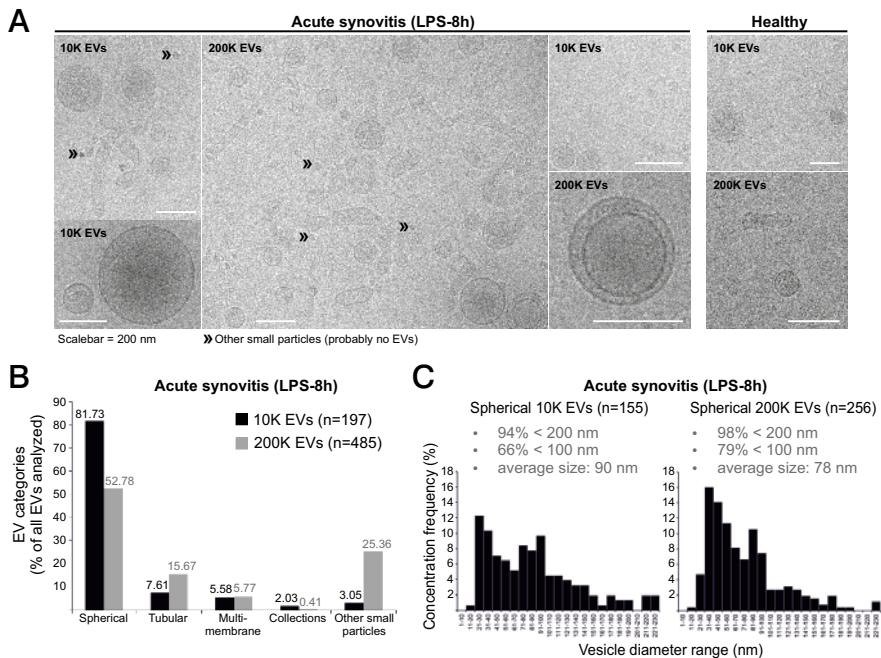
Figure 1 Cryo-TEM analysis of EVs isolated from a joint with acute synovitis and floated in sucrose gradients. **A)** Representative images of 10K and 200K EVs at LPS-8h, compared to the healthy situation which was analysed in identical manner in our previous work [15]. **B)** Quantification of typical EV morphologies in SF at LPS-8h. The 200K centrifugation step retrieved also a significant number of particles without a clear membrane, referred to as "other small particles"; examples are indicated with » in 1A (these particles are not considered EVs; possibly these are lipoproteins [30]). **C)** Size distribution for spherical 10K and 200K EVs from SF for LPS-8h.

EV dynamics in LPS-induced arthritis

Supplementary Figure 1A shows the details for the single EV-based high-resolution FCM and gating strategy as was used in this study. High-resolution FCM revealed that the majority of EVs floated in fractions F3-F9 at densities 1.10-1.21 g/ml (Figure 2A). The total EV count and the percentage of CD44+ EVs strongly increased at LPS-8h compared to LPS-0h (Figure 2A). Western blot analysis confirmed the expression of CD9 (tetraspanin) on EVs derived from both healthy SF and synovitis SF (Figure 2B). In addition, 3 other EV-associated proteins were detected in the LPS-8h samples (Figure 2B): CD44 (HYase-receptor, synovial fibroblast marker), AnxA1 (anti-inflammatory protein) and MHC-II (marker for antigen-presenting cells), which were all undetectable in the LPS-0h samples. For MHC-II a specific enrichment on 200K EVs was found at LPS-8h (Figure 2B).
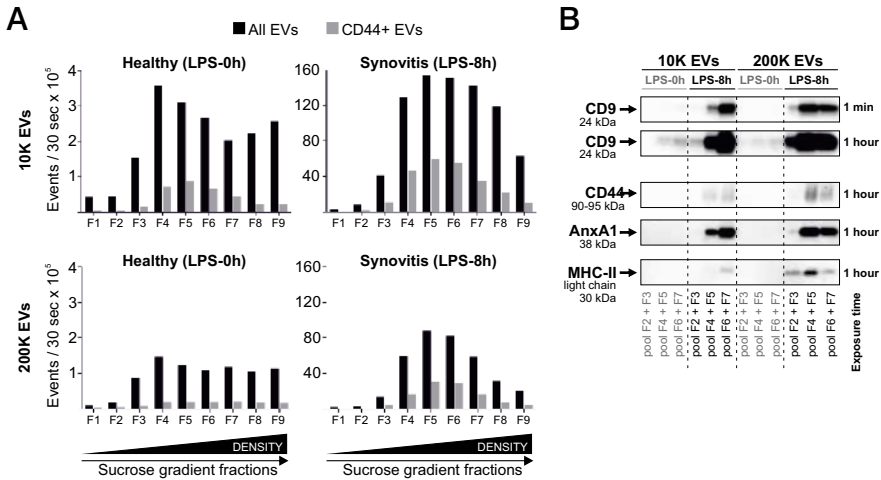
Figure 2 Flow cytometric analysis and protein analysis of SF-derived EVs during LPS-induced synovitis. **A)** Single EV-based high-resolution FCM of SF-derived 10K and 200K EVs at LPS-0h (baseline; n=1) and LPS-8h (n=1). Single EVs (PKH67+) were measured per 30 seconds in sucrose density gradient fractions containing EVs labelled with anti-CD44 antibody and the generic dye PKH67 (see Supplementary Figure 1A for gating strategy). The majority of EVs floated in fractions F3-F9 at densities 1.10-1.21 g/ml. Fractions F10, F11 and F12 (not shown) contained free PKH67 dye and unbound fluorophore-conjugated that interfere with high-resolution FCM; these fractions were therefore not taken along in the analysis. Densities of individual fractions (g/ml) are: F1=1.06, F2= 1.08, F3=1.10, F4=1.12, F5=1.14, F6=1.16, F7=1.18, F8=1.20, F9=1.21. **B)** Detection of CD9 (general EV marker), CD44 (HYase-receptor; synovial fibroblast marker), AnxA1 (Annexin-A1; anti-inflammatory protein) and MHC-II (major histocompatibility complex; marker for antigen-presenting cells) by Western blot in EVs from pools of gradient fractions from 2A.

In a time course experiment, we analysed the EV numbers during the phase of acute inflammation and the resolution phase (Figure 3). At LPS-8h, maximal EV concentrations were reached, with a 22-fold and 3-fold increase compared to LPS-0h for 10K and 200K EVs, respectively (Figure 3A). Thereafter, a steep decline in the number of both 10K and 200K EVs followed over the next 16 hours. At LPS-168h, EV concentrations had returned to baseline.

The number of CD44+ EVs rose substantially in the first 8 hours after LPS administration with a 37-fold and 7-fold increase compared to LPS-0h for 10K and 200K CD44+ EVs, respectively (Figure 3A). At LPS-24h, the number of CD44+ 10K EVs had fallen by a factor 2 compared to LPS-8h. In contrast, the numbers of CD44+ 200K EV increased 1.3-fold compared to LPS-8h, while CD44- 200K EVs declined 8-fold during that time. This resulted in 45% of 200K EVs being CD44+ at LPS-24h,
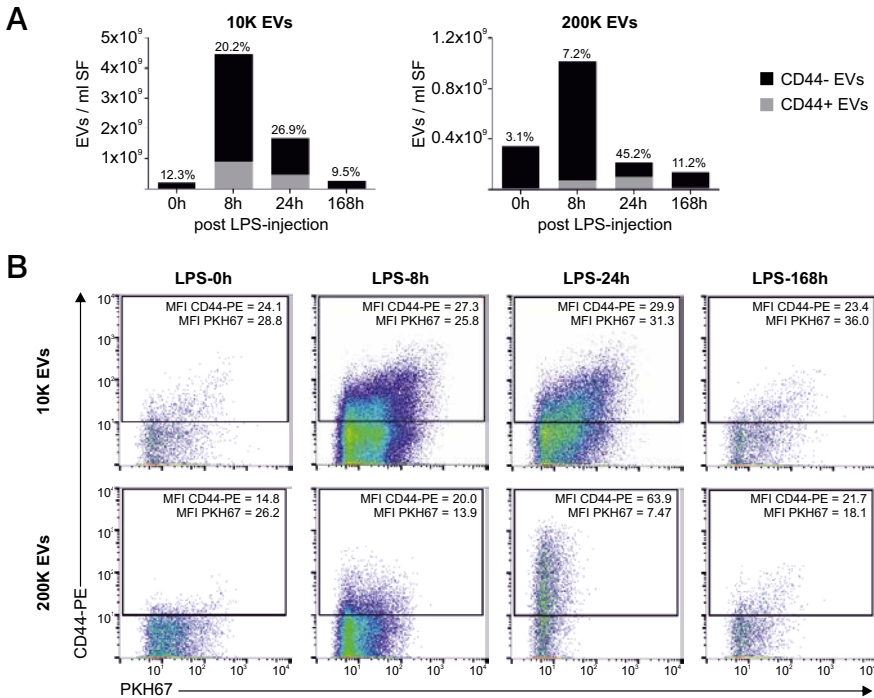
A

B

Figure 3 Single EV-based high-resolution FCM of SF-derived EVs during LPS-induced synovitis. **A)** EV concentration in SF calculated as sum of single-EV measurements (PKH67+ events) in sucrose density gradient fractions F3-F9 containing EVs labelled with anti-CD44 antibody and the generic dye PKH67 (see Supplementary Figure 1A for gating strategy and details for calculation). Bars are pools of 3 animals. For each time point 0.2 ml cell-free SF per animal was pooled to acquire a starting volume of 0.6 ml SF per condition for isolation of EVs. Percentages above bars represent CD44+ EVs (grey bars). **B)** Representative scatter plots for EVs measured in fraction 6 (density = 1.16 g/ml) of sucrose density gradients. Dots represent single measured events in 30 seconds. The square gates (set as such based on an isotype control for the anti-CD44 antibody) hold the CD44+ EVs in which the mean fluorescent intensity (MFI) is the geometric mean of the fluorescent signal on the x-axis (PKH67) or y-axis (CD44-PE) in the gate. See Supplementary Figure 1B for additional plots.

of which approximately one third newly originated from, or infiltrated into the joint between LPS-8h and LPS-24h. In contrast to the 10K CD44+ EVs, this population is characterised by a high mean fluorescent intensity (MFI) for CD44, a low MFI for PKH67 (Figure 3B) and a high forward scatter (rw-FSC) (Supplementary Figure 1B), emphasizing a difference with the majority of EVs in the joint.

Functional characteristics of EV-enriched pellets

In the 3D primary chondrocyte culture with SF-derived EV-enriched pellets (harvested from SF at LPS-0h, LPS-8h and LPS-24h), incubation of cells for 24 hours with EVp from LPS-8h or LPS-24h resulted in significant downregulation of gene expression for a number of genes that are involved in joint inflammation, including inducible nitric oxide synthase (iNOS), interleukin-6 (IL-6), interleukin-1-receptor-1 (IL-1R1), metallo-proteinases ADAMTS-5, and matrix metalloproteinases MMP-3 (stromelysin-1) and MMP-13 (collagenase-3) (Figure 4). For IL-1R1, the effect was only significant for

3
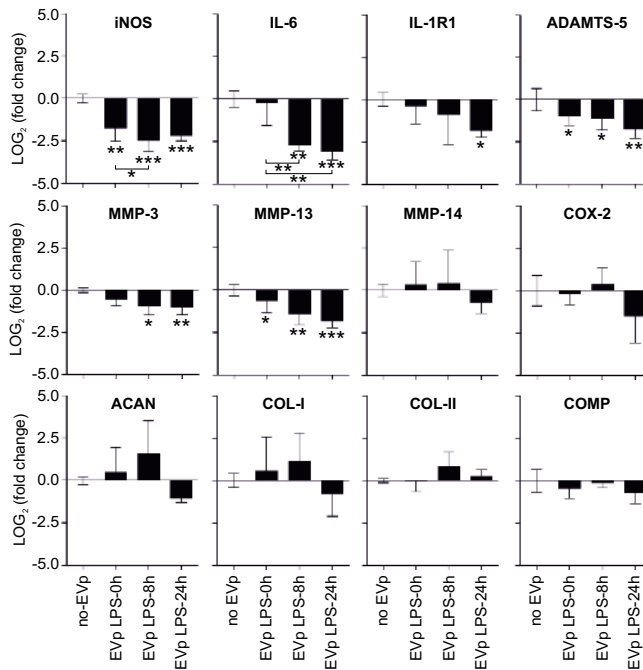
Figure 4 Gene expression changes in chondrocyte 3D cultures after 24 hours incubation with medium only (no EVp) or with EVp (pooled 10K + 200K) from healthy joints (LPS-0h) or acute synovitis at LPS-8h or LPS-24h. Bars represent the mean effect + STDEV of EVp from multiple EVp donors on chondrocytes from 2 cell donors (see Supplementary Table 1 for details). * $p < 0.05$, ** $p < 0.01$, *** $p < 0.001$ (compared to no-EVp or EVp LPS-0h; linear mixed model). iNOS, inducible nitric oxide synthase; IL-6, interleukin-6; IL-1R1, interleukin-1-receptor-1; ADAMTS-5, a disintegrin and metalloproteinase with thrombospondin motif-5; MMP, matrix metalloproteinase; COX-2, cyclooxygenase-2; ACAN, aggrecan; COL-I, collagen type I; COL-II, collagen type II A1; COMP, cartilage oligomeric matrix protein.

incubation with EVp from LPS-24h. Interestingly, in the case of iNOS, ADAMTS-5 and MMP-13 also naive EVp from non-LPS stimulated SF (LPS-0h) had a downregulating effect. For MMP-14 (membrane-type MMP-1), cyclooxygenase-2 (COX-2) and the matrix components collagen-I (COL-I), collagen-II type A1 (COL-II), cartilage oligomeric matrix protein (COMP) and aggrecan (ACAN), no significant changes in gene expression were observed in any of the conditions.

For all genes showing an inflammation mitigating effect of the EVp from SF samples collected at LPS-8h and LPS-24h (Figure 4), EVp from LPS-spiked SF samples, as well as LPS alone, steered gene expression towards a more pro-inflammatory profile, thereby eliminating the possibility of a direct LPS-driven effect (Supplementary Figure 2). Also, the reactions of chemokine CCL2 and prostaglandin-E2 (PGE2) upon stimulation with EVp was different than upon incubation with LPS control samples
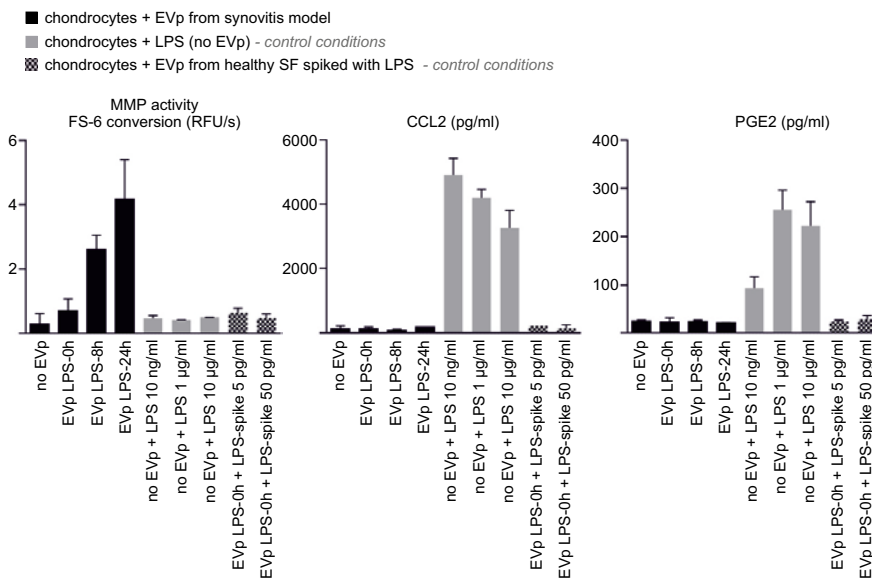
Figure 5 Activity of total matrix metalloproteinases (MMPs) and production of C-C motif chemokine 2 (CCL2) and prostaglandin-E2 (PGE2) in chondrocyte culture medium. Chondrocyte 3D cultures of 1 cell donor were incubated for 24 hours with medium only (no EVp) or with EVp (pooled 10K + 200K) from healthy joints (LPS-0h) or acute synovitis at LPS-8h or LPS-24h (black bars). Control conditions included LPS-containing culture medium (grey bars) or EVp from healthy SF spiked with 2 concentrations of LPS (dotted bars). Graphs represent mean effects of EVp from 2 EVp donors on chondrocytes from 1 cell donor, with error bars being the range (highest and lowest observed values; n=2). For samples included per condition, see Supplementary Table 1.

(Figure 5). Additionally, compared to medium controls, MMP activity was upregulated after incubation with naive EVp and increased gradually for the LPS-8h and LPS-24h conditions. The LPS control conditions, on the contrary, did not induce MMP activity.

DISCUSSION

Extracellular vesicle dynamics were profoundly different between healthy and synovitis SF, characterised by a large increase in total EV concentration in the inflamed condition, even if EV morphology appeared to be grossly similar. When monitoring total EV concentrations during acute inflammation, EVs in SF followed a steep increase, peaking at around 8 hours post-induction and decreasing over a time-course of 168 hours, mirroring the increase and decrease of inflammation-related soluble factors measured previously in these same samples [24]. The results show that EV production and/or infiltration is an active process during the acute phase of synovitis, which is in accordance with earlier statements about the role of EVs in joint inflammation [6,31] and with the high EV concentrations found in patients with arthritis [4,14,32]. The results also indicate that, if measured with high-resolution FCM, the EV concentration in SF could potentially be used as a biomarker for the presence of joint inflammation.

Remarkably, at LPS-24h, when the total concentration of EVs returned almost to baseline values, a population of 200K EVs, highly enriched for CD44, makes up 45% of all 200K EVs present at that time point. The most prevalent inflammatory cell type in acute LPS-induced arthritis is the neutrophil [24], which is known to express CD44 [20]. CD44 has been proposed to interact with HA for neutrophil adhesion and migration [20]. Whereas other potential sources of CD44 are known in the joint, such as synovial fibroblasts [15], it is likely that in the current study the neutrophils were the predominant source of the CD44+ EVs, given their abundance. An additional, but admittedly not conclusive, indication is that, at LPS-8h, EVs carried AnxA1, which has been detected in multiple studies on neutrophil-derived EVs (in SF) [14,33,34].

In addition to AnxA1, we showed the presence of 200K MHC-II+ EVs at LPS-8h. Most likely, these EVs originate from antigen-presenting cells that are typically carriers of MHC-II. We did not succeed in detecting CD14, a marker for monocytes/macrophages, which may suggest that monocyte/macrophage-derived EVs play only a minor role during acute synovitis compared to those derived from neutrophils and antigen-presenting cells. This assumption is in line with the observation that in RA-patients CD14+ EVs were less abundantly present compared to CD66b+ EVs (neutrophil-derived) [14].

The results of the functional studies revealed that the EV-enriched pellets harvested from SF at both LPS-8h and LPS-24h, were functionally active. Interestingly, for some genes the LPS-24h condition reached the highest significant effects, which is remarkable as EV concentrations at LPS-24h are already on their return to baseline. Incubation of chondrocytes with EVp had an inherent inflammation-attenuating effect, which resulted in significant downregulation of genes involved in inflammation, even without stimulation of chondrocytes with a catabolic stimulus such as IL-1β, as was used in similar studies [14]. The genes showing most significant inflammation-attenuating effects (iNOS, IL-6, IL-1R1 and ADAMTS-5) are all involved in inflammatory pathways in joint diseases [35]. COX-2, however, which is also a pro-inflammatory marker, was not affected. This could possibly be explained by the fact that COX-2 is under the control of nitric oxide, which is downstream of (the already downregulated) iNOS [36]. The fact that for MMP-3 and MMP-13 significant downregulation was found, but not for MMP-14, was expected, since MMP-3 and MMP-13 are generally involved in joint inflammation [35], whereas MMP-14 is known for its inflammation-cascading role in more chronic joint diseases such as RA [37].

Ross *et al.* investigated the direct effect of LPS-induced equine synovitis on gene expression in the cartilage and found upregulation of catabolic enzymes related to human OA (MMP-1, ADAMTS-4 and ADAMTS-5) [22]. From the measurements of CCL2 and PGE2 production in the chondrocyte culture medium in our study, however, it can be concluded that inflammation-induced EVp do not aggravate the inflammation cascade. On the other hand, EVp did clearly induce MMP activity. This can explain the parallel downregulation of MMP-3 and MMP-13 gene expression as a negative feedback mechanism, and could be a (short-lasting) controlled matrix remodelling event during the late phase of the acute inflammation. In contrast to the known catabolic function of MMPs in chronic inflammation, MMPs can induce tissue remodelling in the joint as well [38]. In acute synovitis they might in this way facilitate fast travelling of important signalling molecules, possibly EVs, into the dense cartilage. Whether EVs during acute synovitis exert possible pro-inflammatory effects on other articular cell types (*e.g.* synovial fibroblasts) is a topic for future study. Synovial fluid derived EVs from RA and OA patients are able to induce chemokine and cytokine release in synovial fibroblasts [4,5], but these pathologies feature more chronic forms of inflammation in which the synoviocytes themselves already express an (auto) inflammatory phenotype [39]. In addition, EVs are thought to function as modulators of cytokine effects on cells [40]. Whereas the results shown here only reflect the situation after 24h of culture, measurements at multiple time points are prerequisite for final conclusions about the synergy between cytokines and EVs.

It is an interesting assumption that EVs during acute inflammation not only have the earlier reported immunogenic effects [3,7,11,12], possibly even via MHC-II [41-43], but also could convey an anti-inflammatory message to the surrounding tissue, initiating the downregulation of the catabolic cascade induced by locally produced soluble molecules, such as PGE2. This would be in line with the findings of Headland *et al.*, who showed that these EVs are protectors of cartilage during joint inflammation [14] and would explain why in our experiment also naive EVs (LPS-0h) repressed inflammatory gene expression. The repression of catabolic processes such as inflammation underscores the recent concept that EVs may play an important role in maintaining joint homeostasis [10]. Furthermore, the resolution phase of acute inflammation is now envisioned as an orchestrated process for which specific molecules, and possibly also EVs, are responsible [44,45]. Most likely, the content of the EV is the most important component with regard to functionality. The finding that AnxA1, an anti-inflammatory protein that is thought to act as inhibitor of flares of inflammation in RA and gout [33,46], is present on EVs, could suggest that such a role may be more than just hypothetical. However, potentially the EV membrane may be more than just an envelope and could play a role too.

In conclusion, this study presents, for the first time, the EV-dynamics in SF during the course of acute synovitis, from the initiation up to the resolution. There is a large increase of EVs in SF during the acute phase of the inflammation, but at later time points, when the synovitis is resolving and overall EV numbers dwindle, a subpopulation of CD44+ EVs remains present in the joint. The presence of AnxA1 and MHC-II on inflammation-induced EVs suggest a possible role in immune regulation. Functional testing of ultracentrifugation pellets enriched with inflammation-induced EVs *in vitro* showed strong indications for the presence of an anti-inflammatory (protective) effect on cartilage gene expression and induction of matrix remodelling. To verify that these effects are specifically induced by these EVs, additional studies should be undertaken with purified populations of EVs. Nevertheless, the data of this study concur with the theory that EVs are important mediators during inflammatory processes in the joint. Based on our findings, we postulate that subsets of EVs produced during an LPS-induced acute flare, could act as protectors of the joint during the resolution phase of the inflammation.

3

ACKNOWLEDGEMENTS

We thank Tsjester Huppes (DVM, Department of Equine Sciences, Faculty of Veterinary Medicine, Utrecht University) for helping with the animal experiments, and Johannes Bergmann (master student, Utrecht University) for performing cryo-TEM.

DISCLOSURE

During this study, the Wauben research group, Utrecht University, Faculty of Veterinary Medicine, Department of Biochemistry and Cell Biology, had a collaborative research agreement with BD Biosciences Europe, Erembodegem, Belgium, to optimise analysis of EVs using the BD Influx™ flow cytometer.

REFERENCES

1. Attur, M. G.; Dave, M.; Akamatsu, M.; Katoh, M.; Amin, A. R. Osteoarthritis or osteoarthrosis: the definition of inflammation becomes a semantic issue in the genomic era of molecular medicine. *Osteoarthritis Cartilage* **2002***, 10*, 1-4.

2. Rahmati, M.; Mobasheri, A.; Mozafari, M. Inflammatory mediators in osteoarthritis: A critical review of the state-of-the-art, current prospects, and future challenges. *Bone* **2016***, 85*, 81-90.

3. Berckmans, R. J.; Nieuwland, R.; Tak, P. P.; Boing, A. N.; Romijn, F. P.; Kraan, M. C.; Breedveld, F. C.; Hack, C. E.; Sturk, A. Cell-derived microparticles in synovial fluid from inflamed arthritic joints support coagulation exclusively via a factor VII-dependent mechanism. *Arthritis Rheum.* **2002***, 46*, 2857-2866.

4. Berckmans, R. J.; Nieuwland, R.; Kraan, M. C.; Schaap, M. C.; Pots, D.; Smeets, T. J.; Sturk, A.; Tak, P. P. Synovial microparticles from arthritic patients modulate chemokine and cytokine release by synoviocytes. *Arthritis Res. Ther.* **2005***, 7*, R536-44.

5. Reich, N.; Beyer, C.; Gelse, K.; Akhmetshina, A.; Dees, C.; Zwerina, J.; Schett, G.; Distler, O.; Distler, J. H. Microparticles stimulate angiogenesis by inducing ELR(+) CXC-chemokines in synovial fibroblasts. *J. Cell. Mol. Med.* **2011***, 15*, 756-762.

6. Buzas, E. I.; Gyorgy, B.; Nagy, G.; Falus, A.; Gay, S. Emerging role of extracellular vesicles in inflammatory diseases. *Nat. Rev. Rheumatol.* **2014***, 10*, 356-364.

7. Thery, C.; Ostrowski, M.; Segura, E. Membrane vesicles as conveyors of immune responses. *Nat. Rev. Immunol.* **2009***, 9*, 581-593.

8. Yanez-Mo, M.; Siljander, P. R.; Andreu, Z.; Zavec, A. B.; Borras, F. E.; Buzas, E. I.; Buzas, K.; Casal, E.; Cappello, F.; Carvalho, J.; Colas, E.; Cordeiro-da Silva, A.; Fais, S.; Falcon-Perez, J. M.; Ghobrial, I. M.; Giebel, B.; Gimona, M.; Graner, M.; Gursel, I.; Gursel, M.; Heegaard, N. H.; Hendrix, A.; Kierulf, P.; Kokubun, K.; Kosanovic, M.; Kralj-Iglic, V.; Kramer-Albers, E. M.; Laitinen, S.; Lasser, C.; Lener, T.; Ligeti, E.; Line, A.; Lipps, G.; Llorente, A.; Lotvall, J.; Mancek-Keber, M.; Marcilla, A.; Mittelbrunn, M.; Nazarenko, I.; Nolte-'t Hoen, E. N.; Nyman, T. A.; O'Driscoll, L.; Olivan, M.; Oliveira, C.; Pallinger, E.; Del Portillo, H. A.; Reventos, J.; Rigau, M.; Rohde, E.; Sammar, M.; Sanchez-Madrid, F.; Santarem, N.; Schallmoser, K.; Ostenfeld, M. S.; Stoorvogel, W.; Stukelj, R.; Van der Grein, S. G.; Vasconcelos, M. H.; Wauben, M. H.; De Wever, O. Biological properties of extracellular vesicles and their physiological functions. *J. Extracell Vesicles* **2015***, 4*, 27066.

9. EL Andaloussi, S.; Mager, I.; Breakefield, X. O.; Wood, M. J. Extracellular vesicles: biology and emerging therapeutic opportunities. *Nat. Rev. Drug Discov.* **2013***, 12*, 347-357.

10. Malda, J.; Boere, J.; van de Lest, C. H.; van Weeren, P.; Wauben, M. H. Extracellular vesicles - new tool for joint repair and regeneration. *Nat. Rev. Rheumatol.* **2016***, 12*, 243-249.

11. Cloutier, N.; Tan, S.; Boudreau, L. H.; Cramb, C.; Subbaiah, R.; Lahey, L.; Albert, A.; Shnayder, R.; Gobezie, R.; Nigrovic, P. A.; Farndale, R. W.; Robinson, W. H.; Brisson, A.; Lee, D. M.; Boilard, E. The exposure of autoantigens by microparticles underlies the formation of potent inflammatory components: the microparticle-associated immune complexes. *EMBO Mol. Med.* **2013***, 5*, 235-249.

12. Distler, J. H.; Jungel, A.; Huber, L. C.; Seemayer, C. A.; Reich, C. F.,3rd; Gay, R. E.; Michel, B. A.; Fontana, A.; Gay, S.; Pisetsky, D. S.; Distler, O. The induction of matrix metalloproteinase and cytokine expression in synovial fibroblasts stimulated with immune cell microparticles. *Proc. Natl. Acad. Sci. U. S. A.* **2005***, 102*, 2892-2897.

13. Jungel, A.; Distler, O.; Schulze-Horsel, U.; Huber, L. C.; Ha, H. R.; Simmen, B.; Kalden, J. R.; Pisetsky, D. S.; Gay, S.; Distler, J. H. Microparticles stimulate the synthesis of prostaglandin E(2) via induction of cyclooxygenase 2 and microsomal prostaglandin E synthase 1. *Arthritis Rheum.* **2007***, 56*, 3564-3574.

14. Headland, S. E.; Jones, H. R.; Norling, L. V.; Kim, A.; Souza, P. R.; Corsiero, E.; Gil, C. D.; Nerviani, A.; Dell'Accio, F.; Pitzalis, C.; Oliani, S. M.; Jan, L. Y.; Perretti, M. Neutrophil-derived microvesicles enter cartilage and protect the joint in inflammatory arthritis. *Sci. Transl. Med.* **2015***, 7*, 315ra190.

15. Boere, J.; van de Lest, C. H.; Libregts, S. F.; Arkesteijn, G. J.; Geerts, W. J.; Nolte-'t Hoen, E. N.; Malda, J.; van Weeren, P. R.; Wauben, M. H. Synovial fluid pretreatment with hyaluronidase facilitates isolation of CD44+ extracellular vesicles. *J. Extracell Vesicles* **2016***, 5*, 31751.

16. Kato, T.; Miyaki, S.; Ishitobi, H.; Nakamura, Y.; Nakasa, T.; Lotz, M. K.; Ochi, M. Exosomes from IL-1beta stimulated synovial fibroblasts induce osteoarthritic changes in articular chondrocytes. *Arthritis Res. Ther.* **2014***, 16*, R163.

17. Duchez, A. C.; Boudreau, L. H.; Naika, G. S.; Bollinger, J.; Belleannee, C.; Cloutier, N.; Laffont, B.; Mendoza-Villarroel, R. E.; Levesque, T.; Rollet-Labelle, E.; Rousseau, M.; Allaeys, I.; Tremblay, J. J.;

3

Poubelle, P. E.; Lambeau, G.; Pouliot, M.; Provost, P.; Soulet, D.; Gelb, M. H.; Boilard, E. Platelet microparticles are internalized in neutrophils via the concerted activity of 12-lipoxygenase and secreted phospholipase A2-IIA. *Proc. Natl. Acad. Sci. U. S. A.* **2015**, *112*, E3564-73.

18. Ponta, H.; Sherman, L.; Herrlich, P. A. CD44: from adhesion molecules to signalling regulators. *Nat. Rev. Mol. Cell Biol.* **2003**, *4*, 33-45.

19. Murai, T. Lipid Raft-Mediated Regulation of Hyaluronan-CD44 Interactions in Inflammation and Cancer. *Front. Immunol.* **2015**, *6*, 420.

20. Khan, A. I.; Kerfoot, S. M.; Heit, B.; Liu, L.; Andonegui, G.; Ruffell, B.; Johnson, P.; Kubes, P. Role of CD44 and hyaluronan in neutrophil recruitment. *J. Immunol.* **2004**, *173*, 7594-7601.

21. McCoy, A. M. Animal Models of Osteoarthritis: Comparisons and Key Considerations. *Vet. Pathol.* **2015**, *52*, 803-818.

22. Ross, T. N.; Kisiday, J. D.; Hess, T.; McIlwraith, C. W. Evaluation of the inflammatory response in experimentally induced synovitis in the horse: a comparison of recombinant equine interleukin 1 beta and lipopolysaccharide. *Osteoarthritis Cartilage* **2012**, *20*, 1583-1590.

23. Palmer, J. L.; Bertone, A. L. Experimentally-induced synovitis as a model for acute synovitis in the horse. *Equine Vet. J.* **1994**, *26*, 492-495.

24. de Grauw, J. C.; van de Lest, C. H.; van Weeren, P. R. Inflammatory mediators and cartilage biomarkers in synovial fluid after a single inflammatory insult: a longitudinal experimental study. *Arthritis Res. Ther.* **2009**, *11*, R35.

25. Nolte-'t Hoen, E. N.; van der Vlist, E. J.; Aalberts, M.; Mertens, H. C.; Bosch, B. J.; Bartelink, W.; Mastrobattista, E.; van Gaal, E. V.; Stoorvogel, W.; Arkesteijn, G. J.; Wauben, M. H. Quantitative and qualitative flow cytometric analysis of nanosized cell-derived membrane vesicles. *Nanomedicine* **2012**, *8*, 712-720.

26. van der Vlist, E. J.; Nolte-'t Hoen, E. N.; Stoorvogel, W.; Arkesteijn, G. J.; Wauben, M. H. Fluorescent labeling of nano-sized vesicles released by cells and subsequent quantitative and qualitative analysis by high-resolution flow cytometry. *Nat. Protoc.* **2012**, *7*, 1311-1326.

27. Groot Kormelink, T.; Arkesteijn, G. J.; Nauwelaers, F. A.; van den Engh, G.; Nolte-'t Hoen, E. N.; Wauben, M. H. Prerequisites for the analysis and sorting of extracellular vesicle subpopulations by high-resolution flow cytometry. *Cytometry A.* **2016**, *89*, 135-147.

28. Neumann, U.; Kubota, H.; Frei, K.; Ganu, V.; Leppert, D. Characterization of Mca-Lys-Pro-Leu-Gly-Leu-Dpa-Ala-Arg-NH2, a fluorogenic substrate with increased specificity constants for collagenases and tumor necrosis factor converting enzyme. *Anal. Biochem.* **2004**, *328*, 166-173.

29. de Grauw, J. C.; van de Lest, C. H.; van Weeren, P. R. A targeted lipidomics approach to the study of eicosanoid release in synovial joints. *Arthritis Res. Ther.* **2011**, *13*, R123.

30. Sodar, B. W.; Kittel, A.; Paloczi, K.; Vukman, K. V.; Osteikoetxea, X.; Szabo-Taylor, K.; Nemeth, A.; Sperlagh, B.; Baranyai, T.; Giricz, Z.; Wiener, Z.; Turiak, L.; Drahos, L.; Pallinger, E.; Vekey, K.; Ferdinandy, P.; Falus, A.; Buzas, E. I. Low-density lipoprotein mimics blood plasma-derived exosomes and microvesicles during isolation and detection. *Sci. Rep.* **2016**, *6*, 24316.

31. Distler, J. H.; Pisetsky, D. S.; Huber, L. C.; Kalden, J. R.; Gay, S.; Distler, O. Microparticles as regulators of inflammation: novel players of cellular crosstalk in the rheumatic diseases. *Arthritis Rheum.* **2005**, *52*, 3337-3348.

32. Gyorgy, B.; Szabo, T. G.; Turiak, L.; Wright, M.; Herczeg, P.; Ledeczi, Z.; Kittel, A.; Polgar, A.; Toth, K.; Derfalvi, B.; Zelenak, G.; Borocz, I.; Carr, B.; Nagy, G.; Vekey, K.; Gay, S.; Falus, A.; Buzas, E. I. Improved flow cytometric assessment reveals distinct microvesicle (cell-derived microparticle) signatures in joint diseases. *PLoS One* **2012**, *7*, e49726.

33. Cumpelik, A.; Ankli, B.; Zecher, D.; Schifferli, J. A. Neutrophil microvesicles resolve gout by inhibiting C5a-mediated priming of the inflammasome. *Ann. Rheum. Dis.* **2016**, *75*, 1236-1245.

34. Dalli, J.; Norling, L. V.; Renshaw, D.; Cooper, D.; Leung, K. Y.; Perretti, M. Annexin 1 mediates the rapid anti-inflammatory effects of neutrophil-derived microparticles. *Blood* **2008**, *112*, 2512-2519.

35. Wojdasiewicz, P.; Poniatowski, L. A.; Szukiewicz, D. The role of inflammatory and anti-inflammatory cytokines in the pathogenesis of osteoarthritis. *Mediators Inflamm.* **2014**, *2014*, 561459.

36. Kim, S. F.; Huri, D. A.; Snyder, S. H. Inducible nitric oxide synthase binds, S-nitrosylates, and activates cyclooxygenase-2. *Science* **2005**, *310*, 1966-1970.

37. Miller, M. C.; Manning, H. B.; Jain, A.; Troeberg, L.; Dudhia, J.; Essex, D.; Sandison, A.; Seiki, M.; Nanchahal, J.; Nagase, H.; Itoh, Y. Membrane type 1 matrix metalloproteinase is a crucial promoter of synovial invasion in human rheumatoid arthritis. *Arthritis Rheum.* **2009**, *60*, 686-697.

38. Rose, B. J.; Kooyman, D. L. A Tale of Two Joints: The Role of Matrix Metalloproteases in Cartilage Biology. *Dis. Markers* **2016***, 2016*, 4895050.

39. Neumann, E.; Lefevre, S.; Zimmermann, B.; Gay, S.; Muller-Ladner, U. Rheumatoid arthritis progression mediated by activated synovial fibroblasts. *Trends Mol. Med.* **2010***, 16*, 458-468.

40. Szabo, G. T.; Tarr, B.; Paloczi, K.; Eder, K.; Lajko, E.; Kittel, A.; Toth, S.; Gyorgy, B.; Pasztoi, M.; Nemeth, A.; Osteikoetxea, X.; Pallinger, E.; Falus, A.; Szabo-Taylor, K.; Buzas, E. I. Critical role of extracellular vesicles in modulating the cellular effects of cytokines. *Cell Mol. Life Sci.* **2014***, 71*, 4055-4067.

41. Kambayashi, T.; Laufer, T. M. Atypical MHC class II-expressing antigen-presenting cells: can anything replace a dendritic cell? *Nat. Rev. Immunol.* **2014***, 14*, 719-730.

42. Thery, C.; Duban, L.; Segura, E.; Veron, P.; Lantz, O.; Amigorena, S. Indirect activation of naive CD4+ T cells by dendritic cell-derived exosomes. *Nat. Immunol.* **2002***, 3*, 1156-1162.

43. Qu, Y.; Ramachandra, L.; Mohr, S.; Franchi, L.; Harding, C. V.; Nunez, G.; Dubyak, G. R. P2X7 receptor-stimulated secretion of MHC class II-containing exosomes requires the ASC/NLRP3 inflammasome but is independent of caspase-1. *J. Immunol.* **2009***, 182*, 5052-5062.

44. Buckley, C. D.; Gilroy, D. W.; Serhan, C. N. Proresolving lipid mediators and mechanisms in the resolution of acute inflammation. *Immunity* **2014***, 40*, 315-327.

45. Headland, S. E.; Norling, L. V. The resolution of inflammation: Principles and challenges. *Semin. Immunol.* **2015***, 27*, 149-160.

46. Yang, Y. H.; Morand, E.; Leech, M. Annexin A1: potential for glucocorticoid sparing in RA. *Nat. Rev. Rheumatol.* **2013***, 9*, 595-603.

3

SUPPLEMENTARY INFORMATION CHAPTER 3

EXTENDED METHODOLOGY

Experimental LPS-induced acute synovitis in adult horses – 3 *in vivo* studies
In vivo study 1. Experimental synovitis was monitored during 168 hours post intra-articular LPS-injection in 6 adult Warmblood mares. This study was published previously[1]. Briefly, animals received an injection of 0.5 ng LPS from *E. Coli* O55:B5 (Sigma Aldrich, St. Louis, MO, USA) into the left or right middle carpal joint. Synovial fluid was collected by sterile arthrocentesis prior to LPS-injection (LPS-0h, baseline), and at 8 (LPS-8h), 24 (LPS-24h) and 168 (LPS-168h) post LPS-injection. Samples of *in vivo* study 1 were used for Figure 3.

In vivo study 2. This is a similar experiment as *in vivo* study 1 (Cokelaere S.M. et al, manuscript in preparation), in which a total of 8 adult Warmblood horses (2 mares, 6 geldings) received injections of 0.25 ng LPS from *E. Coli* O55:B5 (Sigma Aldrich, St. Louis, MO, USA) into the left and right middle carpal and tarsocrural joints. Synovial fluid was collected by sterile arthrocentesis prior to LPS-injection (LPS-0h, baseline), and at 8 (LPS-8h) and 24 (LPS-24h) hours post LPS-injection. Samples of *in vivo* study 2 were used for Figures 1, 4 and 5.

In vivo study 3. For a more thorough investigation of EV concentration and EV protein content at the peak of the induced synovitis, one adult trotter horse (mare) received single injections of 0.7 ng LPS from *E. Coli* O55:B5 (Sigma Aldrich, St. Louis, MO, USA) into the left middle carpal joint and the right tarsocrural joint. Synovial fluid was collected by sterile arthrocentesis prior to LPS-injection (LPS-0h, baseline) and at 8 hours post LPS-injection (LPS-8h). Samples of *in vivo* study 3 were used for Figures 2 and 4.

SF was cleared from cells by centrifugation at 2,700*g* (4000 rpm) 30 min at RT in a Hettich Universal 32 centrifuge (Hettich, Tuttlingen, Germany) with rotor 1619, aliquoted and stored at −80°C. Extracellular vesicle isolation from SF was performed in a selection of samples from these studies.

EV-depletion of reagents containing BSA and FBS. EV-depleted PBS/0.1% BSA, used for suspension of EVp, was prepared by making a stock solution of 5% (w/v) BSA (GE Healthcare, Amersham, UK) in PBS, which was cleared from EVs and aggregates by ultracentrifugation at 100,000*g* for 16 h at 4°C (Optima™ L-90K or Optima™ XPN-80 centrifuge; SW28 rotor; 28,000 rpm; relative centrifugation force

(RCF) average 103,745g; RCF max 141,371g; κ-factor 245.5; Beckman-Coulter, Fullerton, CA, USA), filtered through a 0.22-μm filter, stored in aliquots at −20°C, and diluted 50× in PBS prior to use.

EV-depleted RPMI/10% FBS, used to stop the PKH67 staining process, was prepared by making a stock solution of 30% (v/v) FBS (PAA Laboratories, GE Healthcare) in Roswell Park Memorial Institute medium (RPMI) (Gibco, Thermo Scientific, Waltham, MA, USA), which was cleared of EVs and aggregates by ultracentrifugation at 100,000g for 16 h at 4°C (as described above), filtered through a 0.22-μm filter, stored in aliquots at −20°C, and diluted 3× in RPMI prior to use.

This protocol for EV depletion of reagents is a standard procedure in our lab[2] and results in very few remaining EVs if the following precautions are taken: a) start with dilutions of BSA (max 5%) and FBS (max 30%) in the buffer/medium of choice; b) use a swing-out rotor; c) use a centrifugation time of at least 16 h; d) leave at least 5 ml of supernatant above the EVp.

3

EV-isolation from SF

For analysis with high-resolution flow cytometry and Western Blot. Stored cell-free SF from *in vivo* studies 1, 2 and 3 (starting volumes 0.6-2 ml) was thawed, incubated with hyaluronidase solution (HYase Type II from sheep testes, Sigma-Aldrich, St. Louis, MO, USA) (1500 U/ml in H_2O; 20 μl per ml SF) for 15 min at 37°C in a water bath while vortexing every 5 min, and centrifuged at 1000g 10 min at RT in an Eppendorf centrifuge (Hettich Mikro 200R with rotor 2424A) to remove aggregates. Then, samples were mixed with PBS to reach a volume of 4.5 ml. Subsequent ultracentrifugation in SW60 tubes (Beckman-Coulter, Fullerton, CA, USA) at 10,000g for 35 min at 4°C (9,900 rpm; RCF average 10,066g; RCF max 13,205g; κ-factor 1667.7) and 200,000g for 120 min at 4°C (44,000 rpm; RCF average 198,835g; RCF max 260,849g; κ-factor 84.4) resulted in 10K and 200K EVp. For these steps a SW60-Ti rotor in a Beckman-Coulter Optima™ L-90K or Optima™ XPN-80 ultracentrifuge was used.

For analysis with Cryo-TEM. EVs were isolated from SF collected during acute LPS-induced synovitis (LPS-8h; *in vivo* study 2; starting volume 1.2 ml SF). The sample was incubated with HYase and cleared from aggregates as described above, then transferred into MLS50 tubes (Beckman-Coulter, Fullerton, CA, USA) and gently mixed with PBS to reach a volume of 5 ml. Subsequent ultracentrifugation at 10,000g for 35 min at 4°C (10,000 rpm; RCF average 8,025g; RCF max 10,730g; κ-factor 1,777) and 200,000g for 120 min at 4°C (50,000 rpm; RCF average 200,620g; RCF max 268,240g; κ-factor 71.7) resulted in 10K and 200K EVp. For these steps an MLS50 rotor in a Beckman-Coulter Optima™ MAX-E ultracentrifuge was used.

Single-EV-based high-resolution flow cytometry (FCM)

Labelling of EVp with anti-CD44 and PKH67. EVp were resuspended in a mixture of 20 µl EV-depleted PBS/0.1% BSA and 30 µl diluent-C. To each sample 4 µl anti-CD44-PE antibody (clone IM7, PE-conj., eBioscience, San Diego, CA, USA; 0.2 mg/ml) or 4 µl anti-IgG2bκ-PE isotype control antibody (0.2 mg/ml; rat IgG2bκ, PE-conj., eBioscience) was added and incubated for 1 hour at RT on a shaker. Prior to use the anti-CD44-PE and the IgG2bκ-PE stock solutions were centrifuged in order to pellet aggregates (21,000*g*, 20 min, 4°C; Hettich Mikro 200R with rotor 2424A). After CD44-PE or isotype labelling 50 µl diluent-C was added (to create a total volume of 100 µl) and this was mixed with PKH67 staining mix (MIDI-67-1KT kit, Sigma-Aldrich, St. Louis, MO, USA) (1.5 µl PKH67 in 100 µl diluent-C). After 3 min incubation at RT, 50 µl of EV-depleted RPMI/10% FBS was added to stop the staining process. Labelled EVs (250 µl) were then mixed with 1.5 ml 2.5 M sucrose (J.T. Baker, Avantor Performance Materials, Center Valley, PA, USA) in PBS. The prepared EV-sucrose mixture was then overlaid with 15 volumes of 700 µl sucrose solutions with decreasing density (2.0 M – 0.4 M sucrose in PBS) in SW40 tubes (Beckman-Coulter, Fullerton, CA, USA). Gradients were centrifuged at 200,000*g* for 16 hours at 4°C (Beckman-Coulter Optima™ L-90K or Optima™ XPN-80 centrifuge; SW40-Ti rotor; 39,000 rpm; RCF average 192,072*g*; RCF max 270,519*g*; κ-factor 144.5) and 12 fractions of 1 ml were collected from top (F1, lowest density) to bottom (F12, highest density) by using a P1000 pipette. Densities were determined by refractometry.

A background control sample (20 µl EV-depleted PBS/0.1% BSA+30 µl diluent-C, without EVs) was taken along during the entire procedure of PKH67 labelling, anti-CD44 labelling, and sucrose gradient floatation. High-resolution FCM of this control sample did not show significant background events in gradient fractions of interest (data not shown).

Single-EV-based high-resolution FCM. For this technique an optimised jet-in-air-based BD Influx™ flow cytometer (BD Biosciences Europe, Erembodegem, Belgium) was used, as described previously [2-4]. Detection of EVs by this system is based on threshold triggering on the fluorescent light emitted after excitation of fluorescently labelled particles passing the first laser (FL1 signal). The threshold for triggering on FL1 was adjusted to allow an event rate of ≤10 events/s when clean PBS was analysed. The threshold level was kept identical for all measurements in this study. Forward scatter (FSC) of EVs was measured through an adapted small particle detector with a collection angle of 15–25° (reduced wide-angle FSC), by using a high numerical aperture and long working distance lens and by installing a 5-mm obscuration bar in front of the FSC collection lens. These settings allow the best distinction of FSC and FL1 fluorescence for 100 nm and 200 nm yellow-green fluorescent (505/515) carboxylated polystyrene beads (FluoSpheres, Life Technologies, Thermo Scientific,

Waltham, MA, USA) with which the flow cytometer was calibrated. For experiments a 140-µm nozzle was used. The sheath fluid pressure was kept between 4.98 and 5.02 psi and was monitored by an external pressure meter. The sample pressure was set to 4.29 psi. Upon loading the sample the system was boosted until events appeared, the fluidics were then allowed to stabilise for 30 seconds, after which samples were acquired for 30 seconds. In between samples the flow cytometer was washed with FACSrinse and PBS. Data were acquired using BD FACS™ Sortware v1.0.1.654 (BD Biosciences, San Jose, CA, USA) and analysed with FlowJo v10.07 software (FlowJo, Ashland, OR, USA).

EV concentration per fraction was calculated based on the number of events per 30 seconds and the flow rate that was determined by a volume measurement using ddH$_2$O. The EV concentration per ml of SF was calculated by taking the sum of EVs in sucrose fractions F3-F9, corrected for the SF starting volume.

Cryo-TEM

Preparation of samples. EVp were resuspended in 250 µl PBS, mixed with 1.25 ml 2 M sucrose solution (in PBS) (total volume = 1.5 ml) in MLS50 tubes (Beckman-Coulter, Fullerton, CA, USA) and carefully overlaid with sucrose solutions of 1.4, 0.4, and 0 M (sucrose in PBS) to create 2 small discontinuous sucrose gradients. Gradients were centrifuged at 200,000*g* for 16 h at 4°C (Beckman-Coulter Optima™ MAX-E centrifuge; MLS50 rotor; 50,000 rpm; RCF average 200,620*g*; RCF max 268,240*g*; κ-factor 71.1). After centrifugation, 5 fractions of 1 ml were collected from bottom (F5) to top (F1) by using a peristaltic pump connected to a capillary tube reaching to the bottom of the centrifuge tube. Densities were determined by refractometry. Then, sucrose gradient fractions F2, F3, and F4 were pooled per gradient and diluted by adding 9 ml PBS to SW40 tubes (Beckman-Coulter, Fullerton, CA, USA). EVs were again pelleted at 200,000*g* for 60 min at 4°C (Beckman-Coulter Optima™ L-90K or Optima™ XPN-80 centrifuge; SW40-Ti rotor; 39,000 rpm; RCF average 192,072*g*; RCF max 270,519*g*; κ-factor 144.5).

Cryo-TEM. EVp were carefully resuspended in 20 µl PBS and stored on ice for 1–2 h until vitrification using a Vitrobot™ Mark IV system (FEI, Eindhoven, Netherlands). Three microliters of EV sample was directly placed onto a glow-discharged 2/2 copper grid (Quantifoil, Jena, Germany). Excess sample was removed with 595 filter paper (Schleicher & Schuell, Whatman Plc., Kent, UK) in the Vitrobot chamber for 1 s at 100% relative humidity, with subsequent plunging into liquid ethane (3.5 purity). Residual ethane was removed with filter paper and grids were stored in cryo-boxes under liquid N$_2$ for later imaging. For cryo-TEM, grids were transferred to a Gatan 626 cryo-holder (Gatan Inc., Pleasanton, CA, USA), which was inserted into a Tecnai™ 20 transmission electron microscopy (FEI) with LaB$_6$ filament operated at 200 kV.

3

Images were acquired with a 4,000×4,000 Eagle charge coupled device (CCD) camera (FEI) at a 19,000× magnification, 5–10 µm under focus.

Note that only 1.2 ml starting volume was needed of this synovitis SF sample to successfully image the isolated EVs, whereas previously, for healthy SF, 12 ml was needed to reach similar detection efficiency [4].

Morphological analysis of EVs. Individual EVs were categorised as "single EVs" (1 EV with a single membrane), "multi-membrane EVs" (2 EVs merged together, or 1 EV with double membrane), "collections of EVs" (more than 2 EVs merged into 1 entity), or "other small particles" (very small vesicle-like particles without clear membrane). Single EVs were further subcategorised into "spherical EVs" (diameter ratio ≥0.7) or "tubular EVs" (diameter ratio <0.7). Multi-membrane EVs and collections of EVs were counted as 1 entity. For size distribution of spherical EVs, the smallest and largest diameter of each individual EV was measured with the "measure tool" in ImageJ (1.48v) and the "diameter ratio" (smallest diameter/largest diameter) was determined. The average diameter for each EV [(smallest+largest diameter)/2] was used for the size distribution graphs.

Western blotting. The same sucrose fractions that were analysed by high-resolution FCM were used for protein identification by Western blotting. Gradient fractions of 375 µl were pooled in pairs (*i.e.* fractions F2+F3 [low density], F4+F5 [medium density], F6+F7 [high density]) and diluted in 3.4 ml PBS in SW60 tubes (Beckman-Coulter, Fullerton, CA, USA). EVs were pelleted at 200,000g (44.000 rpm; RCF average 198,835g; RCF max 260,849g; κ-factor 84.4) using an SW60-Ti rotor in a Beckman-Coulter Optima™ L-90K or Optima™ XPN-80 ultracentrifuge (Beckman-Coulter, Fullerton, CA, USA), 90 min at 4°C. EVp were resuspended in 65 µl non-reducing SDS-PAGE sample buffer (50mM TRIS pH 6.8, 2% SDS, 10% glycerol, 0.02% bromophenol blue), heated at 100°C, run on 4-20% Criterion TGX gels (Bio-Rad, Hercules, CA, USA), and transferred onto 0.2 µm PVDF membranes. After blocking for 1 hour in 5% Protifar (Nutricia, Zoetermeer, the Netherlands) in PBS 0.1% Tween-20, proteins were labelled with primary antibodies against CD9 (clone HI9, Biolegend, San Diego, CA, USA; dilution 1:1000), CD44 (clone IM7, PE-conj., eBioscience, San Diego, CA, USA; dilution 1:400), MHC Class II (clone CVS20, Bio-Rad (AbD Serotec), Hercules, CA, USA; dilution 1:400) and Annexin-A1 (clone 29/Annexin-1, BD Transduction Labs, San Jose, CA, USA; dilution 1:400). HRP-conjugated goat-anti-mouse IgG (Nordic Immunology Laboratories, Susteren, the Netherlands; dilution 1:5000) was used for detection by chemiluminescence (SuperSignal West Pico Chemiluminescent Substrate, Thermo Scientific, Waltham, MA, USA). Chemiluminescence was visualised using a ChemiDoc™ MP Imaging System (Bio-Rad, Hercules, CA, USA) and analysed with Bio-Rad Image Lab V5.1 software (Bio-Rad, Hercules, CA, USA).

3D primary chondrocyte culture with SF-derived EVp

Chemicals used for media. DMEM (high glucose, with GlutaMAX and pyruvate) and Fungizone were purchased from Invitrogen (Thermo Scientific, Waltham, MA, USA), DMEM/F12 1:1 mixture (w/o phenol red) and fetal bovine serum (FBS, high performance) from Gibco (Thermo Scientific, Waltham, MA, USA), Pen/Strep (10.000 U/ml penicillin, 10.000 µg/ml streptomycin) from PAA Laboratories (GE Healthcare, Amersham, UK), recombinant human basic fibroblast growth factor (bFGF) from AbD Serotec (Bio-Rad, Hercules, CA, USA), insulin-transferrin-selenium (ITS) from Costar Corning (Tewksbury, MA, USA), bovine serum albumin (BSA) and L-ascorbic-acid-2-phosphate from Sigma-Aldrich (St. Louis, MO, USA), DMSO from Merck-Millipore (Darmstadt, Germany).

3D chondrocyte culture. Fresh articular cartilage was harvested post-mortem, with owner consent, from the distal articular surfaces of the metacarpal bones of two adult Warmblood horses (1 mare, 1 stallion) that were euthanised for reasons other than joint disease at the Utrecht University Equine Hospital. Full thickness cartilage was washed in Hanks balanced salt solution (Gibco, Thermo Scientific, Waltham, MA, USA) with 1% Pen/Strep, then minced in pieces of approximately 2 mm³ and digested overnight at 37°C in 1.5 x their volume of DMEM containing 1% Pen/Strep and 0.15% (w/v) collagenase-II (Wortington, Lakewood, NJ, USA). Subsequently, primary chondrocytes were collected through a cell strainer, washed and suspended in freezing medium (DMEM with 1% Pen/Strep, 20% FBS and 10% DMSO) for immediate freezing of aliquots in liquid nitrogen (passage 0). Frozen chondrocytes of the 2 donors were thawed and separately cultured in monolayer for 7 days (37°C, 5% CO_2) in expansion medium (DMEM with 1% Pen/Strep, 0.5% Fungizone, 10% FBS, 0.1 mM L-ascorbic-acid-2-phosphate and 1 ng/ml human bFGF). Confluent cells were trypsinised and seeded (passage 1) in 96-well plates (round bottom, ultra-low attachment, Costar Corning, Tewksbury, MA, USA), 2000.000 cells per well in 200 µl chondrogenic medium (DMEM/F12 w/o phenol red with 1% Pen/Strep, 0.5% Fungizone, 1% ITS, 1.25 mg/ml BSA and 0.1 mM L-ascorbic-acid-2-phosphate). To form 3D cell cultures, plates were centrifuged at 41*g* (500 rpm) 5 min at RT in a 5804 Eppendorf centrifuge with an A2DWP rotor (Eppendorf, Hamburg, Germany). 3D cultures were then given 48 hours to grow in chondrogenic medium (37°C, 5% CO_2).

Preparing EVp suspensions. EVs were isolated from 1 ml SF from *in vivo* studies 2 and 3 according to the isolation protocol above. 10K and the 200K EVp were both resuspended in 100 µl chondrogenic medium and pooled (10K+200K for each condition, in 200 µl suspension). Note that these EVs were not subjected to density gradient floatation.

3

Incubation of cells with EVp suspensions. At the day of incubation, 3D cultures were transferred to coated 12-well plates (TC-coated, Greiner Bio-One, Kremsmünster, Austria) containing 900 µl chondrogenic medium. Cells were incubated for 24 hours with 100 µl EVp (derived from 0.5 ml SF) or 100 µl medium ("no EVp"). Chondrocytes of donor 1 and donor 2 received identical EVp (EVp set 1). Culture medium was collected and stored in aliquots at –80°C for further analysis. Cells were processed for RNA isolation and subsequent qPCR analysis. This experiment was later repeated for chondrocyte donor 1 by incubation with EVp of new SF samples from *in vivo* study 2 (EVp set 2). An overview of conditions and EVp sets used for this functional study is depicted in Supplementary Table 1.

LPS control conditions: 1) LPS only (10 ng/ml, 1 µg/ml or 10 µg/ml), and 2) EVp from healthy SF (LPS-0h) spiked with 0.005 ng/ml or 0.05 ng/ml LPS prior to ultracentrifugation. Doses for LPS spiking were based on what was maximally expected in 10 ml SF of a joint injected with 0.5 ng of LPS, and a 10-fold dilution when the inflammation is resolving after 8 hours.

Gene expression analysis (qPCR). RNA was isolated from stimulated chondrocytes by use of the RNeasy Mini Isolation Kit (Qiagen, Hilden, Germany) according to manufacturer's instructions. RNA quality and quantity was determined with a Nanodrop ND-1000 spectrophotometer (Thermo Scientific, Waltham, MA, USA) and was of adequate quality to proceed with quantitative PCR (qPCR) analysis. Selected samples were checked in a Bioanalyzer 2100 (Agilent Technologies, Santa Clara, CA, USA) with resulting RNA Integrity Number (RIN) values close to 10 (indicative for good quality RNA). RNA amplification was followed by cDNA synthesis with the I-script CDNA synthesis kit (Bio-Rad, Hercules, CA, USA), according to the manufacturer's instructions. 80 ng RNA was used as input for the reaction (in a volume of 20 µl). For qPCR a CFX384 Touch Real-time PCR detection system with C1000 Touch thermal cycler (Bio-Rad, Hercules, CA, USA) was used. Volumes of 10 µl per sample were run in mono in 384-well PCR plates (Bio-Rad, Hercules, CA, USA), containing 4 µl cDNA, 6 µl SYBR Green mix (Bio-Rad, Hercules, CA, USA) with 100 µmol of both forward and reverse primers. Primer sets for the equine genes of interest were designed with PerlPrimer v.1.1.14, based on known sequences from the public databases (www.ensembl.org/index.html and www.ncbi.nlm.nih.gov) and verified using BLAST (http://blast.ncbi.nlm.nih.gov/). For primer sequences, amplicon size and annealing temperatures see Supplementary Table 2. Primers were ordered at Eurogentec (Maastricht, the Netherlands). Amplicon size was checked on agarose gel and sequences were confirmed by sequencing on an ABI Prism 3130XL genetic analyzer (Applied Biosystems, Nieuwerkerk aan den IJssel, the Netherlands). Gene expression was normalised according to 3 reference genes, *i.e.* ribosomal protein S19

(RPS19), ribosomal protein L13 (RPL13) and tyrosine 3/tryptophan 5-monooxygenase activation protein (YWHAZ), for which average Ct-values were ≤ 25. The average Ct-values for the genes of interest were ≤ 30.

MMP assay. 35 µl non-diluted chondrocyte culture medium was incubated with 35 µl FS-6 solution, which is 10 µM Mca-Lys-Pro-Leu-Gly-Leu-Dap(DNP)-Ala-Arg-NH$_2$ trifluoroacetate salt (Bachem, Bubendorf, Switzerland) in MMP buffer, and immediately measured in black flat bottom 384-well plates (Greiner Bio-One, Kremsmünster, Austria) using a CLARIOstar plate reader (BMG Labtech GmbH, Ortenberg, Germany). The fluorescent signal was measured in real-time over 48 minutes for which a linear slope (relative fluorescence units/second (RFU/s)) was calculated as a measure of general MMP activity. MMP buffer: 0.1 M Tris, 0.1 M NaCl, 10 mM CaCl2, 0.05% Triton X-100, 0.1% (w/v) PEG-6000 (J.T. Baker, Avantor Performance Materials, Center Valley, PA, USA), pH 7.5.

CCL2 enzyme-linked immunosorbent assay (ELISA). A sandwich ELISA was designed using antibodies directed against equine CCL2. EIA/RIA 96-well plates (flat bottom, Costar Corning, Tewksbury, MA, USA) were coated overnight at 4°C with capture antibody (rabbit anti-equine CCL2, King Fisher, Saint Paul, MN, USA) 1 µg/ml in coating buffer (100 mM Na$_2$CO$_3$, 100 mM NaHCO$_3$, pH 9.6), 100 µl per well. After blocking for 90 min at RT in PBS 1% BSA, wells were incubated for 90 minutes at RT with 100 µl chondrocyte culture medium or 100 µl recombinant CCL2 (for a standard curve of 0-2.5 ng/ml, King Fisher, Saint Paul, MN, USA), both diluted in PBS 1% BSA 0.1% Tween-20. Subsequently, wells were incubated 60 min at RT with detection antibody (biotinylated rabbit anti-equine CCL2, King Fisher, Saint Paul, MN, USA) 0.02 µg/ml in PBS 1% BSA 0.1% Tween-20, 100 µl per well, followed by incubation 30 min at RT in high sensitivity streptavidin-horseradish peroxidase (Thermo Scientific, Waltham, MA, USA) 10 ng/ml in PBS 1% BSA, 100 µl per well. The signal was developed with TMB substrate solution (Thermo Scientific, Waltham, MA, USA) 30 min at RT and the reaction was stopped with 0.18 M sulfuric acid, both 100 µl per well. Color development was quantified in a plate reader (Tecan, Männedorf, Switzerland) using wavelengths 450 and 540 nm.

3

1. de Grauw JC, van de Lest CH, van Weeren PR. Inflammatory mediators and cartilage biomarkers in synovial fluid after a single inflammatory insult: a longitudinal experimental study. *Arthritis Res Ther* **2009**;11:R35.

2. van der Vlist EJ, Nolte-'t Hoen EN, Stoorvogel W, Arkesteijn GJ, Wauben MH. Fluorescent labeling of nano-sized vesicles released by cells and subsequent quantitative and qualitative analysis by high-resolution flow cytometry. *Nat Protoc* **2012**; 7:1311-26

3. Nolte-'t Hoen EN, van der Vlist EJ, Aalberts M, Mertens HC, Bosch BJ, Bartelink W, et al. Quantitative and qualitative flow cytometric analysis of nanosized cell-derived membrane vesicles. *Nanomedicine* **2012**;8:712-20

4. Boere J, van de Lest CH, Libregts SF, Arkesteijn GJ, Geerts WJ, Nolte-'t Hoen EN, et al. Synovial fluid pretreatment with hyaluronidase facilitates isolation of CD44+ extracellular vesicles. *J Extracell Vesicles* **2016**;5:31751

3

Supplementary Table 1 Overview of conditions for repeated 3D chondrocyte culture experiments. Test conditions were EVp (pooled 10K + 200K) from healthy joints (LPS-0h) or joints with acute synovitis (LPS-8h; LPS-24h). Control conditions included culture medium (no EVp), LPS-containing culture medium, or EVp from healthy SF spiked with 2 concentrations of LPS.

Culture exp. #	Chondrocyte donor	Condition	EVp set	EVp donor	Samples used for
1	1	No EVp (medium control)	-	-	Fig. 4
1	1	No EVp (medium control)	-	-	Fig. 4
1	1	EVp LPS-0h	Set 1	Horse **2-A** (*in vivo* study 2)	Fig. 4
1	1	EVp LPS-0h	Set 1	Horse **3-A** (*in vivo* study 3)	Fig. 4
1	1	EVp LPS-8h	Set 1	Horse **2-A** (*in vivo* study 2)	Fig. 4
1	1	EVp LPS-24h	Set 1	Horse **3-A** (*in vivo* study 3)	Fig. 4
1	2	No EVp (medium control)	-	-	Fig. 4
1	2	No EVp (medium control)	-	-	Fig. 4
1	2	EVp LPS-0h	Set 1	Horse **2-A** (*in vivo* study 2)	Fig. 4
1	2	EVp LPS-0h	Set 1	Horse **3-A** (*in vivo* study 3)	Fig. 4
1	2	EVp LPS-8h	Set 1	Horse **2-A** (*in vivo* study 2)	Fig. 4
1	2	EVp LPS-24h	Set 1	Horse **3-A** (*in vivo* study 3)	Fig. 4
2	1	No EVp (medium control)	-	-	Fig. 4; Fig.5; Fig. S2
2	1	No EVp (medium control)	-	-	Fig. 4; Fig.5; Fig. S2
2	1	EVp LPS-0h	Set 2	Horse **2-B** (*in vivo* study 2)	Fig. 4; Fig.5; Fig. S2
2	1	EVp LPS-0h	Set 2	Horse **2-C** (*in vivo* study 2)	Fig. 4; Fig.5; Fig. S2
2	1	EVp LPS-8h	Set 2	Horse **2-A** (*in vivo* study 2)	Fig. 4; Fig.5; Fig. S2
2	1	EVp LPS-8h	Set 2	Horse **2-D** (*in vivo* study 2)	Fig. 4; Fig.5; Fig. S2
2	1	EVp LPS-24h	Set 2	Horse **2-B** (*in vivo* study 2)	Fig. 4; Fig.5; Fig. S2
2	1	EVp LPS-24h	Set 2	Horse **2-C** (*in vivo* study 2)	Fig. 4; Fig.5; Fig. S2
2	1	No EVp (medium control) + LPS 10 ng/ml	-	-	Fig.5; Fig. S2
2	1	No EVp (medium control) + LPS 1 µg/ml	-	-	Fig.5; Fig. S2
2	1	No EVp (medium control) + LPS 10 µg/ml	-	-	Fig.5; Fig. S2
2	1	EVp LPS-0h + LPS-spike 5 pg/ml	Set 2	Horse **2-B** (*in vivo* study 2)	Fig.5; Fig. S2
2	1	EVp LPS-0h + LPS-spike 50 pg/ml	Set 2	Horse **2-C** (*in vivo* study 2)	Fig.5; Fig. S2

Supplementary Table 2 Nucleotide sequences (5'-3'), amplicon size and optimal annealing temperatures (T_a) of forward (Fw) and reverse (Rv) primers used for qPCR. Primer sets for the equine genes of interest were designed with PerlPrimer v.1.1.14, based on known sequences from the public databases (www.ensembl.org/index.html and www.ncbi.nlm.nih.gov) and verified using BLAST (http://blast.ncbi.nlm.nih.gov/).
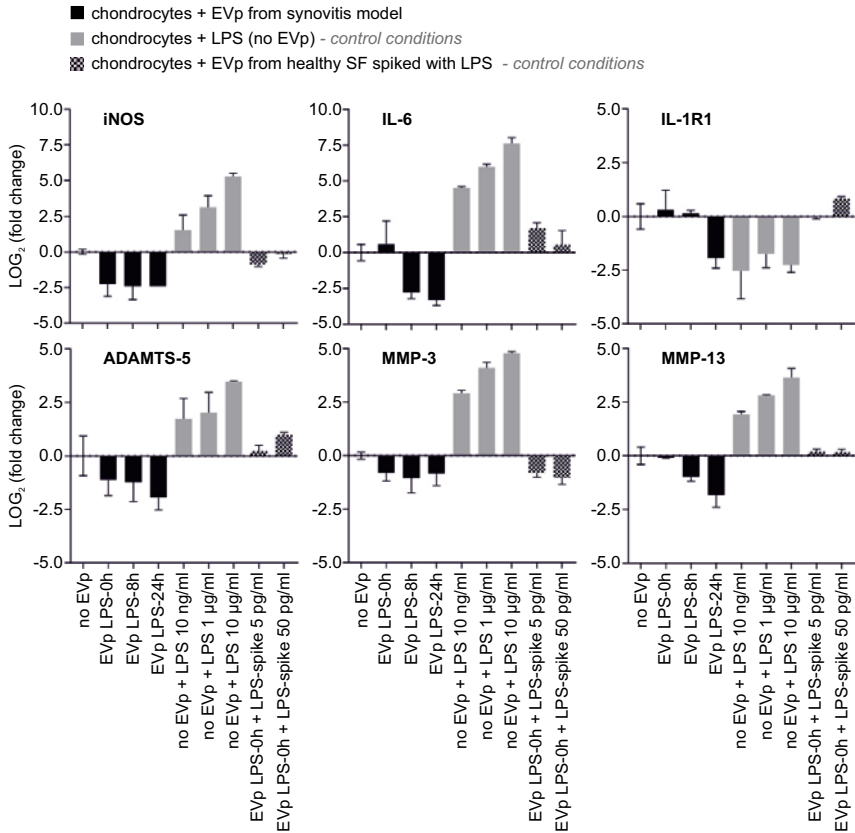
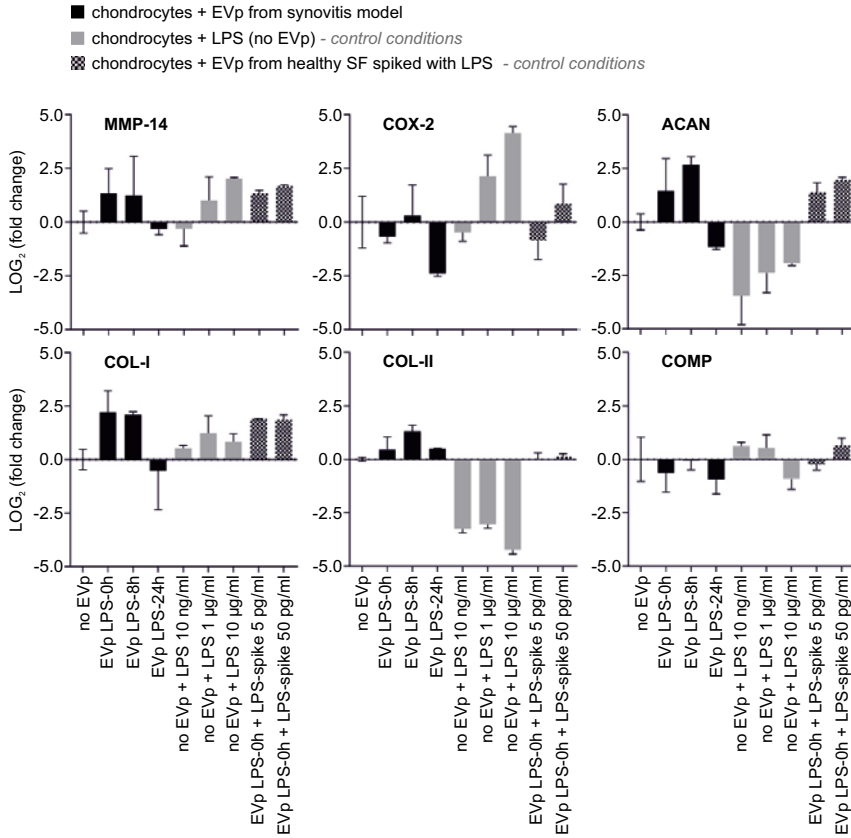| Gene	Name	Amplicon (bp)	T_a(°C)		Primer sequence (5'-3')
COX-2	cyclooxygenase-2	203	65	Fw	GTATCCGCCCACAGTCAAAGA
				Rv	ACAAGCGTTCATCATCCCATTC
ADAMTS-5	a disintegrin and metalloproteinase with thrombospondin motif-5	107	65	Fw	AGCCACGCCAGCATTGAGAACC
				Rv	AGTGTGGTGGCCGCGTTCTT
IL-6	interleukin-6	89	62	Fw	GACGGATGCTTCCAATCTG
				Rv	GTACTCCAGGTATATCTGAAACTC
MMP-3	matrix metalloproteinase-3	96	65	Fw	AAATAGCAGAAGACTTTCCAGG
				Rv	TCAAACTGTGAAGATCCACTG
MMP-13	matrix metalloproteinase-13	90	55.5	Fw	CAAGGGATCCAGTCTCTCTATGGT
				Rv	GGATAAGGAAGGGTCACATTTGTC
MMP-14 (MT-1MMP)	matrix metalloproteinase-14 (membrane type-1-MMP)	91	60.5	Fw	GGACTGTCCGGAATGAGGATCT
				Rv	TTGGAATGCTCAAGGCCCA
iNOS	inducible nitric oxide synthase	96	64	Fw	CACCAAAGAGGCTGAGAG
				Rv	CACCTTCAGGAATGTGGG
IL-1R1	interleukin-1 receptor-1	112	58	Fw	TGGTACAGGGATTCTTGC
				Rv	GAGTTAGAGGTGGACCCT
ACAN	aggrecan	115	64	Fw	AAGACAGGGTCTCGCTGCCCAA
				Rv	ATGCCGTGCATCACCTCGCA
COMP	cartilage oligomeric matrix protein	104	65	Fw	CCACGTGAATACGGTCACAG
				Rv	ACGTCTGCTCCATCTGCTTC
COL-I	collagen type I	93	62	Fw	CGTGACCTCAAGATGTGC
				Rv	AGAAGACCTTGATGGCGT
COL-II	collagen type II A1	79	55.5	Fw	GGCAATAGCAGGTTCACGTACA
				Rv	CGATAACAGTCTTGCCCCACTT
Ref. gene	Name	Amplicon (bp)	T_a(°C)		Primer sequence (5'-3')
RPS19	ribosomal protein S19	144	63	Fw	CACGATGCCTGGAGTTACTG
				Rv	GGAGCAAGCTCTTTATGTTTGG
RPL13	ribosomal protein L13	112	63	Fw	GCGGAAGAACTCAAATTGG
				Rv	GCCTTGAAGTTCTTCTCCT
YWHAZ	tyrosine 3/tryptophan 5-monooxygenase activation protein	179	61	Fw	CAAGCGGAGAGCAAAGTC
				Rv	AGACCCAATCTGATAGGATGT
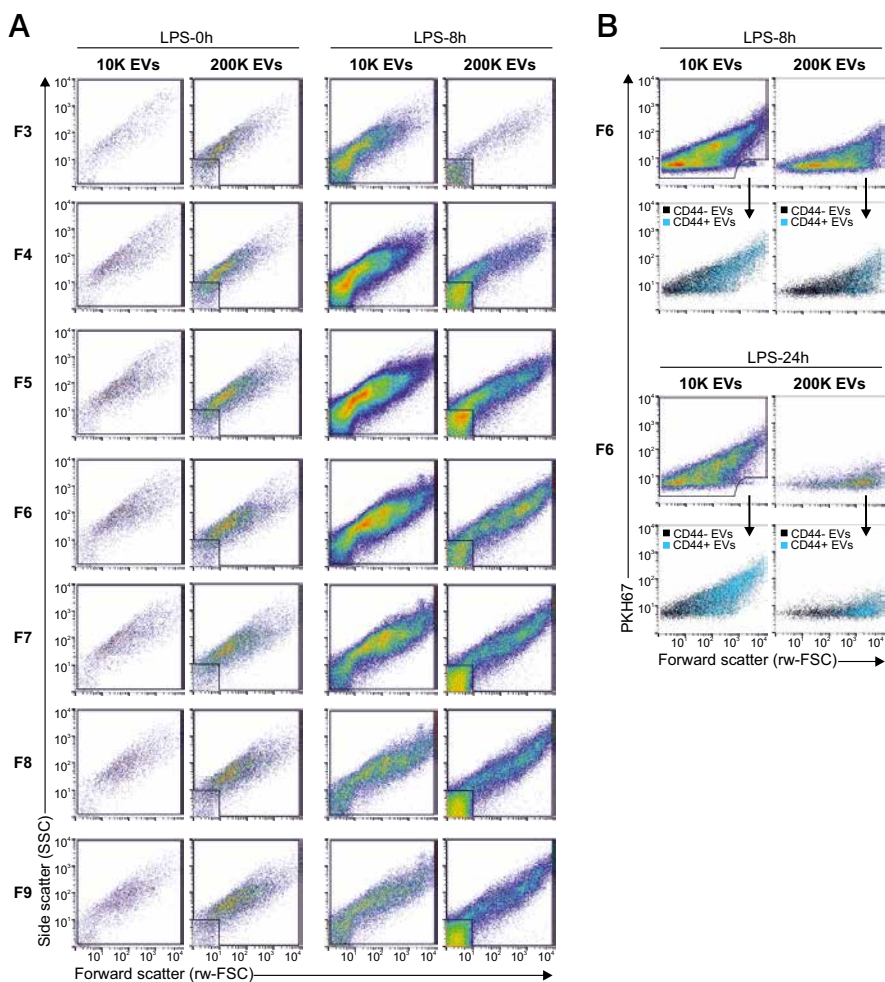
Supplementary Figure 1 High-resolution FCM details and gating strategy for Figures 2 and 3. **A)** Reduced wide-angle Forward scatter (rw-FSC) and side scatter (SSC) for PKH67+ EVs in fractions F3-F9 of sucrose density gradients with gating strategy used for data in Figures 1A and 3A. Dots represent single EVs measured in 30 seconds. Importantly, for 200K EVs the left lower corner was omitted, due to background caused by artefacts, possibly lipoproteins, in the sample (Sódar *et al.*, Sci Rep. 2016;18;6:24316). Plots show a dramatically increased EV concentration at LPS-8h, with peak values in F4-F7. Densities of individual fractions (g/ml) are: F3=1.10, F4=1.12, F5=1.14, F6=1.16, F7=1.18, F8=1.20, F9=1.21. For Figure 3A: EV concentration per fraction was calculated based on the number of events per 30 seconds and the flow rate that was determined by a volume measurement using ddH_2O.

Supplementary Figure 1 (*Continued*)

The EV concentration per ml of SF was calculated by taking the sum of EVs in fractions F3-F9, corrected for the SF starting volume (0.6 ml). **B)** Reduced wide-angle forward scatter (rw-FSC) and PKH67 intensity of PKH67+ EVs (in black) were plotted for LPS-8h and LPS-24h and overlaid (in blue) with the signal for CD44+ EVs, corresponding to the square gates in Figure 3B. Differences in light scattering properties of EVs can be observed for the different time points and between 10K and 200K EVs. Note that the majority of 200K EVs at LPS-24h is CD44+ (blue) and has an extremely high forward scatter compared to the EVs at LPS-8h.

■ chondrocytes + EVp from synovitis model
■ chondrocytes + LPS (no EVp) - *control conditions*
▨ chondrocytes + EVp from healthy SF spiked with LPS - *control conditions*

Supplementary Figure 2 See continued figure and description on next page.

Supplementary Figure 2 (*Continued*)

Repeat of chondrocyte 3D culture experiment (Figure 4), including LPS control conditions. Gene expression was measured after 24 hours incubation with culture medium only (no EVp) or with EVp (pooled 10K + 200K) from healthy joints (LPS-0h) or joints with acute synovitis (LPS-8h; LPS-24h) (black bars). Additional control conditions included LPS-containing culture medium (grey bars) or EVp from healthy SF spiked with 2 concentrations of LPS (dotted bars). Graphs represent mean effects of EVp from 2 EVp donors on chondrocytes from 1 cell donor, with error bars being the range (highest and lowest observed values; n=2). For samples included per condition, see Supplementary Table 1. iNOS, inducible nitric oxide synthase; IL-6, interleukin-6; IL-1R1, interleukin-1-receptor-1; ADAMTS-5, a disintegrin and metalloproteinase with thrombo-spondin motif-5; MMP, matrix metalloproteinase; COX-2, cyclooxygenase-2; ACAN, aggrecan; COL-I, collagen type I; COL-II, collagen type II A1; COMP, cartilage oligomeric matrix protein.

4

Phospholipid characterisation of synovial fluid derived extracellular vesicles harvested during LPS-induced synovitis

Identification of novel naturally occurring short-chain carboxylic acid N-modified phosphatidylserine subclasses

Janneke Boere [a]
Jos F. Brouwers [b]
Stefan M. Cokelaere [a]
Jos Malda [a,c]
Marca H.M. Wauben [b]
P. René van Weeren [a]
Chris H. A. van de Lest [a,b]

Departments of Equine Sciences[a] and Biochemistry & Cell Biology[b] of Faculty of Veterinary Medicine, Utrecht University, Utrecht, the Netherlands; Department of Orthopaedics[c], University Medical Center Utrecht, Utrecht, the Netherlands

The results of functional experiments are awaited before this manuscript will be submitted for publication

ABSTRACT

Objective. Given that the lipidome of extracellular vesicles (EVs) is relatively unexplored, and that EVs are a major contributor to a multitude of pathologies, EV lipidomics is a potential tool to study EV-mediated processes during disease. The objectives of this study were to investigate the lipidome of synovial fluid (SF) EVs in healthy equine joints and joints with bacterial lipopolysaccharide (LPS)-induced synovitis. Focus was on non-neutral lipids, including the phospholipids and sphingolipids.

Methods. Isolation of EVs from equine SF was performed by differential ultracentrifugation with final steps at 10,000g (10K) and 200,000g (200K) for healthy SF (n=3) harvested prior to LPS-injection, and synovitis SF (n=3) harvested at 24 hours post LPS-injection, followed by EV purification in OptipPrep^{TM} density gradients. EV lipids were extracted by the Bligh & Dyer method, followed by hydrophilic and hydrophobic interaction liquid chromatography and mass spectrometry. Principal component analysis and heatmap correlation analysis was used to identify disease- and EV-specific lipidomes.

Results. In addition to generally known EV phospholipids, at least four novel glycerophospholipid subclasses were found, of which structures were deduced to be phosphatidylserine (PS) molecules with the amino-group linked to a carboxylic acid varying in chain length from 1 to 4 carbons, *i.e. N*-formyl-PS, *N*-acetyl-PS, *N*-propionyl-PS and *N*-butyryl-PS, respectively. These lipids were enriched in 200K EVs, and their presence was increased during LPS-induced synovitis. Results were verified by comparison of the chromatographic mobility of heterogeneous and synthetically produced candidate lipids.

Conclusion. A number of not earlier described glycerophospholipid subclasses were found which were identified as short-chain carboxylic acid modifications of PS. These *N*-modified PS molecules were associated with SF-derived EVs and are therefore highly likely involved in synovitis. Hypotheses about the potential origin and function of the *N*-modified PS molecules are postulated.

INTRODUCTION

The understanding of the molecular mechanisms of disease has recently been boosted by the increased knowledge on extracellular vesicles (EVs), which are important mediators of intercellular communication. These vesicles are a heterogeneous group of bilayered proteolipid spheres, 20 nm – 1 μm in size, produced by all cell types [1]. Various physiological and pathological processes, including immune responses, are partially under the control of EVs [2,3]. They are therefore of major interest to be studied in detail for both mechanistic reasons and as possible biomarkers for disease [4-6].

The EV membrane, which is composed of glycerophospholipids, interspersed with glyco(sphingo)lipids, cholesterol, sphingomyelin (SM), prostaglandins, integrins, tetraspanins, cell adhesion molecules and growth factor receptors, creates a protected environment for bioactive molecules, such as proteins and nucleic acids that are to be transported over longer distances [1,7,8]. In addition, the EV membrane composition is essential for interactions with target cells, which – as alternative to internalisation by endocytosis – can consist of either membrane fusion or direct ligand-receptor binding [9]. Finally, EVs might carry (precursors of) potentially bioactive lipids to be released in the extracellular space or to be used for interaction with the target cell. In this respect, the relatively unexplored EV lipidome is potentially a significant library of information when it comes to unraveling the multitude of EV types and functionalities. The studies that focused on EV lipidomics in the last 2 decades have provided an overview of general lipid distribution and variations thereof in EVs derived from different cell types [8,10-16]. It is postulated that the origin of EVs is reflected in their lipid signature: microvesicles (EVs shed from the cell membrane) resemble the parental plasma membrane, whereas exosomes (EVs derived from the lumen of multivesicular bodies after fusion with the plasma membrane) undergo lipid sorting resulting in enrichment of SM, cholesterol, phosphatidylserine (PS) and phosphatidyl-ethanolamine (PE) [12,13].

Previously, we found that a small population of EVs is enriched in synovial fluid (SF) from horses that underwent lipopolysaccharide (LPS)-induced acute synovitis (Boere *et al.*, manuscript in preparation). This population of EVs, highly positive for CD44, appeared to stay present as a separate population in the joint at 24 hours post LPS-injection, a moment at which the majority of synovitis-induced EVs (peak at 8 hours post LPS injection) had been cleared. This small subpopulation of EVs could potentially give us important information about the role of EVs during (the resolving phase of) acute synovitis and was, therefore, chosen as target for lipidomic analysis.

4

CD44 is the receptor for hyaluronic acid (hyaluronan) [17], the main extracellular matrix component of SF [18]. CD44 is, besides being present on certain EVs, also present on multiple cell types, among which synovial fibroblasts and neutrophils [19,20]. Recently, CD44 has been associated with lipid rafts, which are cholesterol and sphingolipid enriched microdomains of the plasma membrane [17]. Interestingly, it was found that CD44 ligand binding ability was increased after cholesterol depletion in lipid rafts, causing dispersion of CD44 within the membrane [21]. This process was observed during inflammation and cancer and, therefore, is thought to be disease-induced. Although typical lipid rafts have not yet been described in EVs, the knowledge that membrane lipid remodeling as a reaction to disease can regulate functionality of membrane molecules, provides enough reason for the detailed analysis of the EV lipidome during synovitis.

The comparison of the EV lipid composition between SF from healthy and inflamed joints can potentially indicate bioactive lipids that could act as a target or active substance for future treatments, or can point to lipid-mediated regulation of disease mechanisms. Different lipidomic profiles in SF of patients suffering from osteoarthritis and rheumatoid arthritis compared to healthy controls have previously been detected [22,23] and underline the relationship of the lipidome with changes in joint homeostasis.

Highly sensitive and high-resolution mass spectrometry techniques, such as heated electrospray ionisation liquid chromatography tandem mass spectrometry (HESI-LC-MS[2]) can, in addition to studying overall lipid composition in body fluids, tissues, cells or EVs, be used to help in identification and structural characterisation of new (sub) classes of lipid species, even if they only make up trace amounts of the total lipidome of the study object. Here, we exploited this technique to screen for EV lipids that might be involved in acute synovitis.

MATERIALS AND METHODS

Ethical considerations for animal experiments. All *in vivo* experiments were approved by the Utrecht University Animal Ethics Committee (DEC), the Animal Welfare Body (IvD), and the Central Authority for Scientific Procedures on Animals (CCD) under license number 10800. All procedures were performed according to the Dutch Experiments on Animals Act and conform to the EU standards (European Directive 2010/63/EU).

Experimental LPS-induced acute synovitis in adult horses and collection of SF.
Experimental synovitis was monitored during 24 hours post intra-articular injection of
bacterial LPS in 8 skeletally mature Warmblood horses with no known history of
orthopaedic disorders (Cokelaere S.M. *et al.*, manuscript in preparation). Samples of
3 randomly selected animals were used for EV isolation. Briefly, animals received
injections of 0.25 ng LPS from *E. Coli* O55:B5 (Sigma Aldrich, St. Louis, MO, USA) into
the left and right middle carpal and tarsocrural joints. Synovial fluid was collected by
sterile arthrocentesis prior to LPS-injection (LPS-0h, baseline) and at 24 hours post
LPS-injection (LPS-24h). Synovial fluid was cleared from cells by centrifugation at
2,700g (4,000 rpm) for 30 min at RT in a Universal 32 centrifuge (Hettich, Tuttlingen,
Germany) with rotor 1619, aliquoted and stored at -80°C until used for EV isolation.

Extracellular vesicle isolation from SF. Isolation of EVs from SF was performed for
healthy SF (LPS-0h; n=3) and synovitis SF (LPS-24h; n=3). Stored cell-free SF (see
above) was thawed, pooled for left + right middle carpal joints (volume LPS-0h = 1.5
ml per animal; volume LPS-24h = 0.8 ml per animal) and incubated with hyaluronidase
solution (HYase Type II from sheep testes, Sigma-Aldrich, St. Louis, MO, USA) (1500
U/ml in H_2O; 20 µl per ml SF) for 15 min at 37°C in a water bath while vortexing every
5 min. Then, PBS was added to reach a volume of 2 ml, after which the solution was
centrifuged at 1000g for 10 min at RT in an Eppendorf centrifuge (Hettich Mikro 200R
with rotor 2424A, Hettich, Tuttlingen, Germany) to remove aggregates. Next, samples
were transferred into MLS50 tubes (Beckman-Coulter, Fullerton, CA, USA) and gently
mixed with PBS to reach a volume of 5 ml. EVs were pelleted with 2 sequential ultra-
centrifugation steps of 10,000g (35 min, 10,000 rpm; RCF average 8,025g; RCF max
10,730g; κ-factor 1,777) and 200,000g (120 min, 50,000 rpm; RCF average 200,620g;
RCF max 268,240g; κ-factor 71.7) using an MLS50 rotor in a Beckman-Coulter
Optima™ MAX-E ultracentrifuge (Beckman-Coulter, Fullerton, CA, USA) at 4°C. The
resulting 10,000g (10K) and 200,000g (200K) EV-pellets were resuspended in 250 µl
PBS.

OptiPrep^TM density gradient purification. Resuspended 10K and 200K EV-pellets
were mixed with 1.25 ml pure OptiPrep^TM (60% Iodixanol; Sigma-Aldrich, St. Louis,
MO, USA) (total volume = 1.5 ml) in MLS50 tubes (Beckman-Coulter, Fullerton, CA,
USA) and carefully overlaid with 2 ml iodixanol 40% (in PBS), 1 ml iodixanol 10% (in
PBS) and 500 µl PBS to create discontinuous gradients. An empty control gradient
without EV-suspension was taken along. Gradients were centrifuged at 200,000g for
16 h at 15°C (Beckman-Coulter Optima™ MAX-E centrifuge, Beckman-Coulter,
Fullerton, CA, USA; MLS50 rotor; 50,000 rpm; RCF average 200,620g; RCF max
268,240g; -factor 71.1). After centrifugation 5 fractions of 1 ml were collected from
bottom (fraction 5) to top (fraction 1) by using a peristaltic pump connected to a

4

capillary tube reaching to the bottom of the centrifuge tube. The 3 middle fractions (density F2 = 1.05 g/mol; density F3 = 1.11 g/mol; density F4 = 1.22 g/mol) were pooled (total volume = 3 ml) and frozen at -20°C until used for lipid extraction.

Lipid extraction and lipidomics. Lipids were extracted according to the Bligh & Dyer method [24] with slight modifications. To 0.8 ml sample 1 ml chloroform and 2 ml methanol were added, and mixed thoroughly. After 30 min 1 ml 0.9% NaCl and 1 ml chloroform were added, and after mixing the two phases were separated by centrifugation for 5 min at 2,000g (Universal 32 centrifuge, Hettich, Tuttlingen, Germany, with rotor 1619). The lower chloroform phase, containing lipids, was transferred to a conical glass tube and kept aside. To the remaining sample (upper phase) another 1 ml of chloroform was added for a second round of identical separation, after which the lower chloroform phase was again isolated and pooled with the first chloroform extract. To remove the remaining OptiPrep™ from the samples the pooled lipid extract was washed once with 2 ml 2 M NaCl and, after evaporation of the chloroform, stored dry under a nitrogen atmosphere at -20°C for no longer than 14 days before analysis.

For chromatography, dried lipid extract was dissolved in 50 μl chloroform/methanol (1:1), of which 10 μl was injected onto a hydrophilic interaction liquid chromatography (HILIC) column (Kinetex 2.6 μm, Phenomenex, Torrance, CA, USA) at a flow rate of 1 ml/min to resolve different lipid classes, essentially as described elsewhere [15]. Column effluent was introduced into an LTQ-XL mass spectrometer (Thermo Scientific, Waltham, MA, USA) and analyzed in the negative ion mode using a heated electrospray ionisation (ESI) source. Capillary and source heater temperature were set to 400°C and 450°C, respectively. Ion spray voltage was -2.5 kV, capillary voltage was -8 V and tube lens voltage was -77 V. Full scan spectra were collected in the range from 450–950 m/z at a FWHM of 0.4 Da. For identification of acyl composition, MS[2] spectra were collected from the 3 most abundant m/z signals for each survey scan, using dynamic exclusion for 3 seconds.

Chromatographic mobility analysis of unidentified phospholipids was performed by reverse phase chromatography according to Retra *et al.* [25], or by HILIC chromatograph as described above. Mass spectrometric detection was done using negative mode ESI, on a 4000 QTRAP mass spectrometry system (Applied Biosystems, Nieuwerkerk aan den IJssel, The Netherlands). Source temperature was set to 450°C and nitrogen was used as curtain gas. The declustering potential was set to -80 V and the collision energy set to 35 V. For optimal sensitivity and selectivity, quantification of tested lipids was performed in multiple reaction monitoring (MRM, also known as "Selected Reaction Monitoring" (SRM) mode).

Chemical synthesis of *N*-modified PS. *N*-acetyl-PS, *N*-propionyl-PS and *N*-butyryl-PS were prepared by a one-step reaction of 18:0/18:1 PS (1-stearoyl-2-oleoyl-*sn*-glycero-3-phospho-L-serine sodium salt (SOPS), Avanti Polar Lipids, Alabaster, AL, USA) with the corresponding anhydride (acetic, propionic or butyric anhydride, all from Sigma-Aldrich, St. Louis, MO, USA). Briefly, 1 ml 1 mM SOPS in chloroform/methanol (1:1) was placed on ice, after which 10 µl 6 M HCl and 20 µl of the appropriate anhydride were added. After mixing, 200 µl saturated NaHCO₃ solution was added and the reaction was allowed to proceed for 30 min on ice. The reaction was stopped by extraction of the phospholipids by Bligh & Dyer as described above.

N-formyl-PS was synthesised in two steps. First, a stable *N*-hydroxysuccinimide(NHS)/formate ester was prepared by NHS-activation of formic acid: 1 ml 10 mM formic acid (set to pH 5 with 1 M NaOH) was mixed with 1.2 mg NHS and 0.8 mg 1-ethyl-3-[3-dimethylaminopropyl]carbodiimide (EDC). The reaction was allowed to stand for 30 min at RT. Then, the NHS/formate ester was allowed to react with the amino group of SOPS (amide reaction): to the NHS-formic acid ester, 1 µmol SOPS in 3 ml chloroform/methanol (1:2) and 0.2 ml 0.1 M phosphate buffer (pH 8) were added. This mixture was allowed to stand for 2 hours, after which the phospholipids were extracted by Bligh & Dyer as described above. Yields for the anhydride reaction and the NHS reaction were $> 80\%$ and $\sim 40\%$, respectively.

Biostatistics. Data were converted to mzXML format and analyzed using XCMS v1.50.1 running under R v3.3.2 [26,27]. Featured peaks were normalised to the total peak intensity of the corresponding sample, and annotated based on their m/z value, retention time and, if available, MS² spectrum.

Non-linear iterative partial least squares principal component analysis (PCA) was performed on pareto-scaled annotated normalised data, using the R-package pcaMethods v1.66.0. Heatmap and cluster analysis was performed on Spearman correlations between all individual lipids, using the R-package ComplexHeatmap v1.12.0.

RESULTS

Lipids were successfully extracted from EVs that were isolated from synovitis SF by pelleting at 10,000*g* (10K) and 200,000*g* (200K) ultracentrifugation and purified by OptiPrep™ density gradients. In addition, lipids were extracted from the remaining EV-depleted supernatant and from control density gradients without EVs, serving as background control. Automated peak detection of extracted lipids and subsequent alignment of peaks resulted in a total of 946 detected features. After background

subtraction, isotope and adduct correction, 239 lipids were identified. Annotation of the lipids was based on their chromatographic mobility (lipid class), their m/z ratio, and, if available, their MS^2-spectrum. Note that, due to the fact that neutral lipids like di- and tri-glycerides, cholesterol and ceramides all elute at the front of the chromatographic separation, neutral lipids were not included in the analysis.

Principal component analysis of the lipids revealed that EVs from healthy vs. synovitis SF and 10K vs. 200K EVs had distinct lipid profiles (Figure 1A). Furthermore, EV lipids were clearly distinguished from lipids in the EV-depleted supernatant. A more detailed look at the loading plot of the PCA revealed the lipids that were most prominently responsible for the distinguished lipid profiles between samples (Figure 1B). Along with some poly-unsaturated PE, saturated hexosylceramides (HexCer) and 36:1 PS, EVs from LPS-induced synovitis samples contained relatively high amounts of at least 4 yet unidentified phospholipid subclasses (marked as PL-X_n, Figure 1B). In addition to these specific synovitis-related EV-lipids (oriented towards the lower end of the plot), also the most common forms of PS, PE, phosphatidylcholine (PC), phosphatidic acid (PA), bis(monoacylglycero)phosphate (BMP) and SM were found (towards the left and upper ends of the plot, correlating with the healthy EV samples).

An HPLC-MS contour plot of a 200K synovitis EV sample indicated that the unidentified lipids displayed a chromatographic mobility between that of phosphatidylinositol (PI) and PS (Figure 2A). To our surprise, MS^2 analysis of the four major unidentified phospholipids (PL-X_1 to PL-X_4) and the nearby eluting 36:1 PS had, except for a higher precursor mass, identical fragmentation spectra. This indicated that these lipids were all 18:0/18:1 glycerophospholipids of which only the head group was different (Figure 2B–F). Note that for all newly found lipid classes also other molecular species (*e.g.* 18:0/18:2) could be identified. Since the PCA revealed that, together with the unknown phospholipids, the level of PS (18:0/18:1) was increased in the LPS-induced synovitis EVs, we hypothesised that the unknown phospholipids were modifications of the PS head group. Finally, based on the incremental mass difference of 14 Da between the individual unknown phospholipid subclasses, it was argued that this could be a repeating addition of a CH_2 (14.0266 Da) to the head group. We concluded that the modifications were amide-bonds between the amino group of serine and small carboxylic acids, of which the proposed structures are depicted in Figure 3. The lipids were denoted as *N*-formyl-PS (PS-C1), *N*-acetyl-PS (PS-C2), *N*-propionyl-PS (PS-C3) and *N*-butyryl-PS (PS-C4). In addition, based on their retention time patterns (Figure 2A) additional variations (PS-C5, PS-C6 and possibly other) could occur, although the identity of these lipids was not confirmed by MS^2-data.
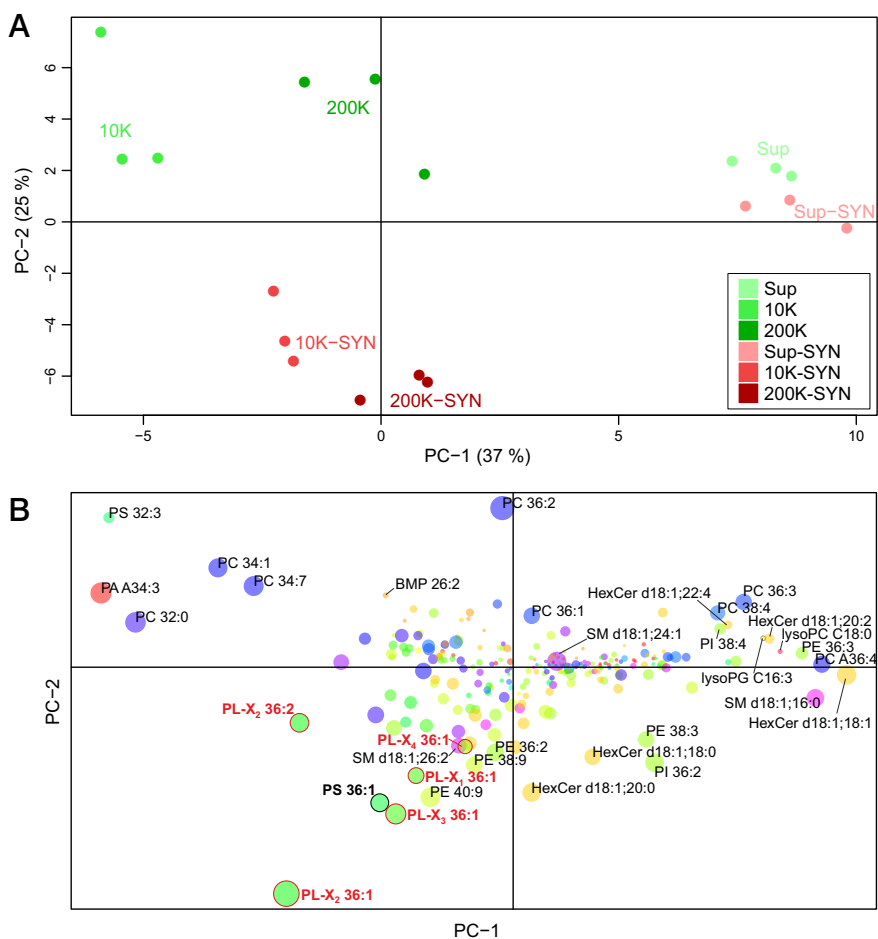
4

Figure 1 Principal component analysis (PCA) of lipids isolated from synovial fluid EVs and from EV-depleted synovial fluid (sup) from healthy joints vs. LPS-induced synovitis. **A)** PCA score plot of principal component-1 (PC-1) and PC-2, showing a clear segregation of samples in the original sample groups. Lipids were extracted from EVs pelleted with steps of 10,000*g* (10K) and 200,000*g* (200K) during differential ultracentrifugation and purified in OptiPrep™ density gradients. In addition, lipids were extracted from the remaining EV-depleted supernatant (sup). Samples were analysed from both healthy joints and joints with LPS-induced synovitis (SYN). Each dot represents one animal (n=3 per condition). **B)** The corresponding PCA loading plot indicating individual lipids found in the samples. The size of the dots represents the log of the summed intensity of the lipid. Dot colours are roughly indicative for the chromatographic retention time; variation of green: PS/PE/PI, blue: PC, yellow: HexCer, purple: SM, red: PA. A selected number of lipids are annotated with corresponding numbers of carbon atoms and double bonds in their two fatty acyl chains.

Figure 1 (*Continued*)

Unknown phospholipid (sub)classes are indicated in red. Abbreviations: BMP, bis(monoacyl-glycero)phosphate; HexCer, hexosylceramide; PA, phosphatidic acid; PC, phosphatidylcho-line; PE, phosphatidylethanolamine; PI, phosphatidylinositol; PL-X$_{1/2/3/4}$, unknown phospholipid (sub)classes; PS, phosphatidylserine; SM, sphingomyelin.
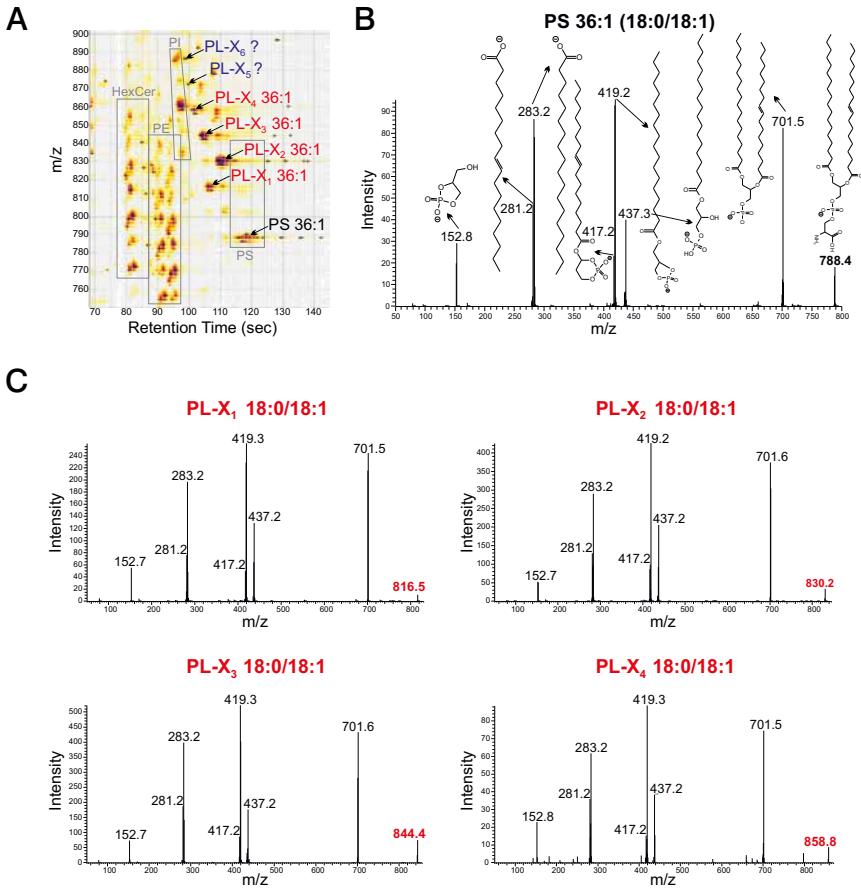
Figure 2 LC-MS^2 analysis of 36:1 PS and unknown PS (sub)classes. **A)** Partial contour plot of lipids found in synovial fluid EVs from a representative LPS-induced synovitis sample, showing the m/z and chromatographic mobility of the unidentified lipid classes (PL-X$_n$) compared to some of the other lipid classes. Note that, based on retention time, multiple unknown phospholipid (sub)classes were found. **B)** MS^2 fragmentation spectrum of 36:1 PS including the proposed molecular structures of individual fragments. **C)** MS^2 fragmentation spectra of the 4 most abundant unknown phospholipid (sub)classes. Abbreviations: HexCer, hexosyl-ceramide; m/z, mass-to-charge ratio; PE, phosphatidylethanolamine; PI, phosphatidylinositol; PL-X$_{1-6}$, unknown phospholipid (sub)classes; PS, phosphatidylserine.
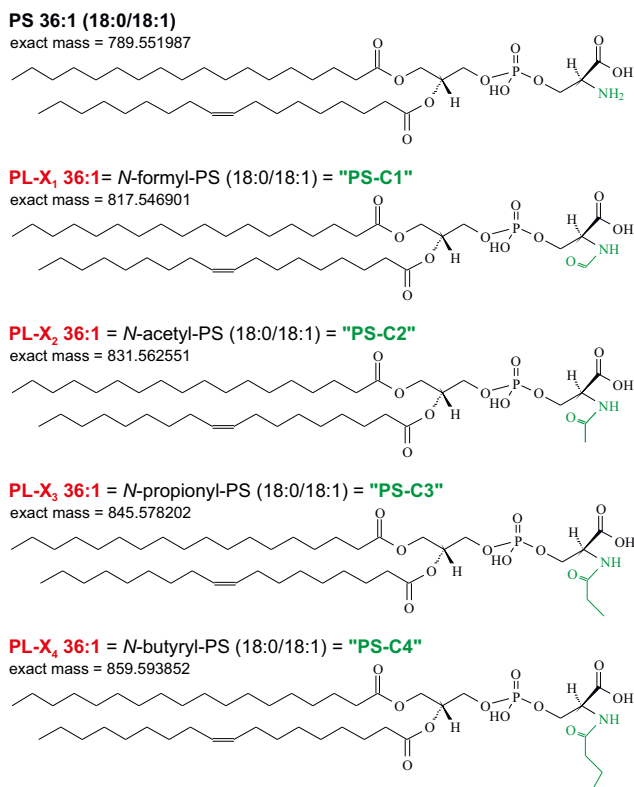
Figure 3 Lewis structure of phosphatidylserine (PS) and the proposed structures of naturally occurring *N*-modified variations of PS. Abbreviations: PL-X$_{1-4}$, unknown phospholipid (sub) classes.

To test our hypothesis, PS-C1, PS-C2, PS-C3 and PS-C4 were produced synthetically (all 18:0/18:1) and their chromatographic mobility was compared to their endogenous counterparts by both hydrophilic (HILIC) and hydrophobic (Reverse Phase) interaction chromatography (Figure 4). Here the detection was based on multiple reaction monitoring of the precursor ions (788.5 for PS, 816.5 for PS-C1, 830.5 for PS-C2, 844.5 for PS-C3 and 858.5 for PS-C4), and the three 701.5, 281.2 and 283.2 characteristic fragment ions representing the 36:1 glycerophospholipid backbone and the two fatty acyl fragments 18:1 and 18:0, respectively. This analysis showed identical retention times for synthetic and endogenous lipids on both chromato-graphic media (Figure 4), confirming that the proposed structures in Figure 3 were representing the unknown phospholipid (sub)classes.
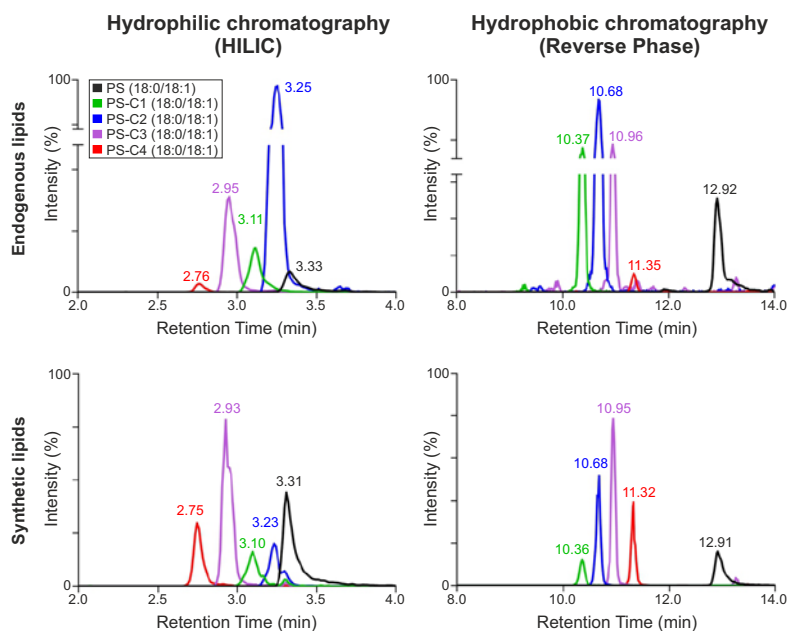
Figure 4 Chromatographic mobility of endogenous lipids (isolated from synovial fluid EVs during LPS-induced synovitis, purified in OptiPrep™ density gradients) compared to synthetically produced modifications of PS: *N*-formyl-PS (PS-C1), *N*-acetyl-PS (PS-C2), *N*-propionyl-PS (PS-C3) and *N*-butyryl-PS (PS-C4). In the left two panels, the mobility of a hydrophilic interaction column (HILIC) is depicted, and in the right panels the mobility on a hydrophobic interaction column (Reverse Phase). The detection was based on an MS-analysis (in multiple reaction monitoring mode) of the precursor ions (788.5 for PS, 816.5 for PS-C1, 830.5 for PS-C2, 844.5 for PS-C3 and 858.5 for PS-C4), and the three 701.5, 281.2 and 283.2 characteristic fragment ions representing the 36:1 glycerophospholipid backbone and the two fatty acyl fragments 18:1 and 18:0, respectively. Only the signals for the precursor mass to 701.5 transitions are plotted, however, the identities for all peaks were confirmed by the transition to the fatty acyl fragments. Note that the differences in retention times of the synthetic lipids compared to the endogenous lipids were all less than 40 ms.

Finally, to get more insight into the distribution of lipids among the sample groups and how they related to each other, a correlation analysis was performed in which the Pearson correlation coefficient was calculated between all individual lipid species. On the correlation coefficient between the 75 most abundant lipids a cluster analysis was performed and plotted in a correlation matrix (Figure 5). Roughly 3 large lipid clusters appeared, which, according to the group distribution of samples, could mainly be attributed to 1) healthy EVs, 2) synovitis EVs, and 3) EV-depleted supernatant. In addition, this analysis confirmed that EVs, especially from LPS-induced synovitis samples, are enriched in *N*-modified PS lipids. Of note, in the EV-depleted supernatant, enrichment was found for lysophospholipid and for phospholipids containing a high degree of unsaturation, both independent from the disease state (healthy/synovitis) of the joint.

DISCUSSION

In this study we show the existence of a number of previously *in vivo* undescribed glycerophospholipid subclasses, which were identified as short-chain carboxylic acid modifications of PS, in the lipidome of EVs extracted from SF of inflamed joints. Phosphatidylserine is made up of a glycerol backbone esterified with 2 fatty acyl chains of variable length and saturation at the *sn*-1 and *sn*-2 carbons of the glycerol moiety. At the *sn*-3 position a phosphate is covalently linked to serine, giving the lipid head group a net negative charge [28]. Only very few earlier reports have described naturally occurring PS modifications at the serine amine group ($-NH_2$) [29,30]. Here, we describe for the first time an *in vivo* short-chain modification of this sort.

N-modified PS was enriched in SF-derived EVs, particularly in 200K EVs, and its presence is increased during LPS-induced synovitis. By LC-MS[2] analysis (at least) four novel glycerophospholipid subclasses were found. Structurally, these consisted of PS molecules of which the amino-group was linked to a carboxylic acid that varied in chain length from C1 to C4, *i.e.* *N*-formyl-PS (PS-C1), *N*-acetyl-PS (PS-C2), *N*-propionyl-PS (PS-C3) and *N*-butyryl-PS (PS-C4). The chromatographic mobility, on both hydrophobic and hydrophilic interaction columns, and fragmentation spectra of these naturally occurring PS-modifications were identical to synthetically produced homologues, confirming their identity.

The modifications of the head group had a relatively large influence on the hydrophobicity of the lipids, as evidenced by the reduced retention times in the hydrophobic chromatographic mobility analysis. The first modification that results in PS-C1 causes the strongest shift towards a shorter retention time from the original
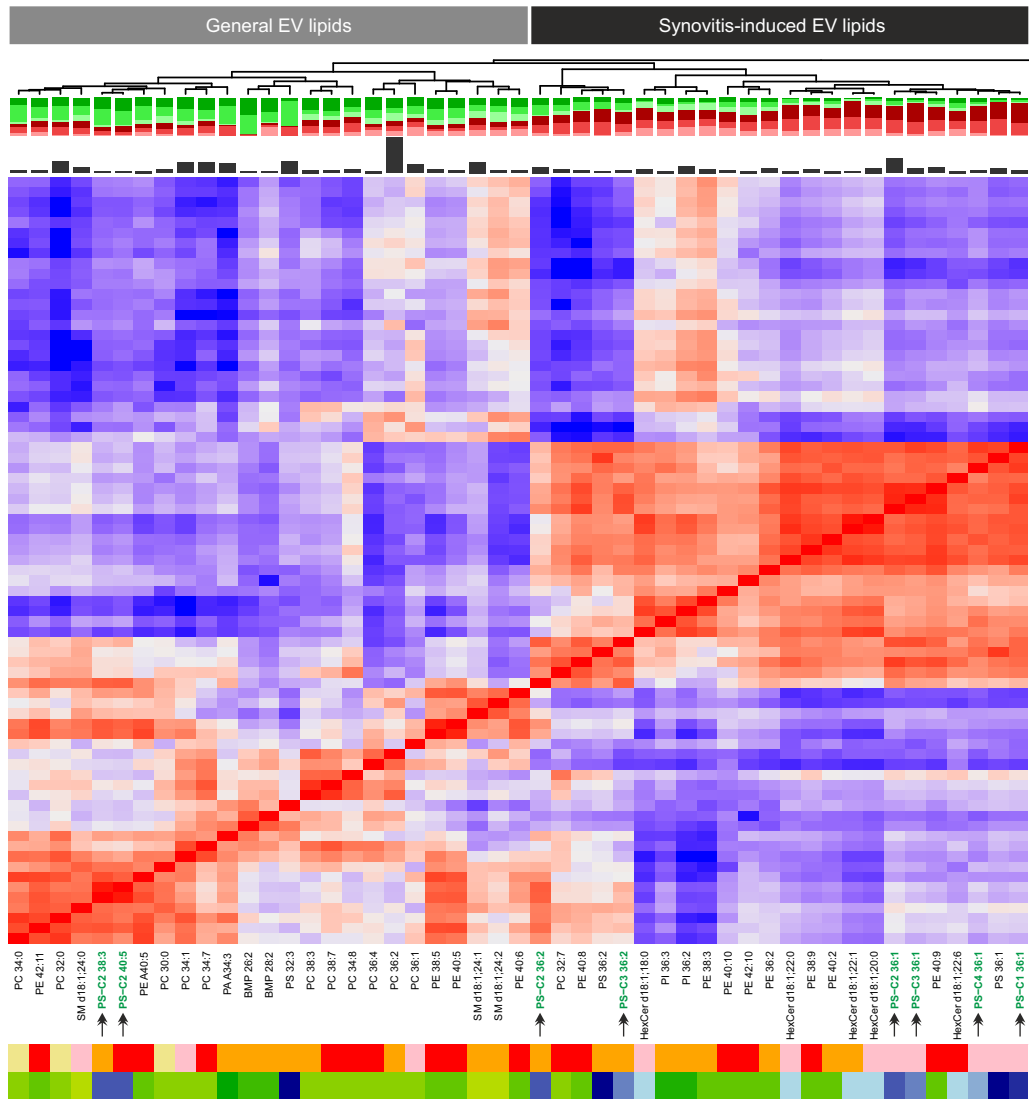
Figure 5 Combined heatmap (cluster dendrogram) of the Spearman correlations between the 75 most abundant lipids in all sample groups. Lipids were extracted from synovial fluid EVs pelleted with subsequent 10,000*g* (10K) and 200,000*g* (200K) ultracentrifugation and purified in OptiPrep^TM density gradients. In addition, lipids were extracted from the remaining EV-depleted supernatant (sup). Samples were analysed from both healthy joints and joints with LPS-induced synovitis (SYN). A possible interpretation of the resulting clusters is given at the
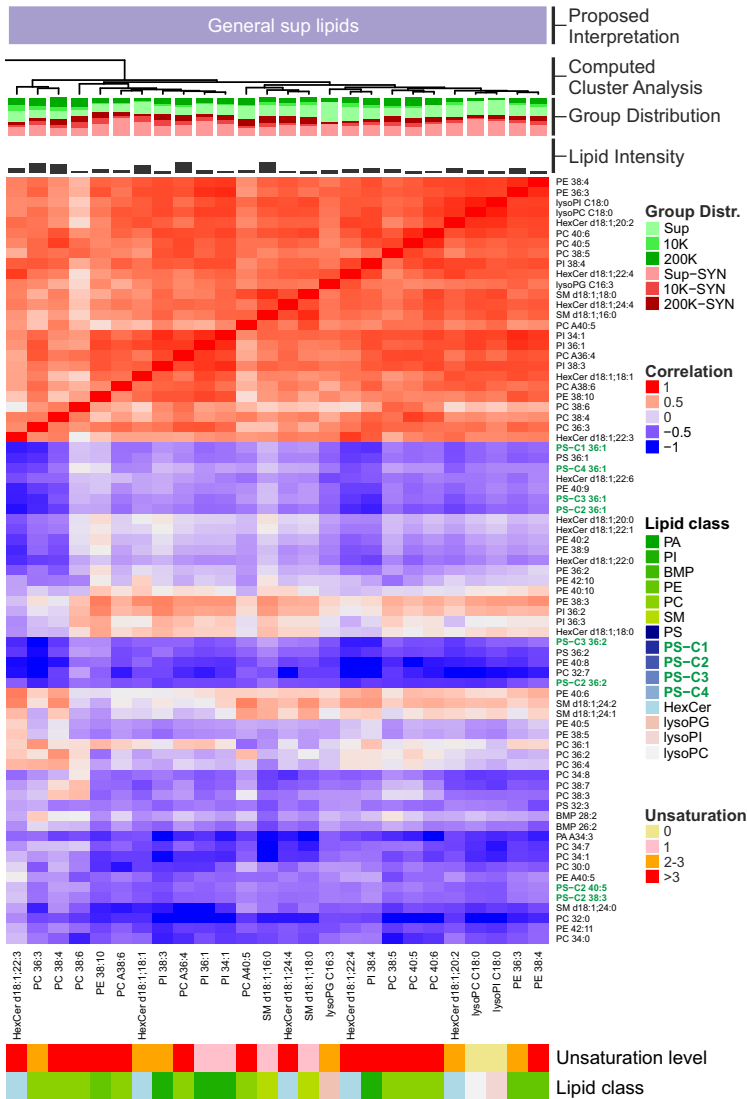
top of the figure. PS variations *N*-formyl-PS (PS-C1), *N*-acetyl-PS (PS-C2), *N*-propionyl-PS (PS-C3) and *N*-butyryl-PS (PS-C4) are shown in green. Abbreviations: BMP, bis(monoacylglycero)-phosphate; HexCer, hexosylceramide; PA, phosphatidic acid; PC, phosphatidylcholine; PE, phosphatidylethanolamine; PI, phosphatidylinositol; PS, phosphatidylserine; SM, sphingomyelin.

4

PS. At first sight, this was not expected, since by this modification the phospholipid head group becomes less hydrophilic, and thus a longer retention time was expected. The conversion of the charged amino group to a non-charged amide in the modified PS, leading to a lower number of charged groups, could possibly be the explanation for the decreased hydrophobic interaction force between the acyl chains of PS and the reverse phase column, and thus for the shorter retention time. As expected, the increasing acyl chain length for PS-C2 to -C4 resulted in an increased retention time compared to PS-C1. Masking the amino-group and attachment of an acyl chain also resulted in a decreased hydrophilic interaction, thus a reduced retention time on the HILIC-column. The stronger retention time shift of PS-C1 compared to PS-C2 can be explained by the physical properties of the aldehyde-oxygen of PS-C1 compared to the keto-oxygens of PS-C2, -C3 and -C4.

Regarding the *in vivo* formation of these lipids, the proposed lipid structures are rather peculiar when realizing that in eukaryotic lipid biosynthesis chain elongation or shortening is thus far known to only take place by an even numbers of carbon atoms (*i.e.* acetyl-CoA is used as a building block or is liberated during β-oxidation). In the individual PS modifications described here, the lipid structure is each time elongated by one carbon only. Currently, the mechanism of formation of these lipids remains elusive.

A second enigma regarding the *in vivo* synthesis of these lipids is the short-chain character of the carboxylic acids by which PS is modified (as small as 1 carbon), which is very uncommon. In 2007, a somewhat similar PS modification was described in mouse brain, pig brain, the RAW-264.7 macrophage tumour cell line and yeast, which was referred to as a family of *N*-acyl-PS. That family has, in contrast to our findings, very long *N*-linked acyl chains consisting of at least 14 carbon atoms (mass > 998), *e.g.* *N*-arachidonoyl-PS, *N*-oleoyl-PS and *N*-palmitoyl-PS [29]. Also *N*-modifications of other glycerophospholipids described in the past, such as *N*-acyl-phosphatidylethanolamine (*N*-acyl-PE), consist of long-chain acyl groups [31]. These, or similar, long-chain modifications were not found in our samples.

Based on the biosynthesis of *N*-acyl-PE, which is proposed to occur by the Ca^{2+} dependent transacylase-mediated transfer of the *sn*-1-acyl chain of a phospholipid onto the amine of PE [31], it is conceivable that short-chain *N*-modified PS is produced in an analogous manner. However, since the formyl group we encountered is not part of any known phospholipid, and the short-chain carboxy-esters are rather uncommon, a direct transfer as seen with *N*-acyl-PE is unlikely. *N*-terminal formylation, however, is a known process taking place during mitochondrial protein synthesis, producing *N*-formyl-methionine for the initiation of translation. These formyl groups become

metabolically available after posttranslational removal by deformylases [32]. Interestingly, mitochondrial *N*-formyl peptides can cause airway contraction and lung neutrophil infiltration via formyl peptide receptor activation [33], demonstrating a functional role for *N*-terminal formylation.

Another possible mechanism for the synthesis of *N*-modified PS is the direct addition of the appropriate carboxylic acid to the amino group of PS. A candidate group of enzymes catalysing these reactions are the *N*-acyl-L-amino-acid aminohydrolases, of which especially aminoacylase 1 (ACY1) is of interest, since it can catalyse the reverse reaction [34]. Furthermore, ACY1 has been found to be associated with exosomes, indicating its potential role in exosome maturation [35].

This is the first report describing the occurrence of the short-chain *N*-modified PS lipids *in vivo*. The lipids have come to our attention because of the enrichment in the synovitis samples studied. Importantly, we were also able to detect them in SF from healthy joints (although at very low concentrations for which reason they may thus far have gone unnoticed). In addition, they were detected in samples in which the total 200K pellet was used (without purification of EVs in OptiPrep™ density gradients) and in fresh non-centrifuged and non-hyaluronidase treated SF (immediate Bligh & Dyer extraction). This rules out the possibility that the new lipid classes would be an artefact of LPS-contamination, hyaluronidase treatment or EV ultracentrifugation and purification procedures. Furthermore, preliminary results revealed that *N*-acetyl PS is also present in human SF from a patient with arthritis, in EVs from human breast milk and in EVs from murine peritoneal mast cells (data not shown). Together, these findings strongly support the physiological presence of *N*-modified PS in humans and several other mammals, and in both healthy and diseased tissues. In all healthy samples of all species tested so far, however, only very low concentrations of the lipids could be detected. Of note, *N*-acetyl-PS was the most abundant modification found in all samples tested so far. The relatively higher yield of *N*-acetyl-PS, *N*-propionyl-PS and *N*-butyryl-PS in the equine samples (compared to samples of other species tested; results not shown) might be explained by the hindgut fermentation process in these herbivores, of which acetic, propionic and butyric acid are the main volatile fatty acid fermentation products [36] which after uptake are transported throughout the body.

Principal component and cluster analysis pointed out distinct lipidomes for healthy and synovitis EVs and showed that these differ from the set of lipids in EV-depleted SF. Among other lipids, all 36:1 and 36:2 *N*-modified PS species were strongly associated with synovitis EVs, although also being present to a much lesser extent in EVs from healthy samples. This result indicates the potential value of further and

4

more in-depth lipidomic studies of EVs and the possible relationships with pathological processes.

The relatively high abundance of lysophospholipids (loss of one fatty acyl chain) and lipids with a high level of unsaturation (double bonds) in the EV-depleted supernatant can be explained by the fact that these lipids are more soluble than non-hydrolysed lipids due to their sterically changed structure and are, therefore, less strongly associated with lipid bilayers. It must be noted that also small amounts of lysophospholipids could be detected in all EVs, with or without synovitis, but they were primarily enriched in EV-depleted SF. This indicates that EVs are not so much the transporters of lysophospholipids, as has been suggested in multiple studies [37], but are more likely to be their producers, shedding them into the extra-vesicular space. Indeed, previous investigations have found phospholipases associated with EVs [37,38]. Together with a range of membrane (precursor) lipids, EVs might in fact represent the biological toolbox for lysophospholipid synthesis outside the cell. Since lysophospholipids are known as "functional lipids" [39] (*e.g.* a form of lysophosphatidylserine (lyso-PS) in schistosomes activates toll-like receptor-2 in humans [40]) this would be an additional way for EVs to transmit signals passively and actively. Furthermore, lysophospholipids in EV-membranes, even at low concentrations, are known to have functional roles too. For example, the binding of C-reactive protein (CRP) to PC, which activates the complement system and enhances phagocytosis, requires the nearby incorporation of lysophosphatidylcholine (lyso-PC) in the cell membrane [41]. This also supports the theory that membrane interaction, be it on cells or EVs (*e.g.* interaction of CD44 with hyaluronan [17,19,21]), could be dependent on modification and reorganisation of lipids.

The exact biological function of short-chain *N*-modified PS is still unclear. A first clue for a possible function was reported in 1979 when Martin and Lagunoff documented that synthetic *N*-acetyl-PS had an inhibiting effect on concanavalin-A-induced mast cell histamine secretion [30]. They also tested two additional *N*-substituted derivates of PS for which the same result was obtained and concluded that any blockage of the serine head group would interfere with its specific interaction on mast cells. Later, more examples of biologically active modifications of phospholipids were documented. The long-chain *N*-arachidonyl-PS described by Guan *et al.* was suggested to be a biosynthetic precursor of the previously discovered naturally occurring signalling lipid *N*-arachidonyl-L-serine, which has vasodilatory and anti-inflammatory properties, such as the ability to suppress LPS-induced TNF-alpha production in several murine cell lines and *in vivo* [29,42]. As for functional modifications of PE, *N*-acyl-PE itself is thought to be involved in the physiologic regulation of dietary fat intake [43], whereas one of its derivates *N*-arachidonyl-ethanolamine (formed after

hydrolysis of *N*-arachidonyl-PE by NAPE-phospholipase-D) is a member of the anandamides family and acts as a fatty acid neurotransmitter in the endogenous cannabinoid system in the central and peripheral nervous system [44,45]. The latter supposedly also would have an anti-inflammatory function by down-regulation of mast cell activity [46]. Based on these examples, it can thus be postulated that short-chain *N*-modified PS molecules potentially can become bioactive when they are hydrolyzed by phospholipases that are carried within EVs [37,38], or by enzymes actively produced in the EV surrounding in specific (patho)physiologic circumstances.

The membrane asymmetry that is typically seen in cells, with the amine-containing PS and PE segregated in the inner leaflet and the choline-containing PC and SM enriched in the outer leaflet, is lost in most EVs. This is due to the absence of active enzymes (flippases, floppases and scramblases) that in cell membranes secure lipid asymmetry. Consequently, PS and PE in most EVs are directed towards both the EV lumen and the surrounding matrix [47,48]. Although PS exposure is a hallmark of cellular apoptosis and serves as an "eat me" flag [49], not all exposed PS on EVs is functionally equivalent. In the case of apoptosis, for example, additional mechanisms are required for final phagocytosis by dendritic cells, *e.g.* the activation of caspase 3, among several others [28,49]. There are no indications that such additional mechanisms are in place in EVs to cause PS-mediated phagocytosis. The random distribution of PS in the EV membrane, however, does enable lipases in both the EV lumen and the surrounding matrix to hydrolyze phospholipids of which the products are (bioactive) lysophospholipids as mentioned earlier. This process was already observed in 1995 when membrane microvesicles, particularly rich in lyso-PC and lysophosphatidyleth-anolamine (lyso-PE), as well as elevated levels of phospholipase A_2 (PLA_2) could be isolated from SF from patients with knee arthritis [37]. The authors concluded that, upon loss of phospholipid asymmetry, microvesicles provide a preferential substrate for PLA_2. Furthermore, phospholipase C and D digestion fragments of *N*-modified-PS (*i.e. N*-acyl-serine phosphate and *N*-acyl-serine, respectively) can be classified as potentially bioactive compounds, based on multiple similar examples from literature. *N*-palmitoyl-serine phosphate is a potential inhibitor of lysophosphatidic acid (lyso-PA) receptors [50] and has been shown to activate endoplasmic reticulum Ca^{2+}-ATPase, resulting in increased cytosolic calcium levels [51]. The phospholipase D product *N*-arachidonyl-serine was shown to have vasodilatory, migratory, neuro-protective, angiogenic, as well as neuroregenerative properties; and *N*-oleoyl-serine is an extremely potent anti-osteoporotic agent [52]. Analogously, specific biological effects can be expected from digestion products of *N*-modified PS.

Conformational changes of the EV lipid membrane, with formation of *N*-modified PS being an example thereof, might also promote or inhibit protein-lipid interactions in

4

these areas of the membrane. Based on preliminary data we have indications that the binding of annexin-V to PS is abolished after modification of the amino group *in vitro*. Interestingly, in 2002, Berckmans *et al.* found that annexin-V binding was impaired on SF EVs from a patient with rheumatoid arthritis (in comparison to plasma EVs) [53]. Considering the *in vivo* increase of EV-associated *N*-modified PS in SF during joint inflammation in our study, inhibition of PS-annexin-V binding can be interpreted as a protective mechanism, possibly preventing pathological mineralisation of the surrounding tissue. In cases of chronic inflammation, EVs have been linked to pathological mineralisation, for example in atherosclerotic lesions and cardiac valve calcification in cardiovascular disease, in calcific tendonitis and in osteophyte formation in osteoarthritis [54-57]. These EVs, derived from local tissue cells, phenotypically resemble matrix vesicles responsible for the initiation of endochondral ossification [58] and hydroxyapatite formation through annexin-V-containing PS-calcium-phosphate complexes. It would be highly favorable to inhibit the formation of such complexes in conditions such as acute inflammation in which massive amounts of EVs are produced. This is especially important, since during osteoarthritis matrix changes (increased quantities of type I collagen and reduced proteoglycan levels) may promote this type of mineralisation [59]. Furthermore, PS on microvesicles was found to be responsible for the successful uptake of the EVs by phagocytosis into the target cell *in vitro*, and this uptake could be prevented by incubation with annexin-V [60]. This could imply that modifications of PS, as described here, are mechanisms to prevent annexin-binding, resulting in full exposure of PS for other protein interactions, possibly with proteins on the target cell membrane. In addition, the induced negative charge of the modified head group makes the EV overall charge more negative, which would also favor interaction with the cell membrane, which is positively charged.

Regarding the possible protective or modulating roles of modifications of PS during inflammation, one can think of inhibiting local blood coagulation, since PS is one of the enhancers of the coagulation cascade [28,61]. Also, PS can supposedly evoke immune suppression and tolerance through activation of the TAM and TIM receptors on cells. Extracellular vesicles were found to actively bind these receptors with their exposed PS [28,62]. Whether modifications of PS influence PS receptor-ligand binding and consequently play a role in immune modulation needs to be further investigated.

Taken together, we here describe for the first time natural occurring short-chain *N*-modifications of PS, for which we have indications that these are involved in joint inflammation. Proposed mechanisms of action are enzymatic hydrolysis (resulting in the formation of potential bioactive components, such as lyso-lipids and *N*-modified (phospho-)serine), changes in protein-lipid interactions, changes in EV-cell

interactions and changes in activation or modulation of the immune response. Conclusions about the biosynthesis, metabolism and exact function of the newly described family of PS cannot be made before results of more detailed research become available. *In vitro* testing of synthetic preparations of *N*-modified PS and its lyso-forms will be the next step in unravelling the details of these interesting molecules.

4

REFERENCES

1. Yanez-Mo, M.; Siljander, P. R.; Andreu, Z.; Zavec, A. B.; Borras, F. E.; Buzas, E. I.; Buzas, K.; Casal, E.; Cappello, F.; Carvalho, J.; Colas, E.; Cordeiro-da Silva, A.; Fais, S.; Falcon-Perez, J. M.; Ghobrial, I. M.; Giebel, B.; Gimona, M.; Graner, M.; Gursel, I.; Gursel, M.; Heegaard, N. H.; Hendrix, A.; Kierulf, P.; Kokubun, K.; Kosanovic, M.; Kralj-Iglic, V.; Kramer-Albers, E. M.; Laitinen, S.; Lasser, C.; Lener, T.; Ligeti, E.; Line, A.; Lipps, G.; Llorente, A.; Lotvall, J.; Mancek-Keber, M.; Marcilla, A.; Mittelbrunn, M.; Nazarenko, I.; Nolte-'t Hoen, E. N.; Nyman, T. A.; O'Driscoll, L.; Olivan, M.; Oliveira, C.; Pallinger, E.; Del Portillo, H. A.; Reventos, J.; Rigau, M.; Rohde, E.; Sammar, M.; Sanchez-Madrid, F.; Santarem, N.; Schallmoser, K.; Ostenfeld, M. S.; Stoorvogel, W.; Stukelj, R.; Van der Grein, S. G.; Vasconcelos, M. H.; Wauben, M. H.; De Wever, O. Biological properties of extracellular vesicles and their physiological functions. *J. Extracell Vesicles* **2015**, *4*, 27066.

2. De Toro, J.; Herschlik, L.; Waldner, C.; Mongini, C. Emerging roles of exosomes in normal and pathological conditions: new insights for diagnosis and therapeutic applications. *Front. Immunol.* **2015**, *6*, 203.

3. Thery, C.; Ostrowski, M.; Segura, E. Membrane vesicles as conveyors of immune responses. *Nat. Rev. Immunol.* **2009**, *9*, 581-593.

4. Boukouris, S.; Mathivanan, S. Exosomes in bodily fluids are a highly stable resource of disease biomarkers. *Proteomics Clin. Appl.* **2015**, *9*, 358-367.

5. Gamez-Valero, A.; Lozano-Ramos, S. I.; Bancu, I.; Lauzurica-Valdemoros, R.; Borras, F. E. Urinary extracellular vesicles as source of biomarkers in kidney diseases. *Front. Immunol.* **2015**, *6*, 6.

6. Verma, M.; Lam, T. K.; Hebert, E.; Divi, R. L. Extracellular vesicles: potential applications in cancer diagnosis, prognosis, and epidemiology. *BMC Clin. Pathol.* **2015**, *15*, 6-015-0005-5. eCollection 2015.

7. Yoon, Y. J.; Kim, O. Y.; Gho, Y. S. Extracellular vesicles as emerging intercellular communicasomes. *BMB Rep.* **2014**, *47*, 531-539.

8. Skotland, T.; Sandvig, K.; Llorente, A. Lipids in exosomes: Current knowledge and the way forward. *Prog. Lipid Res.* **2017**, *66*, 30-41.

9. Mulcahy, L. A.; Pink, R. C.; Carter, D. R. Routes and mechanisms of extracellular vesicle uptake. *J. Extracell Vesicles* **2014**, *3*, 10.3402/jev.v3.24641. eCollection 2014.

10. Subra, C.; Laulagnier, K.; Perret, B.; Record, M. Exosome lipidomics unravels lipid sorting at the level of multivesicular bodies. *Biochimie* **2007**, *89*, 205-212.

11. Record, M.; Carayon, K.; Poirot, M.; Silvente-Poirot, S. Exosomes as new vesicular lipid transporters involved in cell-cell communication and various pathophysiologies. *Biochim. Biophys. Acta* **2014**, *1841*, 108-120.

12. Llorente, A.; Skotland, T.; Sylvanne, T.; Kauhanen, D.; Rog, T.; Orlowski, A.; Vattulainen, I.; Ekroos, K.; Sandvig, K. Molecular lipidomics of exosomes released by PC-3 prostate cancer cells. *Biochim. Biophys. Acta* **2013**, *1831*, 1302-1309.

13. Laulagnier, K.; Motta, C.; Hamdi, S.; Roy, S.; Fauvelle, F.; Pageaux, J. F.; Kobayashi, T.; Salles, J. P.; Perret, B.; Bonnerot, C.; Record, M. Mast cell- and dendritic cell-derived exosomes display a specific lipid composition and an unusual membrane organization. *Biochem. J.* **2004**, *380*, 161-171.

14. Laulagnier, K.; Vincent-Schneider, H.; Hamdi, S.; Subra, C.; Lankar, D.; Record, M. Characterization of exosome subpopulations from RBL-2H3 cells using fluorescent lipids. *Blood Cells Mol. Dis.* **2005**, *35*, 116-121.

15. Brouwers, J. F.; Aalberts, M.; Jansen, J. W.; van Niel, G.; Wauben, M. H.; Stout, T. A.; Helms, J. B.; Stoorvogel, W. Distinct lipid compositions of two types of human prostasomes. *Proteomics* **2013**, *13*, 1660-1666.

16. Skotland, T.; Ekroos, K.; Kauhanen, D.; Simolin, H.; Seierstad, T.; Berge, V.; Sandvig, K.; Llorente, A. Molecular lipid species in urinary exosomes as potential prostate cancer biomarkers. *Eur. J. Cancer* **2017**, *70*, 122-132.

17. Murai, T. Lipid Raft-Mediated Regulation of Hyaluronan-CD44 Interactions in Inflammation and Cancer. *Front. Immunol.* **2015**, *6*, 420.

18. Dahl, L. B.; Dahl, I. M.; Engstrom-Laurent, A.; Granath, K. Concentration and molecular weight of sodium hyaluronate in synovial fluid from patients with rheumatoid arthritis and other arthropathies. *Ann. Rheum. Dis.* **1985**, *44*, 817-822.

19. Boere, J.; van de Lest, C. H.; Libregts, S. F.; Arkesteijn, G. J.; Geerts, W. J.; Nolte-'t Hoen, E. N.; Malda, J.; van Weeren, P. R.; Wauben, M. H. Synovial fluid pretreatment with hyaluronidase facilitates isolation of CD44+ extracellular vesicles. *J. Extracell Vesicles* **2016**, *5*, 31751.

20. Ponta, H.; Sherman, L.; Herrlich, P. A. CD44: from adhesion molecules to signalling regulators. *Nat. Rev. Mol. Cell Biol.* **2003**, *4*, 33-45.

21. Murai, T.; Sato, C.; Sato, M.; Nishiyama, H.; Suga, M.; Mio, K.; Kawashima, H. Membrane

cholesterol modulates the hyaluronan-binding ability of CD44 in T lymphocytes and controls rolling under shear flow. *J. Cell. Sci.* **2013***, 126*, 3284-3294.

22. Kosinska, M. K.; Liebisch, G.; Lochnit, G.; Wilhelm, J.; Klein, H.; Kaesser, U.; Lasczkowski, G.; Rickert, M.; Schmitz, G.; Steinmeyer, J. A lipidomic study of phospholipid classes and species in human synovial fluid. *Arthritis Rheum.* **2013***, 65*, 2323-2333.

23. Kosinska, M. K.; Liebisch, G.; Lochnit, G.; Wilhelm, J.; Klein, H.; Kaesser, U.; Lasczkowski, G.; Rickert, M.; Schmitz, G.; Steinmeyer, J. Sphingolipids in human synovial fluid--a lipidomic study. *PLoS One* **2014***, 9*, e91769.

24. Bligh, E. G.; Dyer, W. J. A rapid method of total lipid extraction and purification. *Can. J. Biochem. Physiol.* **1959***, 37*, 911-917.

25. Retra, K.; Bleijerveld, O. B.; van Gestel, R. A.; Tielens, A. G.; van Hellemond, J. J.; Brouwers, J. F. A simple and universal method for the separation and identification of phospholipid molecular species. *Rapid Commun. Mass Spectrom.* **2008***, 22*, 1853-1862.

26. Smith, C. A.; Want, E. J.; O'Maille, G.; Abagyan, R.; Siuzdak, G. XCMS: processing mass spectrometry data for metabolite profiling using nonlinear peak alignment, matching, and identification. *Anal. Chem.* **2006***, 78*, 779-787.

27. Tautenhahn, R.; Bottcher, C.; Neumann, S. Highly sensitive feature detection for high resolution LC/MS. *BMC Bioinformatics* **2008***, 9*, 504-2105-9-504.

28. Birge, R. B.; Boeltz, S.; Kumar, S.; Carlson, J.; Wanderley, J.; Calianese, D.; Barcinski, M.; Brekken, R. A.; Huang, X.; Hutchins, J. T.; Freimark, B.; Empig, C.; Mercer, J.; Schroit, A. J.; Schett, G.; Herrmann, M. Phosphatidylserine is a global immunosuppressive signal in efferocytosis, infectious disease, and cancer. *Cell Death Differ.* **2016***, 23*, 962-978.

29. Guan, Z.; Li, S.; Smith, D. C.; Shaw, W. A.; Raetz, C. R. Identification of N-acylphosphatidylserine molecules in eukaryotic cells. *Biochemistry* **2007***, 46*, 14500-14513.

30. Martin, T. W.; Lagunoff, D. Inhibition of mast cell histamine secretion by N-substituteed derivatives of phosphatidylserine. *Science* **1979***, 204*, 631-633.

31. Leung, D.; Saghatelian, A.; Simon, G. M.; Cravatt, B. F. Inactivation of N-acyl phosphatidylethanol-amine phospholipase D reveals multiple mechanisms for the biosynthesis of endocannabinoids. *Biochemistry* **2006***, 45*, 4720-4726.

32. Escobar-Alvarez, S.; Goldgur, Y.; Yang, G.; Ouerfelli, O.; Li, Y.; Scheinberg, D. A. Structure and activity of human mitochondrial peptide deformylase, a novel cancer target. *J. Mol. Biol.* **2009***, 387*, 1211-1228.

33. Wenceslau, C. F.; Szasz, T.; McCarthy, C. G.; Baban, B.; NeSmith, E.; Webb, R. C. Mitochondrial N-formyl peptides cause airway contraction and lung neutrophil infiltration via formyl peptide receptor activation. *Pulm. Pharmacol. Ther.* **2016***, 37*, 49-56.

34. Lindner, H.; Hopfner, S.; Tafler-Naumann, M.; Miko, M.; Konrad, L.; Rohm, K. H. The distribution of aminoacylase I among mammalian species and localization of the enzyme in porcine kidney. *Biochimie* **2000***, 82*, 129-137.

35. Brandt, L. E.; Ehrhart, E. J.; Scherman, H.; Olver, C. S.; Bohn, A. A.; Prenni, J. E. Characterization of the canine urinary proteome. *Vet. Clin. Pathol.* **2014***, 43*, 193-205.

36. Goachet, A. G.; Harris, P.; Philippeau, C.; Julliand, V. Effect of physical training on nutrient digestibility and faecal fermentative parameters in Standardbred horses. *J. Anim. Physiol. Anim. Nutr. (Berl)* **2014***, 98*, 1081-1087.

37. Fourcade, O.; Simon, M. F.; Viode, C.; Rugani, N.; Leballe, F.; Ragab, A.; Fournie, B.; Sarda, L.; Chap, H. Secretory phospholipase A2 generates the novel lipid mediator lysophosphatidic acid in membrane microvesicles shed from activated cells. *Cell* **1995***, 80*, 919-927.

38. Subra, C.; Grand, D.; Laulagnier, K.; Stella, A.; Lambeau, G.; Paillasse, M.; De Medina, P.; Monsarrat, B.; Perret, B.; Silvente-Poirot, S.; Poirot, M.; Record, M. Exosomes account for vesicle-mediated transcellular transport of activatable phospholipases and prostaglandins. *J. Lipid Res.* **2010***, 51*, 2105-2120.

39. Kim, H. Y. Phospholipids: a neuroinflammation emerging target. *Nat. Chem. Biol.* **2015***, 11*, 99-100.

40. van der Kleij, D.; Latz, E.; Brouwers, J. F.; Kruize, Y. C.; Schmitz, M.; Kurt-Jones, E. A.; Espevik, T.; de Jong, E. C.; Kapsenberg, M. L.; Golenbock, D. T.; Tielens, A. G.; Yazdanbakhsh, M. A novel host-parasite lipid cross-talk. Schistosomal lyso-phosphatidylserine activates toll-like receptor 2 and affects immune polarization. *J. Biol. Chem.* **2002***, 277*, 48122-48129.

41. Volanakis, J. E.; Wirtz, K. W. Interaction of C-reactive protein with artificial phosphatidylcholine bilayers. *Nature* **1979***, 281*, 155-157.

42. Milman, G.; Maor, Y.; Abu-Lafi, S.; Horowitz, M.; Gallily, R.; Batkai, S.; Mo, F. M.; Offertaler, L.; Pacher, P.; Kunos, G.; Mechoulam, R. N-arachidonoyl

4

L-serine, an endocannabinoid-like brain constituent with vasodilatory properties. *Proc. Natl. Acad. Sci. U. S. A.* **2006***, 103*, 2428-2433.

43. Gillum, M. P.; Zhang, D.; Zhang, X. M.; Erion, D. M.; Jamison, R. A.; Choi, C.; Dong, J.; Shanabrough, M.; Duenas, H. R.; Frederick, D. W.; Hsiao, J. J.; Horvath, T. L.; Lo, C. M.; Tso, P.; Cline, G. W.; Shulman, G. I. N-acylphosphatidylethanolamine, a gut- derived circulating factor induced by fat ingestion, inhibits food intake. *Cell* **2008***, 135*, 813-824.

44. Devane, W. A.; Hanus, L.; Breuer, A.; Pertwee, R. G.; Stevenson, L. A.; Griffin, G.; Gibson, D.; Mandelbaum, A.; Etinger, A.; Mechoulam, R. Isolation and structure of a brain constituent that binds to the cannabinoid receptor. *Science* **1992***, 258*, 1946-1949.

45. Di Marzo, V.; Deutsch, D. G. Biochemistry of the endogenous ligands of cannabinoid receptors. *Neurobiol. Dis.* **1998***, 5*, 386-404.

46. Schmid, H. H. Pathways and mechanisms of N-acyletanolamine biosynthesis: can anandamide be generated selectively? *Chem. Phys. Lipids* **2000***, 108*, 71-87.

47. Bevers, E. M.; Comfurius, P.; Dekkers, D. W.; Zwaal, R. F. Lipid translocation across the plasma membrane of mammalian cells. *Biochim. Biophys. Acta* **1999***, 1439*, 317-330.

48. Kastelowitz, N.; Yin, H. Exosomes and microvesicles: identification and targeting by particle size and lipid chemical probes. *Chembiochem* **2014***, 15*, 923-928.

49. Segawa, K.; Nagata, S. An Apoptotic 'Eat Me' Signal: Phosphatidylserine Exposure. *Trends Cell Biol.* **2015***, 25*, 639-650.

50. Bittman, R.; Swords, B.; Liliom, K.; Tigyi, G. Inhibitors of lipid phosphatidate receptors: N-palmitoyl-serine and N-palmitoyl-tyrosine phosphoric acids. *J. Lipid Res.* **1996***, 37*, 391-398.

51. Jan, C. R.; Lu, Y. C.; Jiann, B. P.; Chang, H. T.; Wang, J. L.; Chen, W. C.; Huang, J. K. Novel effect of N-palmitoyl-L-serine phosphoric acid on cytosolic Ca2+ levels in human osteoblasts. *Pharmacol. Toxicol.* **2003***, 93*, 71-76.

52. Hanus, L.; Shohami, E.; Bab, I.; Mechoulam, R. N-Acyl amino acids and their impact on biological processes. *Biofactors* **2014***, 40*, 381-388.

53. Berckmans, R. J.; Nieuwland, R.; Tak, P. P.; Boing, A. N.; Romijn, F. P.; Kraan, M. C.; Breedveld, F. C.; Hack, C. E.; Sturk, A. Cell-derived microparticles in synovial fluid from inflamed arthritic joints support coagulation exclusively via a factor VII-dependent mechanism. *Arthritis Rheum.* **2002***, 46*, 2857-2866.

54. Gohr, C. M.; Fahey, M.; Rosenthal, A. K. Calcific tendonitis : a model. *Connect. Tissue Res.* **2007***, 48*, 286-291.

55. Hunter, L. W.; Charlesworth, J. E.; Yu, S.; Lieske, J. C.; Miller, V. M. Calcifying nanoparticles promote mineralization in vascular smooth muscle cells: implications for atherosclerosis. *Int. J. Nanomedicine* **2014***, 9*, 2689-2698.

56. Kirsch, T.; Swoboda, B.; Nah, H. Activation of annexin II and V expression, terminal differentiation, mineralization and apoptosis in human osteoarthritic cartilage. *Osteoarthritis Cartilage* **2000***, 8*, 294-302.

57. Genge, B. R.; Wu, L. N.; Wuthier, R. E. Mineralization of annexin-5-containing lipid-calcium-phosphate complexes: modulation by varying lipid composition and incubation with cartilage collagens. *J. Biol. Chem.* **2008***, 283*, 9737-9748.

58. Anderson, H. C. Vesicles associated with calcification in the matrix of epiphyseal cartilage. *J. Cell Biol.* **1969***, 41*, 59-72.

59. Jubeck, B.; Gohr, C.; Fahey, M.; Muth, E.; Matthews, M.; Mattson, E.; Hirschmugl, C.; Rosenthal, A. K. Promotion of articular cartilage matrix vesicle mineralization by type I collagen. *Arthritis Rheum.* **2008***, 58*, 2809-2817.

60. Wei, X.; Liu, C.; Wang, H.; Wang, L.; Xiao, F.; Guo, Z.; Zhang, H. Surface Phosphatidylserine Is Responsible for the Internalization on Microvesicles Derived from Hypoxia-Induced Human Bone Marrow Mesenchymal Stem Cells into Human Endothelial Cells. *PLoS One* **2016***, 11*, e0147360.

61. Lentz, B. R. Exposure of platelet membrane phosphatidylserine regulates blood coagulation. *Prog. Lipid Res.* **2003***, 42*, 423-438.

62. Miyanishi, M.; Tada, K.; Koike, M.; Uchiyama, Y.; Kitamura, T.; Nagata, S. Identification of Tim4 as a phosphatidylserine receptor. *Nature* **2007***, 450*, 435-439.

4

5

Extracellular vesicles in synovial fluid from juvenile horses: a first exploratory study

Janneke Boere [a]
Chris H. A. van de Lest [a,b]
Janny C. de Grauw [a]
Saskia G.M. Plomp [a]
Sten F. W. M. Libregts [b]
Ger J. A. Arkesteijn [b,c]
Jos Malda [a,d]
Marca H.M. Wauben [b]
P. René van Weeren [a]

Departments of Equine Sciences[a], Biochemistry & Cell Biology[b], and Infectious Diseases and Immunology[c] of Faculty of Veterinary Medicine, Utrecht University, Utrecht, the Netherlands; Department of Orthopaedics[d], University Medical Center Utrecht, Utrecht, the Netherlands

ABSTRACT

Background. There is increasing knowledge on extracellular vesicle (EV) profiles in health and disease in various body fluids, including more recently in synovial fluid (SF). However, the EV profiles in SF during normal growth and development remain unknown.

Objectives. To measure basic parameters of EVs in SF during the first months after birth when joint development is at its most dynamic, and compare outcomes with mature animals and with profiles of known SF biomarkers.

Study design. SF and serum from ten healthy foals (12d-13m) and 6 adult horses (6-15y) were repeatedly sampled for biomarker analysis. EV isolation was performed in 7 SF samples from 3 foals (12d-7m) and 2 samples from adults (8y).

Methods. Biomarkers for cartilage matrix turnover (GAG, MMP activity, CTX-II, C2C) and inflammation (CCL2, PGE2) were measured in SF and serum. EVs were isolated from SF by differential ultracentrifugation (10,000g and 200,000g) and purified by sucrose density gradient floatation. EV concentration and characteristics were determined by high-resolution flow cytometry, buoyant density and Western blotting.

Results. Biomarker profiles in SF and serum reflected the high metabolic activity of juvenile joints. No significant changes in EV parameters, *i.e.* EV concentration, light scattering characteristics, buoyant density and EV protein markers CD9 and CD44, were found in SF from foals compared to adults.

Main limitations. EV isolation, purification and analysis from SF is technically challenging and could only be performed for 7 foal samples in this study, limiting the statistical power of the EV data.

Conclusions. Basic EV parameters in healthy SF are not indicative for the typical dynamic joint metabolism in growing foals and do not resemble known biomarker patterns. However, it cannot be excluded that more in-depth functional analyses may reveal differences between juvenile and mature EVs in SF.

INTRODUCTION

Biomarkers in synovial fluid (SF) and serum reflect physiological processes and are valuable tools for early diagnosis of pathological conditions [1]. In foals, changes in these markers can be a reaction to pathological conditions, such as septic arthritis and osteochondrosis (OC) [2-7], but can also reflect the process of growth and development. During the first months of life musculoskeletal development is to a large extent steered by physical adaptation of growing tissues to external factors, like biomechanical loading [8]. It is also during this time that catabolic processes in the articular cartilage can be counteracted and that early OC lesions can spontaneously resolve [9]. Biomarker studies have confirmed that the immature joint is characterised by quickly changing anabolic and catabolic parameters as a result of the high metabolic activity of juvenile cartilage [3-6].

There is an increasing interest in the possible role in health and disease of extracellular vesicles (EVs), which can be found in many, if not all, body fluids [10]. These cell-derived membrane enclosed vesicles (0.04-5 µm) convey cell-cell communication by stable transfer of proteins, lipids and nucleic acids [11] and have been identified in SF as well [12,13]. In the late 1960s, a particular type of EVs, so-called "matrix vesicles", was studied for its role in bone development [14]. These were later confirmed to be the crucial initiators of mineralisation of cartilage during endochondral ossification [15]. To date many more functions of EVs have come to light, *e.g.* as regulators of immune processes [16] and as important actors in joint disease [13,17,18]. Furthermore, EVs from embryonic stem cells have been shown to promote cartilage regeneration *in vitro* [19] and osteochondral regeneration *in vivo* [20] and have been postulated as a possible new tool for cartilage and bone repair [21]. Since there currently is no knowledge on SF-derived EVs in immature animals or humans, we set out to investigate basic EV parameters in SF from healthy foals and adult horses. We hypothesised that basic EV parameters, such as EV concentration, would vary with age and would reflect the developmental stage of the articular tissues. As a positive control and to provide data to which possible differences in EV parameters could be related, profiles of biomarkers known to reflect growth and development were measured in serum and SF of both age groups.

MATERIALS AND METHODS

Extended methodology can be found as supplementary information. Extracellular vesicle isolation and analysis protocols were based on previous reported work by our group [12].

Ethical considerations. All *in vivo* experiments were approved by the Utrecht University Animal Ethics Committee (DEC), the Animal Welfare Body (IvD), and the Central Authority for Scientific Procedures on Animals (CCD) under license number 10800. All procedures were performed according to the Dutch Experiments on Animals Act and conform to the EU standards (European Directive 2010/63/EU). *In vivo* procedures were non-invasive with only minor discomfort for the animals, did not cause adverse effects and did not lead to humane end points (euthanasia) in any of the animals. All *in vivo* and post-mortem experiments were conducted with owners' consent.

SF and blood collection from healthy foals. Over a time-period of 1 year, serum and SF samples were collected from 10 healthy immature Haflinger horses (age: 12d-13m). See Supplementary Table 1 for specification of samples. After routine blood sampling from the jugular vein, the animals were sedated with detomidine (Domosedan[a]) 0.02 mg/kg bwt i.v. and SF samples were taken by arthrocentesis of one middle carpal or radiocarpal joint and one tarsocrural joint. Serum was prepared by centrifugation (20 min 2,700*g*, RT) and stored at −80°C. Synovial fluid was centrifuged (30 min 2,700*g*, RT) and stored at −80°C. See supplementary information for details.

SF collection from healthy adult horses. Synovial fluid was collected post-mortem from 8 adult Warmblood horses that were euthanised for reasons other than joint disease at the Utrecht University Equine Hospital. See Supplementary Table 1 for specification of samples. Synovial fluid (5-10 ml; no blood contamination) was collected by arthrocentesis from the middle or radiocarpal and tarsocrural joints within 2 hours after euthanasia and cleared from cells as described above.

GAG assay. Proteoglycan content was estimated by measuring sulphated glyco-saminoglycan (GAG) concentration by use of the 1,9-Dimethyl-Methylene Blue (DMMB) assay [22] adapted for use in 96-well plates. Synovial fluid was pre-treated with hyaluronidase (HYase Type II from sheep testes[b]) (30U/ml in H_2O), 30 min at 37°C. Synovial fluid and serum were both diluted in PBS/EDTA buffer before use. See supplementary information for details.

MMP assay. A fluorimetric assay to determine overall matrix metalloproteinase (MMP) activity based on cleavage of the fluorogenic peptide substrate FS-6 was used as described previously [23] with minor modifications. See supplementary information for details.

CTX-II, C2C and CCL2 enzyme-linked immunosorbent assays (ELISA)
CTX-II and C2C. Quantitative determination of two degradation products of type II collagen, C-terminal crosslinked telopeptide type II collagen (CTX-II) and collagenase cleaved neopeptide type II collagen (C2C) was performed using two commercial ELISA kits (Serum Pre-Clinical CartiLaps® (CTX-II) ELISA[c] and C2C Cartilage Degradation Competition Assay[d]) according to the manufacturers' instructions. Synovial fluid was diluted 1:1 in the provided dilution buffers.

CCL2. Pro-inflammatory C-C motif chemokine 2 (CCL2; MCP-1) recruits monocytes, memory T cells, and dendritic cells to sites of tissue injury and infection and is implicated in the pathogenesis of several diseases characterised by monocytic infiltrates, such as (rheumatoid) arthritis. Here it was used to identify systemic and intra-articular pro-inflammatory activity. A sandwich ELISA was designed using antibodies directed against equine CCL2. See supplementary information for details.

Prostaglandin-E2 (PGE2) measurement. After addition of 100 µl internal standard (25,24-dimethyl-PGF2a, 40 pg/µl) to 200 µl SF or serum, and acidifying the solution with 200 µl 0.2 M NH_4COOH pH 3.3, eicosanoids were extracted by mixing each sample with 800 µl ethyl acetate 0.002% butylated hydroxytoluene. After thorough mixing and centrifugation at 15,000*g* for 5 minutes the lower water phase was frozen for 30 min at –80°C and the upper organic (liquid) phase collected. This extraction was repeated with another 800 µl ethyl acetate 0.002% butylated hydroxytoluene. After evaporation of the pooled ethyl acetate extracts (speedvac) the dried samples were dissolved in 60 µl 30% methanol and analysed by liquid chromatography-mass spectrometry (LC/MS), as described previously [24] using a 4000 QTRAP system[e]. A standard curve of a known mixture of synthetic prostaglandins (6.25-200 pg/µl) was included for analysis.

Extracellular vesicle isolation from SF. Cell-free SF (starting volume 2 ml) was thawed, incubated with hyaluronidase solution (HYase Type II from sheep testes[b]) (1500 U/ml in H_2O; 20 µl per ml SF) for 15 min at 37°C, and centrifuged at 1000*g* (10 min, RT) to remove aggregates. Samples were topped up with PBS and subsequently ultracentrifuged at 10,000*g* (35 min, 4°C) and 200,000*g* (120 min, 4°C) resulting in 10K and 200K EV-pellets. See supplementary information for details.

Single-EV-based high-resolution flow cytometry. Single-EV-based high-resolution flow cytometry (FCM) was performed using an optimised jet-in-air-based BD Influx™ flow cytometer[f] as described previously [12,25]. See supplementary information for details. Labelling of EVs with PKH67 and anti-CD44 antibody was performed as described previously [25] with minor modifications, followed by density gradient

floatation in sucrose in order to separate labelled EVs from unbound dye and antibody (see supplementary information). Twelve fractions of 1 ml were collected from top (F1, lowest density) to bottom (F12, highest density). Densities were determined by refractometry. Sucrose fractions were diluted 1:10 in PBS prior to measurement.

Western blotting. The same sucrose fractions that were analysed by high-resolution FCM were used for protein identification by Western blotting. Gradient fractions of 375 µl were pooled in pairs (*i.e.* fractions F4+F5 [medium density] and F6+F7 [high density]), diluted in PBS and EVs were pelleted by ultracentrifugation at 200,000*g* (90 min, 4°C). Pellets were resuspended in 65 µl non-reducing SDS-PAGE sample buffer, pooled for each foal (containing fractions F4-F7), and processed for Western blotting using antibodies against CD9 (tetraspanin; general EV marker), CD44 (hyaluronic acid [hyaluronan] receptor; synovial fibroblast marker), major histocompatibility complex class II (MHC-II) and annexin-A1 (AnxA1). See supplementary information for details.

Statistical analysis. Al data were analysed in R v3.3.2 (http://www.R-project.org). Weighted Spearman rank (rho) correlations were calculated using the R-package 'wCorr' v1.8.0. In this analysis repeated sampling of the same animal was penalised by the number of times the subject was sampled. Differences with p-values < 0.05 were considered significant.

RESULTS

Biomarkers in SF and serum during development

To verify the previously reported differences in SF soluble components between immature and adult horses [2-6], SF was first analysed for several factors related to matrix turnover (Figure 1) and joint inflammation (Figure 2). Data from 10 foals (12 days - 13 months, repeated measurements, total n=22) and 6 adult horses (6-15 years, n=6), with no signs of disease at the time of sampling, showed that concentrations of GAG, MMP activity and CTX-II in SF significantly decreased when age increased from foal age until adulthood (Figure 1A–C). C2C and PGE2 in SF, on the other hand, were significantly higher in adult horses compared to foals (Figure 1D, 2A). CCL2 concentration did not differ between foals and adults (Figure 2B). In the group of foals, no significant correlation with age in the first year of life was found for any of the parameters measured in SF. Overall, GAG and C2C were the most stable factors. PGE2 levels were low and also very stable in all foals (Figure 2A), except for one animal, which might have had an unnoticed joint reaction.
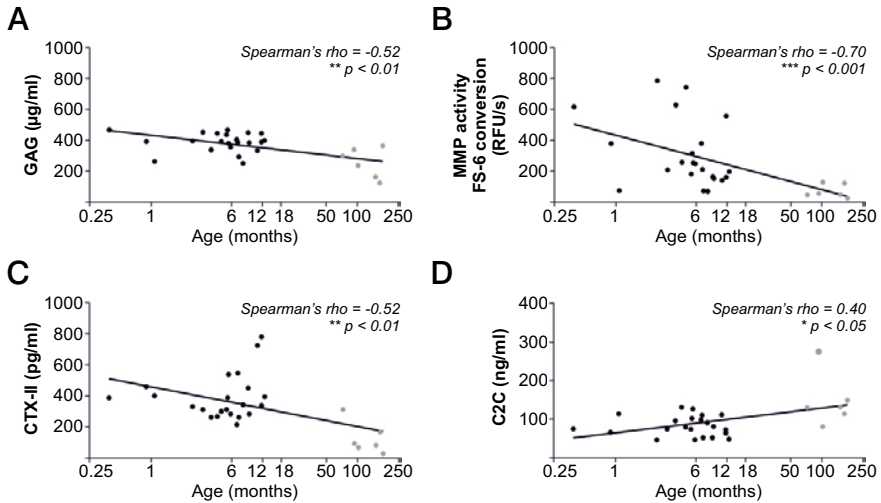
Figure 1 Weighted Spearman rank correlations for soluble factors related to cartilage matrix turnover measured in SF from 10 foals (12 days - 13 months, repeated measurements, total n=22; black dots) and 6 adult horses (6-15 years, n=6; grey dots). Age (x-axis) is presented on a logarithmic scale. **A)** Glycosaminoglycan (GAG). **B)** Activity of total matrix metalloproteinases (MMP). **C)** C-terminal crosslinked telopeptide type II collagen (CTX-II); **D)** Collagenase cleaved neoepitope type II collagen (C2C). There were significant correlations with age from foal to adult, but for none of the parameters a correlation with age was found in the first 13 months of life.

5

Figure 2 Weighted Spearman rank correlations for inflammatory mediators measured in SF from 10 foals (12 days - 13 months, repeated measurements, total n=22; black dots) and 6 adult horses (6-15 years, n=6; grey dots). Age (x-axis) is presented on a logarithmic scale. **A)** Prostaglandin-E2 (PGE2). The dots in circles are repeated measurements from 1 foal with recurrent high PGE2 levels (included in Spearman's rho). **B)** C-C motif chemokine 2 (CCL2). For both parameters no correlation with age was found in the first 13 months of life (foals only). ns, not significant.

Additionally, GAG, MMP activity, CCL2 and PGE2 were monitored in serum of the same foals (Figure 3). No samples from adult animals were included for this analysis. GAG in serum was very stable during the first year of life (Figure 3A), similar to results in SF. In contrast, MMP activity in serum significantly decreased with increasing age ($p<0.05$) (Figure 3B), and displayed remarkably high levels in the first month of life (measured in 3 individuals). Average GAG content in serum was about 6-fold less than in SF, whereas for MMPs the initial activity in serum was about 4-fold higher than in SF. Ultimately, MMP activity levels reached the same order of magnitude in SF and serum in the older foals. For CCL2, only in the first month of life very high levels were found (measured in 3 individuals), after which levels dropped dramatically and were positively correlated with age later in development ($p<0.05$) (Figure 3C). PGE2 was low in the first 5 months in all foals. Later in development, an increase in PGE2 serum concentration was found ($p<0.05$), however, this was predominantly due to repeatedly high levels of PGE2 in only 2 foals (Figure 3D).

EVs in SF during development

In order to confirm whether our previously established protocol [12] was suitable to isolate EVs from SF of foals, EV-protein markers were analysed by Western blotting. Indeed, all EV samples of foals contained CD9 and CD44, albeit the relative intensity of the bands was variable and the detection of CD44 was relatively weak (Supplementary Figure 1). Overall, CD44 was more abundant in 200K EVs. Especially high concentrations of CD44 were found in one sample (D1-2m16d). This particular sample was also positive for AnxA1, whereas EVs of all other animals were AnxA1 negative in the western blot. All samples were negative for MHC-II (marker for antigen presenting cells) (results not shown).

Subsequently, EVs isolated from SF samples from 3 foals (12 days - 7 months, repeated measurements) and 2 adult horses (8 years) were analysed by high-resolution FCM. Supplementary Figure 2 displays the gating strategy and scatter plots used to calculate the total number of EVs. Although higher levels of total numbers of EVs and CD44+ EVs were found in foals when compared to adult horses (Figure 4A), there was no significant correlation between the decrease in EV concentration and increasing age. There was neither a significant correlation during the first 7 months of life (for all foal EVs: Spearman's rho = -0.77, p=ns; for foal CD44+ EVs: Spearman's rho = 0.01, p=ns). Separate evaluation of EVs isolated by ultracentrifugation at 10,000g (10K EVs, Figure 4B) or 200,000g (200K EVs, Figure 4C) did not reveal major changes between age groups either. Concentrations of total 10K or 200K EVs, as well as the percentages of CD44+ EVs, were variable between animals and did not correlate with age. Of note, one animal (D1-2m16d) showed an increased amount of 10K EVs with a remarkably high percentage of CD44+ EVs and decreased 200K EV
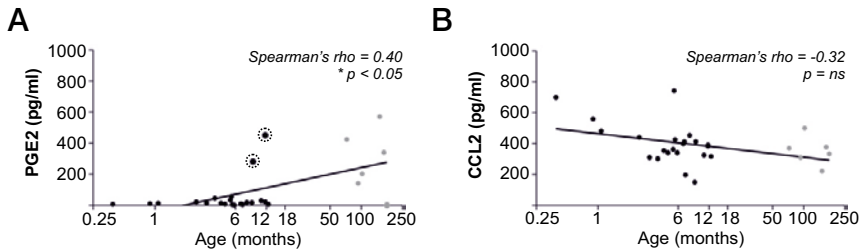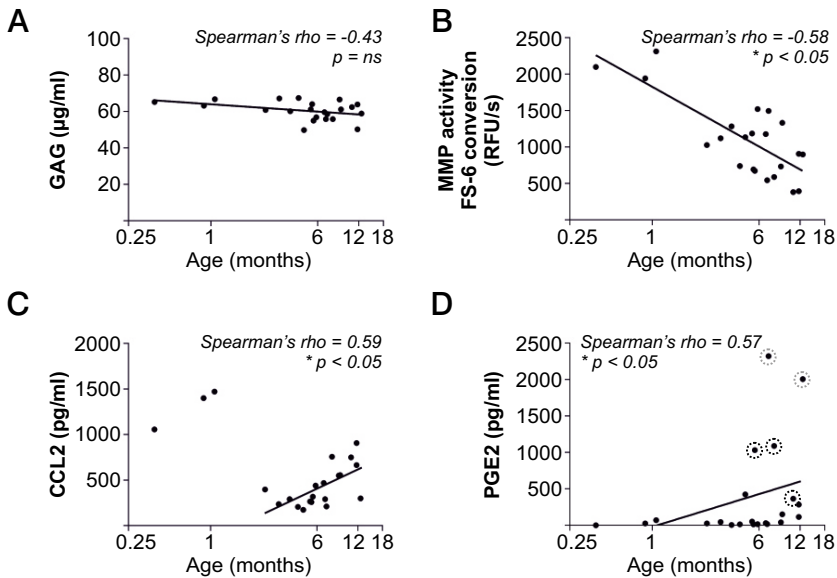
Figure 3 Weighted Spearman rank correlations for soluble factors measured in serum from 10 foals (12 days - 13 months, repeated measurements, total n=22). Age (x-axis) is presented on a logarithmic scale. **A)** Glycosaminoglycan (GAG). **B)** Activity of total matrix metallo-proteinases (MMP). **C)** C-C motif chemokine 2 (CCL2). **D)** Prostaglandin-E2 (PGE2). The dots in circles are repeated measurements from 2 foals (black and grey circles, respectively) with recurrent high PGE2 levels (included in Spearman's rho); these were different animals than the one with high PGE2 levels in SF in Figure 2A. ns, not significant.

5

numbers which corroborated our Western blot results for this specific animal (Supplementary Figure 1). The high-resolution FCM measurement of the same animal 2 weeks after birth (D1-0m12d) did not show these high numbers.

When analyzing the buoyant density of EV-containing sucrose fractions we found that for both foals and adult horses, SF-derived 10K EVs float at slightly higher density (1.12-1.16 g/ml) compared to 200K EVs (1.10-1.14 g/ml) (Figure 5).

Finally, based on the high-resolution FCM scatter plots (Supplementary Figure 2) we cannot exclude possible differences in EV composition between EVs from foals and adult horses. However, to confirm the observed differences in rwFSCxPKH67 scatter patterns (*e.g.* observed in 200K EVs of foals and adult EVs) more samples need to be analysed.
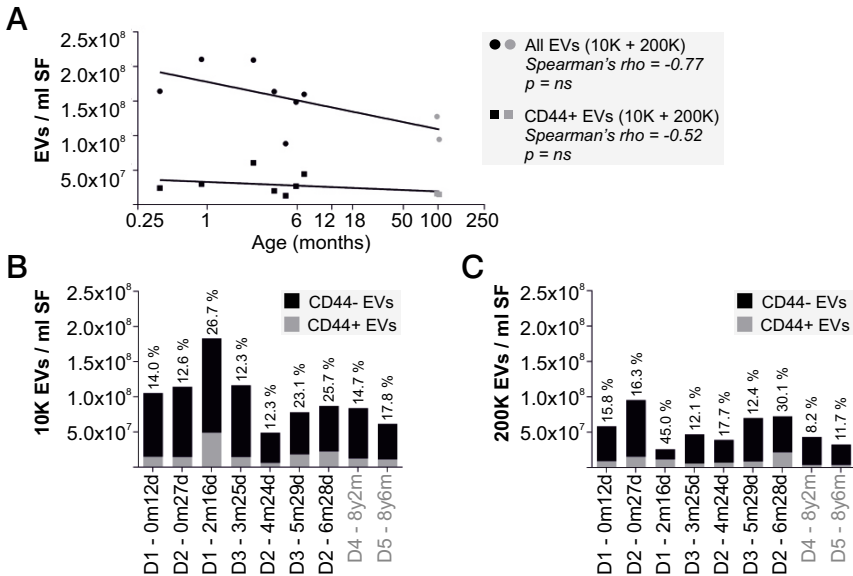
Figure 4 Analysis of EV concentrations in SF from 3 foals (12 days - 7 months, repeated measurements for donors D1, D2 and D3; black dots/squares) and 2 adult horses (8 years; donors D4 and D5; grey dots/squares). Data were calculated from high resolution FCM analysis of EVs present in sucrose density gradient fractions. Prior to measurement, EVs were labelled with PKH67 (generic labelling of all EVs) and anti-CD44 antibody (labelling CD44+ EVs). **A)** Weighted Spearman rank correlations for concentration of total EVs and CD44+ EVs (10K + 200K) from immature to mature age (on logarithmic scale). No significant correlation with age was found in the first 13 months of life (foals only). ns, not significant. **B)** CD44+ and CD44- 10K EV concentrations for individual animals from 4a. **C)** CD44+ and CD44- 200K EV concentrations for individual animals from 4A. Bars represent the sum of CD44+ EVs (grey) and CD44- EVs (black). Percentages CD44+ EVs are indicated above bars. ns, not significant.
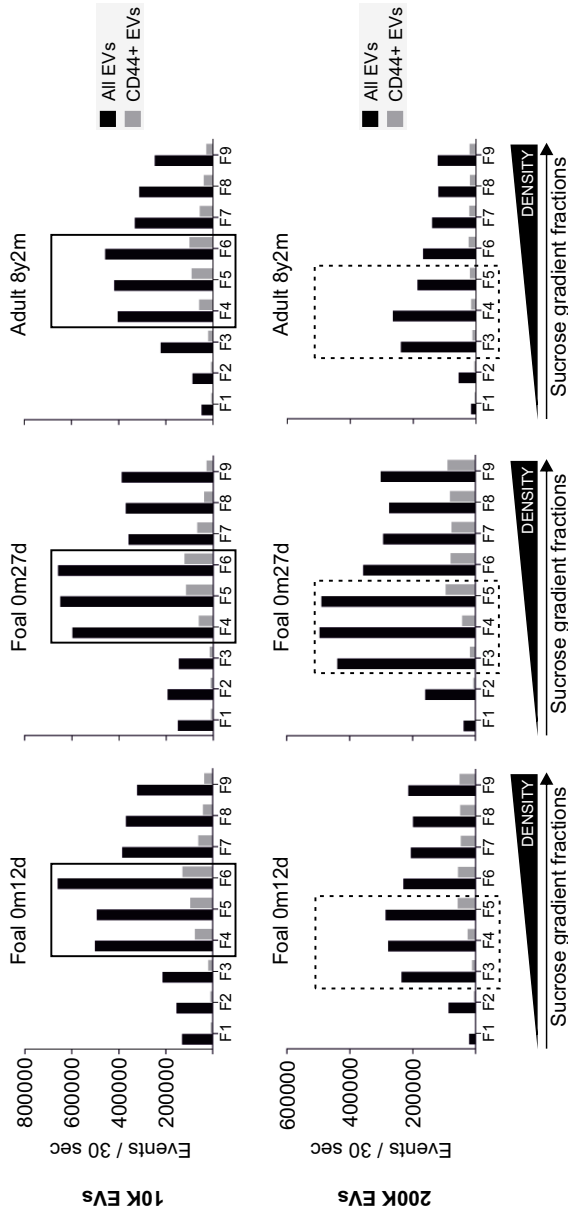
Figure 5 Quantitative analysis (high-resolution FCM) of EVs in individual sucrose fractions with different buoyant density. Prior to measurement, EVs were labelled with PKH67 (labelling all EVs) and anti-CD44 antibody (labelling CD44+ EVs). Results are shown for 2 foals (< 1 month) and 1 adult horse (8 years). Black and dotted boxes indicate the fractions with highest concentrations of EVs (most events/30s), for 10K and 200K EVs respectively. Densities of individual fractions (g/ml) are: F1=1.06, F2=1.08, F3=1.10, F4=1.12, F5=1.14, F6=1.16, F7=1.18, F8=1.20, F9=1.21.

5

DISCUSSION

Biomarker analysis in SF (10 foals, 6 adults) and serum (10 foals) largely confirmed the patterns seen in other studies regarding markers of growth, development and inflammation [2-6], for which age was also a determining factor. Certain factors in SF (GAG, C2C and PGE2) and in serum (GAG) had stable concentrations in the first year of life with low inter-individual variation. Other factors in both SF (MMP activity, CTX-II and CCL2) and serum (MMP activity, CCL2 and PGE2) had a variable concentration and displayed a relatively high variation between animals of roughly the same age. This latter finding may reflect the highly dynamic nature of the immature joint in which day-to-day variations may play a prominent role. This makes biomarker-based predictions about developing pathologies, such as OC, in individual animals very challenging.

An interesting marker for our study was the inflammatory mediator CCL2. In both SF and serum high levels of CCL2 were found only in the first month, but they soon dropped to a baseline value comparable to the adult situation. This may suggest that (regulatory) pro-inflammatory and immune processes are active in the joint immediately after birth for a relatively short while. Active MMP levels followed a similar trend, confirming the high matrix turnover in immature animals reported previously [3-5].

The most recent study describing similar markers in SF of foals was performed in 2011[2] in which stable levels of most factors were described in healthy controls. Furthermore, an age-related increase in type II collagen degradation was suggested, based on a decreased CPII:C2C ratio of C-propeptide of type II procollagen (CPII) (marker for type II collagen synthesis) and C2C (marker for type II collagen cleavage) over time. In the current study, we did not determine the collagen synthesis marker CPII, making ratio calculation impossible. However, our results are not contradictory, as the decreased ratio in the former study was caused by decreasing CPII content with C2C levels remaining constant, which was also the case in the current study. The level of CTX-II, an additional non-collagenase dependent marker of type II collagen breakdown was relatively high in all foals, also suggesting active type II collage turnover. High levels of CTX-II (in serum) in young animals have been found in other studies as well and have been linked to growth plate activity, not to articular cartilage metabolism [26]. As the process of endochondral ossification in the horse is still ongoing during the first year of life, this may well explain the relatively high levels of this marker in SF of foals.

In addition to these biomarkers in SF, we hypothesised that EVs in SF could also reflect the dynamic changes during joint development. They might for instance play a role in promoting tissue turnover, stimulating tissue regeneration in areas with lesions, or possibly repressing local inflammation, as has been shown in other biological and pathological processes in the body [13,16-18] and studies regarding cartilage and bone regeneration [19,20]. Although the number of samples available for EV analysis from SF was a limiting factor, the results of this study nevertheless give an indication of the dynamics of SF-derived EVs in joints of immature animals during the first 7 months of life. This study is unique, since it includes a cohort of healthy foals of similar breed, housing, feeding and exercise regime, and it targets the most dynamic period of joint development, which is 0-6 months after birth [8]. Despite the limitations regarding statistical power, important observations could be made.

Against expectations, this study did not reveal any significant differences between immature animals (12 days – 7 months) and adults (8 years) with respect to the total number of EVs in SF and the number of CD44+ EVs. CD44, a transmembrane glycoprotein, is a highly interesting protein regarding joint homeostasis and inflammation. We recently found a CD44+ EV subset in SF of healthy equine joints [12], which increased in SF of joints with acute synovitis [Boere *et al.*, unpublished results]. So far, CD44 is known as a marker for multiple cell types, including synovial fibroblasts and neutrophils [12,27], which could be relevant for the current study. In addition, CD44 is the receptor for hyaluronic acid (hyaluronan) [28], the main component of the SF's extracellular matrix [29]. However, in this study, there was no difference in the number of CD44+ EVs related to age, suggesting this EV-associated protein does not have a prominent role in joint development.

Overall, our results are comparable to data from EVs in SF of healthy adult horses [12]. This is in sharp contrast to the EV populations in SF from adult horses with induced acute synovitis [Boere *et al.*, unpublished results] or in SF from adult human patients with inflammatory joint disease [13,17,18], which all show significantly increased concentrations of EVs when compared to healthy adult SF samples.

Qualitative EV-analysis revealed that for both foals and adult horses SF-derived 10K EVs have a slightly higher buoyant density compared to 200K EVs. More importantly, based on differences in the high-resolution FCM scatter plots (rwFSCxPKH67) we cannot exclude that EVs in foals and adult horses are (functionally) different. These findings prompt the analysis of more samples as well as in-depth functional analysis of these SF-derived EVs.

5

CONCLUSION

The current study shows that healthy joint development is not reflected by the number of EVs present in SF. This is in contrast to pathological conditions, such as joint inflammation, which have been shown to increase the number of EVs in SF. One interpretation of the results could be that healthy EVs are not, or only marginally, involved in controlling healthy joint homeostasis in immature and mature animals. Given the major role EVs have in regulation of other biological processes, this conclusion seems somewhat counterintuitive. Whereas apparently physiologic growth and development is not reflected in the concentration of EVs, it can be conjectured that more specific aspects, such as their functionality, which is determined by their cargo (*e.g.* growth factors, miRNAs etc.), might be related to developmental stage of the joint. A first hint that EVs derived from foals and adult horses might be (functionally) different comes from differences in high resolution FCM scatter plots observed in this exploratory study. Hence, further studies focusing on more specific characteristics of juvenile SF EVs, such as their cargo and signalling function, are needed, as these may indicate whether distinct differences between juvenile and mature SF EVs exist and what the biological relevance of any such differences might be.

MANUFACTURERS' ADDRESSES

[a]Pfizer, Capelle aan den IJssel, the Netherlands
[b]Sigma-Aldrich, St. Louis, MO, USA
[c]Immunodiagnostics, Tyne & Wear, UK
[d]Ibex Technologies Inc., Montreal, Quebec, Canada
[e]Applied Biosystems, Nieuwerkerk aan den IJssel, the Netherlands
[f]BD Biosciences Europe, Erembodegem, Belgium

ACKNOWLEDGEMENTS

DISCLOSURE

During this study, the Wauben research group, Utrecht University, Faculty of Veterinary Medicine, Department of Biochemistry and Cell Biology, had a collaborative research agreement with BD Biosciences Europe, Erembodegem, Belgium, to optimise analysis of EVs using the BD Influx™ flow cytometer.

5

REFERENCES

1. Frisbie, D. D.; Al-Sobayil, F.; Billinghurst, R. C.; Kawcak, C. E.; McIlwraith, C. W. Changes in synovial fluid and serum biomarkers with exercise and early osteoarthritis in horses. *Osteoarthritis Cartilage* **2008***, 16*, 1196-1204.

2. de Grauw, J. C.; Donabedian, M.; van de Lest, C. H.; Perona, G.; Robert, C.; Lepage, O.; Martin-Rosset, W.; van Weeren, P. R. Assessment of synovial fluid biomarkers in healthy foals and in foals with tarsocrural osteochondrosis. *Vet. J.* **2011***, 190*, 390-395.

3. Brama, P. A.; van den Boom, R.; DeGroott, J.; Kiers, G. H.; van Weeren, P. R. Collagenase-1 (MMP-1) activity in equine synovial fluid: influence of age, joint pathology, exercise and repeated arthrocentesis. *Equine Vet. J.* **2004***, 36*, 34-40.

4. Brama, P. A.; TeKoppele, J. M.; Beekman, B.; van Weeren, P. R.; Barneveld, A. Matrix metalloprotein-ase activity in equine synovial fluid: influence of age, osteoarthritis, and osteochondrosis. *Ann. Rheum. Dis.* **1998***, 57*, 697-699.

5. Brama, P. A.; TeKoppele, J. M.; Beekman, B.; van El, B.; Barneveld, A.; van Weeren, P. R. Influence of development and joint pathology on stromelysin enzyme activity in equine synovial fluid. *Ann. Rheum. Dis.* **2000***, 59*, 155-157.

6. van den Boom, R.; Brama, P. A.; Kiers, G. H.; de Groot, J.; van Weeren, P. R. Assessment of the effects of age and joint disease on hydroxyproline and glycosaminoglycan concentrations in synovial fluid from the metacarpophalangeal joint of horses. *Am. J. Vet. Res.* **2004***, 65*, 296-302.

7. Donabedian, M.; van Weeren, P. R.; Perona, G.; Fleurance, G.; Robert, C.; Leger, S.; Bergero, D.; Lepage, O.; Martin-Rosset, W. Early changes in biomarkers of skeletal metabolism and their association to the occurrence of osteochondrosis (OC) in the horse. *Equine Vet. J.* **2008***, 40*, 253-259.

8. Brama, P. A.; TeKoppele, J. M.; Bank, R. A.; Barneveld, A.; van Weeren, P. R. Development of biochemical heterogeneity of articular cartilage: influences of age and exercise. *Equine Vet. J.* **2002***, 34*, 265-269.

9. van Weeren, P. R.; Jeffcott, L. B. Problems and pointers in osteochondrosis: Twenty years on. *Vet. J.* **2013***, 197*, 96-102.

10. Yuana, Y.; Boing, A. N.; Grootemaat, A. E.; van der Pol, E.; Hau, C. M.; Cizmar, P.; Buhr, E.; Sturk, A.; Nieuwland, R. Handling and storage of human body fluids for analysis of extracellular vesicles. *J. Extracell Vesicles* **2015***, 4*, 29260.

11. EL Andaloussi, S.; Mager, I.; Breakefield, X. O.; Wood, M. J. Extracellular vesicles: biology and emerging therapeutic opportunities. *Nat. Rev. Drug Discov.* **2013***, 12*, 347-357.

12. Boere, J.; van de Lest, C. H.; Libregts, S. F.; Arkesteijn, G. J.; Geerts, W. J.; Nolte-'t Hoen, E. N.; Malda, J.; van Weeren, P. R.; Wauben, M. H. Synovial fluid pretreatment with hyaluronidase facilitates isolation of CD44+ extracellular vesicles. *J. Extracell Vesicles* **2016***, 5*, 31751.

13. Berckmans, R. J.; Nieuwland, R.; Kraan, M. C.; Schaap, M. C.; Pots, D.; Smeets, T. J.; Sturk, A.; Tak, P. P. Synovial microparticles from arthritic patients modulate chemokine and cytokine release by synoviocytes. *Arthritis Res. Ther.* **2005***, 7*, R536-44.

14. Anderson, H. C. Vesicles associated with calcification in the matrix of epiphyseal cartilage. *J. Cell Biol.* **1969***, 41*, 59-72.

15. Anderson, H. C. Matrix vesicles and calcification. *Curr. Rheumatol. Rep.* **2003***, 5*, 222-226.

16. Thery, C.; Ostrowski, M.; Segura, E. Membrane vesicles as conveyors of immune responses. *Nat. Rev. Immunol.* **2009***, 9*, 581-593.

17. Buzas, E. I.; Gyorgy, B.; Nagy, G.; Falus, A.; Gay, S. Emerging role of extracellular vesicles in inflammatory diseases. *Nat. Rev. Rheumatol.* **2014***, 10*, 356-364.

18. Reich, N.; Beyer, C.; Gelse, K.; Akhmetshina, A.; Dees, C.; Zwerina, J.; Schett, G.; Distler, O.; Distler, J. H. Microparticles stimulate angiogenesis by inducing ELR(+) CXC-chemokines in synovial fibroblasts. *J. Cell. Mol. Med.* **2011***, 15*, 756-762.

19. Vonk, L. A.; van Dooremalen, S.; Coffer, P. J.; Saris, D. B.; Lorenowicz, M. J. MSC-derived extracellular vesicles stimulate cartilage regeneration and modulate inflammatory responses. Paper presented at the 13th world congress of the International Cartilage Repair Society, Sept 26, 2016, Sorrento, Italy. **2016**.

20. Zhang, S.; Chu, W. C.; Lai, R. C.; Lim, S. K.; Hui, J. H.; Toh, W. S. Exosomes derived from human embryonic mesenchymal stem cells promote osteochondral regeneration. *Osteoarthritis Cartilage* **2016***, 24*, 2135-2140.

21. Malda, J.; Boere, J.; van de Lest, C. H.; van Weeren, P.; Wauben, M. H. Extracellular vesicles - new tool for joint repair and regeneration. *Nat. Rev. Rheumatol.* **2016***, 12*, 243-249.

22. Farndale, R. W.; Buttle, D. J.; Barrett, A. J. Improved quantitation and discrimination of sulphated glycosaminoglycans by use of dimethylmethylene blue. *Biochim. Biophys. Acta* **1986***, 883*, 173-177.

23. Neumann, U.; Kubota, H.; Frei, K.; Ganu, V.; Leppert, D. Characterization of Mca-Lys-Pro-Leu-Gly-Leu-Dpa-Ala-Arg-NH2, a fluorogenic substrate with increased specificity constants for collagenases and tumor necrosis factor converting enzyme. *Anal. Biochem.* **2004***, 328*, 166-173.

24. de Grauw, J. C.; van de Lest, C. H.; van Weeren, P. R. A targeted lipidomics approach to the study of eicosanoid release in synovial joints. *Arthritis Res. Ther.* **2011***, 13*, R123.

25. van der Vlist, E. J.; Nolte-'t Hoen, E. N.; Stoorvogel, W.; Arkesteijn, G. J.; Wauben, M. H. Fluorescent labeling of nano-sized vesicles released by cells and subsequent quantitative and qualitative analysis by high-resolution flow cytometry. *Nat. Protoc.* **2012***, 7*, 1311-1326.

26. Duclos, M. E.; Roualdes, O.; Cararo, R.; Rousseau, J. C.; Roger, T.; Hartmann, D. J. Significance of the serum CTX-II level in an osteoarthritis animal model: a 5-month longitudinal study. *Osteoarthritis Cartilage* **2010***, 18*, 1467-1476.

27. Ponta, H.; Sherman, L.; Herrlich, P. A. CD44: from adhesion molecules to signalling regulators. *Nat. Rev. Mol. Cell Biol.* **2003***, 4*, 33-45.

28. Murai, T.; Sato, C.; Sato, M.; Nishiyama, H.; Suga, M.; Mio, K.; Kawashima, H. Membrane cholesterol modulates the hyaluronan-binding ability of CD44 in T lymphocytes and controls rolling under shear flow. *J. Cell. Sci.* **2013***, 126*, 3284-3294.

29. Dahl, L. B.; Dahl, I. M.; Engstrom-Laurent, A.; Granath, K. Concentration and molecular weight of sodium hyaluronate in synovial fluid from patients with rheumatoid arthritis and other arthropathies. *Ann. Rheum. Dis.* **1985***, 44*, 817-822.

5

SUPPLEMENTARY INFORMATION CHAPTER 5

EXTENDED METHODOLOGY

SF and blood collection from healthy foals. Animals were kept in a herd in free-stall barns and at pasture at horse dairy farm Riga Ranch (Nieuwveen, the Netherlands). After separation of selected animals from the herd, 10 ml blood was drawn from the jugular vein, immediately followed by sedation of the animal with detomidine (Domosedan, Pfizer, Capelle aan den IJssel, the Netherlands) 0.02 mg/kg bwt i.v.. After 5-10 min, SF samples (5-10 ml) were drawn by sterile arthrocentesis of either the radiocarpal or the middle carpal joint and one tarsocrural joint by using an 18Gx1½" needle and a 10 ml syringe. All procedures were performed within 20 minutes. Animals were assisted during recovery from sedation and returned to the herd within a few hours.

Blood was immediately transferred into serum tubes, kept on ice for 4 hours and centrifuged at 2,700g (4000 rpm) for 20 min at RT in a Hettich Universal 32 centrifuge (Hettich, Tuttlingen, Germany) with rotor 1619. Serum was stored in aliquots at -80°C. SF was transferred into plain 15 ml tubes immediately after collection and centrifuged at 2,700g (4000 rpm) for 30 min at RT in a Hettich Universal 32 centrifuge (Hettich, Tuttlingen, Germany) with rotor 1619. Cell-free SF was kept on ice for 4 hours and stored in 2 ml aliquots at -80°C.

GAG assay. Synovial fluid first underwent hyaluronic acid digestion by 1:1 incubation with hyaluronidase solution (HYase Type II from sheep testes, Sigma-Aldrich, St. Louis, MO, USA) (30U/ml in H_2O), 30 min at 37°C, followed by 1:5 dilution in PBS/EDTA buffer (0.04M Na_2HPO_4, 0.06M $H_2NaPO_4 \cdot 2H_2O$, 0.01M $Na_2EDTA \cdot 2H2O$). Serum was diluted 1:20 in PBS/EDTA buffer. Chondroitin Sulphate (CS) (Sigma C4384, 0.5 mg/ml in PBS) was diluted in PBS/EDTA buffer for a standard curve of 0.3-10 µg/ml. For the assay 100 µl diluted sample or 100 µl diluted CS standard was incubated with 200 µl DMMB staining solution (16 mM 1,9-Dimethyl-Methylene Blue [Sigma-Aldrich, St. Louis, MO, USA], 40 mM NaCl, 0.5% Ethanol, 0.3 % glycine [Sigma-Aldrich, St. Louis, MO, USA], pH 3.0) and measured immediately in a plate reader (Tecan, Männedorf, Switzerland) using wavelengths 525 and 595 nm.

MMP assay. 35 µl sample (SF or serum diluted 20-fold in MMP buffer) was incubated with 35 µl FS-6 solution, which is 10 µM Mca-Lys-Pro-Leu-Gly-Leu-Dap(DNP)-Ala-Arg-NH_2 trifluoroacetate salt (Bachem, Bubendorf, Switzerland) in MMP buffer, and immediately measured in black flat bottom 384-well plates (Greiner Bio-One, Kremsmünster, Austria) using a CLARIOstar plate reader (BMG Labtech GmbH,

Ortenberg, Germany). The fluorescent signal was measured in real-time over 48 minutes for which a linear slope (relative fluorescence units/second (RFU/s)) was calculated as a measure of general MMP activity. MMP buffer: 0.1 M Tris, 0.1 M NaCl, 10 mM $CaCl_2$, 0.05% Triton X-100, 0.1% (w/v) PEG-6000 (J.T. Baker, Avantor Performance Materials, Center Valley, PA, USA), pH 7.5.

CCL2 enzyme-linked immunosorbent assay (ELISA). EIA/RIA 96-well plates (flat bottom, Costar Corning, Tewksbury, MA, USA) were coated overnight at 4°C with capture antibody (rabbit anti-equine CCL2, King Fisher, Saint Paul, MN, USA) 1 μg/ml in coating buffer (100 mM Na_2CO_3, 100 mM $NaHCO_3$, pH 9.6), 100 μl per well. After blocking for 90 min at RT in PBS 1% BSA, wells were incubated for 90 minutes at RT with 100 μl diluted SF, 100 μl diluted serum or 100 μl recombinant CCL2 solution (King Fisher, Saint Paul, MN, USA). SF was diluted 1:1 in 1M NaCl 0.5% BSA 2% Tween-20. Dilution of serum (1:1) and standard (39-2500 pg/ml recombinant CCL2) was done in PBS 1% BSA 0.1% Tween-20. Subsequently, wells were incubated for 60 min at RT with detection antibody (biotinylated rabbit anti-equine CCL2, King Fisher, Saint Paul, MN, USA) 0.02 μg/ml in PBS 1% BSA 0.1% Tween-20, 100 μl per well, followed by incubation for 30 min at RT in high sensitivity streptavidin-horseradish peroxidase (Thermo Scientific, Waltham, MA, USA) 10 ng/ml in PBS 1% BSA, 100 μl per well. The signal was developed with TMB substrate solution (Thermo Scientific, Waltham, MA, USA) 30 min at RT and the reaction was stopped with 0.18 M sulfuric acid, both 100 μl per well. Color development was quantified in a plate reader (Tecan, Männedorf, Switzerland) using wavelengths 450 and 540 nm.

5

Extracellular vesicle depletion of reagents containing BSA and FBS. EV-depleted PBS/0.1% BSA, used for suspension of EV pellets, was prepared by making a stock solution of 5% (w/v) BSA (GE Healthcare, Amersham, UK) in PBS. This solution was cleared from aggregates and EVs by ultracentrifugation at 100,000g for 16 h at 4°C (Optima™ L-90K or Optima™ XPN-80 centrifuge; SW28 rotor; 28,000 rpm; relative centrifugation force (RCF) average 103,745g; RCF max 141,371g; κ-factor 245.5; Beckman-Coulter, Fullerton, CA, USA), filtered through a 0.22-μm filter, stored in aliquots at −20°C, and diluted 50× in PBS prior to use.

EV-depleted RPMI/10% FBS, used to stop the PKH67 staining process, was prepared by making a stock solution of 30% (v/v) FBS (PAA Laboratories, GE Healthcare) in Roswell Park Memorial Institute medium (RPMI) (Gibco, Thermo Scientific), which was cleared of EVs and aggregates by ultracentrifugation at 100,000g for 16 h at 4°C (as described above), filtered through a 0.22-μm filter, stored in aliquots at −20°C, and diluted 3× in RPMI prior to use.

This protocol for EV and aggregate depletion of reagents is a standard procedure in our lab[1] and results in very few remaining EVs if the following precautions are taken:

a) start with dilutions of BSA (max 5%) and FBS (max 30%) in the buffer/medium of choice; b) use a swing-out rotor; c) use a centrifugation time of at least 16 h; d) leave at least 5 ml of supernatant above the EV pellet.

Extracellular vesicle isolation from SF. Stored cell-free SF (starting volume 2ml) was thawed, incubated with hyaluronidase solution (HYase Type II from sheep testes, Sigma-Aldrich, St. Louis, MO, USA) (1500 U/ml in H_2O; 20 µl per ml SF) for 15 min at 37°C in a water bath while vortexing every 5 min, and centrifuged at 1000g 10 min at RT in an Eppendorf centrifuge (Hettich Mikro 200R with rotor 2424A) to remove aggregates. Then, samples were mixed with PBS to reach a volume of 4.5 ml. Subsequent ultracentrifugation in SW60 tubes (Beckman-Coulter, Fullerton, CA, USA) at 10,000g for 35 min at 4°C (9,900 rpm; RCF average 10,066g; RCF max 13,205g; κ-factor 1667.7) and 200,000g for 120 min at 4°C (44,000 rpm; RCF average 198,835g; RCF max 260,849g; κ-factor 84.4) resulted in 10K and 200K EV pellets. For these steps a SW60-Ti rotor in a Beckman-Coulter Optima™ L-90K or Optima™ XPN-80 ultracentrifuge was used.

Single-EV-based high-resolution flow cytometry
Labelling of EVs with anti-CD44 and PKH67. EV-containing 10K and 200K pellets were resuspended in a mixture of 20 µl EV-depleted PBS/0.1% BSA and 30 µl diluent-C. To each sample 4 µl anti-CD44-PE antibody (clone IM7, PE-conj., eBioscience, San Diego, CA, USA; 0.2 mg/ml) or 4 µl anti-IgG2bκ-PE isotype control antibody (0.2 mg/ml; rat IgG2bκ, PE-conj., eBioscience) was added and incubated for 1 hour at RT on a shaker. Prior to use the anti-CD44-PE and the IgG2bκ-PE stock solutions were centrifuged in order to pellet aggregates (21,000g, 20 min, 4°C; Hettich Mikro 200R with rotor 2424A). After CD44-PE or isotype labelling 50 µl diluent-C was added (to create a total volume of 100 µl) and this was mixed with PKH67 staining mix (MIDI-67-1KT kit, Sigma-Aldrich, St. Louis, MO, USA) (1.5 µl PKH67 in 100 µl diluent-C). After 3 min incubation at RT, 50 µl of EV-depleted RPMI/10% FBS was added to stop the staining process. Labelled EVs (250 µl) were then mixed with 1.5 ml 2.5 M sucrose (J.T. Baker, Avantor Performance Materials, Center Valley, PA, USA) in PBS. The prepared EV-sucrose mixture was then overlaid with 15 volumes of 700 µl sucrose solutions with decreasing density (2.0 M – 0.4 M sucrose in PBS) in SW40 tubes (Beckman-Coulter, Fullerton, CA, USA). Gradients were centrifuged at 200,000g for 16 hours at 4°C (Beckman-Coulter Optima™ L-90K or Optima™ XPN-80 centrifuge; SW40-Ti rotor; 39,000 rpm; RCF average 192,072g; RCF max 270,519g; κ-factor 144.5) and 12 fractions of 1 ml were collected from top (F1, lowest density) to bottom (F12, highest density) by using a P1000 pipette. Densities were determined by refractometry. A background control sample (20 µl EV-depleted PBS/0.1% BSA+30 µl diluent-C, without EVs) was taken along during the entire procedure of PKH67

labelling, anti-CD44 labelling, and sucrose gradient floatation. High-resolution flow cytometry (FCM) of this control sample did not show significant background events in gradient fractions of interest (data not shown).

Single-EV-based high-resolution FCM. For this technique an optimised jet-in-air-based BD Influx™ flow cytometer (BD Biosciences Europe, Erembodegem, Belgium) was used, as described previously [1-3]. Detection of EVs by this system is based on threshold triggering on the fluorescent light emitted after excitation of fluorescently labelled particles passing the first laser (FL1 signal). The threshold for triggering on FL1 was adjusted to allow an event rate of ≤10 events/s when clean PBS was analysed. The threshold level was kept identical for all measurements in this study. Forward scatter (FSC) of EVs was measured through an adapted small particle detector with a collection angle of 15–25° (reduced wide-angle FSC), by using a high numerical aperture and long working distance lens and by installing a 5-mm obscuration bar in front of the FSC collection lens. These settings allow the best distinction of FSC and FL1 fluorescence for 100 nm and 200 nm yellow-green fluorescent (505/515) carboxylated polystyrene beads (FluoSpheres, Life Technologies, Thermo Scientific, Waltham, MA, USA) with which the flow cytometer was calibrated. For experiments a 140-µm nozzle was used. The sheath fluid pressure was kept between 4.98 and 5.02 psi and was monitored by an external pressure meter. The sample pressure was set to 4.29 psi. Upon loading the sample the system was boosted until events appeared, the fluidics were then allowed to stabilise for 30 seconds, after which samples were acquired for 30 seconds. In between samples the flow cytometer was washed with FACSrinse and PBS. Data were acquired using BD FACS™ Sortware v1.0.1.654 (BD Biosciences, San Jose, CA, USA) and analysed with FlowJo v10.07 software (FlowJo, Ashland, OR, USA).
EV concentration per fraction was calculated based on the quantitative EV analysis and the flow rate that was determined by a volume measurement using ddH$_2$O. The EV concentration per ml of SF was calculated by taking the sum of EVs in sucrose fractions, divided by the SF starting volume (ml).

Western blotting. The same sucrose fractions that were analysed by high-resolution FCM were used for protein identification by Western blotting. Gradient fractions of 375 µl were pooled in pairs (F4+F5 [medium density] and F6+F7 [high density]) and diluted in 3.4 ml PBS in SW60 tubes (Beckman-Coulter, Fullerton, CA, USA). EVs were pelleted at 200,000*g* (44.000 rpm; RCF average 198,835*g*; RCF max 260,849*g*; κ-factor 84.4) using an SW60-Ti rotor in a Beckman-Coulter Optima^{TM} L-90K or Optima^{TM} XPN-80 ultracentrifuge (Beckman-Coulter, Fullerton, CA, USA), 90 min at 4°C. EV pellets were resuspended in 65 µl non-reducing SDS-PAGE sample buffer (50mM TRIS pH 6.8, 2% SDS, 10% glycerol, 0.02% bromophenol blue) and pooled for each foal. Thus, each sample contained EVs from F4, F5, F6 and F7.

5

Samples were heated at 100°C, run on 4-20% Criterion TGX gels (Bio-Rad, Hercules, CA, USA), and transferred onto 0.2 μm PVDF membranes. After blocking for 1 hour in 5% Protifar (Nutricia, Zoetermeer, the Netherlands) in PBS 0.1% Tween-20, proteins were labelled with primary antibodies against CD9 (clone HI9, Biolegend, San Diego, CA, USA; dilution 1:1000), CD44 (clone IM7, PE-conj., eBioscience, San Diego, CA, USA; dilution 1:400), MHC-II (clone CVS20, Bio-Rad (AbD Serotec), Hercules, CA, USA; dilution 1:400) and Annexin-A1 (clone 29/Annexin-1, BD Transduction Labs , San Jose, CA, USA; dilution 1:400). HRP-conjugated goat-anti-mouse IgG (Nordic Immunology Laboratories, Susteren, the Netherlands; dilution 1:5000) was used for detection by chemiluminescence (SuperSignal West Pico Chemiluminescent Substrate, Thermo Scientific, Waltham, MA, USA). Chemiluminescence was visualised using a ChemiDoc™ MP Imaging System (Bio-Rad, Hercules, CA, USA) and analysed with Bio-Rad Image Lab V5.1 software (Bio-Rad, Hercules, CA, USA).

1. van der Vlist EJ, Nolte-'t Hoen EN, Stoorvogel W, Arkesteijn GJ, Wauben MH. Fluorescent labeling of nano-sized vesicles released by cells and subsequent quantitative and qualitative analysis by high-resolution flow cytometry. *Nat Protoc* **2012**;7:1311-26

2. Nolte-'t Hoen EN, van der Vlist EJ, Aalberts M, Mertens HC, Bosch BJ, Bartelink W, et al. Quantitative and qualitative flow cytometric analysis of nanosized cell-derived membrane vesicles. *Nanomedicine* **2012**; 8:712-20

3. Boere J, van de Lest CH, Libregts SF, Arkesteijn GJ, Geerts WJ, Nolte-'t Hoen EN, et al. Synovial fluid pretreatment with hyaluronidase facilitates isolation of CD44+ extracellular vesicles. *J Extracell Vesicles* **2016**;5:31751

Supplementary Table 1 Additional information on experimental animals. Age, sex and breed of all animals used in this study. In the foals repeated samples from the same animal were taken during the first year of life. Indicated is which data sets were used as input for the different figures. SF, synovial fluid; SE, serum; EV, purified extracellular vesicles floated in sucrose gradients.

Condition	Animal	Age	Sex	Breed	Fig. 1+2	Fig. 3	Fig. 4	Fig. 5	Suppl. Fig. 1	Suppl. Fig. 2
1	Foal 1	0m12d	Male	Haflinger	SF	SE	EV	EV	EV	EV
2	Foal 2	0m27d	Male	Haflinger	SF	SE	EV	EV	-	EV
3	Foal 3	1m2d	Male	Haflinger	SF	SE	-	-	-	-
4	Foal 1	2m16d	Male	Haflinger	SF	SE	EV	-	EV	-
5	Foal 4	3m6d	Male	Haflinger	SF	SE	-	-	-	-
6	Foal 5	3m25d	Female	Haflinger	SF	SE	EV	-	EV	-
7	Foal 6	4m10d	Female	Haflinger	SF	SE	-	-	-	-
8	Foal 2	4m24d	Male	Haflinger	SF	SE	EV	-	EV	-
9	Foal 4	5m10d	Male	Haflinger	SF	SE	-	-	-	-
10	Foal 6	5m14d	Female	Haflinger	SF	SE	-	-	-	-
11	Foal 7	5m19d	Female	Haflinger	SF	SE	-	-	-	-
12	Foal 5	5m29d	Female	Haflinger	SF	SE	EV	-	EV	-
13	Foal 8	6m22d	Female	Haflinger	SF	SE	-	-	-	-
14	Foal 2	6m28d	Male	Haflinger	SF	SE	EV	-	EV	-
15	Foal 9	7m2d	Female	Haflinger	SF	SE	-	-	-	-
16	Foal 7	7m25d	Female	Haflinger	SF	SE	-	-	-	-
17	Foal 10	8m21d	Female	Haflinger	SF	SE	-	-	-	-
18	Foal 8	8m27d	Female	Haflinger	SF	SE	-	-	-	-
19	Foal 7	10m22d	Female	Haflinger	SF	SE	-	-	-	-
20	Foal 10	11m20d	Female	Haflinger	SF	SE	-	-	-	-
21	Foal 8	11m25d	Female	Haflinger	SF	SE	-	-	-	-
22	Foal 9	12m16d	Female	Haflinger	SF	SE	-	-	-	-
23	Adult 1	6y1m	Female	Dutch Warmblood	SF	-	-	-	-	-
24	Adult 2	7y9m	Female	Dutch Warmblood	SF	-	-	-	-	-
25	Adult 3	8y2m	Female	Dutch Warmblood	-	-	EV	EV	-	EV
26	Adult 4	8y6m	Female	Dutch Warmblood	-	-	EV	-	-	EV
27	Adult 5	8y7m	Female	Dutch Warmblood	SF	-	-	-	-	-
28	Adult 6	12y9m	Male	Dutch Warmblood	SF	-	-	-	-	-
29	Adult 7	13y9m	Female	Dutch Warmblood	SF	-	-	-	-	-
30	Adult 8	14y9m	Male	Dutch Warmblood	SF	-	-	-	-	-

5
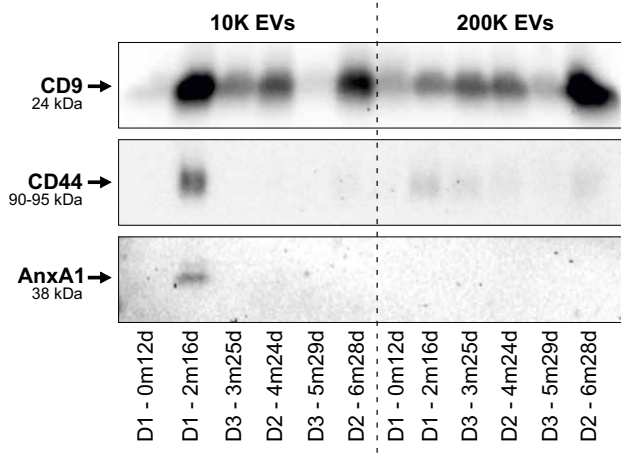
Supplementary Figure 1 Protein analysis (Western blotting) of SF-derived EVs from 6 samples of 3 foals (12 days - 7 months, repeated measurements for donors D1, D2 and D3). Each sample is a pool of sucrose fractions F4-F7 (see Figure 5). Analysis is shown for CD9 (tetraspanin; general EV-marker), CD44 (hyaluronic acid receptor, synovial fibroblast marker) and AnxA1 (annexin-A1, anti-inflammatory protein).
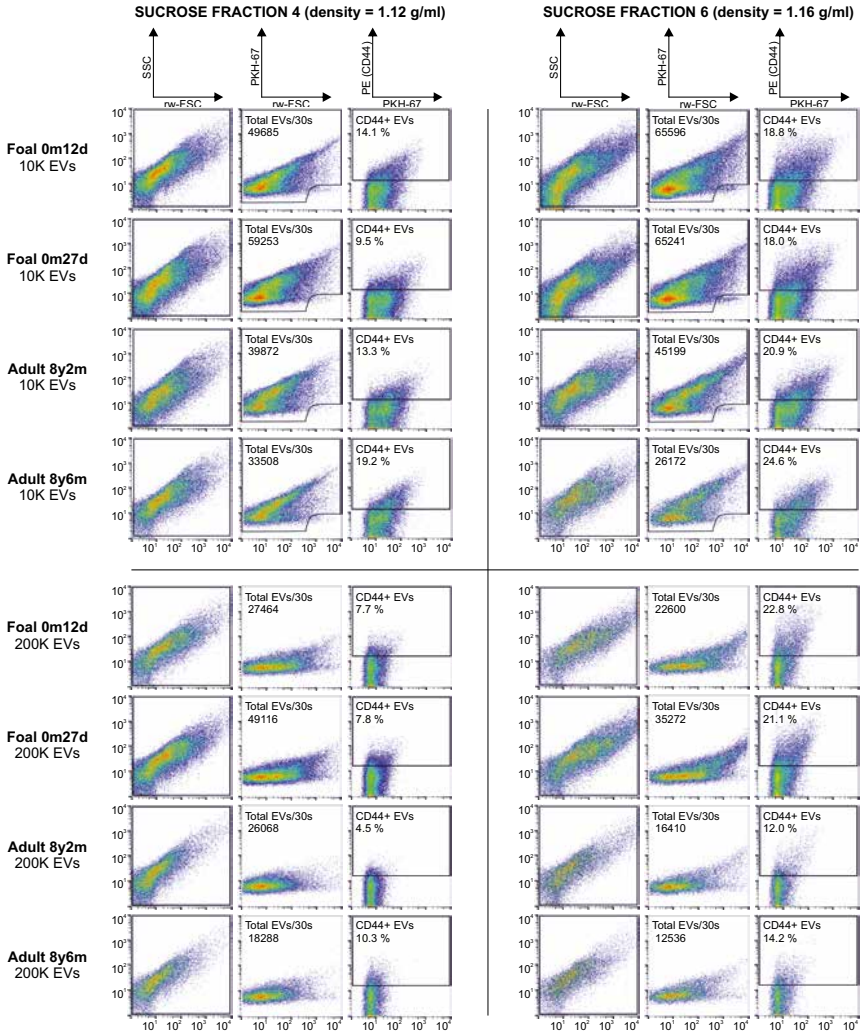
Supplementary Figure 2 High-resolution flow cytometry (FCM) of sucrose gradient fraction. Scatter plots displaying reduced-wide angle forward scatter (rw-FSC), side scatter (SSC), PKH67 fluorescence and CD44-expression of 10K and 200K EVs in sucrose fractions 4 and 6. Prior to measurement, EVs were labelled with PKH67 (labelling all EVs) and stained with either PE-conjugated anti-CD44 (labelling CD44+ EVs) or PE-conjugated isotype antibodies (Ig-control labelling) and subjected to density gradient floatation to separate EVs from free dye and unbound antibodies. Results are shown for 2 foals (< 1 month) and 2 adult horses (8 years). Gating excluded background events (in rwFSCxSSC and rwFSCxPKH67), resulting in the final event rate per sample (EVs/30s). Gating for CD44-expression was based on the anti-CD44 isotype control sample (data not shown). Percentages CD44+ EVs are indicated in the corresponding gates.

6

Extracellular vesicles – new tool for joint repair and regeneration

Perspectives – Opinion

Janneke Boere [a]
Jos Malda [a,c]
Chris H. A. van de Lest [a,b]
P. René van Weeren [a]
Marca H. M. Wauben [b]

Departments of Equine Sciences[a] and Biochemistry & Cell Biology[b] of Faculty of Veterinary Medicine, Utrecht University, Utrecht, the Netherlands; Department of Orthopaedics[c], University Medical Center Utrecht, Utrecht, the Netherlands

ABSTRACT

Cell-derived extracellular vesicles (EVs), present in synovial fluid and cartilage extracellular matrix (ECM), are involved in joint development and in the regulation of joint homeostasis. Although the exact function of EVs in these processes remains incompletely defined, the knowledge already acquired in this field suggests a role for these EVs as biomarkers of joint disease, and as a new tool to restore joint homeostasis and enhance articular tissue regeneration. In addition to direct injection of therapeutic EVs into the target site, surface coating of scaffolds and embedding of EVs in hydrogels might also lead to novel therapeutic possibilities. Based on the existing literature of EVs in synovial fluid and articular tissues, and investigation of the molecular factors (including microRNAs) active in joint homeostasis (or during its disturbance), we postulate novel perspectives for the implementation of EVs as a regenerative medicine approach in joint repair.

INTRODUCTION

Extracellular vesicles (EVs) are small membrane-enclosed particles actively released by cells (Box 1). These structures are found in all tissue types and body fluids studied to date, including synovial fluid and blood [1,2]. This heterogeneous group of particles (varying in size from ~40 nm to 5 μm) can be formed by direct budding off the cell membrane, or released after fusion of endosomal multivesicular bodies with the plasma membrane [3]. Among other functions, EVs act as protective carriers for biologically active signalling molecules (such as proteins, enzymes, mRNAs, microRNAs (miRNAs), DNA fragments and lipids) and contain ligands for receptors on the cell membrane of recipient cells. Upon binding to the target cell, EVs can signal from the plasma membrane or, alternatively, fuse with the cell membrane and deliver their cargo into the cytosol, thereby activating or inhibiting specific cellular processes. Extracellular vesicles can also be internalised via endocytosis, subsequently releasing their cargo in endosomal compartments [4]. Hence, EVs are efficient shuttling vehicles that participate in intercellular communication in a variety of biological processes *in vivo* [5,6], even over long distances [7,8].

> **BOX 1** EV types and nomenclature
>
> Extracellular vesicle (EV) is a generic name for all secreted lipid-bilayer-enclosed, cell-derived vesicles, defined in 2011 by the International Society for Extracellular Vesicles. However, other terms are often used to refer to EVs, including exosomes, microvesicles, apoptotic bodies, matrix vesicles, ectosomes, prostasomes, membrane particles and shedding vesicles. The different names are mainly based on particular research fields, physiological or pathological condition, vesicle morphology (mainly size), cell type of origin and route of biogenesis (membrane-shed or endosomal-derived). As several different EV types share overlapping characteristics, and often no unique markers are available to clearly distinguish between EV types, the classification of EVs is difficult, and comparison of research data based on terminology alone can lead to inconsistencies and is not recommended [81]. In this Perspectives article, we use the generic term "extracellular vesicles" for all EVs, with the exception of matrix vesicles, which are a well-defined EV type.

6

As early as 1969, matrix vesicles – a specialised type of EVs present in the growth plate of developing bone – were shown to initiate cartilage calcification during endochondral ossification [9]. During this process, matrix vesicles derived from chondroblasts and osteoblasts collect inorganic phosphate and calcium from the extracellular matrix (ECM), contributing to mineralisation by the formation of hydroxyapatite crystals in the vesicle lumen. Eventually, the deposition of these

crystals in the ECM results in further mineralisation of cartilage [10]. With the discovery of a range of growth factors and proteins, including bone morphogenetic proteins (BMPs) and vascular endothelial growth factor (VEGF), in matrix vesicles, these structures were thought to be also involved in the regulation of neovascularisation and the differentiation of chondrocytes and osteoblasts in the growth plate [11]. Despite the fact that these mineralizing matrix vesicles have not been directly implicated in joint repair and regeneration, they are an example of EVs that facilitate tissue development and regulate homeostasis.

Synovial fluid derived EVs, first isolated 2 decades ago [12], were found in patients with rheumatoid arthritis (RA) [2,12] and were suggested to play a part in this inflammation-driven disorder. Nowadays, EV-mediated communication in the joint has become a new field of interest, especially in the context of inflammatory joint diseases [13].

Based on the existing knowledge of EVs derived from synovial fluid and articular tissue, as well as from *in vitro* studies, we evaluate the role of EVs in the maintenance and restoration of joint homeostasis, and discuss their potential for use in tissue regeneration. Taking into account findings concerning molecular factors (including miRNAs) in joint biology and pathology, we define a concept for clinical application of EVs in the field of joint repair and regeneration.

EVs IN THE JOINT

Inflammatory joint disease

All joint diseases, including RA and osteoarthritis (OA) as the most prevalent, are characterised by a disturbance of the fine balance between anabolic and catabolic cues [14]. Any disturbance of joint homeostasis is reflected in the levels of soluble factors (such as cytokines, enzymes and growth factors) in the synovial fluid, and possibly also in the numbers and content of EVs. In theory, EVs in the synovial fluid can be derived from two sources: directly from cells in the synovial lining (fibro-blast-like synoviocytes (FLSs), macrophage-like synoviocytes and leukocytes recruited from the circulation) or from resting chondrocytes in the cartilage; or indirectly from the blood plasma, of which synovial fluid is an ultrafiltrate. Therefore, various mechanisms of EV-mediated communication in action during deregulation of joint homeostasis could result in inflammatory joint disease (Figure 1).

Evidence in support of a role for EVs during synovial inflammation is provided by studies showing that synovial-fluid-derived EVs from patients with RA or OA can induce cytokine and growth factor release by synoviocytes *in vitro* [15-17]. Furthermore,

the catabolic interaction of EVs, derived from IL-1 -stimulated synoviocytes, with chondrocytes *in vitro* also provides important insights into EV-mediated tissue degradation during joint inflammation [18]. Leukocyte and erythrocyte-derived EVs, found at high concentrations in the synovial fluid of patients with RA, expose platelet tissue-factor (also known as coagulation factor III or CD142) and support thrombin generation *in vitro*, suggesting their involvement in hypercoagulation and fibrin deposition [2]. Furthermore, EVs derived from T cells or monocytes increased the synthesis of matrix metalloproteinases (MMPs), prostaglandin G/H synthase 2 (PTGS2, also known as cyclooxygenase-2 (COX-2)), microsomal prostaglandin E synthase 1 (PTGES) and prostaglandin E_2 (PGE_2) in FLSs, and resulted in the activation of nuclear factor κB (NFκB), activator protein 1 (AP-1) and JNK (c-Jun N-terminal kinases) signalling pathways in these FLSs [19,20]. These findings demonstrate an EV-mediated, catabolic effect of immune cells on the cartilage and the synovial membrane.

Studies have suggested the existence of specific EV types and functionalities in different joint diseases, and disease-dependent, morphological EV signatures have been found [21]. For example, Zhang and colleagues described a membrane-bound form of TNF in EVs shed by RA, but not OA, FLSs [22]. In addition, platelet-derived EVs were found in synovial fluid of patients with RA, but not in patients with OA [23]. In this study, Boilard and colleagues identified platelet glycoprotein VI, a collagen receptor, as a trigger for EV production in arthritis [23], and found that collagen-induced EVs co-localised with leukocytes in the synovial fluid, where they were able to stimulate FLSs by activating the IL-1 receptor [23]. Importantly, this was the first observation that suggested a role for ECM molecules (specifically collagen) in cell-activation and EV production. The authors proposed that the synovial membrane would be the ideal location in the joint for interaction between ECM of the synovial membrane and cells from the circulation, theoretically enabling collagen-receptor-mediated platelet activation (and subsequent EV production) via fenestrations in the microvasculature [23]. In addition, a 2015 study has suggested that platelet-derived EVs in synovial fluid are internalised by neutrophils [24], a process that has been suggested to enhance inflammation. Interestingly, conversion of arachidonic acid by EV-associated arachidonate 12(S)-lipoxygenase (12S-LOX) to 12(S)-hydroxyeicosatetraenoic acid (12[S]-HETE) was found to be necessary for platelet-derived EV internalisation by immune cells. This conversion seems to be driven by the catalytic activity of secreted phospholipase A_2 IIA ($sPLA_2$-IIA) from the inflamed synovial fluid, which can release arachidonic acid from phospholipids in the EV membrane.

Several EV-related mechanisms have been suggested to act during inflammation, including recognition of pathogen-shed EVs by immune cells, EV-mediated shuttling

6

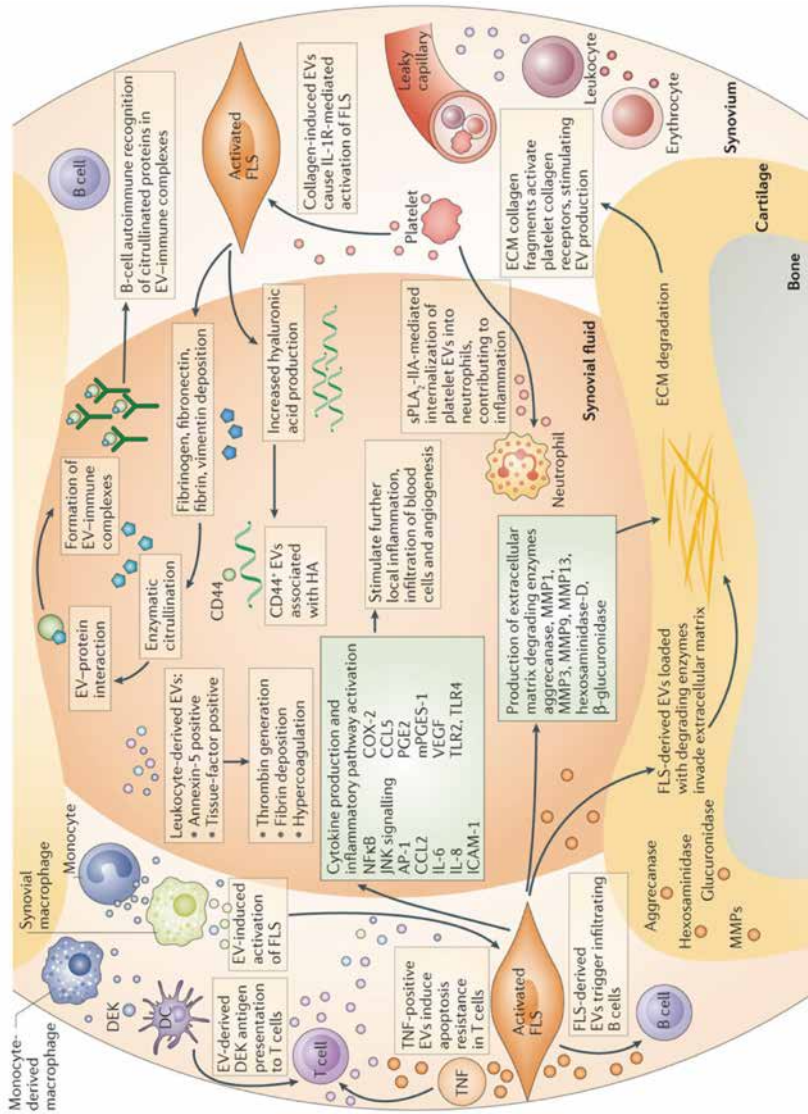**Figure 1** Proposed mechanisms of EV-mediated communication in inflammatory joint disease. During local inflammation, infiltrating leukocytes (T cells, B cells, monocytes, monocyte-derived macrophages) and resident synovial macrophages activate fibroblast-like synoviocytes (FLSs) in the synovial membrane by EV-mediated cell-to-cell communication. Activated FLSs further maintain inflammation by production of cytokines and enzymes.

Figure 1 (*Continued*)

By the release of their own EVs, FLSs signal back to immune cells and enzyme-loaded, FLS-derived EVs can invade aggrecan-rich extracellular matrix (ECM). Leukocyte-derived EVs can carry factors that cause local hypercoagulation. Activated-platelet-derived EVs cause IL-1 receptor-mediated activation of FLSs and can be internalised by activated neutrophils, maintaining the inflammatory phenotype of the two cell types. B cells recognise citrullinated proteins in EV-immune complexes, which might be part of the autoimmune process in rheumatoid arthritis. AP1, activator protein 1; CCL2, C–C motif chemokine 2; CCL5, C–C motif chemokine 5; COX-2, cyclooxygenase 2 (prostaglandin G/H synthase 2); DC, dendritic cell; HA, hyaluronic acid; ICAM, intercellular adhesion molecule; JNK, c-Jun N-terminal kinase; MMP, matrix metalloproteinase; PGE, prostaglandin E; mPGES-1, microsomal prostaglandin E synthase 1; sPLA2-IIA, secreted phospholipase A2-IIA; TLR, Toll-like receptor; VEGF, vascular endothelial growth factor. This figure was used with permission from the Nature Publishing Group.

of inflammation-related cytokines and lipid mediators, and the transportation by EVs of proteolytic enzymes that cause tissue destruction [4,13]. Immune complexes formed after recognition of EV-associated citrullinated proteins (such as vimentin and fibrinogen) by the immune system have also been found [25]; these processes might propagate inflammation in autoimmune diseases. Indeed, citrullinated proteins were detected in EVs from patients with RA, OA and reactive arthritis [26], and EV-associated factors have been discovered that could trigger joint inflammation, including DEK, an autoantigen known to attract neutrophils, CD8+ T cells and natural killer (NK) cells [27]. Extracellular vesicles carrying these antigens have been proposed to facilitate their efficient uptake by dendritic cells (DCs) for antigen presentation [27].

Finally, the expression of Toll-like receptors (TLRs) in RA and OA is upregulated in chondrocytes [28] and FLSs [29], resulting in increased cytokine, chemokine and enzyme production. Consequently, targeting of TLR signalling, specifically of TLR4, has been suggested as a therapy for these diseases [30]. The indication that EVs are able to activate monocytes in a TLR2 and TLR4-dependent manner [31] – two TLR family members previously associated with inflammatory joint diseases [32,33] – suggests that TLR activation in joint inflammation might be mediated by EVs.

ECM–EV interactions

Extracellular vesicles produced by RA FLSs might have the ability to infiltrate aggrecan-rich ECM, as was suggested by Lo Cicero and colleagues after finding aggrecanase activity in these EVs [34]. Similarly, hexosaminidase D and β-glucuronidase activity detected in EVs derived from synovial fluid and FLSs from patients with RA and OA was linked to cartilage degradation [35,36]. Although direct evidence is still

6

lacking, EVs are now thought to have a role in the catabolic cascade during inflammatory joint diseases by contributing to the primary degradation of the ECM.

In the context of cancer, EVs positive for the hyaluronic acid (HA) receptor CD44 have been associated with binding of HA in the extracellular environment [37]. Hyaluronic acid, a nonsulfated glycosaminoglycan, is also abundant in the joint, in both synovial fluid and cartilage ECM. Production of HA by FLSs and chondrocytes is regulated by the HA concentration in the synovial fluid, which is affected, in turn, by the disease state in the joint [38]. Interestingly, CD44 was detected on EVs isolated from healthy synovial fluid, and from chondrocyte or synoviocyte-derived culture media (J.B., unpublished data), indicating that HA can also serve as a matrix for EV binding in synovial fluid and cartilage ECM. Differences in HA concentration during inflammatory events might, therefore, be associated with changes in EV binding and diffusion in the joint.

EV-associated miRNAs

Extracellular vesicle mediated transfer of miRNAs – silencing molecules that target specific mRNAs during post-transcriptional regulation of gene expression – has been described in the past decade [5]. Nowadays, EVs are acknowledged as vehicles that efficiently protect fast-degrading RNA molecules, enabling their safe transport within the extracellular space. Given the crucial role of miRNAs in cell function, the transport of these molecules might be one the most important mechanisms by which EVs facilitate intercellular communication.

Two interesting examples of this functional link between EVs and miRNAs involve miR-140 and miR-146a. Although these miRNAs have not been associated with EVs in the joint, they are involved in joint homeostasis and disease, and have been associated with EVs in other tissues [39-41]. MiRNA-140, one of the few miRNAs highly expressed in chondrocytes, is an important regulator of cartilage homeostasis [42]. Expression levels of miR-140 were found to be lower in human articular cartilage from patients with OA than from healthy controls, and IL-1β could suppress miR-140 expression in articular chondrocytes [43]. In addition, mRNA expression of a disintegrin and metalloproteinase with thrombospondin motifs 5 (ADAMTS5) and aggrecan core protein were regulated by miR-140, suggesting a role for this miRNA in regulating the balance between ECM formation and degradation [43]. These effects were only present in IL-1β-stimulated cells and, therefore, seem to be specific for catabolic processes – an important observation in relation to potential treatment options. In addition to its function as a general immune-regulatory factor, miRNA-146a, differentially expressed in both RA and OA [44], also has a role during osteoclastogenesis in RA [45]. Given these observations, EV-mediated transfer of miRNAs is likely to be a mechanism in

pathological processes in the joint and, hence, a promising target deserving future research.

EV APPLICATIONS IN THE JOINT

Biomarkers

The special features of EVs, including their particular composition, mechanisms of regulated release and cargo-protective properties, have led to hope that these structures can be used as biomarkers to monitor physiological and pathological processes [46-48]. For example, in cancer research, the potential of circulating tumour-derived EVs as biomarkers in liquid biopsies is currently being investigated for use in early tumour detection, in defining disease stage and in prediction of treatment outcome [49]. Joint disease-specific EV signatures might also be identified in the circulation or synovial fluid.

Based on the reports of EVs from synovial fluid and blood of patients with RA and OA discussed in this Perspectives, we hypothesise that at least three possible EV biomarker types could be defined for joint diseases (Figure 2): immune-cell-derived inflammatory EVs in the circulation could be a sign of early-onset joint disease; EVs in the synovial fluid of patients could provide information about inflammation type, disease state and progression; and EVs derived from FLSs and chondrocytes, isolated from healthy individuals, could provide information about predisposition for autoimmune disease or cartilage disorders. Furthermore, considering the possible role of EV-associated miRNAs in inflammatory joint disease, evaluation of miRNA levels in synovial-fluid-derived EVs from patients with RA or OA would further substantiate the involvement of EVs in deregulated joint homeostasis, and might lead to the development of novel diagnostic tools.

Restoration of joint homeostasis

In addition to containing information related to the disease state of an individual, EVs could also be applied as therapy to counteract inflammatory events at the tissue level (Figure 2). Previous successful attempts to target synovial inflammation in experimental arthritis with liposomes loaded with glucocorticoids or with an immuno-suppressive peptide showed the potential of targeted therapies [50,51]. Furthermore, EVs derived from IL-10-stimulated or IL-10-expressing DCs have shown their potential as modulators of the inflammatory immune response during experimentally induced joint disease [52]. Interestingly, besides EV periarticular injection, systemic injection also had a therapeutic effect in the same study [52].

6

a EVs as biomarkers
- Blood
- Synovial fluid
- Tissue biopsies

b Restoration of joint homeostasis
- Therapeutic blocking of EV-mediated pathological processes
- Intra-articular or systemic administration of anti-inflammatory EVs
- Intra-articular or systemic administration of immunosuppressive EVs

FLS

Targeting activated cell

Immune cells

→ Reduction of cytokine release
→ Inhibition of inflammatory signalling pathways

c Tissue repair

miRNA

IGF-1, TGF-β, BMP-7, BMP-2, PDGF

EVs derived from cultured MSCs or iPSC

Bio-inspired artificial nanovesicles loaded with miRNAs or growth factors of interest

- Surface coating of polymer scaffolds with EVs
- Embedding of EVs in hydrogel matrices
- Application in 3D-bioprinting technology

→ Controlled kinetics for EV release and degradation
→ Promoting cell proliferation and ECM production
→ Promoting chondrogenesis
→ Regulation of immunogenic processes in and around the scaffold
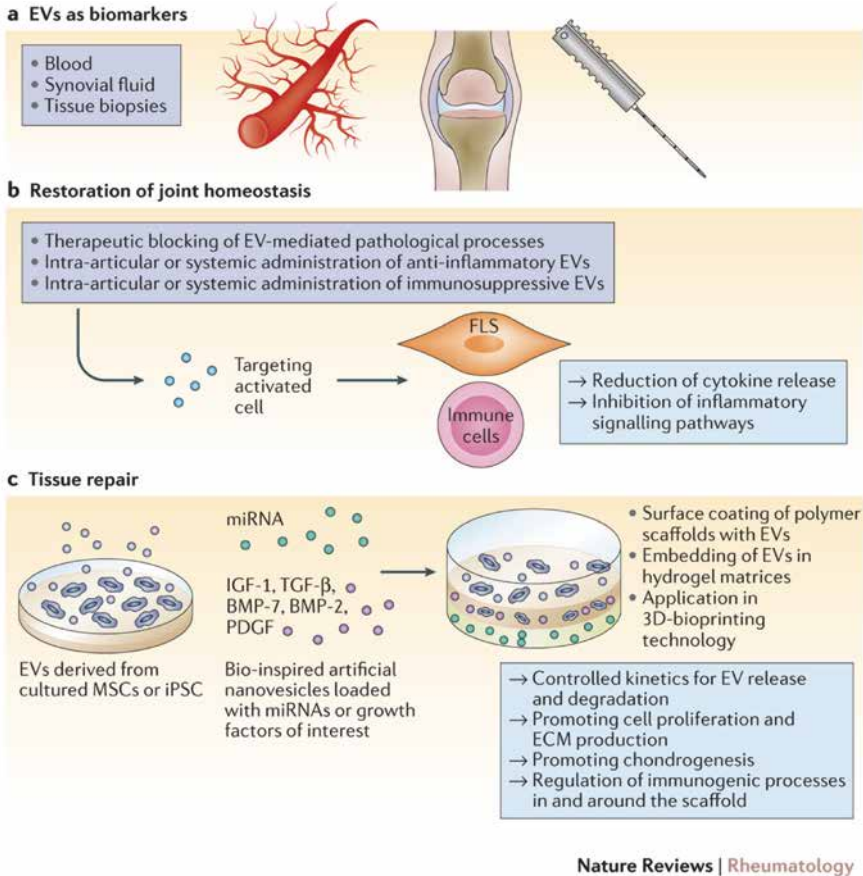
Nature Reviews | Rheumatology

Figure 2 Proposed applications of EVs in joint disease. **A)** Extracellular vesicles have biomarker potential for joint diseases, both to predict disease development in healthy individuals and to monitor disease progression in patients. In the blood, circulating inflammatory EVs can be an alert for early onset of inflammatory joint diseases. In synovial fluid, EVs from patients can provide information about inflammation type, disease state and disease progression. In the context of tissue biopsies, EVs derived from cultured synovial tissue could indicate predisposition for development of autoimmune disease and cartilage disorders. **B,C)** Regulatory EVs can be exploited for intra-articular injection or for application in biomaterials designed for implantation purposes to restore joint homeostasis and improve tissue repair in patients. BMP, bone morphogenetic protein; IGF-1, insulin-like growth factor 1; iPSC, induced pluripotent stem cell; miRNA, microRNA; MSC, mesenchymal stem/stromal cell; PDGF, platelet derived growth factor; TGF-β, transforming growth factor-β. This figure was used with permission from the Nature Publishing Group.

Extracellular vesicles derived from multipotent mesenchymal stem/stromal cells (MSCs) have also been demonstrated to exert immunosuppressive and anti-inflammatory effects [53]; for example, in a clinical trial using MSC-derived EVs as treatment, symptoms were considerably mitigated in a patient with therapy-refractory graft-versus-host disease [54]. Therefore, the role of MSCs as modulators of joint homeostasis, which includes previously described anti-inflammatory properties [55], suggests these cells as interesting therapeutic alternatives in the restoration of homeostasis in the inflamed joint (relevant, for example, for patients with RA). Based on the current knowledge of EV-mediated immune regulation [56], MSC-derived EVs could become a part of these therapeutic efforts for joint diseases [53].

Tissue repair

Extracellular vesicles also hold potential as inducers of tissue regeneration, given that they affect regulatory processes including cell recruitment, proliferation and differentiation [57]. Current regenerative treatments for articular cartilage often rely on the use of biomaterials combined with autologous chondrocytes expanded *in vitro* [58]. In this context, the use of MSCs as a cellular therapy is increasingly gaining attention despite difficulties in controlling undesired ossification of the newly formed tissue [59]. New advances in cocultures of primary chondrocytes with allogeneic MSCs have simplified the treatment [60], and resulted in a shift from *in vitro* expansion and subsequent reimplantation to a single-stage procedure [61]. As MSCs establish a regenerative microenvironment by secreting bioactive molecules [62], the supposed underlying mechanism by which these cells enhance chondrogenic differentiation is thought to be based on trophic factors. Consequently, soluble biomolecules – and, possibly, EVs – are likely to be the main effectors in the MSC-driven regenerative pathway [53]. In line with this assumption, in a scenario of tissue injury, mRNA and miRNA-laden EVs from local MSCs in the tissue could lead to genetic reprogramming and induction of cell dedifferentiation, instructing a cell-cycle "reboot" and starting the regeneration process [63,64]. These regenerative approaches could be simplified, potentially, by the replacement of cultured MSCs with the MSC secretome, or even by specific MSC-derived EVs. This is an exciting prospect and might lead to an off-the-shelf regenerative treatment with fewer regulatory constraints than the present strategies, as no living cells would be injected into patients [65]. Moreover, the efficacy of MSC-derived EVs (or of EVs derived from other cell types, such as induced pluripotent stem cells) might be further enhanced by the incorporation of selected biological molecules, such as miRNAs and proteins, which support chondrogenesis [66,67] (Figure 2).

6

CHALLENGES AND TRANSLATION

EV preparation and selection

Although ultracentrifugation and density gradient flotation are recommended techniques for EV isolation for analytical and experimental purposes, these procedures are not feasible for clinical applications (Box 2). One of the biggest challenges for the future is the large-scale production and isolation of (engineered) EVs for clinical application. Therefore, the development of robust, scalable biological production procedures and of appropriate EV isolation methods is urgently needed. Furthermore, detailed knowledge of the complex lipid, protein and nucleic acid composition of EVs could be used to design bio-inspired synthetic carriers with lower variability than that of EVs produced biologically. For example, EV lipid membrane selection or modification could be used to improve the delivery of EVs and their interaction with target cells. Some EV lipids can interact with specific lipid receptor proteins on target cells (for instance, phosphatidylserine binding to TIMD-4, or glycosphingolipids binding to sialoadhesin), and EVs have been shown to carry bioactive lipids (such as eicosanoids and lysophospholipids) and enzymes that convert structural lipids into bioactive molecules (examples of these enzymes include sPLA$_2$-IIA, 12S-LOX and prostaglandin synthases) [24,68]. Hence, targeted delivery of these bioactive compounds to particular cells might enhance their effect and specificity of this therapeutic approach.

BOX 2 Isolation and purification of EVs

Isolation of EVs, particularly from body fluids, is challenging, and the quality of the EV isolation procedure determines the validity of the claim of EV-mediated functional effects [1,81]. Lack of sufficient information about EV isolation procedures and EV characteristics complicates the interpretation of data and hampers the comparability of studies. Moreover, limited centrifugation steps, omission of density gradient centrifugation and lack of EV-depleted controls preclude conclusions that observed functional effects are caused solely via EVs [81]. Skriner and colleagues [26] were among the first to isolate EVs from synovial fluid using a multistep centrifugation protocol followed by sucrose density gradient flotation and size determination by electron microscopy. These steps justify their conclusion that the effects observed can be fully attributed to small EVs (<300 nm). In previous reports of EVs derived from synovial fluid, EV characteristics were not specified and the EV fraction isolated most likely contained several EV subtypes as well as nonvesicular particulates. Immune complexes are also known to be present in synovial fluid and can hamper EV analysis, providing an additional reason to purify EVs using ultracentrifugation and density gradient flotation [82]. Finally, to provide researchers with guidelines, the International Society for Extracellular Vesicles (ISEV) published the minimal experimental requirements for definition of EVs and their function in 2014 [81].

EV delivery

Achieving effective and controlled delivery of EVs to disease sites is challenging, but is paramount to the efficient restoration of joint homeostasis and sustained positive effect on the regenerative process. Different modes of EV delivery could include intravenous (systemic) EV injection, intra-articular EV injection, and surface coating of scaffolds or embedding in hydrogel matrices [57]. Systemic EV injection can result in passive targeting to inflamed joints owing to increased synovial vascular permeability, as has been observed in arthritic joints [51,69]. Conversely, intra-articular injection of EVs, possibly in combination with other therapeutics or regenerative cells, is a direct application at the affected site.

The use of EV-mediated delivery is expected to be more efficient than using soluble proteins or RNA molecules, which are usually prone to fast degradation after injection. However, in view of the gradual clearance of EVs from the joint space, a more sustained effect might be achieved by temporarily immobilizing EVs on or within a biomaterial scaffold. A wide range of scaffolds for musculoskeletal regenerative applications is currently being evaluated, generally in combination with cells and bioactive molecules [70]. Coating with, or incorporation of, EVs is an additional opportunity to optimise the functionality of these scaffolds (Figure 2). More specifically, EVs could be bound on the surface of polymer scaffolds by specific linkers, antibodies or ECM components such as HA [37].

Alternatively, EVs could also be incorporated within a hydrogel matrix. Hydrogels recapitulate several features of the natural ECM and enable the encapsulation of cells and EVs. Polymer network density and degradation kinetics of hydrogels can be adjusted and tailored to the specific release kinetics of EVs. For this purpose, the field can take particular advantage of the extensive experience available in the embedding of liposomes for drug delivery applications [71]. Moreover, it has been suggested that EV surface modification with functional polymers can be used to modulate their release kinetics further [72]. Nevertheless, how specific biomaterials interact with embedded EVs and preserve their activity needs further research. For example, combinatorial use of different hydrogels loaded with distinct EV populations within a single construct could further facilitate the controlled and sequential release of the different fractions of embedded EVs. Three-dimensional (3D)-printing technologies now have the ability to generate these multimaterial constructs with precisely defined anatomical architectures [73,74], and cell or EV-laden hydrogels can be used as potential building blocks for the production of tissue analogues.

6

Experimental considerations

In previous clinical trials of EV therapy, these structures were shown to be generally well-tolerated and to have a low risk of immunogenicity and toxicity [75]. However, important questions remain about the kinetics and biodistribution of EVs. The distribution of systemically administered EVs has been demonstrated to be dependent on dose, route of administration and cellular origin of the EVs [76]. No biodistribution data exists for articular tissues yet, and detailed investigations of EV distribution and clearance from the synovial fluid and articular tissues will be necessary for each EV therapy. Directing EVs to the target site and decreasing the risk of fast clearance from the tissues of interest, as has been achieved in cancer research [777], might be a way to increase treatment efficiency.

The future development of EV-mediated therapeutic approaches for joint diseases requires further elucidation of the potential roles of EVs in joint homeostasis and regeneration. Advanced bioreactor systems and *ex vivo* culture models can, to a certain extent, be used for this purpose, but animal models will be indispensable for translation to the clinic. For translational studies in musculoskeletal diseases, the horse is generally seen as the best animal model for joint disease, whereas the dog is better suited for intervertebral disk disease (IVDD) studies [78,79]. The prevalence of OA and IVDD in horses and dogs, respectively, is considerable, enabling the design of clinical trials that use them as experimental animals and therapeutic target animals simultaneously, an important factor from an ethical perspective. A practical advantage of the equine model is the large size of the joints, which enables sequential sampling of relevant quantities of synovial fluid for the monitoring of EV profiles. Furthermore, comparative studies of human and equine articular cartilage have shown great similarities in thickness and composition between the two species [80].

CONCLUSIONS

Extracellular vesicles have a prominent role in joint development and in the regulation of intra-articular homeostasis. Although their composition and function in the joint are not yet clearly understood, EVs are envisaged as next-generation biomarkers of the pathophysiological state of the joint. Further, an important role for EVs in future therapies for the treatment of joint disorders is also foreseen, in particular as they provide a simpler and safer alternative to current cell-based therapeutic options. Extracellular vesicles can also be combined with scaffolds, either bound on their surface or embedded within scaffold matrices, enabling the controlled release of specific populations of EVs. Bioengineering approaches could further assist in defining the location of EV delivery by 3D generation of organised tissue constructs.

Research on biomaterial-based release of well-defined EV populations is still in its infancy, but holds considerable promise. However, the therapeutic use of EVs demands high-quality standardisation of isolation and analysis techniques to yield reproducible EV preparations. In this regard, synthetic alternatives to cell-derived EVs might simplify production and scalability of EV-based therapeutic delivery systems, further enhancing their therapeutic potential.

6

REFERENCES

1. Witwer, K. W.; Buzas, E. I.; Bemis, L. T.; Bora, A.; Lasser, C.; Lotvall, J.; Nolte-'t Hoen, E. N.; Piper, M. G.; Sivaraman, S.; Skog, J.; Thery, C.; Wauben, M. H.; Hochberg, F. Standardization of sample collection, isolation and analysis methods in extracellular vesicle research. *J. Extracell Vesicles* **2013***, 2*, 20360.

2. Berckmans, R. J.; Nieuwland, R.; Tak, P. P.; Boing, A. N.; Romijn, F. P.; Kraan, M. C.; Breedveld, F. C.; Hack, C. E.; Sturk, A. Cell-derived microparticles in synovial fluid from inflamed arthritic joints support coagulation exclusively via a factor VII-dependent mechanism. *Arthritis Rheum.* **2002***, 46*, 2857-2866.

3. Thery, C.; Zitvogel, L.; Amigorena, S. Exosomes: composition, biogenesis and function. *Nat. Rev. Immunol.* **2002***, 2*, 569-579.

4. Thery, C.; Ostrowski, M.; Segura, E. Membrane vesicles as conveyors of immune responses. *Nat. Rev. Immunol.* **2009***, 9*, 581-593.

5. Valadi, H.; Ekstrom, K.; Bossios, A.; Sjostrand, M.; Lee, J. J.; Lotvall, J. O. Exosome-mediated transfer of mRNAs and microRNAs is a novel mechanism of genetic exchange between cells. *Nat. Cell Biol.* **2007***, 9*, 654-659.

6. Yanez-Mo, M.; Siljander, P. R.; Andreu, Z.; Zavec, A. B.; Borras, F. E.; Buzas, E. I.; Buzas, K.; Casal, E.; Cappello, F.; Carvalho, J.; Colas, E.; Cordeiro-da Silva, A.; Fais, S.; Falcon-Perez, J. M.; Ghobrial, I. M.; Giebel, B.; Gimona, M.; Graner, M.; Gursel, I.; Gursel, M.; Heegaard, N. H.; Hendrix, A.; Kierulf, P.; Kokubun, K.; Kosanovic, M.; Kralj-Iglic, V.; Kramer-Albers, E. M.; Laitinen, S.; Lasser, C.; Lener, T.; Ligeti, E.; Line, A.; Lipps, G.; Llorente, A.; Lotvall, J.; Mancek-Keber, M.; Marcilla, A.; Mittelbrunn, M.; Nazarenko, I.; Nolte-'t Hoen, E. N.; Nyman, T. A.; O'Driscoll, L.; Olivan, M.; Oliveira, C.; Pallinger, E.; Del Portillo, H. A.; Reventos, J.; Rigau, M.; Rohde, E.; Sammar, M.; Sanchez-Madrid, F.; Santarem, N.; Schallmoser, K.; Ostenfeld, M. S.; Stoorvogel, W.; Stukelj, R.; Van der Grein, S. G.; Vasconcelos, M. H.; Wauben, M. H.; De Wever, O. Biological properties of extracellular vesicles and their physiological functions. *J. Extracell Vesicles* **2015***, 4*, 27066.

7. Zomer, A.; Maynard, C.; Verweij, F. J.; Kamermans, A.; Schafer, R.; Beerling, E.; Schiffelers, R. M.; de Wit, E.; Berenguer, J.; Ellenbroek, S. I.; Wurdinger, T.; Pegtel, D. M.; van Rheenen, J. In Vivo imaging reveals extracellular vesicle-mediated phenocopying of metastatic behavior. *Cell* **2015***, 161*, 1046-1057.

8. Ridder, K.; Keller, S.; Dams, M.; Rupp, A. K.; Schlaudraff, J.; Del Turco, D.; Starmann, J.; Macas, J.; Karpova, D.; Devraj, K.; Depboylu, C.; Landfried, B.; Arnold, B.; Plate, K. H.; Hoglinger, G.; Sultmann, H.; Altevogt, P.; Momma, S. Extracellular vesicle-mediated transfer of genetic information between the hematopoietic system and the brain in response to inflammation. *PLoS Biol.* **2014***, 12*, e1001874.

9. Anderson, H. C. Vesicles associated with calcification in the matrix of epiphyseal cartilage. *J. Cell Biol.* **1969***, 41*, 59-72.

10. Anderson, H. C. Matrix vesicles and calcification. *Curr. Rheumatol. Rep.* **2003***, 5*, 222-226.

11. Nahar, N. N.; Missana, L. R.; Garimella, R.; Tague, S. E.; Anderson, H. C. Matrix vesicles are carriers of bone morphogenetic proteins (BMPs), vascular endothelial growth factor (VEGF), and noncollagenous matrix proteins. *J. Bone Miner. Metab.* **2008***, 26*, 514-519.

12. Fourcade, O.; Simon, M. F.; Viode, C.; Rugani, N.; Leballe, F.; Ragab, A.; Fournie, B.; Sarda, L.; Chap, H. Secretory phospholipase A2 generates the novel lipid mediator lysophosphatidic acid in membrane microvesicles shed from activated cells. *Cell* **1995***, 80*, 919-927.

13. Buzas, E. I.; Gyorgy, B.; Nagy, G.; Falus, A.; Gay, S. Emerging role of extracellular vesicles in inflammatory diseases. *Nat. Rev. Rheumatol.* **2014***, 10*, 356-364.

14. Goldring, M. B.; Marcu, K. B. Cartilage homeostasis in health and rheumatic diseases. *Arthritis Res. Ther.* **2009***, 11*, 224.

15. Berckmans, R. J.; Nieuwland, R.; Kraan, M. C.; Schaap, M. C.; Pots, D.; Smeets, T. J.; Sturk, A.; Tak, P. P. Synovial microparticles from arthritic patients modulate chemokine and cytokine release by synoviocytes. *Arthritis Res. Ther.* **2005***, 7*, R536-44.

16. Messer, L.; Alsaleh, G.; Freyssinet, J.; Zobairi, F.; Leray, I.; Gottenberg, J.; Sibilia, J.; Toti-Orfanoudakis, F.; Wachsmann, D. Microparticle-induced release of B-lymphocyte regulators by rheumatoid synoviocytes. *Arthritis Research & Therapy* **2009***, 11*, R40.

17. Reich, N.; Beyer, C.; Gelse, K.; Akhmetshina, A.; Dees, C.; Zwerina, J.; Schett, G.; Distler, O.; Distler, J. H. Microparticles stimulate angiogenesis by inducing ELR(+) CXC-chemokines in synovial fibroblasts. *J. Cell. Mol. Med.* **2011***, 15*, 756-762.

18. Kato, T.; Miyaki, S.; Ishitobi, H.; Nakamura, Y.; Nakasa, T.; Lotz, M. K.; Ochi, M. Exosomes from IL-1beta stimulated synovial fibroblasts induce osteoarthritic changes in articular chondrocytes. *Arthritis Res. Ther.* **2014***, 16*, R163.

19. Distler, J. H.; Jungel, A.; Huber, L. C.; Seemayer, C. A.; Reich, C. F.,3rd; Gay, R. E.; Michel, B. A.; Fontana, A.; Gay, S.; Pisetsky, D. S.; Distler, O. The induction of matrix metalloproteinase and cytokine expression in synovial fibroblasts stimulated with immune cell microparticles. *Proc. Natl. Acad. Sci. U. S. A.* **2005**, *102*, 2892-2897.

20. Jungel, A.; Distler, O.; Schulze-Horsel, U.; Huber, L. C.; Ha, H. R.; Simmen, B.; Kalden, J. R.; Pisetsky, D. S.; Gay, S.; Distler, J. H. Microparticles stimulate the synthesis of prostaglandin E(2) via induction of cyclooxygenase 2 and microsomal prostaglandin E synthase 1. *Arthritis Rheum.* **2007**, *56*, 3564-3574.

21. Gyorgy, B.; Szabo, T.,G.; Turiak, L.; Wright, M.; Herczeg, P.; Ledeczi, Z.; Kittel, A.; Polgar, A.; Toth, K.; Derfalvi, B.; Zelenak, G.; Borocz, I.; Carr, B.; Nagy, G.; Vekey, K.; Gay, S.; Falus, A.; Buzas, E.,I. Improved flow cytometric assessment reveals distinct microvesicle (cell-derived microparticle) signatures in joint diseases. *PloS one* **2012**, *7*, e49726.

22. Zhang, H.; Liu, C.; Su, K.; Yu, S.; Zhang, L.; Zhang, S.; Wang, J.; Cao, X.; Grizzle, W.; Kimberly, R. P. A Membrane Form of TNF-α Presented by Exosomes Delays T Cell Activation-Induced Cell Death. *The Journal of Immunology* **2006**, *176*, 7385-7393.

23. Boilard, E.; Nigrovic, P. A.; Larabee, K.; Watts, G. F.; Coblyn, J. S.; Weinblatt, M. E.; Massarotti, E. M.; Remold-O'Donnell, E.; Farndale, R. W.; Ware, J.; Lee, D. M. Platelets amplify inflammation in arthritis via collagen-dependent microparticle production. *Science* **2010**, *327*, 580-583.

24. Duchez, A. C.; Boudreau, L. H.; Bollinger, J.; Belleannee, C.; Cloutier, N.; Laffont, B.; Mendoza-Villarroel, R. E.; Levesque, T.; Rollet-Labelle, E.; Rousseau, M.; Allaeys, I.; Tremblay, J. J.; Poubelle, P. E.; Lambeau, G.; Pouliot, M.; Provost, P.; Soulet, D.; Gelb, M. H.; Boilard, E. Platelet microparticles are internalized in neutrophils via the concerted activity of 12-lipoxygenase and secreted phospholipase A2-IIA. *Proc. Natl. Acad. Sci. U. S. A.* **2015**, *112*, E3564-73.

25. Cloutier, N.; Tan, S.; Boudreau, L. H.; Cramb, C.; Subbaiah, R.; Lahey, L.; Albert, A.; Shnayder, R.; Gobezie, R.; Nigrovic, P. A.; Farndale, R. W.; Robinson, W. H.; Brisson, A.; Lee, D. M.; Boilard, E. The exposure of autoantigens by microparticles underlies the formation of potent inflammatory components: the microparticle-associated immune complexes. *EMBO Mol. Med.* **2013**, *5*, 235-249.

26. Skriner, K.; Adolph, K.; Jungblut, P. R.; Burmester, G. R. Association of citrullinated proteins with synovial exosomes. *Arthritis Rheum.* **2006**, *54*, 3809-3814.

27. Mor-Vaknin, N.; Punturieri, A.; Sitwala, K.; Faulkner, N.; Legendre, M.; Khodadoust, M. S.; Kappes, F.; Ruth, J. H.; Koch, A.; Glass, D.; Petruzzelli, L.; Adams, B. S.; Markovitz, D. M. The DEK nuclear autoantigen is a secreted chemotactic factor. *Mol. Cell. Biol.* **2006**, *26*, 9484-9496.

28. Sillat, T.; Barreto, G.; Clarijs, P.; Soininen, A.; Ainola, M.; Pajarinen, J.; Korhonen, M.; Konttinen, Y. T.; Sakalyte, R.; Hukkanen, M.; Ylinen, P.; Nordstrom, D. C. Toll-like receptors in human chondrocytes and osteoarthritic cartilage. *Acta Orthop.* **2013**, *84*, 585-592.

29. Hu, F.; Li, Y.; Zheng, L.; Shi, L.; Liu, H.; Zhang, X.; Zhu, H.; Tang, S.; Zhu, L.; Xu, L.; Yang, Y.; Li, Z. Toll-like receptors expressed by synovial fibroblasts perpetuate Th1 and th17 cell responses in rheumatoid arthritis. *PLoS One* **2014**, *9*, e100266.

30. Gomez, R.; Villalvilla, A.; Largo, R.; Gualillo, O.; Herrero-Beaumont, G. TLR4 signalling in osteoarthritis-finding targets for candidate DMOADs. *Nat. Rev. Rheumatol.* **2015**, *11*, 159-170.

31. Bretz, N. P.; Ridinger, J.; Rupp, A. K.; Rimbach, K.; Keller, S.; Rupp, C.; Marme, F.; Umansky, L.; Umansky, V.; Eigenbrod, T.; Sammar, M.; Altevogt, P. Body fluid exosomes promote secretion of inflammatory cytokines in monocytic cells via Toll-like receptor signaling. *J. Biol. Chem.* **2013**, *288*, 36691-36702.

32. Kim, H. A.; Cho, M. L.; Choi, H. Y.; Yoon, C. S.; Jhun, J. Y.; Oh, H. J.; Kim, H. Y. The catabolic pathway mediated by Toll-like receptors in human osteoarthritic chondrocytes. *Arthritis Rheum.* **2006**, *54*, 2152-2163.

33. Liu-Bryan, R.; Terkeltaub, R. Chondrocyte innate immune myeloid differentiation factor 88-dependent signaling drives procatabolic effects of the endogenous Toll-like receptor 2/Toll-like receptor 4 ligands low molecular weight hyaluronan and high mobility group box chromosomal protein 1 in mice. *Arthritis Rheum.* **2010**, *62*, 2004-2012.

34. Lo Cicero, A.; Majkowska, I.; Nagase, H.; Di Liegro, I.; Troeberg, L. Microvesicles shed by oligodendroglioma cells and rheumatoid synovial fibroblasts contain aggrecanase activity. *Matrix Biol.* **2012**, *31*, 229-233.

35. Pasztoi, M.; Sodar, B.; Misjak, P.; Paloczi, K.; Kittel, A.; Toth, K.; Wellinger, K.; Geher, P.; Nagy, G.; Lakatos, T.; Falus, A.; Buzas, E. I. The recently

6

identified hexosaminidase D enzyme substantially contributes to the elevated hexosaminidase activity in rheumatoid arthritis. *Immunol. Lett.* **2013***, 149*, 71-76.

36. Pasztoi, M.; Nagy, G.; Geher, P.; Lakatos, T.; Toth, K.; Wellinger, K.; Pocza, P.; Gyorgy, B.; Holub, M. C.; Kittel, A.; Paloczy, K.; Mazan, M.; Nyirkos, P.; Falus, A.; Buzas, E. I. Gene expression and activity of cartilage degrading glycosidases in human rheumatoid arthritis and osteoarthritis synovial fibroblasts. *Arthritis Res. Ther.* **2009***, 11*, R68.

37. Mu, W.; Rana, S.; Zoller, M. Host matrix modulation by tumor exosomes promotes motility and invasiveness. *Neoplasia* **2013***, 15*, 875-887.

38. Smith, M. M.; Ghosh, P. The synthesis of hyaluronic acid by human synovial fibroblasts is influenced by the nature of the hyaluronate in the extracellular environment. *Rheumatol. Int.* **1987***, 7*, 113-122.

39. Bellingham, S. A.; Coleman, B. M.; Hill, A. F. Small RNA deep sequencing reveals a distinct miRNA signature released in exosomes from prion-infected neuronal cells. *Nucleic Acids Res.* **2012***, 40*, 10937-10949.

40. Cheng, L.; Sun, X.; Scicluna, B. J.; Coleman, B. M.; Hill, A. F. Characterization and deep sequencing analysis of exosomal and non-exosomal miRNA in human urine. *Kidney Int.* **2014***, 86*, 433-444.

41. Gernapudi, R.; Yao, Y.; Zhang, Y.; Wolfson, B.; Roy, S.; Duru, N.; Eades, G.; Yang, P.; Zhou, Q. Targeting exosomes from preadipocytes inhibits preadipocyte to cancer stem cell signaling in early-stage breast cancer. *Breast Cancer Res. Treat.* **2015***, 150*, 685-695.

42. Hong, E.; Reddi, A. H. MicroRNAs in chondrogenesis, articular cartilage, and osteoarthritis: implications for tissue engineering. *Tissue Eng. Part B. Rev.* **2012***, 18*, 445-453.

43. Miyaki, S.; Nakasa, T.; Otsuki, S.; Grogan, S. P.; Higashiyama, R.; Inoue, A.; Kato, Y.; Sato, T.; Lotz, M. K.; Asahara, H. MicroRNA-140 is expressed in differentiated human articular chondrocytes and modulates interleukin-1 responses. *Arthritis Rheum.* **2009***, 60*, 2723-2730.

44. Yamasaki, K.; Nakasa, T.; Miyaki, S.; Ishikawa, M.; Deie, M.; Adachi, N.; Yasunaga, Y.; Asahara, H.; Ochi, M. Expression of MicroRNA-146a in osteoarthritis cartilage. *Arthritis Rheum.* **2009***, 60*, 1035-1041.

45. Nakasa, T.; Shibuya, H.; Nagata, Y.; Niimoto, T.; Ochi, M. The inhibitory effect of microRNA-146a expression on bone destruction in collagen-induced arthritis. *Arthritis Rheum.* **2011***, 63*, 1582-1590.

46. Boukouris, S.; Mathivanan, S. Exosomes in bodily fluids are a highly stable resource of disease biomarkers. *Proteomics Clin. Appl.* **2015**.

47. Cheng, L.; Sharples, R. A.; Scicluna, B. J.; Hill, A. F. Exosomes provide a protective and enriched source of miRNA for biomarker profiling compared to intracellular and cell-free blood. *J. Extracell Vesicles* **2014***, 3*, 23743.

48. Julich, H.; Willms, A.; Lukacs-Kornek, V.; Kornek, M. Extracellular vesicle profiling and their use as potential disease specific biomarker. *Front. Immunol.* **2014***, 5*, 413.

49. Skog, J.; Wurdinger, T.; van Rijn, S.; Meijer, D. H.; Gainche, L.; Sena-Esteves, M.; Curry, W. T.,Jr; Carter, B. S.; Krichevsky, A. M.; Breakefield, X. O. Glioblastoma microvesicles transport RNA and proteins that promote tumour growth and provide diagnostic biomarkers. *Nat. Cell Biol.* **2008***, 10*, 1470-1476.

50. Vanniasinghe, A. S.; Manolios, N.; Schibeci, S.; Lakhiani, C.; Kamali-Sarvestani, E.; Sharma, R.; Kumar, V.; Moghaddam, M.; Ali, M.; Bender, V. Targeting fibroblast-like synovial cells at sites of inflammation with peptide targeted liposomes results in inhibition of experimental arthritis. *Clin. Immunol.* **2014***, 151*, 43-54.

51. Metselaar, J. M.; van den Berg, W. B.; Holthuysen, A. E.; Wauben, M. H.; Storm, G.; van Lent, P. L. Liposomal targeting of glucocorticoids to synovial lining cells strongly increases therapeutic benefit in collagen type II arthritis. *Ann. Rheum. Dis.* **2004***, 63*, 348-353.

52. Kim, S. H.; Lechman, E. R.; Bianco, N.; Menon, R.; Keravala, A.; Nash, J.; Mi, Z.; Watkins, S. C.; Gambotto, A.; Robbins, P. D. Exosomes derived from IL-10-treated dendritic cells can suppress inflammation and collagen-induced arthritis. *J. Immunol.* **2005***, 174*, 6440-6448.

53. Heldring, N.; Mager, I.; Wood, M. J.; Le Blanc, K.; Andaloussi, S. E. Therapeutic Potential of Multipotent Mesenchymal Stromal Cells and Their Extracellular Vesicles. *Hum. Gene Ther.* **2015***, 26*, 506-517.

54. Kordelas, L.; Rebmann, V.; Ludwig, A. K.; Radtke, S.; Ruesing, J.; Doeppner, T. R.; Epple, M.; Horn, P. A.; Beelen, D. W.; Giebel, B. MSC-derived exosomes: a novel tool to treat therapy-refractory graft-versus-host disease. *Leukemia* **2014***, 28*, 970-973.

55. MacDonald, G. I.; Augello, A.; De Bari, C. Role of mesenchymal stem cells in reestablishing immunologic tolerance in autoimmune rheumatic diseases. *Arthritis Rheum.* **2011***, 63*, 2547-2557.

56. Robbins, P. D.; Morelli, A. E. Regulation of immune responses by extracellular vesicles. *Nat. Rev. Immunol.* **2014**, *14*, 195-208.

57. De Jong, O. G.; Van Balkom, B. W.; Schiffelers, R. M.; Bouten, C. V.; Verhaar, M. C. Extracellular vesicles: potential roles in regenerative medicine. *Front. Immunol.* **2014**, *5*, 608.

58. Grande, D. A.; Schwartz, J. A.; Brandel, E.; Chahine, N. O.; Sgaglione, N. Articular cartilage repair: where we have been, where we are now, and where we are headed. *Cartilage* **2013**, *4*, 281-285.

59. Savkovic, V.; Li, H.; Seon, J. K.; Hacker, M.; Franz, S.; Simon, J. C. Mesenchymal stem cells in cartilage regeneration. *Curr. Stem Cell. Res. Ther.* **2014**, *9*, 469-488.

60. De Windt, T. S.; Hendriks, J. A.; Zhao, X.; Vonk, L. A.; Creemers, L. B.; Dhert, W. J.; Randolph, M. A.; Saris, D. B. Concise review: unraveling stem cell cocultures in regenerative medicine: which cell interactions steer cartilage regeneration and how? *Stem Cells Transl. Med.* **2014**, *3*, 723-733.

61. US National Library of Medicine. IMPACT: Safety and feasibility of a single-stage procedure for focal cartilage lesions of the knee. https://clinicaltrials.gov/ct2/show/NCT02037204. **2014**.

62. Caplan, A. I.; Correa, D. The MSC: an injury drugstore. *Cell. Stem Cell.* **2011**, *9*, 11-15.

63. Camussi, G.; Deregibus, M. C.; Bruno, S.; Cantaluppi, V.; Biancone, L. Exosomes/microvesicles as a mechanism of cell-to-cell communication. *Kidney Int.* **2010**, *78*, 838-848.

64. Bruno, S.; Grange, C.; Deregibus, M. C.; Calogero, R. A.; Saviozzi, S.; Collino, F.; Morando, L.; Busca, A.; Falda, M.; Bussolati, B.; Tetta, C.; Camussi, G. Mesenchymal stem cell-derived microvesicles protect against acute tubular injury. *J. Am. Soc. Nephrol.* **2009**, *20*, 1053-1067.

65. Baglio, S. R.; Pegtel, D. M.; Baldini, N. Mesenchymal stem cell secreted vesicles provide novel opportunities in (stem) cell-free therapy. *Front. Physiol.* **2012**, *3*, 359. doi: 10.3389/fphys.2012.00359.

66. Lamichhane, T. N.; Sokic, S.; Schardt, J. S.; Raiker, R. S.; Lin, J. W.; Jay, S. M. Emerging roles for extracellular vesicles in tissue engineering and regenerative medicine. *Tissue Eng. Part B. Rev.* **2015**, *21*, 45-54.

67. Vonk, L. A.; van Dooremalen, S.; Coffer, P. J.; Saris, D. B.; Lorenowicz, M. J. MSC-derived extracellular vesicles stimulate cartilage regeneration and modulate inflammatory responses. Paper presented at the 13th world congress of the International Cartilage Repair Society, Sept 26, 2016, Sorrento, Italy. **2016**.

68. Record, M.; Carayon, K.; Poirot, M.; Silvente-Poirot, S. Exosomes as new vesicular lipid transporters involved in cell-cell communication and various pathophysiologies. *Biochim. Biophys. Acta* **2014**, *1841*, 108-120.

69. Cloutier, N.; Pare, A.; Farndale, R. W.; Schumacher, H. R.; Nigrovic, P. A.; Lacroix, S.; Boilard, E. Platelets can enhance vascular permeability. *Blood* **2012**, *120*, 1334-1343.

70. Smith, B. D.; Grande, D. A. The current state of scaffolds for musculoskeletal regenerative applications. *Nat. Rev. Rheumatol.* **2015**, *11*, 213-222.

71. Samad, A.; Sultana, Y.; Aqil, M. Liposomal drug delivery systems: an update review. *Curr. Drug Deliv.* **2007**, *4*, 297-305.

72. Sawada, S.; Yasuoka, J.; Sato, Y.; Shimoda, A.; Seo, N.; Harada, N.; Shiku, H.; Akiyoshi, K. Functional polymer gel–exosomes hybrids for drug delivery system and tissue engineering. *ISEV Annual Meeting; Abstract P4C-192* **2014**.

73. Malda, J.; Visser, J.; Melchels, F. P.; Jungst, T.; Hennink, W. E.; Dhert, W. J.; Groll, J.; Hutmacher, D. W. 25th anniversary article: Engineering hydrogels for biofabrication. *Adv Mater* **2013**, *25*, 5011-5028.

74. Visser, J.; Peters, B.; Burger, T. J.; Boomstra, J.; Dhert, W. J.; Melchels, F. P.; Malda, J. Biofabrication of multi-material anatomically shaped tissue constructs. *Biofabrication* **2013**, *5*, 035007-5082/5/3/035007. Epub 2013 Jul 2.

75. Dai, S.; Wei, D.; Wu, Z.; Zhou, X.; Wei, X.; Huang, H.; Li, G. Phase I clinical trial of autologous ascites-derived exosomes combined with GM-CSF for colorectal cancer. *Mol. Ther.* **2008**, *16*, 782-790.

76. Wiklander, O. P.; Nordin, J. Z.; O'Loughlin, A.; Gustafsson, Y.; Corso, G.; Mager, I.; Vader, P.; Lee, Y.; Sork, H.; Seow, Y.; Heldring, N.; Alvarez-Erviti, L.; Smith, C. E.; Le Blanc, K.; Macchiarini, P.; Jungebluth, P.; Wood, M. J.; Andaloussi, S. E. Extracellular vesicle in vivo biodistribution is determined by cell source, route of administration and targeting. *J. Extracell Vesicles* **2015**, *4*, 26316.

77. Ohno, S.; Takanashi, M.; Sudo, K.; Ueda, S.; Ishikawa, A.; Matsuyama, N.; Fujita, K.; Mizutani, T.; Ohgi, T.; Ochiya, T.; Gotoh, N.; Kuroda, M. Systemically injected exosomes targeted to EGFR deliver antitumor microRNA to breast cancer cells. *Mol. Ther.* **2013**, *21*, 185-191.

78. Bergknut, N.; Rutges, J. P.; Kranenburg, H. J.; Smolders, L. A.; Hagman, R.; Smidt, H. J.; Lagerstedt, A. S.; Penning, L. C.; Voorhout, G.; Hazewinkel, H. A.; Grinwis, G. C.; Creemers, L. B.; Meij, B. P.; Dhert, W. J. The dog as an animal model

6

for intervertebral disc degeneration? *Spine (Phila Pa. 1976)* **2012***, 37*, 351-358.

79. Hurtig, M. B.; Buschmann, M. D.; Fortier, L. A.; Hoemann, C. D.; Hunziker, E. B.; Jurvelin, J. S.; Mainil-Varlet, P.; McIlwraith, C. W.; Sah, R. L.; Whiteside, R. A. Preclinical studies for cartilage repair: recommendations from the International Cartilage Repair Society. *Cartilage* **2011***, 2*, 137-152.

80. Malda, J.; Benders, K. E.; Klein, T. J.; de Grauw, J. C.; Kik, M. J.; Hutmacher, D. W.; Saris, D. B.; van Weeren, P. R.; Dhert, W. J. Comparative study of depth-dependent characteristics of equine and human osteochondral tissue from the medial and lateral femoral condyles. *Osteoarthritis Cartilage* **2012***, 20*, 1147-1151.

81. Lotvall, J.; Hill, A. F.; Hochberg, F.; Buzas, E. I.; Di Vizio, D.; Gardiner, C.; Gho, Y. S.; Kurochkin, I. V.; Mathivanan, S.; Quesenberry, P.; Sahoo, S.; Tahara, H.; Wauben, M. H.; Witwer, K. W.; Thery, C. Minimal experimental requirements for definition of extracellular vesicles and their functions: a position statement from the International Society for Extracellular Vesicles. *J. Extracell Vesicles* **2014***, 3*, 26913.

82. Gyorgy, B.; Modos, K.; Pallinger, E.; Paloczi, K.; Pasztoi, M.; Misjak, P.; Deli, M. A.; Sipos, A.; Szalai, A.; Voszka, I.; Polgar, A.; Toth, K.; Csete, M.; Nagy, G.; Gay, S.; Falus, A.; Kittel, A.; Buzas, E. I. Detection and isolation of cell-derived microparticles are compromised by protein complexes resulting from shared biophysical parameters. *Blood* **2011***, 117*, e39-48.

6

7

General Discussion

This thesis addresses a potentially highly relevant, though as yet relatively untouched, avenue in extracellular vesicle (EV) research: the (possible) involvement of EVs in joint biology and joint disease.

Joint diseases, with rheumatoid arthritis (RA) and osteoarthritis (OA) as most prevalent ones, represent a significant burden to human society, both in terms of loss of quality of life and as a significant part of total healthcare costs. Current demographic and societal developments (*i.e.* the rapid increase of life expectancy and the decreasing acceptance of disability) aggravate the problem quickly [1]. In veterinary medicine, a similar situation exists, especially in horses, a species kept for its locomotor performance and in which joint disorders are, depending on equestrian discipline, invariably ranking first or second (after tendon injuries) as cause of lameness, and thus of disability to perform. In a survey of US horse owners in 1998, it was estimated that 60% of all lameness was related to OA and approximately $145 million was spent on veterinary bills relating to the problem [2]. Given the increasing burden human and equine joint diseases have on our society, new insights in joint biology and disease in both species are more needed than ever.

Although multiple previous studies had already postulated a role for synovial fluid (SF) derived EVs in human joint inflammation, many of those early publications in this field did not take into account the strict conditions and precautions in sample preparation and vesicle isolation of which it has become clear that they imperatively need to be respected to guarantee the generation of pure samples, and hence to avoid drawing of erroneous conclusions. We here have taken the research in this field one step further by first focusing on the development and optimisation of sample processing methodology, which was then applied to study the basic EV parameters of equine SF samples representing healthy joint homeostasis, joint inflammation and joint development.

EV RESEARCH: BASIC LESSONS

The key requirement for robust EV research is standardisation of sample processing and EV isolation procedures. This is now fully recognised within the scientific community and the area has seen an enormous improvement during the last 5 years, mainly as a result of initiatives from the International Society for Extracellular Vesicles (ISEV; https://www.isev.org/). Not only have EV analysis techniques been optimised and described in detail [3-5], also general experimental guidelines and requirements have been published for robust EV research [6,7]. Furthermore, open online training courses are now organised for young EV researchers [8] and recently the online

7

crowdsourcing knowledgebase "EV-Track" (http://evtrack.org/index.php) has been launched that aims at centralising knowledge on EV biology and methodology [9]. This online platform integrates information about important requirements for EV research, such as isolation and purification methods and particle analysis methods, all done in order to boost the quality and reproducibility of future EV experiments and publications. By uploading protocol details of individual EV experiments to the platform, researchers will be given an "EV-metric score", which reflects the quality and quantity of used techniques. Conclusions drawn from publications with low EV-metric scores will ultimately be perceived with skepticism by the EV community. There is little doubt that such initiatives will prove to be of utmost importance in the upcoming decade in which it is expected that a multitude of fundamental and translational research groups in the field of medical biology will focus on EVs.

Isolation of EVs

Recent publications addressing the fine-tuning of EV isolation from a variety of biological fluids, each having its own typical composition, show the difficulties researchers encounter in establishing efficient isolation methods of EVs from these fluids [10-15]. It has become clear that specific protocols need to be developed for each individual fluid.

Synovial fluid is a particularly complicated medium to isolate EVs from, mainly because of its high viscosity, which is caused by the elevated concentration of hyaluronic acid [16,17]. After testing multiple strategies, digestion of SF with hyaluronidase prior to ultra-centrifugation and the use of a final ultracentrifugation step of $> 100,000g$ were the major protocol amendments that finally contributed to a high EV yield without causing significant harm to the vesicles (as evaluated by morphology and functionality testing). These were the first steps to come to a standardised protocol for EV research in SF (Chapter 2).

Of note, standardised and careful collection of fluids prior to EV isolation is indispensable for preventing contamination of samples with non-relevant EVs. Contamination of SF with peripheral blood during arthrocentesis, for example, causes major errors in EV measurements. Due to the high EV counts in blood [18], even a small contamination can cause major influx of blood-derived EVs into the SF sample and, hence, significantly mask the local EVs of interest. This applies mainly to healthy SF samples that contain relatively low concentrations of EVs. In SF samples from inflamed joints, the situation is different. In those conditions, an increase in blood-derived EVs can be expected in SF due to the increased permeability of the vasculature in the synovial membrane, which is a hallmark of joint inflammation. In this case the influx of blood-derived EVs in the joint can contribute to EV-driven

pathological processes in the joint and should, therefore, be considered part of the ongoing pathological process and not as sample contamination. For the research described in this thesis, careful inspection of samples was performed, taking into account disease condition and research questions.

Characterisation, quantification and visualisation of EVs

Although the finding of cell-specific markers on EVs can be an indication for the cell type of origin, *e.g.* Annexin-A1 positive EVs in inflammatory joints are most likely derived from neutrophils [19], this is not a clear-cut method for typing of EVs. Extracellular vesicles can travel over long distances in the body and can cross most endothelial and epithelial barriers, *e.g.* the blood-brain-barrier and the synovial membrane [20], and, therefore, the pool of EVs isolated from body fluids most likely has multiple origins. This challenges the development of a marker profile to identify EVs, especially since it is not yet known which cell-derived markers are transferred onto EVs.

The more general EV markers, such as the tetraspanin CD9, are regularly detected on EVs of different origins, but a more comprehensive range of markers is needed to fully prove that the particles studied are truly EVs and are derived from a specific cell type. In addition, more knowledge is needed about various components of EVs, especially of the membrane of EVs, as this can provide important information about the route of origin (endosomal or cell-membrane derived), possible interactions, working mechanism and functionality of EVs. In this thesis, we have used a lipidomics approach to get more insight into the lipid composition of SF-derived EVs (Chapter 4). Lipidomics is a highly valuable tool for EV research as it allows for detailed analysis of EV membranes. Moreover, the technique is not dependent on species-specific technical challenges. At the moment, the application of lipidomics in the EV field is gaining ground [21], as is underscored by a recent review paper about this topic [22].

Another technical challenge in EV research is the reliable detection of EVs based on labelling with (fluorescent) markers. The generic fluorescent dye PKH67 has been widely used to visualise EVs and to detect EVs by flow cytometry. However, since this dye not only intercalates in the lipid membrane of EVs, but in all lipid membranes, care should be taken with its use in cell culture and *in vivo* experiments. An experiment performed in our lab, in which PKH67-labelled healthy equine SF-derived EVs were incubated with human chondrocytes, clearly illustrates the problem of non-specific staining of PKH67 in cell culture experiments (Figure 1). This may easily cause mis-interpretation of results. At the moment, better labelling procedures with more specific dyes are being developed which will in a near future ultimately improve the way in which we can analyse EVs. In addition, the use of adequate control conditions is
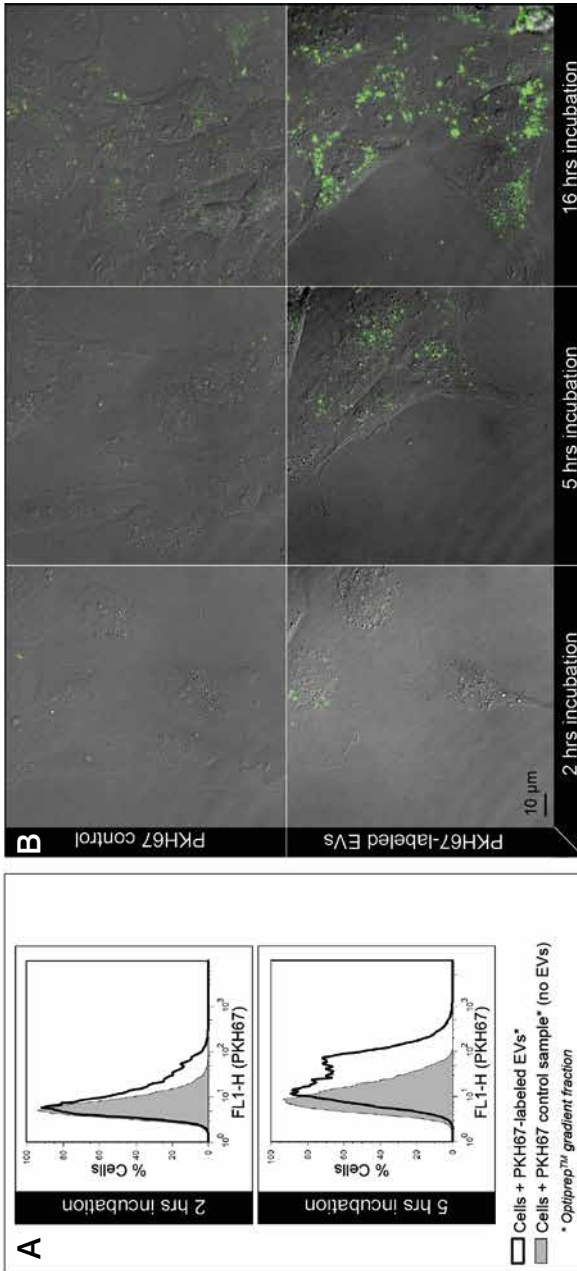
7

Figure 1 Equine SF-derived EVs were isolated by ultracentrifugation, labelled with PKH67 and floated in iodixanol density gradients identical to the methods described in Chapter 2. Labelled 100,000g EVs and corresponding iodixanol control samples (containing PKH67, but no EVs) were diluted 1:4 in cell culture medium and added to C20A4 human chondrocytes in monolayer culture for 16 hours. **A)** Flow cytometry of cells after 2 or 5 hours incubation with EVs showed an increased uptake of fluorescent signal over time compared to the PKH67 control condition. **B)** Specific interaction of EVs with cells was shown by live imaging. Already after 10 minutes incubation, fluorescent dots appeared at the cell membrane and later in the cytoplasm. The fluorescent signal, possibly representing EVs, increased in intensity during 16 hours incubation. PKH67-transfer into cells was clearly more efficient in presence of EVs, but some non-specific staining of cells occurred in the control samples. Similar results were obtained for HFLS 408-05a human fibroblast-like synoviocytes (results not shown).

indispensable and must be given high priority when designing EV-labelling experiments. Finally, electron microscopy images, preferably showing more than one single EV, are now also regarded as a prerequisite for validation of results in EV research [7].

Functional testing of EVs

The unravelling of the functions of EVs in biological processes is the ultimate goal in EV research. Extracellular vesicles collected from biological fluids or *in vitro* cell culture can be subjected to functional testing in *in vitro* or *in vivo* systems in which EV-driven regulation of biological processes can be measured. These functional tests, however, are in a practical sense not straightforward and evoke several technical issues, which urgently need to be addressed in future investigations.

First, sterile purification of EVs is required prior to cell-EV co-culture or *in vivo* EV injection. Given the absence of EV purification procedures in many published studies, the results of those investigations should be classified as questionable at best. The effect that some isolation and purification techniques may have on EVs, potentially affecting their functionality, is a severely complicating factor. A well-known example is the detrimental effect of sucrose from density gradients on the stability of EVs and on the viability of cells in culture. This means that EV purification strategies and methods for further functional testing must be designed with utmost care and need tailoring for each individual experiment.

Another problematic issue in functional testing is the lack of knowledge about which concentrations of EVs should be considered biologically relevant. Quantitative EV analysis (*e.g.* high-resolution flow cytometry) in healthy and diseased biological fluids can give indications of EV production rates in certain tissues or organs, in physiological and pathological conditions, but variable EV isolation yields and unreliable purification outcomes complicate the calculation of EV concentration in samples. A consequence is that the translation of *in vivo* relevant EV concentrations to *in vitro* culture systems should be considered far from reliable at the moment. This urges a highly conservative approach when drawing conclusions from this type of experiments that should go beyond the usual caution that is always needed when interpreting the *in vivo* consequences of *in vitro* experiments.

For comparative studies in which the biological functions of EVs originating from healthy and diseased conditions are evaluated, basically two strategies can be followed: 1) using identical starting volumes of healthy and diseased biological fluids prior to EV isolation, after which EVs or EV-pellets are subsequently suspended in identical volumes of medium or buffer, or 2) after EV isolation from healthy and

7

diseased biological fluids (not necessarily identical volumes), using identical EV concentrations in the final test sample. The latter option requires adequate calculation of concentrations in EV preparation and is limited by the relatively low EV numbers in healthy samples. This approach also does not take into account the possibility that sheer numbers of EVs may make the difference between healthy and diseased conditions, rather than changes in functionality of individual EVs or relative changes in concentrations. In the functional studies in this thesis, we therefore have chosen the first approach in which starting volumes of SF were kept the same, resulting in concentration differences in healthy and diseased samples for EV-cell co-culture. We argued that this approach was most likely to reflect the real-life situation and thus was the best manner to reproduce *in vitro* the EV-effect on cartilage tissue during joint inflammation (high EV counts in SF) or healthy joint homeostasis (low EV counts in SF).

Finally, the use of species other than human to investigate human EV-driven disease processes might be a critical pitfall in EV research. Not only are EV composition and function most likely species-specific, they might also be under the control of species-specific factors, such as enzymes and signalling proteins. The experiment illustrated by Figure 1 revealed that cross-species uptake of EVs is possible *in vitro*, suggesting that EV uptake in cells is a preserved process, giving options for pharmaceutical use of natural EVs from several sources. However, given the species-specific cargo that EVs most likely carry (*e.g.* DNA, miRNA), it is not recommended to perform cross-species experiments for functional testing. If such testing is undertaken, then at least results should be interpreted very cautiously.

In Chapter 3 of this thesis, a functional *in vitro* experiment was designed in which the effect of equine "EV-pellets" (all pelleted material including EVs) on equine primary chondrocytes could be measured. Although proof-of-principle experiments like this are very convenient and efficient to get a first clue about the possible functions of the EVs involved without experiencing the detrimental effects of purification methods, these studies must be repeated with purified EV samples to verify the results and to draw sound conclusions about the actual function of these EVs.

EVs IN JOINT HOMEOSTASIS AND DISEASE

The studies in this thesis presented clear indications for a role for EVs in acute synovitis (Chapter 3), given the close association of EV numbers with the state of inflammation. By using a controlled lipopolysaccharide (LPS)-induced synovitis model, EV dynamics could be studied over time, providing a comprehensive view of

the basic characteristics of the different EV populations in a joint during the course of acute inflammation. This is important and much needed fundamental information, complementary to results of other groups that were based on the analysis of EVs in SF samples from human patients with joint disease [19,23-25]. The most interesting finding was the presence of CD44+ EVs that were shown to be potentially involved in the downregulation of pro-inflammatory mediators, hence suggesting an inflammation resolving effect. This finding, if confirmed to be not species-specific, can be of interest for human research as well.

In addition to the results presented in Chapter 3, an identical experimental setup was used for a preliminary study with SF samples from animals that had received a treatment with meloxicam (a selective Cyclooxygenase (COX)-2 inhibiting non-steroidal anti-inflammatory drug (NSAID)) prior to LPS-injection (results not shown). Interestingly, at 8 hours post LPS-injection, we found a 3-fold increase of CD44+ EVs in SF compared to animals that received placebo treatment (the numbers at 24h post LPS-injection were the same for meloxicam and placebo condition), indicating that the rise of CD44+ EVs occurs at an earlier time point in the joint as a result of NSAID treatment. Although this experiment was only performed with samples from a limited number of animals, these preliminary results suggest that NSAIDs may not directly evoke functional EV population changes, but may cause a change in the dynamics of EV production, EV influx and EV efflux from the joint. Although very speculative, this would be in line with the hypothesis that CD44+ EVs act as anti-inflammatory mediators and are part of the resolving phase of the inflammation, and their net duration of presence in the joint might be stimulated by NSAIDs.

In Chapter 4 we were able to identify so far unknown short-chain carboxylic acid modifications of phosphatidylserine, enriched in 200K EVs that were isolated from SF collected from inflamed joints. Apart from the discovery of these new phospholipid subclasses, that had not been described in living beings before, and are therefore of general biological interest, the observation increases our fundamental knowledge about EVs and can possibly be a first step in the better understanding of the mechanistic aspects of EV functionality in inflamed joints. It is a good illustration of the added value of the use of a lipidomics approach in the study of EVs.

7

One of the premises of this thesis was that EVs not only execute roles during episodes of disease, but also take part in the regulation of healthy joint homeostasis. Along this line of thought, we hypothesised a possible role for EVs in SF in the control of the tightly orchestrated processes in the developing joint. In young individuals, joints are characterised by high metabolic activity of chondrocytes and other cell types present in the tissue that make up the articulation. This is necessary to enable growth and

development and explains why there is still capacity of cartilage lesions to repair spontaneously, as is frequently seen in the case of osteochondrotic lesions in foals during the early juvenile period [26]. This is in sharp contrast to the situation in mature joints where collagen turnover has been shown to be virtually nil [27]. Given the known regulating role of many EVs, it lies therefore at hand to suppose that there may be differences in the EV populations of juvenile and adult joints. The experiments performed for this thesis using SF samples from juvenile and adult equine joints could not demonstrate such differences in basic EV parameters (Chapter 5). However, there is still a possibility that functional differences exist, which were not measured in our studies. Though still speculative at this moment, it can be hypothesised that SF-derived EVs in the growing joint are potentially loaded with so far unknown protective and/or regenerative factors (possibly even derived from local mesenchymal stem cells (MSCs)) that might explain the natural healing capacity of immature articular tissues. This is mere conjecture, however, and the better repair capacity of immature cartilage may be explained as well by the higher metabolic activity of the juvenile chondrocytes and/or to the less compact extracellular matrix due to less dense cross-linking compared to older cartilage [28]. For this, no specific juvenile EV function would be necessary. Further studies are warranted, as no conclusive data exist yet, whilst the area remains a very interesting research topic for future studies.

TRANSLATION TO THE CLINIC

For setting up translational studies focusing at EVs in joint disorders, the choice of the animal model is critical. The overall role and functionality of EVs might be conserved in the system biology of most mammals or even vertebrates [29], but specific EV functions can still be dependent on species-specific diets and other environmental factors [30]. Larger animals are more convenient than the classic laboratory species with regard to sample size and easiness of repeated sampling, but these larger animal species come with the disadvantage that many research tools, especially antibodies and genomic sequences, are not (yet) available. This was also a limitation in our equine studies and it was for this reason that we were not able to verify most of the standard EV markers that are used in human studies. Nevertheless, we were able to show that equine SF-derived EVs from joints with acute inflammation have a different EV signature and may exhibit specific functional effects on equine primary chondrocytes.

The use of animal models is under debate and efforts are made to develop alternatives by using advanced (bio)technology and *in silico* modelling. Currently, there is consensus, however, that animal models are still necessary for various purposes.

The horse is one of the optimal models for orthopaedic research, among other reasons, because of the strong similarities between equine and human joints with respect to cartilage thickness and cellular and biochemical composition of the cartilage extracellular matrix [31]. For this reason, and because of the fact that the horse is a target species in itself with a clear clinical need for improved care for joint disorders, we opted for using this species and therefore, our results can, with certain caution, be extrapolated to the human situation. Possibly in the near future, the horse can also serve as animal model for testing EV-mediated treatment of joint disease or for the assessment of repair of cartilage and bone lesions with EV-loaded scaffolds, for which possibilities are currently being explored [32-35] (Chapter 6). In addition to natural EVs derived from biological fluids, or synthetically prepared EVs loaded with active molecules of interest, now also extracellular matrix derived EVs are considered as supplements for bioscaffolds [36].

FINAL CONCLUSIONS

Many of the early investigations into the possible role of EVs in joint disease have been very helpful in providing explorative and preliminary *in vivo* information, but in most of these publications details are lacking about the technical requirements deemed necessary to day in EV research to make unequivocal conclusions. By using robust analysis techniques, made possible by a well-developed research infrastructure for EV-related experiments and the existence of a productive interdisciplinary network of dedicated scientists, the research presented in this thesis has provided fundamental knowledge on the dynamics and possible role of EVs in joints, both in physiological and in selected pathological conditions. Furthermore, the work offers some first ideas about possible disease-related mechanisms. Taken together, this thesis provides a starting point for further EV research in the fields of joint homeostasis in health and disease, including regenerative medicine of the joint.

7

REFERENCES

1. Lunenfeld, B.; Stratton, P. The clinical consequences of an ageing world and preventive strategies. *Best Pract. Res. Clin. Obstet. Gynaecol.* **2013***, 27*, 643-659.

2. Anonymous. Lameness and Laminitis in US horses. *National animal health monitoring systems 2000, veterinary services – centers for epidemiology in animal health: Fort Collins, CO.* **2000***.

3. Nolte-'t Hoen, E. N.; van der Vlist, E. J.; Aalberts, M.; Mertens, H. C.; Bosch, B. J.; Bartelink, W.; Mastrobattista, E.; van Gaal, E. V.; Stoorvogel, W.; Arkesteijn, G. J.; Wauben, M. H. Quantitative and qualitative flow cytometric analysis of nanosized cell-derived membrane vesicles. *Nanomedicine* **2012***, 8*, 712-720.

4. Mateescu, B.; Kowal, E. J.; van Balkom, B. W.; Bartel, S.; Bhattacharyya, S. N.; Buzas, E. I.; Buck, A. H.; de Candia, P.; Chow, F. W.; Das, S.; Driedonks, T. A.; Fernandez-Messina, L.; Haderk, F.; Hill, A. F.; Jones, J. C.; Van Keuren-Jensen, K. R.; Lai, C. P.; Lasser, C.; Liegro, I. D.; Lunavat, T. R.; Lorenowicz, M. J.; Maas, S. L.; Mager, I.; Mittelbrunn, M.; Momma, S.; Mukherjee, K.; Nawaz, M.; Pegtel, D. M.; Pfaffl, M. W.; Schiffelers, R. M.; Tahara, H.; Thery, C.; Tosar, J. P.; Wauben, M. H.; Witwer, K. W.; Nolte-'t Hoen, E. N. Obstacles and opportunities in the functional analysis of extracellular vesicle RNA - an ISEV position paper. *J. Extracell Vesicles* **2017***, 6*, 1286095.

5. van der Vlist, E. J.; Nolte-'t Hoen, E. N.; Stoorvogel, W.; Arkesteijn, G. J.; Wauben, M. H. Fluorescent labeling of nano-sized vesicles released by cells and subsequent quantitative and qualitative analysis by high-resolution flow cytometry. *Nat. Protoc.* **2012***, 7*, 1311-1326.

6. Witwer, K. W.; Buzas, E. I.; Bemis, L. T.; Bora, A.; Lasser, C.; Lotvall, J.; Nolte-'t Hoen, E. N.; Piper, M. G.; Sivaraman, S.; Skog, J.; Thery, C.; Wauben, M. H.; Hochberg, F. Standardization of sample collection, isolation and analysis methods in extracellular vesicle research. *J. Extracell Vesicles* **2013***, 2*, 10.3402/jev.v2i0.20360. eCollection 2013.

7. Lotvall, J.; Hill, A. F.; Hochberg, F.; Buzas, E. I.; Di Vizio, D.; Gardiner, C.; Gho, Y. S.; Kurochkin, I. V.; Mathivanan, S.; Quesenberry, P.; Sahoo, S.; Tahara, H.; Wauben, M. H.; Witwer, K. W.; Thery, C. Minimal experimental requirements for definition of extracellular vesicles and their functions: a position statement from the International Society for Extracellular Vesicles. *J. Extracell Vesicles* **2014***, 3*, 26913.

8. Lasser, C.; Thery, C.; Buzas, E. I.; Mathivanan, S.; Zhao, W.; Gho, Y. S.; Lotvall, J. The International Society for Extracellular Vesicles launches the first massive open online course on extracellular vesicles. *J. Extracell Vesicles* **2016***, 5*, 34299.

9. EV-TRACK Consortium; Van Deun, J.; Mestdagh, P.; Agostinis, P.; Akay, O.; Anand, S.; Anckaert, J.; Martinez, Z. A.; Baetens, T.; Beghein, E.; Bertier, L.; Berx, G.; Boere, J.; Boukouris, S.; Bremer, M.; Buschmann, D.; Byrd, J. B.; Casert, C.; Cheng, L.; Cmoch, A.; Daveloose, D.; De Smedt, E.; Demirsoy, S.; Depoorter, V.; Dhondt, B.; Driedonks, T. A.; Dudek, A.; Elsharawy, A.; Floris, I.; Foers, A. D.; Gartner, K.; Garg, A. D.; Geeurickx, E.; Gettemans, J.; Ghazavi, F.; Giebel, B.; Kormelink, T. G.; Hancock, G.; Helsmoortel, H.; Hill, A. F.; Hyenne, V.; Kalra, H.; Kim, D.; Kowal, J.; Kraemer, S.; Leidinger, P.; Leonelli, C.; Liang, Y.; Lippens, L.; Liu, S.; Lo Cicero, A.; Martin, S.; Mathivanan, S.; Mathiyalagan, P.; Matusek, T.; Milani, G.; Monguio-Tortajada, M.; Mus, L. M.; Muth, D. C.; Nemeth, A.; Nolte-'t Hoen, E. N.; O'Driscoll, L.; Palmulli, R.; Pfaffl, M. W.; Primdal-Bengtson, B.; Romano, E.; Rousseau, Q.; Sahoo, S.; Sampaio, N.; Samuel, M.; Scicluna, B.; Soen, B.; Steels, A.; Swinnen, J. V.; Takatalo, M.; Thaminy, S.; Thery, C.; Tulkens, J.; Van Audenhove, I.; van der Grein, S.; Van Goethem, A.; van Herwijnen, M. J.; Van Niel, G.; Van Roy, N.; Van Vliet, A. R.; Vandamme, N.; Vanhauwaert, S.; Vergauwen, G.; Verweij, F.; Wallaert, A.; Wauben, M.; Witwer, K. W.; Zonneveld, M. I.; De Wever, O.; Vandesompele, J.; Hendrix, A. EV-TRACK: transparent reporting and centralizing knowledge in extracellular vesicle research. *Nat. Methods* **2017***, 14*, 228-232.

10. Foster, B. P.; Balassa, T.; Benen, T. D.; Dominovic, M.; Elmadjian, G. K.; Florova, V.; Fransolet, M. D.; Kestlerova, A.; Kmiecik, G.; Kostadinova, I. A.; Kyvelidou, C.; Meggyes, M.; Mincheva, M. N.; Moro, L.; Pastuschek, J.; Spoldi, V.; Wandernoth, P.; Weber, M.; Toth, B.; Markert, U. R. Extracellular vesicles in blood, milk and body fluids of the female and male urogenital tract and with special regard to reproduction. *Crit. Rev. Clin. Lab. Sci.* **2016***, 53*, 379-395.

11. Baek, R.; Sondergaard, E. K.; Varming, K.; Jorgensen, M. M. The impact of various preanalytical treatments on the phenotype of small extracellular vesicles in blood analyzed by protein microarray. *J. Immunol. Methods* **2016***, 438*, 11-20.

12. Yuana, Y.; Bertina, R. M.; Osanto, S. Pre-analytical and analytical issues in the analysis of blood microparticles. *Thromb. Haemost.* **2011***, 105*, 396-408.

13. Iwai, K.; Minamisawa, T.; Suga, K.; Yajima, Y.; Shiba, K. Isolation of human salivary extracellular vesicles by iodixanol density gradient ultracentrifugation and their characterizations. *J. Extracell Vesicles* **2016***, 5*, 30829.

14. Zonneveld, M. I.; Brisson, A. R.; van Herwijnen, M. J.; Tan, S.; van de Lest, C. H.; Redegeld, F. A.; Garssen, J.; Wauben, M. H.; Nolte-'t Hoen, E. N. Recovery of extracellular vesicles from human breast milk is influenced by sample collection and vesicle isolation procedures. *J. Extracell Vesicles* **2014***, 3*, 10.3402/jev.v3.24215. eCollection 2014.

15. Gyorgy, B.; Paloczi, K.; Kovacs, A.; Barabas, E.; Beko, G.; Varnai, K.; Pallinger, E.; Szabo-Taylor, K.; Szabo, T. G.; Kiss, A. A.; Falus, A.; Buzas, E. I. Improved circulating microparticle analysis in acid-citrate dextrose (ACD) anticoagulant tube. *Thromb. Res.* **2014***, 133*, 285-292.

16. Hui, A. Y.; McCarty, W. J.; Masuda, K.; Firestein, G. S.; Sah, R. L. A systems biology approach to synovial joint lubrication in health, injury, and disease. *Wiley Interdiscip. Rev. Syst. Biol. Med.* **2012***, 4*, 15-37.

17. Dahl, L. B.; Dahl, I. M.; Engstrom-Laurent, A.; Granath, K. Concentration and molecular weight of sodium hyaluronate in synovial fluid from patients with rheumatoid arthritis and other arthropathies. *Ann. Rheum. Dis.* **1985***, 44*, 817-822.

18. Arraud, N.; Linares, R.; Tan, S.; Gounou, C.; Pasquet, J. M.; Mornet, S.; Brisson, A. R. Extracellular vesicles from blood plasma: determination of their morphology, size, phenotype and concentration. *J. Thromb. Haemost.* **2014***, 12*, 614-627.

19. Headland, S. E.; Jones, H. R.; Norling, L. V.; Kim, A.; Souza, P. R.; Corsiero, E.; Gil, C. D.; Nerviani, A.; Dell'Accio, F.; Pitzalis, C.; Oliani, S. M.; Jan, L. Y.; Perretti, M. Neutrophil-derived microvesicles enter cartilage and protect the joint in inflammatory arthritis. *Sci. Transl. Med.* **2015***, 7*, 315ra190.

20. Alvarez-Erviti, L.; Seow, Y.; Yin, H.; Betts, C.; Lakhal, S.; Wood, M. J. Delivery of siRNA to the mouse brain by systemic injection of targeted exosomes. *Nat. Biotechnol.* **2011***, 29*, 341-345.

21. Haraszti, R. A.; Didiot, M. C.; Sapp, E.; Leszyk, J.; Shaffer, S. A.; Rockwell, H. E.; Gao, F.; Narain, N. R.; DiFiglia, M.; Kiebish, M. A.; Aronin, N.; Khvorova, A. High-resolution proteomic and lipidomic analysis of exosomes and microvesicles from different cell sources. *J. Extracell Vesicles* **2016***, 5*, 32570.

22. Skotland, T.; Sandvig, K.; Llorente, A. Lipids in exosomes: Current knowledge and the way forward. *Prog. Lipid Res.* **2017***, 66*, 30-41.

23. Berckmans, R. J.; Nieuwland, R.; Kraan, M. C.; Schaap, M. C.; Pots, D.; Smeets, T. J.; Sturk, A.; Tak, P. P. Synovial microparticles from arthritic patients modulate chemokine and cytokine release by synoviocytes. *Arthritis Res. Ther.* **2005***, 7*, R536-44.

24. Fourcade, O.; Simon, M. F.; Viode, C.; Rugani, N.; Leballe, F.; Ragab, A.; Fournie, B.; Sarda, L.; Chap, H. Secretory phospholipase A2 generates the novel lipid mediator lysophosphatidic acid in membrane microvesicles shed from activated cells. *Cell* **1995***, 80*, 919-927.

25. Gyorgy, B.; Szabo, T.,G.; Turiak, L.; Wright, M.; Herczeg, P.; Ledeczi, Z.; Kittel, A.; Polgar, A.; Toth, K.; Derfalvi, B.; Zelenak, G.; Borocz, I.; Carr, B.; Nagy, G.; Vekey, K.; Gay, S.; Falus, A.; Buzas, E.,I. Improved flow cytometric assessment reveals distinct microvesicle (cell-derived microparticle) signatures in joint diseases. *PloS one* **2012***, 7*, e49726.

26. Dik, K. J.; Enzerink, E.; van Weeren, P. R. Radiographic development of osteochondral abnormalities, in the hock and stifle of Dutch Warmblood foals, from age 1 to 11 months. *Equine Vet. J. Suppl.* **1999***, (31)*, 9-15.

27. Heinemeier, K. M.; Schjerling, P.; Heinemeier, J.; Moller, M. B.; Krogsgaard, M. R.; Grum-Schwensen, T.; Petersen, M. M.; Kjaer, M. Radiocarbon dating reveals minimal collagen turnover in both healthy and osteoarthritic human cartilage. *Sci. Transl. Med.* **2016***, 8*, 346ra90.

28. Brama, P. A.; TeKoppele, J. M.; Bank, R. A.; Barneveld, A.; van Weeren, P. R. Development of biochemical heterogeneity of articular cartilage: influences of age and exercise. *Equine Vet. J.* **2002***, 34*, 265-269.

29. Vyas, N.; Walvekar, A.; Tate, D.; Lakshmanan, V.; Bansal, D.; Lo Cicero, A.; Raposo, G.; Palakodeti, D.; Dhawan, J. Vertebrate Hedgehog is secreted on two types of extracellular vesicles with different signaling properties. *Sci. Rep.* **2014***, 4*, 7357.

30. Neven, K. Y.; Nawrot, T. S.; Bollati, V. Extracellular Vesicles: How the External and Internal Environment Can Shape Cell-To-Cell Communication. *Curr. Environ. Health. Rep.* **2017***, 4*, 30-37.

31. Malda, J.; Benders, K. E.; Klein, T. J.; de Grauw, J. C.; Kik, M. J.; Hutmacher, D. W.; Saris, D. B.; van Weeren, P. R.; Dhert, W. J. Comparative study of depth-dependent characteristics of equine and human osteochondral tissue from the medial and lateral femoral condyles. *Osteoarthritis Cartilage* **2012***, 20*, 1147-1151.

32. Vonk, L. A.; van Dooremalen, S.; Coffer, P. J.; Saris, D. B.; Lorenowicz, M. J. MSC-derived extra-

7

cellular vesicles stimulate cartilage regeneration and modulate inflammatory responses. Paper presented at the 13th world congress of the International Cartilage Repair Society, Sept 26, 2016, Sorrento, Italy. **2016**.

33. Zhang, J.; Liu, X.; Li, H.; Chen, C.; Hu, B.; Niu, X.; Li, Q.; Zhao, B.; Xie, Z.; Wang, Y. Exosomes/ tricalcium phosphate combination scaffolds can enhance bone regeneration by activating the PI3K/ Akt signaling pathway. *Stem Cell. Res. Ther.* **2016**, *7*, 136-016-0391-3.

34. Zhang, S.; Chu, W. C.; Lai, R. C.; Lim, S. K.; Hui, J. H.; Toh, W. S. Exosomes derived from human embryonic mesenchymal stem cells promote osteochondral regeneration. *Osteoarthritis Cartilage* **2016**, *24*, 2135-2140.

35. Toh, W. S.; Lai, R. C.; Hui, J. H.; Lim, S. K. MSC exosome as a cell-free MSC therapy for cartilage regeneration: Implications for osteoarthritis treatment. *Semin. Cell Dev. Biol.* **2016**.

36. Huleihel, L.; Hussey, G. S.; Naranjo, J. D.; Zhang, L.; Dziki, J. L.; Turner, N. J.; Stolz, D. B.; Badylak, S. F. Matrix-bound nanovesicles within ECM bioscaffolds. *Sci. Adv.* **2016**, *2*, e1600502.

7

ADDENDUM

Nederlandse Samenvatting
About the author
List of publications
PhD Portfolio
Dankwoord | Acknowledgements

Nederlandse Samenvatting

MEMBRAANBLAASJES IN GEWRICHTSVLOEISTOF

Dynamiek tijdens artritis en gewrichtsontwikkeling en de mogelijke rol bij regeneratie van gewrichten en herstel van gewrichtshomeostase

De sterk stijgende incidentie van gewrichtsaandoeningen is op zijn minst zorgwekkend te noemen en vormt een snel in belangrijkheid toenemend maatschappelijk probleem. Naast de ernstige lichamelijke klachten en bewegingsbeperking die dit voor sommige patiënten met zich meebrengt, is het ook een zware praktische en financiële last voor onze gezondheidszorg. Niet alleen in de Westerse maatschappij waar de stijgende levensverwachting en de toename aan obesitas gewrichtsaandoeningen in de hand werkt, maar ook in minder ontwikkelde landen, waar sterftecijfers dalen, maar waar mensen in erbarmelijke arbeidsomstandigheden werken, is de verwachting dat de incidentie van gewrichtsproblemen in de komende decennia alleen maar zal toenemen. Gewrichtsklachten kunnen tijdelijk of blijvend zijn en ontstaan door blessures, overbelasting, trauma, acute of chronische ontsteking, anatomische afwijkingen of auto-immuunziekten. Dit breed spectrum aan oorzaken en bijbehorende klachten maakt afdoende behandeling erg complex en vaak is dat zelfs niet mogelijk. Voor de meest voorkomende gewrichtsziekten, zoals osteoartritis (OA) en reumatoïde artritis (RA), kunnen op dit moment klachten alleen verlicht worden met medicatie, maar een adequate oplossing om de onderliggende oorzaak aan te pakken is niet voor handen. Onderzoek naar het ontstaan en het verloop van gewrichtsziekten is daarom noodzakelijk om in de toekomst betere therapieën te kunnen ontwikkelen. Daarnaast is het belangrijk om ziekteprocessen vroegtijdig op te sporen door middel van zogeheten 'biomarkers' om preventieve behandeling mogelijk te maken.

Ook dieren, met name paarden, lijden aan vergelijkbare aandoeningen. De skelet-en spieropbouw bij paarden is op weefselniveau in hoge mate vergelijkbaar met die bij de mens en net als bij mensen komen acute gewrichtsontsteking en OA vaak voor, wat kan leiden tot ernstige schade aan kraakbeen en bot, uiteindelijk gevolgd door kreupelheid. Het paardengewricht is daarom een uitstekend model voor onderzoek naar humane gewrichtsaandoeningen met als bijkomend groot voordeel dat onder-zoeksresultaten ook gebruikt kunnen worden voor nieuwe ontwikkelingen in de veterinaire kliniek. Het paard fungeert in dit type onderzoek letterlijk zelf als patiënt en als diermodel voor de menselijke patiënt.

Ontsteking in het gewricht (artritis), met name de chronische vorm, is in vele gevallen de aanzet tot een langdurig lijden met als uitkomst vaak een dysfunctioneel gewricht. De moleculaire achtergronden van de oorzaken en het specifieke verloop van ge-wrichtsontsteking zijn nog niet volledig bekend. Wel weten we dat er in het gewricht

een bepaalde homeostase heerst waarbij er in gezonde toestand een balans is tussen weefselopbouw (anabolisme) en –afbraak (katabolisme). De vloeistof in de holte van het gewricht speelt hierin een cruciale rol door het faciliteren van transport van factoren die worden uitgescheiden door de omliggende weefsels: het synoviaalmembraan (de binnenbekleding van het gewrichtskapsel) en het laagje gewrichtskraakbeen dat de uiteinden omhult van de botten die deel uit maken van het gewricht. In het geval van ontsteking is er sprake van een verstoorde gewrichtshomeostase waarbij synoviaalmembraancellen en instromende bloed- en immuuncellen inflammatoire en immuunreactieve factoren uitscheiden, waaronder enzymen, chemokines en cytokines. Bij voortdurende blootstelling van kraakbeencellen aan deze factoren ontstaat er een katabole omslag van de homeostase met als gevolg onomkeerbare kraakbeenschade en verdere ontsteking van het omliggende weefsel.

In dit proefschrift trachten we dieper in te gaan op de moleculaire aspecten van zowel de normale als een verstoorde gewrichtshomeostase. De recente ontwikkelingen in de biologie omtrent cel-cel communicatie door middel van membraanblaasjes, oftewel 'extracellular vesicles' (EVs) in het Engels, hebben er ons toe gebracht ons te richten op dit onderwerp. Membraanblaasjes of EVs komen voor in alle tot dusver onderzochte lichaamsvloeistoffen, ook in gewrichtsvloeistof. Het zijn kleine sferische structuren, uitgescheiden door cellen, met een diameter van 20 nanometer tot 1 micrometer. Ze zijn opgebouwd uit een lipidenmembraan en dragen verscheidene (mogelijk functionele) factoren met zich mee zoals eiwitten, lipiden en genetisch materiaal (RNA en DNA). Alle cellen in ons lichaam scheiden EVs uit als signaal voor de cellen in het direct omliggende weefsel of weefsels verder weg. Ontvangende cellen nemen op hun beurt EVs op of ontvangen een functioneel signaal na hechting van het EV aan de celmembraan. Op deze manier kunnen complexe boodschappen van de ene cel naar de andere cel worden overgedragen, zelfs over relatief lange afstanden in het lichaam.

In de jaren '90 van de vorige eeuw werden voor het eerst EVs beschreven in gewrichtsvloeistof. Het lag voor de hand dat deze, net als de 30 jaar eerder ontdekte 'matrix vesicles' (een variant van EVs in kraakbeen), een functie zouden hebben in het gewricht. Waar matrix vesicles een aantoonbare rol spelen bij de ontwikkeling van kraakbeen naar bot in jonge, zich nog ontwikkelende, gewrichten, was de rol van EVs in gewrichtsvloeistof een moelijker vraagstuk. De vraagstelling die de basis vormt voor dit proefschrift was wat de rol van EVs in gewrichtsvloeistof is ten tijde van acute artritis en ten tijde van gewrichtsontwikkeling in jonge individuen. Later in het proefschrift gaan we ook in op een mogelijke toepassing van EVs voor weefselregeneratie.

Aangezien EV-onderzoek in gewrichtsvloeistof wereldwijd nog in een onderontwikkeld stadium is en daarom de kwaliteit en reproduceerbaarheid van onderzoekstechnieken

nog niet optimaal is, was het van belang aan de start van ons onderzoek een standaard protocol op te zetten voor zorgvuldige isolatie van EVs uit deze vloeistof. In **Hoofdstuk 2** wordt, gebaseerd op literatuuronderzoek, een door ons opgesteld protocol op bruikbaarheid getest voor isolatie van EVs uit gezonde gewrichtsvloeistof van paarden. Een belangrijke stap in dit protocol was de voorbehandeling van gewrichtsvloeistof met het enzym hyaluronidase dat ervoor zorgt dat het in hoge concentraties aanwezige hyaluronzuur wordt afgebroken om zo de hoge viscositeit van de vloeistof te verlagen. Ultracentrifugatiestappen van achtereenvolgens 10,000g, 100,000g en 200,000g en een opzuiverstap d.m.v. een dichtheidsgradiënt zorgen vervolgens voor een goede EV-opbrengst. Door middel van een scala aan hoog-waardige technieken, waaronder hoge-resolutie flowcytometrie en cryo-elektronen-microscopie konden basiskenmerken van EVs uit gezonde gewrichtsvloeistof in kaart worden gebracht. Dit onderzoek vormde de basis voor de vervolghoofdstukken.

In **Hoofdstuk 3** werden EVs geanalyseerd tijdens gewrichtsontsteking in een paarden-model voor acute synovitis (ontsteking van het synoviaalmembraan) waarbij de gewrichtsholte werd geïnjecteerd met 0.5 nanogram lipopolysacharide (LPS), een endotoxine-bevattende structuur afkomstig van de wand van Gram-negatieve bacteriën. Deze injectie veroorzaakt een lokale, steriele, ontstekingsreactie van het synoviaalmembraan waarvan de klinische verschijnselen (zwelling van het gewricht, pijn, kreupelheid) verdwijnen binnen 48 uur. Uit onze analyse bleek dat tijdens deze ontstekingsreactie de concentratie aan EVs in gewrichtsvloeistof in hoge mate toeneemt, waarbij het piekmoment overeenkomt met de piek in concentratie van ontstekingsmediatoren in deze vloeistof, zoals cytokines, prostaglandines, leukotriënen en matrixmetalloproteïnases, die al eerder beschreven werden als kenmerkend voor dit type ontsteking. Een andere bevinding was de hoge concentratie aan CD44-positieve EVs, waarbij de relatieve aanwezigheid het hoogst was 24 uur na LPS-injectie, het moment dat de ontsteking al aan het afnemen is. Een functionele test van monsters die deze EVs bevatten gaf een eerste indicatie dat dit type EV een anti-inflammatoire rol kan spelen als het in contact komt met kraakbeen en mogelijk zo een dempend effect heeft op de ontsteking. Naast de downregulatie van inflammatoire genexpressie in de kraakbeencellen (beschermend effect), zagen we ook een toename in productie van matrixmetalloproteïnases, wat kan wijzen op een stimulering van de omvorming van het in een stresssituatie gebrachte weefsel. Deze resultaten moeten nog nader bevestigd worden in verder onderzoek, maar ze geven alvast belangrijke aanwijzingen voor de rol van EVs in acute synovitis en kunnen als basis dienen voor onderzoek naar EVs bij andere vormen van gewrichtsontsteking.

De lipidensamenstelling van EVs, die gezien kan worden als de blauwdruk van elk EV, geeft inzicht in de verschillende EV types die kunnen worden aangetroffen in

verschillende lichaamsvloeistoffen en ook een indicatie van de functionaliteit van EVs. De in **Hoofdstuk 3** aangetroffen CD44-positieve EV-subpopulatie werd in **Hoofdstuk 4** verder onderzocht. Een gedetailleerde fosfolipidenkarakterisering van EVs geïsoleerd uit gewrichtsvloeistof van paarden 24 uur na LPS-injectie (acute synovitis), onthulde minimaal vier tot nu toe onbekende glycerofosfolipide subklassen die niet of nauwelijks werden aangetroffen in EVs geïsoleerd uit gezonde gewrichts-vloeistof. Deze lipiden werden getypeerd als fosfatidylserinemoleculen waarbij de aminogroep gebonden is aan een variabele carboxylgroep die in ketenlengte verschilt van 1 tot minimaal 4 koolstofatomen. Opvallend is dat deze nieuwe lipiden, te weten *N*-formyl-fosfatidylserine, *N*-acetyl-fosfatidylserine, *N*-propionyl-fosfatidylserine en *N*-butyryl-fosfatidylserine, voornamelijk aangetroffen werden in EVs die voortkwamen uit de 200,000*g* EV-isolatie-stap en niet uit de voorafgaande 10,000*g* stap. Samen gaven deze resultaten een indicatie dat deze lipidemodificatie specifiek is voor een bepaald type EV en dat EVs van dit type een rol kunnen spelen bij (het afremmen van) gewrichtsontsteking. Veronderstelde functies van deze lipidemodificaties zijn 1) vorming van bioactieve componenten (zoals lyso-lipiden) d.m.v. enzymatische hydrolyse, 2) faciliteren van nieuwe potentieel functionele lipide-eiwit interacties, 3) creëren van structurele verandering van de EV-membraan en hierdoor verandering in EV-cel interacties en 4) een rol in mogelijke wijzigingen in de lipide-afhankelijke immuunrespons. Echter, de exacte functie(s) alsmede de biosynthese van deze nieuwe lipiden zal moeten blijken uit aanvullend onderzoek.

Een tweede onderwerp dat aan bod kwam in dit proefschrift **(Hoofdstuk 5)** was de rol van EVs tijdens gewrichtsontwikkeling bij veulens, wat later mogelijk vertaald kan worden naar gewrichtsontwikkeling bij de mens. In de eerste maanden na de geboorte is het gewrichtsmetabolisme zeer hoog, wat zich kenmerkt door snel veranderende biomarkerprofielen in gewrichtsvloeistof (en bloedserum) voor kraak-beenmatrix turnover (glycosaminoglycanen, matrixmetalloproteïnase-activiteit en type-II collageenafbraakproducten) en zelfs ontsteking (pro-inflammatoir chemokine CCL2 en prostaglandine-E2). Dit heeft alles te maken met de hoge mate van botvorming bij jonge dieren waarbij de omvorming van kraakbeen naar bot resulteert in groei van de lange beenderen, een proces bekend als endochondrale ossificatie. Gezien de belangrijke rol van EVs in andere biologische processen, o.a. de rol van 'matrix vesicles' tijdens endochondrale ossificatie, was een rol voor EVs in gewrichts-vloeistof tijdens deze fase van variabele gewrichtshomeostase niet ondenkbaar. De EV-concentraties en EV-karakteristeken in gewrichtsvloeistof verschilden echter niet tussen een groep jonge veulens (12 dagen tot 13 maanden oud) en een groep volwassen paarden (6-15 jaar oud). Ook waren er geen noemenswaardige verschillen tussen monsters genomen van dezelfde dieren op verschillende momenten in hun ontwikkeling. Gebaseerd op deze resultaten moeten we concluderen dat gewrichts-

ontwikkeling niet duidelijk weerspiegeld wordt in EV-concentraties of de door ons gemeten EV-kenmerken. Mogelijk zijn er wel andere kenmerken van EVs in gewrichts-vloeistof die bepalend zijn voor, of bepaald worden door, de fase van ontwikkeling. De inhoud van de EVs, dus de signaalmoleculen die zij transporteren, is daar een goede kandidaat voor, maar die hebben we in deze studie niet bepaald.

Zoals eerder gezegd is kraakbeenschade onomkeerbaar. De meest kenmerkende eigenschap van kraakbeen is dat het een weefsel is dat zichzelf niet kan herstellen, in tegenstelling tot de meeste andere weefsels in ons lichaam. Kraakbeenschade, veroorzaakt door voortdurende ontsteking of door acuut trauma, bijvoorbeeld een sport-blessure, kan daarom levenslange mobiliteitsproblemen veroorzaken. In **Hoofdstuk 6** van dit proefschrift geven we een doorkijk hoe EVs zouden kunnen bijdragen aan de regeneratie van beschadigd kraakbeen en het herstellen van de gewrichtshomeostase. Allereerst zijn EVs, in ieder geval in potentie, bijzonder geschikt als biomarker voor het typeren van gewrichtsaandoeningen. Daarvoor moeten dan wel de verschillende EV-types in bloed, gewrichtsvloeistof en weefselbiopten in de toekomst beter gedefinieerd zijn. Als tweede stap kunnen EVs gesynthetiseerd worden, gevuld met (combinaties van) anti-inflammatoire of immunosuppressieve mediatoren, en lokaal toegediend worden als therapie. Door de zeer efficiënte signaaloverdracht van EVs, die mogelijk zelfs in de tijd kan worden gestuurd, wordt verwacht dat deze therapie betere resultaten oplevert in vergelijking met het toedienen van losse oplosbare mediatoren in het gewricht (een op het moment gangbare therapie). In het geval van kraakbeenschade, kan men denken aan het inzetten van EVs afkomstig van (patiënt-eigen) gekweekte mesenchymale of geïnduceerde pluripotente stamcellen, waarvan de EVs *in vitro* al een gunstig functioneel effect hebben laten zien in andere studies. Ook kunnen synthetische EVs hier voor worden gebruikt, gevuld met factoren die gewrichtsontsteking afremmen en kraakbeenherstel stimuleren, zoals bepaalde miRNAs en groeifactoren. Een andere belangrijke en innovatieve ontwikkeling in het onderzoek naar kraakbeenregeneratie is de opkomst van de zogenaamde 'biofabricatie' waarbij nieuwe technologieën, zoals 3-dimensionele bioprinting, het mogelijk maken om stukjes kraakbeen en bot te produceren en als gepersonaliseerd implantaat aan te bieden aan de patiënt. Het inbouwen van functionele EVs tijdens bioprinting van deze implantaten (opgebouwd uit cellen en matrixelementen) zou latere weefselregeneratie een extra stimulans kunnen geven. Ook het toevoegen van EVs aan 'hydrogels' die gebruikt worden voor het opvullen van kraakbeendefecten, zou een potentieel gunstig effect kunnen hebben op het uiteindelijke herstel van het weefsel. Op dit moment worden de eerste onderzoeken uitgevoerd met betrekking tot dit onderwerp. De verwachting is dat dit snel zijn weg zal vinden naar een klinische toepassing, mits alle technische en ethische obstakels worden overwonnen.

Ten slotte worden in het afsluitende **Hoofdstuk 7** de bevindingen van de in het proefschrift beschreven onderzoeken bediscussieerd en in een breder kader geplaatst. Het belangrijkste vereiste van goed EV-onderzoek is het consequent volgen van een serie van goed uitgewerkte protocollen, zo blijkt ook uit dit proefschrift. Technische beperkingen en verdere uitdagingen worden in **Hoofdstuk 7** toegelicht en er worden adviezen gegeven voor toekomstig onderzoek van EVs in gewrichtsvloeistof.

Conclusie

Het eerder gedane onderzoek naar de functie van EVs in gewrichtsvloeistof gaf slechts in beperkte mate betrouwbare informatie over het exacte proces dat zich *in vivo* afspeelt in het gewricht. De studies in dit proefschrift hebben belangrijke aanvullende fundamentele gegevens geproduceerd en hierdoor inzicht gecreëerd wat betreft de rol van EVs tijdens het verloop van acute synovitis. Ook voor nader onderzoek naar de rol van EVs bij gewrichtsontwikkeling hebben we een goede basis gelegd. Verder zullen de inzichten die uit dit proefschrift voortkomen kunnen helpen bij de ontwikkeling van innovatieve medicatie en bio-engineering gericht op herstel van gewrichtskraakbeen.

The love for all living creatures is the most noble attribute of man
(Charles Darwin)

About the author

Janneke Boere was born on 16 July 1985 in Maastricht, the Netherlands. She grew up with her parents Elly Keijsers and Hub Boere in Zichen-Zussen-Bolder, a small village in Belgium close to the border with Maastricht. After finishing her secondary school in Belgium (Provinciale Secundaire School Voeren), she moved in 2003 to Maastricht where she undertook the studies Molecular Life Sciences (BSc, 2006) and Clinical Molecular Sciences (MSc, 2008). As extension of her MSc internship at the department of Psychiatry & Neuropsychology (Maastricht University), under the supervision of dr. Jos Prickaerts, she was given the opportunity to proceed her research on brain-derived neurotrophic factor in the United States. From May 2008 until May 2009 she settled in Boston and worked as research associate at the R&D department (Discovery Team) of pharmaceutical company Sepracor Inc. (currently Sunovion Pharmaceuticals Inc.) in Marlborough, MA, USA, under the supervision of dr. Rudy Schreiber. In the summer of 2009, she decided to take on a new challenge and moved to the United Kingdom to fulfil her long desired whish of studying animal sciences. Together with 24 candidates worldwide she was selected for the prestigious MSc course Wild Animal Biology at the Royal Veterinary College (University of London), which she successfully completed with a research traineeship at the department of Reproductive Biology at the Zoological Society of London (ZSL) under the supervision of prof. dr. Bill Holt.

After arriving back in the Netherlands, she worked for one year on cancer biology in the MAASTRO lab (department of Radiation Oncology, Maastricht University). In 2012, she started her PhD research at the department of Equine Sciences at Utrecht University under the supervision of prof. dr René van Weeren, in collaboration with the department of Orthopaedics of the University Medical Center Utrecht. Soon after the start of her research, her interest steered into the direction of extracellular vesicles, which has led to an additional collaboration with the research group of prof. dr. Marca Wauben, department of Biochemistry & Cell Biology (Utrecht University). Janneke's PhD project was dominated by her affinity for translational and multidisciplinary research in which she combined veterinary and human medicine in the field of joint disease and regenerative medicine. She investigated the role of extracellular vesicles in synovial fluid of horses with an outlook towards clinical applications for both equine and human joint disease.

Since November 2016, she is working as program manager at Lygature (Utrecht, the Netherlands), where she is responsible for the overall management of research consortia in life sciences aiming at developing innovative medical solutions for patients.

List of publications

Papers derived from this thesis

Boere, J.; van de Lest, C. H.; Libregts, S. F.; Arkesteijn, G. J.; Geerts, W. J.; Nolte-'t Hoen, E. N.; Malda, J.; van Weeren, P. R; Wauben, M. H. Synovial fluid pretreatment with hyaluronidase facilitates isolation of CD44+ extracellular vesicles. *J. Extracell Vesicles* **2016***, 5*, 31751.

Boere, J.*; Malda, J.*; van de Lest, C. H.; van Weeren, P. R.; Wauben, M. H. Extracellular vesicles - new tool for joint repair and regeneration. *Nat. Rev. Rheumatol.* **2016***, 12*, 243-249. * *authors contributed equally*

Boere, J.; van de Lest, C. H.; Libregts, S. F.; Arkesteijn, G. J.; Geerts, W. J.; de Grauw, J. C.; Cokelaere, S. M.; Plomp, S. G.; Malda, J.; Wauben, M. H; van Weeren, P. R. Dynamics and possible functional role of synovial fluid extracellular vesicles in LPS-induced acute synovitis. **2017**. *Submitted.*

Boere, J.; van de Lest, C. H.; de Grauw, J. C.; Plomp, S. G.; Libregts, S. F.; Arkesteijn, G. J.; Malda, J.; Wauben, M. H; van Weeren, P. R. Extracellular vesicles in synovial fluid from juvenile horses: a first exploratory study. **2017**. *Submitted.*

Boere, J. ; Brouwers J. F.; Cokelaere, S. M.; Malda, J.; Wauben, M. H.; van Weeren, P. R.; van de Lest, C. H. Phospholipid characterisation of synovial fluid derived extracellular vesicles harvested during LPS-induced synovitis: identification of novel naturally occurring short-chain carboxylic acid N-modified phosphatidylserine subclasses. *To be submitted.*

Other papers

EV-TRACK Consortium; Van Deun, J.;….; **Boere, J.**; …; Hendrix, A. EV-TRACK: transparent reporting and centralizing knowledge in extracellular vesicle research. *Nat. Methods* **2017***, 14*, 228-232.

Bach, F. C.; de Vries, S. A.; Riemers, F. M.; **Boere, J.**; van Heel, F. W.; van Doeselaar, M.; Goerdaya, S. S.; Nikkels, P. G.; Benz, K.; Creemers, L. B.; Maarten Altelaar, A. F.; Meij, B. P.; Ito, K.; Tryfonidou, M. A. Soluble and pelletable factors in porcine, canine and human notochordal cell-conditioned medium: implications for IVD regeneration. *Eur. Cell. Mater.* **2016***, 32*, 163-180.

De Vry, J.; Vanmierlo, T.; Martinez-Martinez, P.; Losen, M.; Temel, Y.; **Boere, J.**; Kenis, G.; Steckler, T.; Steinbusch, H. W.; De Baets, M.; Prickaerts, J. TrkB in the hippocampus and nucleus accumbens differentially modulates depression-like behavior in mice. *Behav. Brain Res.* **2016***, 296*, 15-25.

Estrada, R. J.; van Weeren, P. R.; van de Lest, C. H.; **Boere, J.**; Reyes, M.; Ionita, J. C.; Estrada, M.; Lischer, C. J. Comparison of healing in forelimb and hindlimb surgically induced core lesions of the equine superficial digital flexor tendon. *Vet. Comp. Orthop. Traumatol.* **2014***, 27*, 358-365.

Estrada, R. J.; van Weeren, P. R.; van de Lest, C. H.; **Boere, J.**; Reyes, M.; Ionita, J. C.; Estrada, M.; Lischer, C. J. Effects of autologous conditioned plasma® (ACP) on the healing of surgically induced core lesions in equine superficial digital flexor tendon. *Pferdeheilkunde*. **2014***, 30*, 6.

Prickaerts, J.; De Vry, J.; **Boere, J.**; Kenis, G.; Quinton, M. S.; Engel, S.; Melnick, L.; Schreiber, R. Differential BDNF responses of triple versus dual reuptake inhibition in neuronal and astrocytoma cells as well as in rat hippocampus and prefrontal cortex. *J. Mol. Neurosci.* **2012***, 48*, 167-175.

Boere, J.; Diaz, D. E.; Holt, W. V. Sperm motility activation, sperm heterogeneity and sperm-female tract interactions in Bennett's wallaby (Macropus rufogriseus rufogriseus). *Reprod. Fertil. Dev.* **2011***, 23*, 603-617.

PhD Portfolio

List of presentations

2016   Increased recovery of CD44+ extracellular vesicles from synovial fluid of healthy joints by incubation with hyaluronidase prior to isolation. Poster presentation. International Society for Extracellular Vesicles (ISEV) Annual Meeting, Rotterdam, NL

2015   Quantitative and qualitative analysis of synovial fluid extracellular vesicles in an equine model for acute synovitis. Poster and oral presentation. Utrecht University Veterinary Science Day, Bunnik, NL

2015   High resolution flow cytometry and lipidomics of synovial fluid derived extracellular vesicle populations during joint inflammation. Oral presentation. International Society for Extracellular Vesicles (ISEV) Annual Meeting, Washington DC, MD, USA

2014   Increased concentration of extracellular vesicles in the synovial fluid during LPS induced inflammation in the joint. Oral presentation. Dutch Society for Matrix Biology (NVMB) Annual Meeting, Amersfoort, NL

2014   Zonal organization in prenatal cartilage: the basis for cartilage tissue engineering? Poster presentation. Dutch Society for Biomaterials and Tissue Engineering (NBTE) Annual Meeting, Lunteren, NL

2014   Cartilage homeostasis might be regulated by extracellular vesicles facilitating intercellular communication between joint cells. Poster presentation. NIRM consortium meeting, Rotterdam, NL

2014   Cartilage homeostasis might be regulated by extracellular vesicles facilitating intercellular communication between joint cells. Poster presentation. FEBS Workshop, Lipids as Molecular Switches, Island of Spetses, Greece

2014   Cartilage homeostasis might be regulated by extracellular vesicles facilitating intercellular communication between joint cells. Poster presentation. 1st MBE (Matrix Biology Europe) conference (XXIVth FECTS meeting), Rotterdam, NL

2014   Extracellular vesicles isolated from equine synovial fluid bind to and are internalized by chondrocytes and synoviocytes in vitro. Oral presentation. International Society for Extracellular Vesicles (ISEV) Annual Meeting, Rotterdam, NL

2013   Intercellular communication in the equine joint: lipidome analysis of cell-derived vesicles. Oral presentation. Dutch Society for Biomaterials and Tissue Engineering (NBTE) Annual Meeting, Lunteren, NL

2013   Lipidome analysis of cell-derived vesicles in the equine joint. Oral presentation. Utrecht University Veterinary Science Day, Soesterberg, NL

2013	Isolation and anaylsis of nano-sized vesicles from equine synovial fluid. Poster presentation. NIRM consortium meeting, Utrecht, NL
2013	Isolation and anaylsis of nano-sized vesicles from equine synovial fluid. Oral presentation. Dutch Society for Matrix Biology (NVMB) Annual Meeting, Lunteren, NL
2012	Similar effects of interleukin-1b on cartilage explant cultures in media supplemented with adult serum, adult synovial fluid or immature serum. Poster presentation. Dutch Society for Biomaterials and Tissue Engineering (NBTE) Annual Meeting, Lunteren, NL

Fulfilled academic courses and workshops

2014	Regenerative Medicine, from Bench to Bedside	Utrecht University, NL
2014	Lipids as Molecular Switches	FEBS, Island of Spetses, Greece
2012	Digital Pictures: Data integrity and display	Utrecht University, NL

Teaching

2012	Lecturing 'Stem cell biology and technologies' Utrecht University Summer School – Regenerative Medicine course
2013	Supervision of research internship BSc Biotechnology (Wijtze Kaastra) 'The role of extracellular vesicles for cartilage homeostasis in the equine joint'
2014	Supervision of research internship MSc Veterinary Sciences (Susan van der Vrande) 'Histological analysis of equine cartilage development'
2016	Supervision of research internship MSc Veterinary Sciences (Lizzy Jager) 'Annexin-binding of *N*-modified PS'

Hier in het midden van nergens
Ligt de kleinste grote stad
Of eigenlijk, het grootste kleine dorp
Een wereldstad, een gat

uit ' Utrecht' (Claudia de Breij)

Dankwoord | Acknowledgements

Een van mijn collega-promovendi vergeleek het promotietraject ooit met een circus-act waarbij de doctor in spe allerlei ingewikkelde, zinvolle of niet zinvolle, kunstjes mag vertonen en vervolgens, richting het einde van het traject, door brandende hoepels moet springen om de eindstreep te halen. Een zeer toepasselijke metafoor. Het is inderdaad een eigenaardig wereldje, de academie. En toch had ik het niet willen missen.

Het eindresultaat van dit lange traject is dan het 'boekje', zoals deze thesis in de academische volksmond genoemd wordt. Ik heb me altijd afgevraagd waar dat verkleinwoord vandaan komt. Het is namelijk een 200 pagina's dik schrijven in zeer compacte wetenschappelijke taal. Dit werk geschreven in gewone mensentaal zou een roman van minstens 1000 pagina's behelzen; dat is zo ongeveer wat er aan gedachten in zit. Dat mag best een 'boek' genoemd worden; laat dat '-je' maar weg.
Een ander zeer opvallend iets aan een 'boekje' is dat de wetenschappelijke inhoud, hoe interessant ook, van relatief ondergeschikt belang lijkt voor de gemiddelde lezer, die in eerste instantie vooral aandacht heeft voor de omslag (het oog wil ook wat), waarna er in snel tempo wordt doorgebladerd naar het dankwoord. Ik heb me dan ook voorgenomen dat ik niet zal bezuinigen op dit hoofdstuk, want achter elke promovendus staat een leger collega's, vrienden en familieleden, en die verdienen een oprecht dankjewel!

***

Allereerst wil ik mijn promotoren prof. dr. René van Weeren, prof. dr. Marca Wauben, prof. dr. Jos Malda en mijn copromotor dr. Chris van de Lest van harte bedanken!

René – *paardendokter, letterkundige, avocat-conseil*. Wat heb ik mij gelukkig mogen prijzen met jou als 1ste promotor. Je hebt met mij nogal wat te verduren gehad. Na een jaar oriënterend onderzoek te hebben gedaan, besloot ik opeens van het vertrouwde kweken van paardencellen het veld van extracellulaire vesicles in te springen. Nog onontgonnen terrein in de veterinaire wereld. Nieuw, spannend, en met een risico. Jij gaf me de ruimte om dit risico te nemen en hebt altijd achter mijn onderzoek gestaan. Je bent de meest nuchtere dierenarts die ik ken, maar ook de meest kritische; dit maakt je een geweldig wetenschapper. Ook blijf je alles van de praktische kant benaderen: was er geen dierenarts beschikbaar in de kliniek voor veldwerk voor mijn onderzoek, dan kwam jij aanscheuren in je Landrover en gingen we samen een middagje paarden vangen bij de paardenmelkerij. René to the rescue! Dank voor je vertrouwen en dank voor je ontelbare verbetersessies van mijn stukken, al dan niet vanuit je huis in Frankrijk. Zonder jou was er geen proefschrift.

Marca – *wetenschapster in hart en nieren, energiebron, ideeënbus*. Dankjewel voor het omarmen van mijn onderzoek. Als jij weer eens een blik vesicle-ideeën open trok tijdens een bespreking met René, Jos en Chris, hield iedereen zijn adem in. Hoe moest al die informatie nu weer in een experiment gegoten worden? Een uitdaging, maar samen zijn we tot een heel leuk onderzoek gekomen! Ik heb veel van je geleerd en ik vond het een eer in jouw groep te mogen werken. Je hebt me geleerd kritisch naar data te kijken en hebt me misschien ook wel geleerd dat ik data-analyse helemaal niet zo leuk vind. Ik zit nu beter op mijn plek, op de grens van wetenschap en management. Dankjewel voor je wetenschappelijk inzicht, je eerlijkheid, je onverwoestbare energie en je (Limburgse) gezelligheid.

Jos – *bioprintgrootheid, (collageen)netwerkbouwer, inspiratiebron*. Niet alleen ik als promovendus heb een groei doorgemaakt tijdens dit traject. Ongeveer gelijktijdig heb jij je eigen onderzoeksgroep opgezet, meerdere initiatieven gestart met buitenlandse universiteiten, de bioprintfaciliteit in Utrecht uit de grond gestampt, een zeer succesvolle summerschool opgericht en een nieuwe masterstudie voor de Universiteit Utrecht gerealiseerd (om maar een paar dingen te noemen). Allemaal in het veld van biofabrication. Je hebt Utrecht op de kaart gezet en hebt in een paar jaar tijd grote stappen gezet in je carrière, waarvoor je complimenten verdient. Door je drukke werkzaamheden had je niet altijd tijd om je in detail te bemoeien met mijn onderzoek, maar ondanks dat heb je significant bijgedragen aan dit proefschrift en heb ik veel van je geleerd. Jouw grootste troef is het samenbrengen van mensen en ideeën en dat is precies de eigenschap die ik in mijn nieuwe baan kan gebruiken. Ik ben er super trots op dat we samen als eerste auteur op een fantastische publicatie staan! Dankjewel voor alles!

Chris – *biochemicus, bierbrouwer, bescheiden held*. Er is geen leven in het lab zonder Chris! Jij stond altijd voor me klaar, op welk moment van de dag ook. Als het ging om lipidenextracties en biochemische analyses was ik het kuiken en jij de moederkip. Je hebt me, zo goed en zo kwaad als het kon, bijgespijkerd in jouw vakgebied, maar eerlijk is eerlijk, ik snap er nog steeds slechts een fractie van. Toch hebben we samen een nieuw lipide weten te beschrijven wat resulteerde in het spannendste hoofdstuk van dit proefschrift. Na nog wat extra onderzoek staat er straks een grote publicatie op jouw naam, waar ik (als jouw trotse rechterhand) deel van mag uitmaken. Bedankt voor je betrokkenheid, je nuchterheid, je grappen en grollen en je heerlijke zelfgebrouwen (lab)bier. Ook dank aan je vrouw Nicole. Samen waren jullie altijd bereid voor een opbeurend gesprek, kopje koffie of barbecue. Bedankt voor jullie mentale steun! Jullie behoren tot de liefste mensen die ik ken.

***

Mijn paranimfen, Elly en Aike:

Elly – *beste vriendin, (nog) niet doctor wél dokter, mijn tweelingzus (volgens anderen)*. We zijn ooit samen gestart met een opleiding in Maastricht en zijn jarenlang huisgenootjes geweest in ons prachtig paleisje aan de Via Regia. Wat was dat een leuke tijd! Daarna zijn onze wegen gescheiden, maar onze vriendschap is gebleven en wordt steeds hechter naarmate we meer dingen meemaken. Ik ben heel blij dat we nog steeds op elkaar kunnen bouwen en heel veel gezellige dingen samen doen, ondanks de afstand. Je hebt ondertussen een uitdagende baan als arts en bent moeder van een mooie dochter; ik kan alleen maar super trots op je zijn. Lieve Elly, ik ben vereerd dat jij naast mij staat op dit belangrijke moment.

Aike – *intelligente hippie, high-speed-high-throughput-fanaat, ~~collega~~/vriend*. Oef, gelukkig maar dat jij mijn paranimf wilde zijn! Aan wie moest ik anders die moeilijke vragen over lipiden doorspelen? Maar dat is natuurlijk niet de enige reden dat jij naast me staat. We hebben door de jaren heen heel wat perikelen gezamenlijk overwonnen: piepende labapparatuur, bacteriën die niet of te snel of te langzaam groeiden, paardensamples centrifugeren tot in het oneindige (daar heb je dat k*tpaard weer), programmeren in R (overwinning voor jou, ondergang voor mij), microscopieplaatjes maken (ik vrees dat ik hier de overwinning boek), zoeken naar de kaasschaaf, of naar lekkere koffie, of naar koekjes, of iets anders eetbaars. Maar we hebben ook Mount Zeus op het Griekse eiland Naxos samen overwonnen. Een helse fietstocht van 12 uur... maar wat was het prachtig! En we toerden met een autootje samen door het Griekse binnenland om de mooiste plekjes te vinden. Het perfecte team: ik sturen, jij kaartlezen (GPS is voor mietjes). Wat een fantastische reis! (Oh wacht, we gingen natuurlijk ook voor de wetenschap naar Griekenland, maar dat ter zijde.) Je bent altijd een waardevolle collega geweest en nu een nog meer waardevolle vriend. Je hebt me onlangs nog gered toen ik bijna verzoop tijdens het wadlopen. Daarom ben jij mijn paranimf! Ondertussen sta jij ook aan het begin van het einde van je AIO-carrière. Laat weten als je hulp nodig hebt met die laatste loodjes, dan ben ik er voor je!

***

Out of the ordinary, I would like to take the opportunity here to thank specific teachers, mentors and supervisors that have unconditionally supported me during my studies and at the start of my career, ultimately contributing to this achievement. **Dr. Willem Voncken** – jij hebt mij in de goede richting gestuurd tijdens de studie MLW en hebt mij telkens opgevangen als het dreigde mis te gaan, ook na mijn studie. Ik hoop dat je nog steeds studenten op deze manier begeleidt en advies geeft. **Dr. Jos Prickaerts** en **dr. Gunter Kenis** – jullie leerden mij celkweken en papers schrijven. En jullie

stuurden me naar Boston, waarvoor eeuwige dank, wat een geweldige ervaring! **Dr. Rudy Schreiber** – je was mijn wetenschappelijke baas bij Sepracor in Boston, maar samen met Ineke heb je er ook voor gezorgd dat ik mijn weg vond in de grote stad. Ik ken niemand zo gastvrij als jullie. Via e-mail en Skype kan ik nog steeds bij je terecht voor advies. Je bent een inspiratiebron! **Dr. Jan Theys** – merci voor de vele motiverende gesprekken in moeilijke tijden. Ik heb veel aan je adviezen gehad. **Prof. dr. Bill Holt** – Thank you for giving me the best practical and mental support I could have during my internship at the Zoological Society in London. I will never forget we went searching for wallabies together at Whipsnade Zoo!

<div align="center">***</div>

Collega's van Biochemie & Celbiologie – ook al was ik niet officieel een B&C AIO, jullie afdeling was mijn thuisbasis. Dankjewel voor alle fijne contacten, leerzame discussies en gezellige uitjes!

Het 'Lunch@Space' clubje – jullie gezelligheid en goede gesprekken maakten veel goed, zelfs de slappe kroketten en de zoute space-soep. Ik ben nog steeds in overleg met Sodexo of we korting kunnen afdwingen als trouwe klant. Tot nu toe zonder succes.

Ruud – *5-sterren analist, experiment-lover, labdancer*. Lieve Rudy, je was mijn maatje in het lab! Met jou was het altijd feest! Je bent niet alleen te goed voor de wereld, maar ook de meest geweldige analist die er is! B&C zonder Ruud is als een pipet zonder puntje. Dankjewel voor al je hulp en gezelligheid in het lab en bedankt voor de eindeloos lange gesprekken. Ik hoop dat je snel de carrièrestappen kan zetten die je van plan was. Het is je gegund, ga ervoor!

Martijn M – *van analist naar PhD, (gitaar)kunstenaar, kattenknuffelaar*. Samen naar Rock Werchter, op druilerige zondagmiddagen kunstzinnige linosnedes maken en op wandelreis in het Marokkaanse Toubkalgebergte. Dankjewel voor deze leuke tijd! We zetten dit voort! Wat goed dat je besloot te gaan promoveren! Ik kijk nu al uit naar al die prachtige plaatjes in je proefschrift waarvoor je uren achter de microscoop hebt zitten turen.

Nick – *GAPR-koning, IB-regelnicht, doctor in relativeren*. Als alle wetenschappers zo relaxt waren als jij, dan was de universiteit een kuuroord. Zelfs toen we onderweg naar Spetses eerst onze posters kwijt raakten op het vliegveld, daarna op een verlaten treinstation strandden en vervolgens de Flying Cat boot ('Flying Kots') in Pyreus op één minuut na misten, was jij de rust zelve. Biertje erbij, niks aan de hand.

Datzelfde gold voor mislukte Western blots: geen bandjes, dan maar weer in de herkansing, niks aan de hand! Dank voor je onuitstaanbare relativeringsvermogen! Ik ben het steeds meer gaan waarderen. Aan alle wetenschappers die dit stukje lezen: GAPR gaat de wereld redden!

Ellen – *super-MSc-analist, organisatietalent, Limburgse vlaaienliefhebster.* We zijn ondertussen goede vriendinnen geworden en ik hoop dat dat nog lang zo mag blijven. Dankjewel voor het luisterende oor en de kopjes thee. Bij jou mocht/mag ik altijd miepen. Ik wens je een nieuwe leuke baan toe waarin je al jouw kwaliteiten kan toepassen. Dat wordt een uitdaging, want dat zijn er best veel!

Tom D – *pipettteermachine, vesicle-RNA-goeroe, vrijetijdsskater.* Ik sta telkens weer versteld van jouw oneindig enthousiasme. Zelfs stomme experimenten vind jij leuk. Vesicle-RNA, here comes Tom! Ik reserveer alvast een plekje voor jouw promotie! Ondertussen gaan we gewoon door met culinaire avondjes en gezellige weekendjes weg ter afleiding.

Marijke – *melk-kundige, vesicle-making-device-hater, gezelligheidsdier.* Vesicles in melk, vesicles in paarden... vesicles in paardenmelk? Het zou je ervan gaan duizelen. Jij hebt deze show al achter de rug! Super trots op je! 'Slapen doe je maar als je dood bent!' ☺ Heel veel succes in Maastricht! Bij Kasper en Tom ben je in goede handen.

Ger en **Sten** – *het influx-team!* Ger, het moeten wel duizenden samples zijn geweest die we samen hebben doorgemeten. Wat een werk! Gelukkig bracht dit goede gesprekken met zich mee. Dank voor al je tijd! Ik heb veel van je geleerd! Sten, ouwe brombeer, wat heb ik met je gelachen! Vooral op die zeldzame momenten dat je eens écht boos werd en dan in het Italiaans tekeer ging. Zeer vermakelijk. Ik heb gelukkig ook aandachtig geluisterd naar jouw technische kennis. En écht héél erg bedankt voor het reviewen van alle influxpapers!

Marthe en **Susanne** – jullie zijn ook al aardig op weg naar de doctorstitel. Heel veel succes de komende tijd! Susanne, telkens als ik een NOS verslaggever in het wild spot, denk ik aan jou. Marthe, jouw talent voor muziek sleept je hier wel doorheen, blijf spelen!

Marije – jij voert elk experiment tot in de perfectie uit. Wat fijn dat je op het einde een aantal experimenten van mij overnam. Dankjewel voor al je hulp!

Jaël – bij jou in het kamertje vond ik de rust om te schrijven. Fijn dat dat kon en dat ik de hele kamer mocht behangen met post-its met details over mijn onderzoek. Heel veel succes met lesgeven!

Petra – jij bent niet alleen secretaresse maar ook de zorgzame moeder van de afdeling. Een kopje thee hier, een goed gesprek daar. En een roos op mijn bureau toen er een familielid overleed. Kleine details die jou bijzonder maken. Fijn dat ik altijd mocht komen kletsen!

Maidina – we have had many chats at the coffee table the last years and I have seen you come a long way. I really hope you will achieve all your dreams!

Mokrish – for a short time we have been writing-roomies. Thanks for your inspiring stories about Malaysia. I hope I can visit you one day there…

Ignace – je hebt B&C verlaten zonder PhD diploma, maar je bent meer gegroeid dan wij allemaal bij elkaar. Het buitenland heeft je goed gedaan. Bedankt voor je vele (vooral lange) emails uit Zuid-Amerika; dit zette alles weer in perspectief. Ik wens je een fantastische nieuwe uitdaging toe in Nederland! Met de bagage van het laatste jaar moet dat zeker lukken.

<div align="center">***</div>

Collega's van de universiteitskliniek voor paarden – bedankt dat ik als onderzoeker zo welkom was om mee te kijken met behandelingen en operaties en altijd klinische vragen op jullie mocht afvuren. **Tsjester, Wim, Harold, Hanneke, Mathijs, Andrea, Annemiek, Henk H, Henk W, Peter** en **Jaimy**: jullie zijn fantastische dierenartsen en -verzorgers. Dank voor jullie hulp bij het verzamelen van onderzoeksmateriaal. Zonder jullie inzet kon ik geen onderzoek doen.

The Tissue Repair research group – it was great being part of this team of biologists, biochemists, vets, orthopaedic surgeons and engineers. In this group, translational ideas for cartilage and bone repair came to life. Keep up the good work!

Saskia – ik moet jou hier het meest in het zonnetje zetten, want jij hebt het laatste jaar mijn experimenten bij elkaar gepipetteerd. Dankjewel voor je eeuwige geduld, je volhardendheid en de vele uren die je in mijn onderzoek hebt gestopt. Ik heb ervan genoten met je samen te werken! De tissue repair groep mag blij zijn met een analist als jij! Ik hoop dat je ook in je vrije tijd nog veel successen mag boeken met de paarden, je grote hobby. Ik blijf je volgen.

Janny – jij bent mijn voorganger en mijn voorbeeld geweest. Jouw proefschrift ligt altijd binnen handbereik. Ik denk zelfs dat ik alle hoofdstukken gelezen heb! Fijn dat ik altijd vragen mocht stellen! En veel dank voor de hulp bij de paardenmelkerij! Je bent de beste dierenarts-onderzoeker die ik ken.

Nikae – veel AIO's mogen aan jou een voorbeeld nemen, petje af! Dank voor je kennis en kunde waar ik af en toe gebruik van mocht maken. En dank voor de gezellige avond in de schouwburg.

Stefan – de allerliefste paardendokter! Heel veel dank voor je uitgebreide hulp in de kliniek. Ook jij bent bijna klaar met je boekje. Nu in galop naar de eindstreep!

***

Collega's van afdeling Orthopedie UMCU – Bedankt aan jullie allemaal om de deur steeds verder open te zetten voor mijn onderzoek. Jullie ongezouten mening heeft mijn werk telkens weer aangescherpt. **Lucienne** and **Riccardo** – the vesicle work is now in your safe hands. Hopefully it will find its way into a clinical application soon. **Mattie** – ik hoor nog steeds dat de pezencoupes die we samen hebben gesneden van zulke goede kwaliteit zijn. Bedankt dat je altijd te hulp schoot waar nodig.

***

Mijn studenten **Wijtze, Susan** en **Lizzy** – jullie hebben stukken van mijn onderzoek op jullie bord gekregen tijdens jullie stages. Bedankt voor jullie inzet gedurende al die maanden! Speciale dank aan Susan, je hebt echt keihard gewerkt en hele mooie resultaten verkregen! Jammer dat net jouw stukje onderzoek niet in dit proefschrift is beland, maar het ligt nog steeds op de publicatieplank!

***

Bijzondere dank gaat uit naar **Carien van Wees**, eigenaar van paardenmelkerij Riga Ranch. Beste Carien, jij stelde jouw bedrijf beschikbaar voor het verzamelen van unieke monsters van een grote groep jonge paarden. Hiermee heb je een belangrijk stuk onderzoek gefaciliteerd. Ook veel dank aan de medewerkers van Riga Ranch voor de voorbereiding van onze bezoeken en de goede nazorg van de dieren.

***

Bedankt aan alle paardeneigenaren die toestemming hebben gegeven voor het gebruiken van monsters van hun zieke paarden voor onderzoek en het beschikbaar stellen van de dieren voor post mortem onderzoek.

***

Collega's van Lygature – sinds november 2016 werk ik bij jullie. Ik had mij geen warmer welkom kunnen wensen. **Jorg en Ton** – bedankt voor het vertrouwen dat ik uiteindelijk toch dat diploma zou halen. **Eric, Pieter** en **Andre** – bedankt dat ik de ruimte kreeg om deze promotie tot een goed einde te brengen. Ondertussen zit ik bij Lygature helemaal op mijn plek! Aan alle collega's: wat fijn dat jullie er zijn!

***

Mijn vrienden...

Ralph – *beste vriend, realist, steunpilaar.* Bedankt dat je me af en toe eraan herinnert dat een werkdag een einde heeft en dat het dan tijd is voor leuke dingen. Blijf dit vooral doen! Bedankt ook voor de vele filosofische bankgesprekken: dat kan alleen met jou. En fijn dat je mijn LBN (Limburgs Beschaafd Nederlands) nog steeds blijft corrigeren. Ooit kan ik net zo goed Nederlands *dan jouw*... ☺

Frank – *theatergenie, lachtherapeut, mensenmens.* Bedankt voor je onvoorwaardelijke steun tijdens de vele lange gesprekken. Ik heb veel aan je gehad. Jij zet mij altijd weer met beide benen op de grond. Jim kwam er als cadeautje bij!

Linda, Irene, Marc, Ramon en de rest van het 'Samen Happen' clubje in Utrecht – Misschien weten jullie het niet, maar jullie zijn een belangrijke stabiele factor geweest! Ik heb genoten (en geniet nog steeds) van de ontelbare etentjes en spelletjesavonden met de nodige flauwe praat. Hier even geen wetenschap! Linda, ik ben super trots dat jij met de band komt spelen op mijn feest! Dierendokter Irene, als dieren genezen gebaseerd was op richtingsgevoel, dan had de diergeneeskunde met jou een probleem ☺ Ik hoop dat je nog veel beestjes beter mag maken! Marc en Ramon, misschien verschillen wij wel het meest van elkaar wat betreft vakgebied. Lief dat jullie altijd interesse tonen! Jullie hebben allemaal heel wat moeten aanhoren over dit PhD-verhaal, waarvoor dank! Als afsluiter volgt er een groot feest... en dan zeur ik er nooit meer over, beloofd!

Vrienden in Maastricht – **Thijs, Ellen, Siamack, Michael, Jorrick, Gaby, Larissa** en **Norbert**. Een aantal van jullie hebben al PhD achter je naam staan en weten hoe belangrijk het is om hierover te kunnen sparren. Fijn dat dat bij jullie altijd kan! Ook fijn om samen met dit groepje van tijd tot tijd de afleiding te zoeken. Alaaf!

Mijn buren – **Anne, Frank** en **Hassan**, dankjewel voor jullie interesse, telkens weer.

Sanaz – finally, the goal is reached! Thanks for always listening, from each continent of the world you were at. I am happy to have you back in the Netherlands!

Friends all over the world – **Jamie, Rane, Jennifer, Ale, Riccardo, Lukas,** and many others… Meeting you was by complete coincidence, but I am overly happy that coincidences like this exist! From a distance we keep following each other's steps, of which this PhD thesis is one. I hope we can keep in touch for a very long time.

***

Lieve familie – jullie hebben vaak gevraagd 'Ben je nou nóg niet klaar met studeren?'. Maar nu is het dan eindelijk klaar en kan ik eindelijk laten zien waar ik al die jaren aan heb gewerkt. Bedankt voor jullie interesse door de jaren heen.

Tiny en **Piet** – Jullie zijn mijn tweede setje ouders. Wat fijn dat ik altijd bij jullie terecht kan! Piet, krijg ik nou eindelijk die duif die je me 25 jaar geleden hebt beloofd?

Sylvia en **Etien** – jullie zijn als mijn grote zus en broer. Ik ben ondertussen al jaren weg uit Limburg, maar telkens als ik bij jullie aanschuif, voelt het weer 'wie vreuger'. Tied veur 'n pafke! Wanneer gaan we weer naar Cadzand?

Mama en **papa** – dit boekje is voor jullie! Als kind al kreeg ik de vrijheid om mij te ontwikkelen in de richting die ik wilde. Ik was het type kind dat liever naar het natuur-historisch museum ging dan een dagje naar de speeltuin. Wat fijn dat dat kon! Dankjewel dat jullie me telkens weer meenamen naar de reuzenschildpad, de mosasaurus, de bijenkast,… Daar is mogelijk de interesse voor biologie ontstaan. Vervolgens wilde ik toch maar bakker worden, of balletdanseres, of dierenarts. Uiteindelijk heb ik, met hulp van jullie, gekozen om Molecular Life Sciences te studeren, en dat sloeg de spijker op de kop. Jullie gaven mij na mijn studie het vertrouwen om de oversteek naar Boston te maken en vervolgens nog een extra studie op te pakken in Londen. Zonder jullie duwtje (nouja, zeg maar 'stevige duw') in de rug had ik dit nooit gedaan. Tijdens mijn promotie hebben jullie altijd voor me klaargestaan, en dat staan jullie nog steeds. Ik kan jullie niet genoeg bedanken voor alle steun die ik altijd van jullie krijg! Jullie zijn fantastische ouders!